

Tuning DNA Stability to Achieve Isothermal DNA Amplification

by

Abu Kausar

A thesis submitted in partial fulfillment of the requirements for the degree of

Doctor of Philosophy

Department of Chemistry  
University of Alberta

©Abu Kausar, 2014

## Abstract

Developing a simple, general, and isothermal self-replicating system is one of the key requirements for a simplified detection platform for nucleic acid sequences specific to a disease causing microorganism. One of the challenges in achieving nucleic-acid templated isothermal amplification is that the product duplex formed after the templated reaction is much more stable than the pre-reaction complex. Consequently, the template remains bound to the complementary nucleic acid formed, preventing the template from initiating another cycle of amplification. To avoid this product inhibition, we introduce different destabilizing linkers in the template, which result in the isothermal amplification of complementary DNA. One of the most active destabilizing groups is an abasic lesion, which we demonstrate can also operate in across-catalytic process that we refer to as lesion-induced DNA amplification or LIDA. Using LIDA, we are able to observe rapid, isothermal self-replication of DNA, of a variety of sequences, by combining two cycles of amplification and using a high concentration of T4 DNA ligase enzyme. Moreover, we find the LIDA process operates in the presence of genomic DNA and can detect a specific sequence in plasmid DNA, suggesting this method may find application in nucleic-acid based diagnostics. Additionally, as DNA ligases have a better discriminating ability than DNA polymerases for mismatches in target DNA, using ligase-based LIDA we are able to achieve very good discrimination between amplification initiated with a matched target versus a mismatched target (discrimination ratio = 47).

Combining a simple amplification method for disease-specific nucleic acid sequences with a simple detection platform is an important step towards the development of a diagnostic tool usable in resource-limited environments. Traditionally, we employ polyacrylamide gel electrophoreses (PAGE) to detect the amplified nucleic acid, requiring that we label one of the DNA probe strands that is incorporated into the self-replication product. In another approach explored, one of the probes is modified with a fluorescent donor (FAM) and another probe modified with a fluorescent acceptor (Cy5). The replication process causes these probes to become covalently attached, which we observe by Förster Resonance Energy Transfer (FRET) providing a real-time method of detection of the amplification process. To further simplify detection, we also combine LIDA with a rapid colorimetric approach developed in our group based on gold nanoparticles, where the target-induced amplification product leads to the disassembly of nanoparticle aggregates resulting in a color change from purple to red. Additionally, we have screened different DNA ligases and demonstrate that we are able to detect down to 14 pM target DNA using *E. coli* DNA ligase (compared with 1.4 nM using T4 DNA ligase), which suggests that identifying or developing an enzyme with no blunt-end ligation would be ideal for further lowering the limit of detection with LIDA. Finally, varying the base across from the abasic site reveals that there is no special base requirement for the isothermal system to work, providing further evidence that LIDA represents a general approach for isothermal target sequence amplification.

## Preface

This project on isothermal DNA amplification by destabilization was highly collaborative. The idea in Chapter 2 was conceived by J. M. Gibbs-Davis. Prior to my joining the project, some of the proof-of-concept experiments were done by J. Lam and R. D. McKay. R. Bhogal and A. Tang synthesized several of the destabilizing templates reported in Chapter 2 and performed some of the thermal denaturation curves reported therein. J. Lam synthesized some of the DNA strands and performed some of the single cycle ligation and amplification experiments as well as some of the thermal denaturation curves in that chapter. The data reported in this chapter for the kinetic experiments on the single cycle ligations and the cross-catalytic amplification was studied by myself. Chapter 2 has been published as Kausar, A.\*, McKay, R. D.\*, Lam, J.\*, Bhogal, R. S., Tang, A. Y. and Gibbs-Davis, J. M. (2011), Tuning DNA Stability to Achieve Turnover in Template for an Enzymatic Ligation Reaction. *Angew. Chem. Int. Ed.*, 50: 8922–8926 (\* Equal contribution). I was responsible for data collection, analysis and manuscript edits. J. M. Gibbs-Davis was the supervisory author and was involved with the project concept and manuscript composition.

Chapter 3 has been published as Kausar, A., Mitran, C. J., Li, Y. and Gibbs-Davis, J. M. (2013), Rapid, Isothermal DNA Self-Replication Induced by a Destabilizing Lesion. *Angew. Chem. Int. Ed.*, 52: 10577–10581. C. J. Mitran, J.M. Gibbs-Davis, and I developed the concept and designed experiments. J. M. Gibbs-Davis and I prepared the manuscript. Y. Li performed many of the LIDA



experiments and thermal denaturation experiments for the **H-DNA-I** system. C. J. Mitran helped me optimize the single cycle amplification and serial ligation experiments of the **DNA-I** system, as well as prepared some of the DNA and performed some of the thermal denaturation experiments for that system.

In Chapter 4, all the experiments described were conceived by myself and J. M. Gibbs-Davis and conducted by me. A manuscript based on this chapter is in preparation. Ligase variation and probe design variation experiments for making the isothermal amplification system better are reported in Chapter 5. Probes for the true blunt end system were designed and synthesized by C. J Mitran. All of the amplification experiments including the blunt-end system were performed by me.

## Acknowledgements

From the core of my heart, I would like to express my deepest sense of gratitude and sincerest thanks to Professor Julianne M. Gibbs-Davis for her constant guidance, thoughtful suggestions, dear cooperation, and untiring endeavors and over all for her keen and sharp supervision throughout the course of my PhD. It was a great opportunity for me to work with a multidisciplinary group which broadened my knowledge in different areas of Chemistry. The training I received in scientific communication both in oral and writing will be a milestone for the rest of my life. She is a dedicated and energetic mentor that helped her maintaining a large research group with many successful projects. I am very thankful to her for giving me the opportunity to work in the DNA project even though I had a very little experience working with biomolecules. Finally, I would like to thank her for the help with crafting and editing the manuscripts and the thesis.

With due deference, I would like to express my cordial thanks to Prof. John Klassen and Prof. Robert Campbell for being in the supervisory committee with periodic monitoring the progress of the project with valuable thought and suggestions. I wish to thank Dr. Klassen and Dr. Campbell for the thoughtful comments and suggestions for improving the thesis.

In the Gibbs-Davis group, we had a very collaborative team of researchers. First of all, I would like to thank Dr. Azam for helping me initial with settlement in Edmonton. He was the first person who inspired me to come to University of

Alberta. I will not forget all the help and support I received for initial settlement as well as suggestions in many decision making situations. I would like to specially mention Yimeng and Katie for their help with studying different parameters of the project. Katie was instrumental in trying to take the project in different directions with special focus on developing simple point-of-care kit. I would like to thank to Delwar and Mike for the help with the gold-nanoparticle project. I should mention Akemi for giving clear conception about some of the topics in Biology. I would like specially thank Eiman and Safeenaz for proof-reading my thesis and important discussion about different topics. I also thank Dr. Hoi and Dr. Ding from Campbell group for the help for the training with microplate-reader and different molecular biology experiment. With gratitude, I like to express my warm thanks to Gareth Lambkin in Biological Services for helping me with different molecular biology techniques. I would like to thank Jade, Alex, Rohan, Harry, Camila, Uchenna, Rosalie and Haleemah for their contribution in the project.

I would like to specially thank my wife, Masuda Akter and my daughter Adiba Kausar for sacrificing their fun time together. I am very fortunate to have such a supportive family. I would like to express warm thanks to my parents and all the family members for their motivation and constant encouragement throughout the course of my study.

Finally, I would like to praise the blessings of Almighty Allah for the bountiful resources, perseverance and the strength bestowed upon me to complete course of the study.

*To my wife Masuda Akter, daughter Adiba Kausar, parents (Abdul Quddus and  
Jahanara Begum)and my late brother Abul Kalam Azad  
whose constant support and inspiration kept me  
motivated all the time*

## Table of Contents

<b>Title</b> .....	i
<b>Abstract</b> .....	ii
<b>Preface</b> .....	iv
<b>Acknowledgements</b> .....	vi
<b>Table of Contents</b> .....	ix
<b>List of Tables</b> .....	xvi
<b>List of Figures</b> .....	xvii
<b>List of Abbreviations/symbols</b> .....	xxvi
<b>Chapter 1</b> .....	1
<b>Introduction</b> .....	1
1.1 Infectious disease diagnostics.....	2
1.2 Diagnostic methods.....	2
1.2.1 Culture and colony based methods.....	2
1.2.2 Immunological methods.....	3
1.2.3 Nucleic acid based diagnostics.....	5
1.3 Nucleic acid amplification methods.....	7
1.3.1 Amplification with thermocycling.....	7
1.3.1.1 Polymerase chain reaction.....	7
1.3.1.2 Ligase chain reaction (LCR).....	13
1.3.2 Isothermal amplification.....	17
1.3.2.1 Strand displacement amplification (SDA).....	17

1.3.2.2 Rolling circle amplification (RCA).....	18
1.3.2.3 Helicase-dependent isothermal amplification (HDA).....	19
1.3.2.4 Nucleic acid sequence-based amplification (NASBA).....	22
1.3.2.5 Exponential amplification reaction (EXPAR).....	23
1.3.2.6 Loop-mediated isothermal amplification.....	24
1.3.2.7 Isothermal amplification using destabilization approach.....	27
1.4 Objectives.....	34
1.5 References.....	39
<b>Chapter 2.....</b>	<b>50</b>
<b>Tuning DNA Stability to Achieve Turnover in Template for an Enzymatic</b>	
<b>Ligation Reaction.....</b>	<b>50</b>
2.1 Introduction.....	51
2.2 Introduction of destabilizing group for isothermal amplification.....	53
2.3 Results and discussions.....	54
2.3.1 Tuning DNA stability with destabilizing groups.....	54
2.3.2 Monitoring ligation with various destabilizing templates.....	56
2.3.3 Monitoring turnover with destabilizing templates.....	58
2.3.4 Effect of concentration of enzyme on turnover number (TON) .....	62
2.3.5 DNA self-replication with a cross-catalytic approach.....	63
2.4 Conclusion.....	67
2.5 Experimental.....	68
2.5.1 General.....	68

2.5.2 Preparation of DNA strands.....	70
2.5.3 Synthesis of the destabilizing templates (strand <b>DNA-II<sub>D</sub></b> , where D ≠ thymidine).....	71
2.5.3.1 Preparation of dimethoxytrityl (DMT)-protected diols.....	71
2.5.3.2 Typical preparation of the mono-DMT protected diols.....	72
2.5.3.3 Preparation of the corresponding phosphoramidites.....	73
2.5.3.4 Preparation of destabilized templates using the synthesized phosphoramidites.....	74
2.5.4 Mass analysis of the DNA strands.....	74
2.5.5 Thermal dissociation experiments.....	75
2.5.6 Melting profile analysis.....	75
2.5.7 Ligation experiments.....	76
2.5.8 Denaturing polyacrylamide gel electrophoresis.....	77
2.5.8.1PAGE analysis of strand purity.....	79
2.6 References.....	80
<b>Chapter 3.....</b>	<b>84</b>
<b>Rapid, Isothermal DNA Self-Replication Induced by a Destabilizing Lesion</b> .....	<b>84</b>
3.1 Introduction.....	85
3.2 Cross-catalytic amplification by destabilization.....	87
3.2.1 Influence of enzyme concentration.....	89
3.2.2 Cross-catalysis in the absence of a destabilizing group.....	91

3.2.3 Cross-catalysis with a mismatch as the destabilizing group.....	92
3.2.4 Determining sequence generality.....	94
3.2.5 Optimizing template-initiated replication by reducing the replicator concentration.....	102
3.2.6 Cross catalysis in the presence of non-complementary DNA.....	106
3.2.7 Cross catalysis initiated by double-stranded plasmid DNA.....	110
3.3 Conclusions.....	114
3.4 Experimental Section.....	115
3.4.1 General.....	115
3.4.2 DNA preparation and characterization.....	115
3.4.3 MALDI characterization.....	117
3.4.4 Thermal denaturation (melting) Studies.....	118
3.4.5 Plasmid preparation.....	119
3.4.6 Ligation experiments.....	120
3.4.7 Plasmid detection.....	121
3.4.8 Serial ligation experiments.....	122
3.4.9 Quantification of replication cycles.....	122
3.4.10 PAGE images.....	124
3.4.11 Supporting tables.....	129
3.5 References.....	131



<b>Chapter 4</b> .....	135
<b>Detection of SNPs using lesion-induced DNA amplification and simplified detection strategies</b> .....	135
4.1 Introduction.....	136
4.2 Discrimination of mismatches in a ligation single cycle.....	140
4.3 Discrimination of mismatches with cross-catalysis.....	142
4.3.1 Specific detection of mismatches.....	147
4.3.1.1 Discrimination between T- and A-target.....	147
4.3.1.2 Discrimination between T- and G-target.....	153
4.3.2 FRET based detection.....	157
4.3.2.1 Detection of DNA-templated ligation with FRET for the single cycle system.....	159
4.3.2.2 Real-time discrimination of mismatches with cross-catalysis.....	162
4.3.3 Colorimetric detection of amplification with gold-nanoparticle.....	166
4.4 Conclusions.....	174
4.5 Experimental.....	175
4.5.1 Materials and instrumentation.....	175
4.5.2 DNA synthesis and purification.....	175
4.5.3 PAGE-based ligation (single cycle and cross-catalysis).....	176
4.5.4 Denaturing polyacrylamide gel electrophoresis.....	177
4.5.5 Real-time FRET experiments (single cycle and cross-catalysis).....	177
4.5.6 Nanoparticle functionalization with DNA.....	178
4.5.7 NP-based colorimetric detection.....	179

4.5.7.1 Nanoparticle hybridization.....	179
4.5.7.2 Cross-catalytic amplification followed by colorimetric detection.....	179
4.6 References.....	181
<b>Chapter 5.....</b>	<b>188</b>
<b>The influence of ligase and probe architecture on lesion-induced DNA amplification.....</b>	<b>188</b>
5.1 Introduction.....	189
5.2 Overview of DNA ligases.....	190
5.2.1 T7 DNA ligase.....	190
5.2.2 T3 DNA ligase.....	191
5.2.3 <i>E. coli</i> DNA ligase.....	191
5.3 Ligation with T7 DNA ligase.....	192
5.3.1 Lesion-induced DNA amplification with T7 DNA ligase.....	192
5.3.2 Single cycle ligation with T7 DNA ligase.....	193
5.3.3 Cross-catalysis with different buffers with T7 DNA ligase.....	196
5.3.4 Cross-catalysis with high concentration T7 DNA ligase in PEG-free buffer.....	197
5.4 Cross-catalysis with <i>E. coli</i> ligase.....	199
5.5 Cross-catalysis with T3 DNA ligase.....	201
5.6 Cross-catalysis with different blunt end system.....	202
5.7 Attempts to reduce background-triggered amplification with ATP and spermidine.....	207
5.8 Varying the deoxynucleotide across from the abasic group.....	209

5.9 Conclusions.....	216
5.10 Experimental Section.....	217
5.10.1 General Materials.....	217
5.10.2 DNA Sequences.....	217
5.10.3 Ligation buffers.....	218
5.10.4 Ligation experiments.....	219
5.10.5 Thermal denaturation experiments.....	219
5.11 References.....	221
<b>Chapter 6.....</b>	<b>222</b>
<b>General conclusions and Future plans.....</b>	<b>222</b>
6.1 General conclusions.....	223
6.2 Future plans.....	228
6.2.1 Reducing background ligation using dual LDR-PCR with destabilization .....	228
6.2.2 Isothermal amplification of longer targets using LIDA.....	230
6.3 Challenges.....	233
6.3.1 Sample Preparation.....	233
6.3.2 Ease of use.....	234
6.3.3 Stability of the reagent.....	235
6.4 References.....	236
Bibliography.....	237

## List of Tables

<b>Table 2.1:</b> DNA sequences used for studying isothermal amplification.....	70
<b>Table 3.1:</b> Melting temperatures ( $T_m$ ) of duplexes formed during cross-catalytic replication.....	96
<b>Table 3.2:</b> DNA Sequences <b>DNA-I</b> , <b>H-DNA-I</b> , and <b>E-DNA-I</b> systems used in this study.....	117
<b>Table 3.3:</b> Ligation results vs. initial template concentration for the <b>DNA-I</b> system.....	129
<b>Table 3.4:</b> Ligation results vs. initial template concentration for the <b>H-DNA-I</b> system.....	130
<b>Table 4.1:</b> DNA sequences used for studying SNP detection.....	140
<b>Table 4.2:</b> DNA sequences used for the nanoparticle study.....	179
<b>Table 5.1:</b> DNA sequences used in Chapter 5.....	217

## List of Figures

### Chapter 1

<b>Figure 1.1:</b> Stepwise scheme of a sandwich ELISA (enzyme-linked immunosorbent assay).....	5
<b>Figure 1.2:</b> Schematic representation of the polymerase chain reaction (PCR) reaction.....	10
<b>Figure 1.3:</b> Schematic diagram of different types of real-time PCR techniques.	12
<b>Figure 1.4:</b> Schematic representation of the ligase chain reaction (LCR).....	14
<b>Figure 1.5:</b> Schematic representation of rolling circle amplification (RCA).....	19
<b>Figure 1.6:</b> Schematic representation of helicase dependent amplification (HDA). .....	21
<b>Figure 1.7:</b> Schematic representation of the nucleic acid sequence-based amplification (NASBA).....	23
<b>Figure 1.8:</b> Schematic representation of loop-mediated isothermal amplification (LAMP).....	26
<b>Figure 1.9:</b> Schematic diagram of a nucleic acid self-replicating system.....	28
<b>Figure 1.10:</b> Schematic diagram of cross-catalytic amplification system.....	29
<b>Figure 1.11:</b> General scheme of surface-promoted replication and exponential amplification (SPREAD) process.....	31
<b>Figure 1.12:</b> General scheme of destabilization of product duplex with ligation–rearrangement reactions.....	33

<b>Figure 1.13:</b> Schematic diagram of isothermal amplification by destabilization with a flexible linker.....	33
--	----

## Chapter 2

<b>Figure 2.1:</b> Schematic diagram of isothermal turnover in DNA-templated ligation reactions using destabilizing templates.....	52
--	----

<b>Figure 2.2:</b> Zoomed-in view of the nicked site with different destabilizing templates.....	53
--	----

<b>Figure 2.3:</b> The thermal dissociation profiles of the nicked duplexes and the product duplexes (template:product).....	56
--	----

<b>Figure 2.4:</b> Single cycle ligation for different destabilizing templates and the correspondence turnover number at different temperature.....	57
---	----

<b>Figure 2.5:</b> Ligation of different length probes with different templates.....	58
--	----

<b>Figure 2.6:</b> Representative PAGE images of the kinetics of ligation with different destabilizing templates.....	61
---	----

<b>Figure 2.7:</b> Schematic diagram of cross-catalytic cycles with destabilizing probes.....	63
---	----

<b>Figure 2.8:</b> Turnover number with single cycle and cross-catalytic with abasic group as a destabilizing group 24 °C.....	65
--	----

<b>Figure 2.9:</b> Comparison of cross-catalysis using varying equivalents of native and destabilizing templates.....	67
---	----

<b>Figure 2.10:</b> Scheme of synthesis of phosphoramidites with destabilizing modification.....	71
--	----

<b>Figure 2.11:</b> PAGE images of the destabilizing templates stained with Stain-All dye.....	79
--	----

### Chapter 3

<b>Figure 3.1:</b> Schematic diagram of cross-catalytic amplification of target DNA using an abasic destabilizing group in an LCR.....	88
--	----

<b>Figure 3.2:</b> Single cycle and cross-catalytic amplification with <b>DNA-I</b> system with native and destabilizing probes at 30 °C.....	90
---	----

<b>Figure 3.3:</b> Kinetics of cross-catalytic replication <b>F-DNA-I</b> with native <b>DNA-I</b> system at different temperatures.....	92
--	----

<b>Figure 3.4:</b> Kinetics of cross-catalytic replication of target <b>F-DNA-I</b> with mismatch as destabilizing template at different temperatures.....	93
--	----

<b>Figure 3.5:</b> Melting profiles of the <b>DNA-I</b> system corresponding to the different product duplex, nicked duplex and replicator ( <b>rDNA</b> ) duplexes.....	94
--	----

<b>Figure 3.6:</b> Melting profiles of the <b>H-DNA-I</b> system corresponding to the different product duplex, nicked duplex and the replicator ( <b>rDNA</b> ) duplexes....	95
---	----

<b>Figure 3.7:</b> Kinetics of Cross-catalytic replication of <b>H-DNA-I</b> with destabilizing probes at 34 °C.....	97
--	----

<b>Figure 3.8:</b> Kinetic traces of cross-catalytic replication of <b>F-H-DNA-I</b> system as a function of time using an abasic modified replicator at different temperatures.	98
--	----

<b>Figure 3.9:</b> Kinetic traces of cross-catalytic amplification with <b>DNA-I</b> system as a function of time using an abasic-modified replicator at different temperatures.....	98
--	----

<b>Figure 3.10:</b> Comparison of melting temperatures ( $T_m$ ) of the product and nicked duplexes for the <b>DNA-I</b> and <b>H-DNA-I</b> systems with the optimum replication temperature.....	99
<b>Figure 3.11:</b> Formation of <b>F-DNA-I</b> as a function of initial <b>DNA-I</b> template concentration and the initial rate as a function of initial <b>DNA-I</b> template.....	100
<b>Figure 3.12:</b> Difference in the concentration of product formed between the reaction initiated with 14 nM and 0 nM <b>H-DNA-I</b> and the number of template-initiated replication cycles as a function of initial template concentration.....	101
<b>Figure 3.13:</b> The concentration of <b>F-DNA-I</b> formed as a function of time with different concentrations of initial <b>DNA-I</b> template and lower replicator concentrations.....	103
<b>Figure 3.14:</b> Schematic diagram of serial ligation and PAGE images.....	104
<b>Figure 3.15:</b> The fluorescent intensity profile of the serial ligation initiated process by 140 fM <b>DNA-I</b> .....	105
<b>Figure 3.16:</b> Cross-catalytic replication of <b>F-DNA-I</b> initiated by <b>DNA-I</b> in the presence of other non-complementary DNA strands.....	107
<b>Figure 3.17:</b> Cross-catalytic replication of <b>F-DNA-I</b> initiated by <b>DNA-I</b> in the presence of varying amounts of salmon sperm DNA.....	109
<b>Figure 3.18:</b> Cross-catalytic replication of <b>F-DNA-I</b> initiated by <b>DNA-I</b> in the presence of 0.09 $\mu\text{g}/\mu\text{L}$ salmon sperm DNA.....	110
<b>Figure 3.19:</b> Application of cross-catalytic for amplification of a particular gene within plasmid DNA.....	112



<b>Figure 3.20:</b> Representative gel image of cross-catalytic amplification of a particular gene within a plasmid DNA.....	113
<b>Figure 3.21:</b> Representative gel images of cross-catalytic amplification of <b>F-DNA-I</b> with destabilizing probes at 30 °C.....	124
<b>Figure 3.22:</b> Representative gel images single cycle amplification of <b>F-DNA-II</b> with 14 nM <b>DNA-I</b> .....	124
<b>Figure 3.23:</b> Representative gel images of cross-catalytic amplification of <b>F-DNA-I</b> with native DNA probes at 30 °C.....	125
<b>Figure 3.24:</b> Representative gel images of cross-catalytic amplification of <b>F-H-DNA-I</b> with destabilizing probes at 34 °C initiated by different concentration of <b>H-DNA-I</b> .....	126
<b>Figure 3.25:</b> Representative gel images of cross-catalytic amplification of <b>F-DNA-I</b> with destabilizing probes at 30 °C initiated by different concentration of <b>DNA-I</b> .....	127
<b>Figure 3.26:</b> Representative gel images of cross-catalytic amplification of <b>F-H-DNA-I</b> with destabilizing probes at 34 °C initiated by different concentration of <b>H-DNA-I</b> with lower probe concentration.....	128

#### Chapter 4

<b>Figure 4.1:</b> Schematic diagram of mismatch discrimination with T4 DNA ligase in single cycle and PAGE images of ligation with different targets.....	142
<b>Figure 4.2:</b> General scheme for isothermal cross-catalytic amplification of <b>DNA-I(X)</b> using an abasic destabilizing group in an LCR.....	144

<b>Figure 4.3:</b> The kinetics of cross-catalytic amplification of <b>F-DNA-I(T)</b> initiated with different <b>DNA-I(X)</b> targets and the linearity of the product formed with <b>(DNA-I(T))</b> .....	146
<b>Figure 4.4:</b> Representative PAGE image of the cross-catalytic amplification with different concentrations of initial target <b>DNA-I(T)</b> .....	147
<b>Figure 4.5:</b> Discrimination of T-target and A-target in a single-cycle ligation.	148
<b>Figure 4.6:</b> Multiplexed assay in the presence of six probes for discrimination of T-target and A-target.....	150
<b>Figure 4.7:</b> Cross-catalytic amplification with separate sets of probes for discrimination of T-target and A-target.....	152
<b>Figure 4.8:</b> Discrimination of T-target and G-target in a single-cycle ligation.	154
<b>Figure 4.9:</b> Multiplexed assay in the presence of six probes for discrimination of T-target and G-target.....	155
<b>Figure 4.10:</b> Cross-catalytic amplification with separate sets of probes for discrimination of T-target and G-target.....	156
<b>Figure 4.11:</b> Normalized excitation and emission spectra of the fluorescein (FAM) and Cy5labeled probes.....	159
<b>Figure 4.12:</b> Fluorescent spectra of the DNA mixture containing different templates (D = T/Ab) in the absence and presence of ligation.....	161
<b>Figure 4.13:</b> Plot of FRET efficiency ( $I_{661}/I_{521}$ ) with respect to time for the single cycle ligation with native and destabilizing templates.....	162
<b>Figure 4.14:</b> Real-time fluorescence spectra of the ligation mixture at different time point from the time of mixing with enzyme.....	163

<b>Figure 4.15:</b> Difference in FRET signal with different mismatches at 30 °C after 35 minutes of mixing.....	164
<b>Figure 4.16:</b> Plot of FRET efficiency with time for cross-catalytic amplification with different targets (match or mismatch) and linearity of FRET efficiency with matched target DNA ( <b>DNA-I(T)</b> ).....	165
<b>Figure 4.17:</b> Formation of NP-aggregate by hybridization of two NPs modified with non-complementary DNA sequences upon addition of the complementary linker DNA.....	168
<b>Figure 4.18:</b> Disassembly of aggregated DNA-linked gold NP by a complementary linker DNA.....	169
<b>Figure 4.19:</b> Thermal denaturation profile of the gold NP–DNA aggregate formed by a linker DNA.....	170
<b>Figure 4.20:</b> Disassembly of aggregated DNA-linked gold NP by different concentration of amplified DNA mixtures demonstrated using a cell phone camera or on a TLC plate.....	171
<b>Figure 4.21:</b> Monitoring the dissociation of the aggregate using UV-vis absorbance spectroscopy.....	173

## Chapter 5

<b>Figure 5.1:</b> Schematic illustration of blunt end, sticky end and pseudo-blunt end systems.....	190
<b>Figure 5.2:</b> Kinetics of cross-catalytic amplification with T7 DNA ligase at 30 °C and 26 °C.....	193

<b>Figure 5.3:</b> PAGE images of single cycle ligation with different templates and probes at different temperatures.....	195
<b>Figure 5.4:</b> Cross-catalytic amplification with T7 DNA ligase with different concentration of PEG in the buffer at 26 °C.....	197
<b>Figure 5.5:</b> Cross-catalytic amplification with T7 DNA ligase at different temperatures in PEG free buffer.....	198
<b>Figure 5.6:</b> Kinetics of cross-catalysis with <i>E. coli</i> DNA ligase at different temperatures.....	200
<b>Figure 5.7:</b> Kinetics of cross-catalysis with <i>E. coli</i> ligase with different concentration of target DNA at 30 °C. ....	200
<b>Figure 5.8:</b> Kinetics of cross-catalysis with T3 DNA ligase at different temperatures.....	201
<b>Figure 5.9:</b> Cross-catalytic amplification with different blunt-end system at 30 °C with T7 and <i>E. coli</i> DNA ligase.....	203
<b>Figure 5.10:</b> Ligation with different single cycle system with different ligases at 25°C.....	206
<b>Figure 5.11:</b> PAGE images of cross-catalytic amplification with different buffers containing different amount of ATP and spermidine.....	208
<b>Figure 5.12:</b> Cross-catalytic amplification of different amplification systems DNA-I(Y), Y = A/T/C/G with matched probe set with T4 DNA ligase at 30 °C. ....	210
<b>Figure 5.13:</b> Single cycle ligation with different nicked duplexes corresponding to DNA-I(Y), Y = A/T/C/G systems at 30°C.....	212

<b>Figure 5.14:</b> Thermal denaturation (melting) profiles of different DNA duplexes (DNA-IIAb:DNA-I(Y)).....	213
<b>Figure 5.15:</b> Cross-catalytic amplification with DNA-I(C) system at different temperatures with T4 DNA ligase.....	214
<b>Figure 5.16:</b> Cross-catalytic amplification with different templates with probe set matching with DNA-I(A) at 30 °C with T4 DNA ligase.....	214

## Chapter 6

<b>Figure 6.1:</b> Schematic representation isothermal LDR-PCR amplification.....	230
<b>Figure 6.2:</b> Schematic representation isothermal lesion-induced amplification of a longer target.....	231
<b>Figure 6.3:</b> DNA sequences used in LIDA of a longer target.....	231
<b>Figure 6.4:</b> PAGE image of cross-catalytic amplification with 14 nM 27-nt long target at 37°C.....	232

## List of Symbols / Abbreviations

Ab	Abasic
cB	<i>cis</i> -butenyl
CEU	Cohesive end units
Bu	Butyl
DMT	Dimethoxytrityl
DNA	Deoxyribonucleic acid
DCM	Dichloromethane
dsDNA	Double stranded deoxyribonucleic acid
$\epsilon$	Molar extinction coefficient
<i>E. coli</i>	<i>Escherichia coli</i>
EDC	1-ethyl-3-(3-dimethylaminopropyl)carbodiimide
EDTA	Ethylenediaminetetraacetic acid
ELISA	Enzyme-linked immunosorbent assay
Et	Ethyl
EXPAR	Exponential amplification reaction
FAM	Fluorescein
fM	Femtomolar
FRET	Fluorescence (or Förster) resonance energy transfer
HCA	Hybrid capture assay
HDA	Helicase dependent isothermal amplification
$\lambda$	Wavelength

LAMP	Loop-mediated isothermal amplification
LCR	Ligase chain reaction
LDR	Ligase detection reaction
LIDA	Lesion induced isothermal amplification
MB	Molecular beacons
$\mu\text{M}$	Micromolar
MALDI-TOF	Matrix-assisted laser desorption/ionization -time-of-flight
NASBA	Nucleic acid sequence-based amplification
nM	Nanomolar
NMR	Nuclear magnetic resonance
NP	Nanoparticle
PCR	Polymerase chain reaction
PAGE	Polyacrylamide gel electrophoresis
PBS	Phosphate buffered saline
PLA	Proximity ligation assay
pM	Picomolar
POC	Point-of-care
RCA	Rolling circle amplification
RNA	Ribonucleic acid
SDA	Strand displacement amplification
SMP2	Smart amplification process version 2
SNP	Single nucleotide polymorphism

SPREAD	Surface promoted replication and exponential amplification of DNA analogues
SSB	Single strand binding proteins
ssDNA	Single stranded deoxyribonucleic acid
SPR	Surface plasmon resonance
TAMRA	Carboxytetramethylrhodamine
THF	Tetrahydrofuran
TLC	Thin layer chromatography
$T_m$	Melting temperature
TON	Turnover number
UV-vis	Ultraviolet-visible
Xy	Xylyl



# **Chapter 1**

## **General Introduction**

## **1.1 Infectious disease diagnostics**

Infectious diseases are caused by the invasion of various pathogenic microorganisms such as bacteria, viruses, parasites, fungi, and prions to the host (human, animal, plant or another microorganism) through different pathways.<sup>1-7</sup> In developing countries, as a result of different initiatives taken by several government and non-government organizations, access to drugs for most of the commonly occurring diseases has improved remarkably over the past decades.<sup>8</sup> The need for accurate diagnostics of disease, however, remains as a major obstacle to disease control in the developing world.<sup>8,9</sup> Current diagnostic tools use complex and expensive processes designed for industrialized countries that are often not suitable for developing countries. Moreover, many of these diagnostic methods need to be performed in a central laboratory, so these methods are not applicable in areas with limited resources. Therefore, it is highly desirable to develop simple, rapid point-of-care (POC) testing devices to reduce the global burden of infectious diseases.<sup>10,11</sup>

## **1.2 Diagnostic methods**

Pathogen diagnostic methods can be divided into three main categories: i) culture and colony based methods, ii) immunological methods, and iii) nucleic acid based diagnostics.

### **1.2.1 Culture and colony based methods**

Culture and colony based diagnostics are the gold standard for detection of the majority of microorganisms. This approach requires a variety of

microbiological laboratory techniques such as microbial growth, visualization, and quantification.<sup>12, 13</sup> These diagnostics identify the microorganisms by growing them in a selective microbiological media to detect and quantify viable cells in the sample. Even though the culture based methods are considered to be accurate, sensitive and inexpensive, the media preparation, colony counting, characterization and quantification make this method time-consuming and very labor intensive. In addition, only a few percent (~1%) of all bacteria are cultureable.<sup>14</sup> Therefore, it is necessary for the laboratories, clinical diagnostics, and food industries to develop alternative detection methods that are rapid, sensitive, and accurate.

### **1.2.2 Immunological methods**

Immunological methods are antibody based methods, which have been used for detection of different targets including bacteria, viruses, and their products (antigen and toxins).<sup>15</sup> These methods rely on the ability of an antibody to bind specifically to an antigen, which is unique to a particular microbial group.<sup>16</sup> In addition to binding, another key feature of this assay is the ability to generate measurable signal upon binding. Immunoassays can be generally classified as homogenous assays or heterogeneous assays. In homogenous assays, it is not necessary to separate the bound and unbound antibodies. This assay is performed in the liquid phase and the antigen-antibody complexes usually show visible or measurable change.<sup>17</sup> Examples of homogeneous assays are agglutination reactions, immunodiffusion, and turbidimetry. In heterogeneous

assays, there are multiple washing steps to separate unbound antibody from the bound antibody.<sup>17</sup>

Enzyme-linked immunosorbent assay (ELISA), a heterogeneous assay, is currently the most commonly used antibody based assay for pathogen detection.<sup>18</sup> There are several variants of ELISA like direct ELISA, sandwich ELISA and competitive ELISA. Among these different types of ELISA assays, the “sandwich ELISA” is the most prevalent one. Sandwich ELISA is used to detect sample antigen, which is a biomarker for the agent of disease. In this assay, an antibody is immobilized on a solid surface to capture the specific antigen to be detected (Figure 1.1).<sup>19, 20</sup> Then the sample containing the antigen is applied to the surface; after waiting for a certain period, the surface is washed to remove unbound antigen. Then a secondary antibody (Detection antibody) is added to bind to the captured antigen followed by addition of the enzyme-linked secondary antibody, which will bind non-specifically to the detection antibody. Finally, the enzyme substrate is added to produce color, fluorescence, or an electrochemical signal, indicating the presence or absence of the target in the original sample. One advantage of this approach is that the signal intensity is proportional to the concentration of the target antigen present in the sample.<sup>19, 21</sup> However, due to the requirement of multiple washing and incubation steps, ELISA and other heterogeneous methods are very time consuming.<sup>22</sup> Moreover, this method requires bulky instruments which limits its application as point-of-care diagnostics.

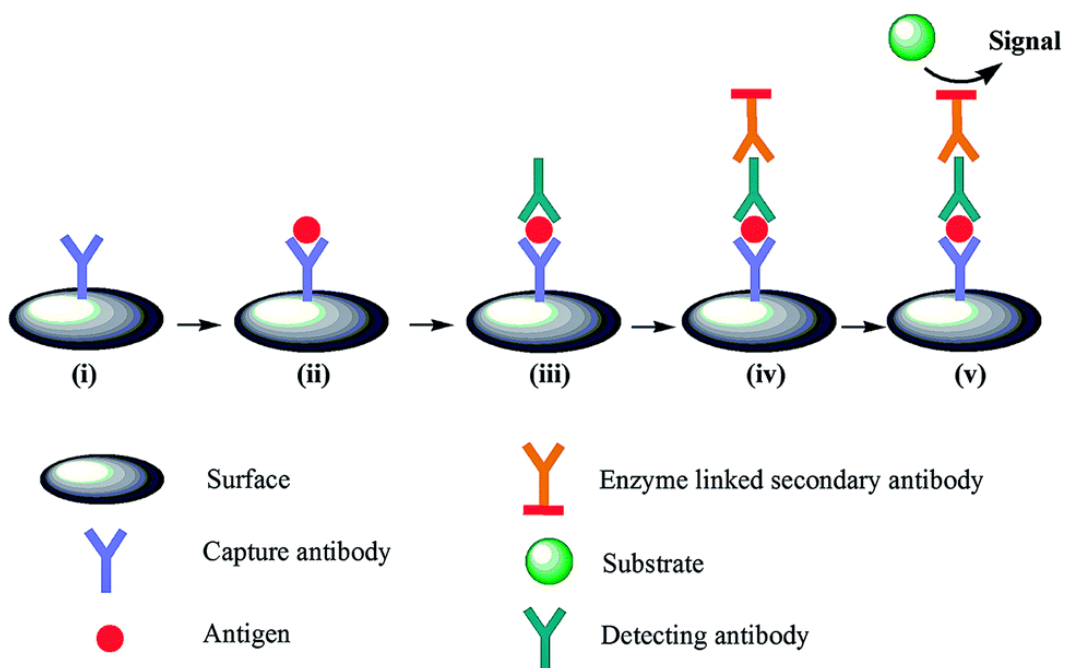


**Figure 1.1** Stepwise scheme of a sandwich ELISA assay. The basic steps are i) immobilization of the capture antibody; ii) introduction of sample containing the target antigen, which will bind to the immobilized antibodies; iii) addition of a secondary antibody (Detection antibody) to bind to the captured antigen iv) addition of the enzyme-linked secondary antibody, that will bind non-specifically to the detection antibody; and v) addition of the enzyme substrate followed by detection. Rinsing is required after each step. Image reproduced with permission from ref. 20. Copyright © 2014 The Royal Society of Chemistry.

### 1.2.3 Nucleic acid based diagnostics

Recently, there has been a lot of focus on developing simple nucleic acid based diagnostics.<sup>23, 24</sup> The basic principal of nucleic acid diagnostics relies on the ability of a nucleic acid strand to bind to the complementary unique sequence of a particular microorganism. As such, nucleic acid based technologies offer sensitive and specific detection and the ability to analyze multiple samples at a time.<sup>25</sup> However, most of the techniques are confined to centralized laboratories and very

few of these methods have been applied in clinical environments.<sup>26, 27</sup> To develop a nucleic acid based diagnostic for use in an area with limited resources, it is important to develop a simple, cheap and portable detection platform. The four basic steps for nucleic acid diagnostics are sample preparation, nucleic acid extraction, amplification of the target sequence, which will be discussed in greater detail below, and detection of the amplified target. Combining the basic steps for nucleic acid diagnostics into one step would be ideal for the development of point-of-care diagnostic systems.<sup>28</sup> Several efforts have been reported to detect antigen or nucleic acids by combining antigen-antibody interactions with nucleic acid amplification: proximity ligation assay (PLA) and hybridization (Hybrid capture assay (HCA) are two examples.<sup>29-31</sup> In PLA, antibodies are modified with nucleic acid strands. The antibody-antigen binding brings these nucleic acid strands close together allowing their ligation followed by amplification of the ligated strand sequence, enabling detection of the antigen.<sup>29, 30</sup> In the HCA method, a DNA sequence associated with the disease as the biomarker is detected; here an RNA probe is used to hybridize with the denatured single-stranded DNA (ssDNA) target. This DNA-RNA hybrid can then specifically bind to an antibody immobilized on the well of a microtiter plate. A second antibody labelled with an enzyme can bind to the hybrid, which yields a colorimetric signal when the substrate is added.<sup>31</sup>

### **1.3 Nucleic acid amplification methods**

Although there are several reports of the direct detection of nucleic acid without amplification, the level of sensitivity obtained using these methods is very low with few exceptions like the bio-barcode gold-nanoparticle based DNA detection reported by the Mirkin group<sup>32</sup> and electrochemical detection using a neutralizer displacement assay by the Kelly group.<sup>33, 34</sup> In general, with current detection technologies it is important to use some form of signal or target amplification to detect the small amount of nucleic acid corresponding to the agent of disease. Nucleic acid amplification techniques can be divided in to two broad classes: i) amplification with thermocycling and ii) isothermal amplification.

#### **1.3.1 Amplification with thermocycling**

In nucleic acid amplification with thermocycling, the sample has to be heated and cooled repeatedly to complete one of the basic cycles of amplification. For this reason, thermal amplification of nucleic acids requires a thermostable enzyme which can withstand the effect of repeated heating and cooling. The polymerase chain reaction (PCR) and ligase chain reaction (LCR) are two examples of temperature-variable nucleic acid amplification.

##### **1.3.1.1 Polymerase Chain Reaction**

The polymerase chain reaction (PCR) is the most widely used method for DNA amplification.<sup>35</sup> Using PCR a single or few copies of DNA can be amplified to many copies of a specific DNA sequence. PCR assays have a wide range of

clinical applications including pathogen detection, gene sequencing, monitoring gene expression, cloning, early detection of bio-threat agents, antimicrobial resistance profiling and many other applications.<sup>36, 37</sup> Target selective amplification is achieved with a pair of DNA strands complementary to the sense and antisense part of the target DNA, which are called primers. Basic PCR consists of three steps: thermal denaturation of the target genomic DNA duplex; annealing of a primer sequence that is complementary to part of the target sequence; and extension of the annealed primer by DNA polymerase (Figure 1.2). This three-step cycle is then repeated many times, each time almost doubling the product molecules. The amplification factor is given by the equation  $n(1+E)^x$ , where  $n$  is the number of initial target strands,  $E$  is the amplification efficiency and  $x$  is the number of PCR cycles.<sup>38</sup> The idea of DNA amplification using polymerase was first introduced by Khorana and co-workers in 1971.<sup>39</sup> The discovery of Taq DNA polymerase - a DNA polymerase derived from *Thermus Aquaticus* - paved the way for PCR by Kary Mullis in 1983. Using Taq DNA polymerase, it was possible to run PCR at higher temperatures, which significantly improved the specificity and rate, while allowing for amplification of longer target sequences.<sup>40-42</sup> Subsequently, various DNA polymerases have been isolated from different species with different extension rates, strand displacement capabilities, proofreading abilities, processivity and fidelity.<sup>43</sup> Processivity is the ability of the enzyme to function repeatedly without dissociating from the substrate (i.e., the primer:target complex); for DNA polymerase, the processivity is quantified as the number of bases added each time the polymerase binds to the



target. The fidelity is the measurement of how error prone a DNA polymerase is and is quantified by the ratio of the right base vs. wrong base incorporation, when both of the nucleotides are present in equal concentrations to compete for the same site.

There are several different variants of PCR techniques, which are designed for specific needs. Hot-Start PCR significantly suppresses non-specific priming and results in sensitive amplification with higher yield.<sup>44, 45</sup> This is done either by heating the reaction mixture before adding the DNA polymerase or by using a specialized enzyme that has been designed such that the polymerase activity is inhibited at room temperature by binding the polymerase with an antibody or other inhibitor which dissociates only at higher temperature.<sup>46-48</sup> There are other techniques that are designed to reduce nonspecific background: these are i) nested PCR, where two sets of PCR primers (an inner primer and outer primer) are used in two successive PCR amplifications,<sup>49</sup> and ii) touchdown PCR, where the annealing temperature is slowly decreased as the PCR cycling progresses. In touchdown PCR, a higher annealing temperature in the initial cycles gives better specificity for primer binding whereas a lower temperature in the later cycles allows faster amplification of specific products formed in the initial cycles.<sup>50</sup> Allele-specific PCR is an application of PCR which detects point mutations in the target DNA. This method relies on the fact that a mismatch between the 3'-end of the primer and the target lowers the rate of amplification.<sup>51</sup> In asymmetric PCR, one of the primers is used in large excess so that the final product predominately yields single-stranded amplicons (product of amplification).<sup>52</sup> This method is

suitable for sequencing where the presence of only one of the strands in the solution is required.<sup>53</sup>

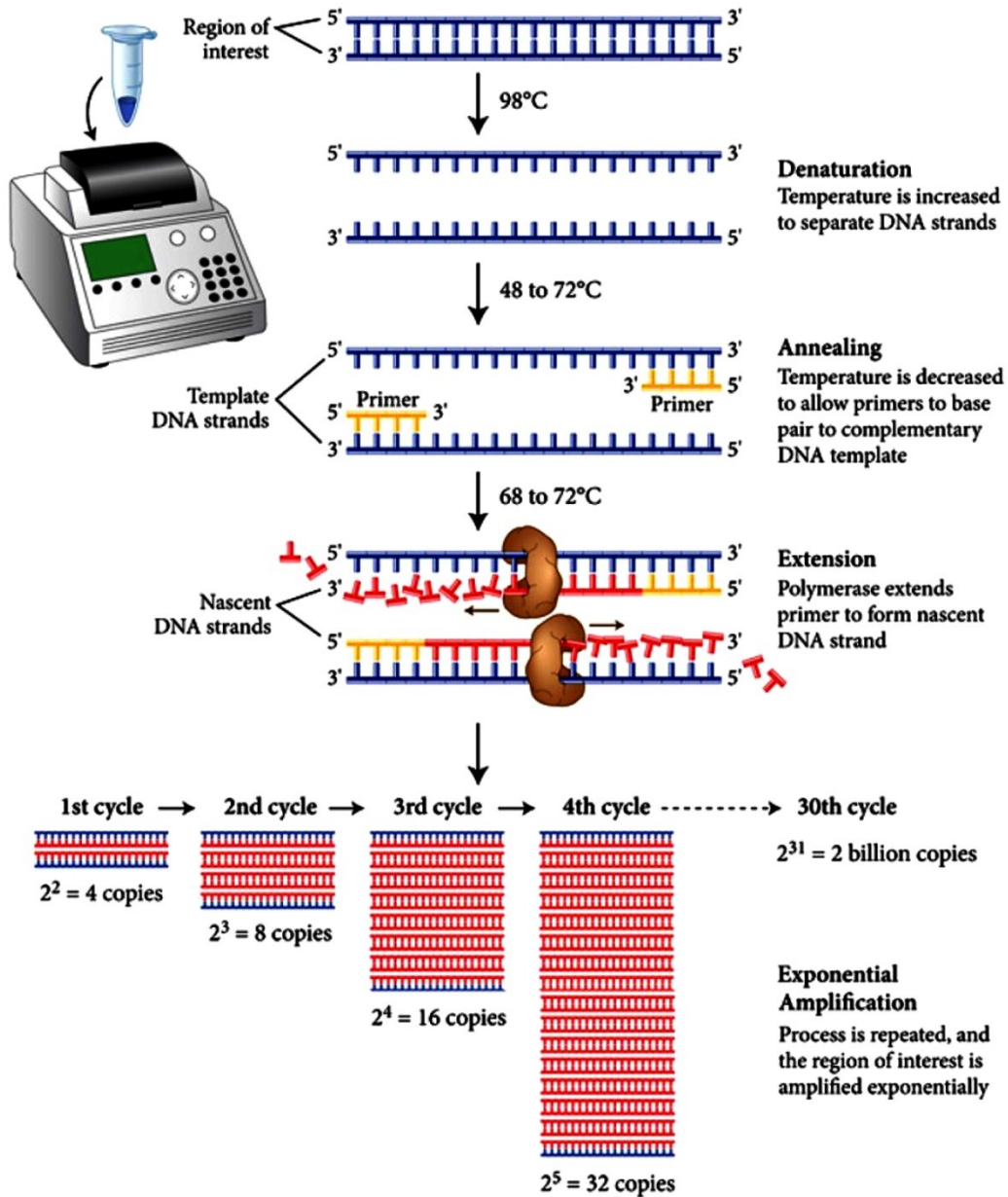


**Figure 1.2:** Schematic representation of the PCR reaction. After denaturation of the target, the primers can bind and polymerase can extend the primers, this cycle is repeated many times to give exponential amplification of the target sequence. Reprinted from [www.neb.com](http://www.neb.com) (2014) with permission from New England Biolabs.

Real-time PCR is a quantitative PCR technique, where the amount of amplified DNA is measured at each cycle throughout the PCR process.<sup>54</sup> This process is different from standard (endpoint) PCR where the amplified product is detected and quantified at the end of the amplification process. The main advantage of real-time PCR is the ability to measure the amount of amplicon in each cycle, which allows one to quantify the amount of starting material in the sample. An additional advantage of real-time PCR is that it uses an integrated system for simultaneous amplification and detection of target, where there is no need for further downstream analysis. Two common methods of detecting product in real-time PCR are i) a general method, where a nonspecific fluorescent dye intercalates with any double-stranded DNA (dsDNA) present in the PCR mixture and ii) a strand-specific method that uses an oligonucleotide primer complementary to the amplicon sequence. In the general detection assays, fluorescent signals generated by the dsDNA intercalating dyes (ethidium bromide or SYBR Green) are proportional to the amount of amplicon formed in each cycle (Figure 1.3A).<sup>55</sup> Strand-specific methods use fluorophore-coupled oligonucleotide probes to hybridize with the complementary amplified product, offering more specificity than the general assay. However the signal originates from the presence of the complementary probes rather than the amplicon itself. Therefore, the hybridization efficiency of the probe is very important to produce a signal that is correlated with the concentration of amplicon in the exponential stage of amplification as that is ultimately used to determine the number of initial target copies. A number of fluorescent reporter probes have been developed, including

hybridization probes, molecular beacons (MB) (Figure 1.3B), TaqMan probes (Figure 1.3C), Sunrise probes, Scorpion primers, and Light-up probes, which are amenable to real-time detection.<sup>56</sup>

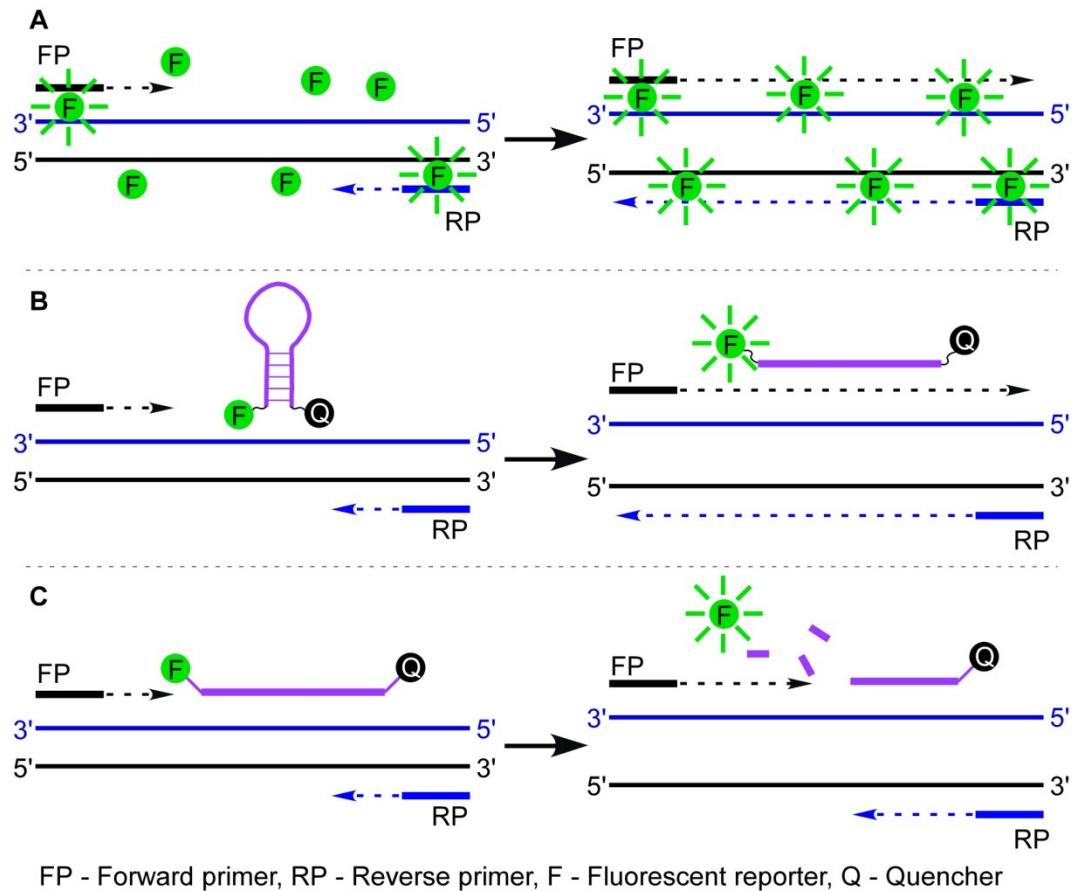


**Figure 1.3:** Schematic diagram of different types of real-time PCR techniques with A) an intercalating dye, which becomes fluorescent when bound to the duplex formed during PCR; B) a molecular beacon, which opens up when hybridized to the amplicon separating the fluorescent group from the quencher; C) a Taqman probe similar to a molecular beacon, where the probe hybridizes to an amplicon downstream from a primer. As the polymerase extends the primer, the probes get chopped up generating fluorescent signal. This figure is adapted and modified from ref. 56. Copyright © 2003 WILEY-VCH Verlag GmbH & Co. KGaA, Weinheim.

In addition to the different PCR methods described above, digital PCR is another new refinement of conventional PCR which can be used to quantify the initial amount of a nucleic acid biomarker in a sample.<sup>57</sup> In digital PCR, reactions are partitioned into many picoliter-sized compartments through dilutions and amplified by PCR. The purpose for dilution of the sample is to have either 0 or 1 target molecule in each compartment. After thermal cycling and data acquisition, the statistical analysis of positive and negative mini-reactions is used to calculate the absolute number of target molecules present in the original sample. There have been many applications of digital PCR, especially in genetic analysis of cancers.<sup>58</sup> Another approach similar to digital PCR is called BEAMing (beads, emulsion, amplification and magnetics) technology; using this method it is possible to amplify millions of templates individually within a single tube.<sup>59-61</sup> In the BEAMing process, a magnetic bead is coated with one of the primers, then the beads are mixed with the target DNA, the mixture is then emulsified by adding oil and emulsifier such that each of the droplets of water contain either zero or one target DNA and bead. If any droplet contains at least one bead and one target, after amplification it will contain thousands of copies of the original DNA molecule which can be analyzed using flow-cytometry by hybridizing with a fluorescent probe. This technique can be used to quantify the fraction of specific mutation present in a DNA population.<sup>62</sup>

### **1.3.1.2 Ligase Chain Reaction (LCR)**

The ligase chain reaction (LCR) is another technique developed to detect specific nucleic acid targets by amplification of a nucleic acid target sequence.

This technique has been used to identify the presence of specific genetic disorders such as sickle cell disease, which is caused by the presence of point mutations.<sup>63</sup> Moreover, LCR method has been applied in infectious disease detection with special importance to the infection caused by microbes that are difficult to detect by traditional culture techniques.<sup>64</sup>

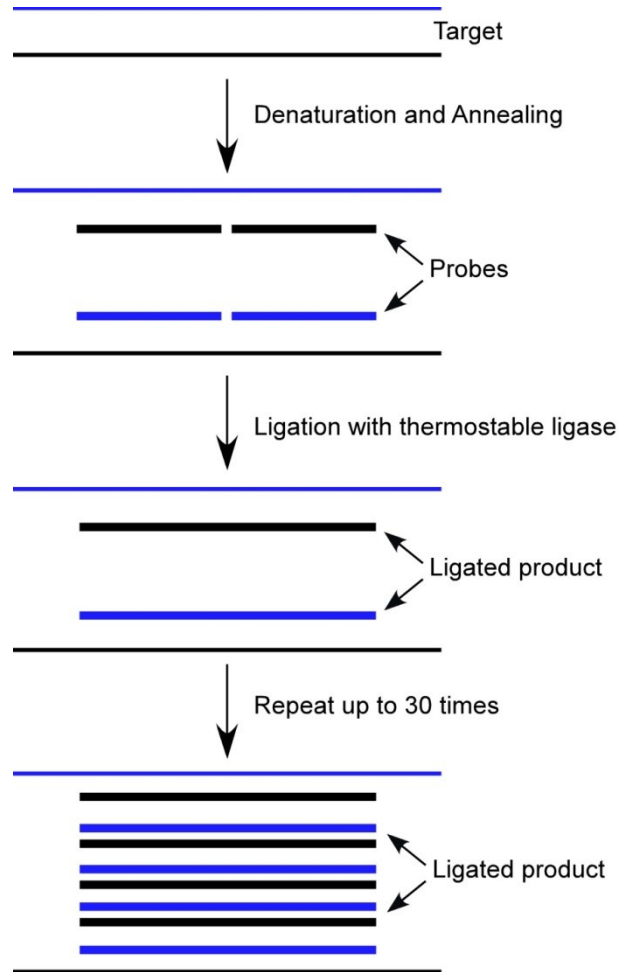


**Figure 1.4:** Schematic representation of the ligase chain reaction (LCR). After denaturation and annealing, the probes will be ligated by a thermostable ligase; this process is repeated many times to achieve exponential amplification. This figure is adapted and modified with permission from ref. 65. Copyright © 1991 National Academy of Sciences.

In typical LCR assays, a thermostable DNA ligase is used to ligate two adjacent probes hybridized to the target DNA strand.<sup>66-69</sup> The first example of ligation of two polynucleotide probes hybridized to a complementary target strand was reported by Besmer et al. in 1972.<sup>70</sup> The first report of using the ligation of oligonucleotide probes to determine sequence variation was reported in 1988.<sup>67,71</sup> Finally, the first example of LCR with cyclic denaturation, hybridization and ligation of two sets of DNA probes was reported in 1989 with the requirement of adding fresh ligase for each cycle.<sup>72</sup> In 1991, Barany used a thermostable DNA ligase eliminating the need for adding fresh ligase after each denaturation step.<sup>65</sup>

Simple LCR involves two pairs of oligonucleotide probes that are complementary to both the sense and the corresponding anti-sense sequence of the target DNA, in contrast to basic PCR where only two oligonucleotide primer sequences are used (Figure 1.4). For LCR, a probe pair consists of two strands, each 25-35 nucleotides long, that are complementary to adjacent sequences on the target and can only be ligated if hybridized to the target. The new oligonucleotide strands formed after ligation become target strands in the subsequent cycles as probes for both the sense and anti-sense sequence of the target are present. Ligase-based amplification systems have some advantages over polymerase-based amplification. Since there is no newly synthesized DNA from single nucleotide building blocks as in PCR, misincorporation of nucleotides is not possible in LCR. Additionally, the LCR reaction is very specific for the 3'-nucleotide, which also allows for higher discriminatory power against mismatches at the 3'-end of

the ligation site.<sup>65, 73</sup> Thus, LCR is very powerful for detecting the identity of a nucleotide at a specific site such as a single-nucleotide polymorphism (SNP).

One drawback of the LCR process is that the probes that are complementary to the corresponding sense and anti-sense target sequences are also complementary to each other. Consequently, the probe pairs can hybridize to each other, which can result in blunt end ligation forming a copy of the target sequence even if there is no target present in the original sample. There are several modifications in the regular LCR process to overcome this inherent problem. For example, the ligase detection reaction (LDR) has been combined with PCR to generate a dual PCR-LDR approach. LDR utilizes only one set of adjacent probes instead of two sets of probes as in LCR, which avoids the problem of blunt-end ligation of the LCR probes.<sup>74-76</sup> In PCR-LDR, the target-induced ligation product is then amplified by PCR using outside primers. Due to the absence of double-stranded probes in PCR-LDR, the background is very low.<sup>74</sup> In Gap LCR, the probes are designed such that a few-base gap results between the two probe oligonucleotides after hybridization to the target. A thermostable polymerase then fills the gap before the ligation of the probes can happen by ligase. As the two pairs of probes do not form blunt duplexes, Gap LCR approach yields more specific detection.<sup>77, 78</sup>



### **1.3.2 Isothermal amplification**

As I discussed earlier, even though PCR and LCR are widely used for different applications, these techniques require thermocycling to denature the product duplex formed after primer extension or probe ligation, respectively. Therefore, these techniques have limited application for use directly at the point-of-care or in resource limited settings. In order to develop a simplified point-of-care diagnostic, several DNA target amplification methods have been developed in the past decades that do not require a thermal cycler. For example, DNA polymerases with strand displacement activity have the ability to displace downstream DNA strands from a duplex during extension, which is the key strategy in many isothermal amplification techniques.<sup>79, 80</sup> Other techniques mimic the natural DNA replication process in vitro such as using the helicase enzyme to unwind duplex DNA in helicase dependent amplification (HDA).

#### **1.3.2.1 Strand displacement amplification (SDA)**

SDA utilizes the strand displacement activity of DNA polymerase to displace downstream DNA strand.<sup>79, 80</sup> After initial heating to denature the DNA target duplex, the primer can bind to the target allowing the subsequent amplification process to be conducted isothermally. SDA involves two sets of target specific outer and inner primers, where the outer primers displace the strands synthesized by the inner primers. The inner primers are designed such that they contain a restriction site as well as a sequence that is complementary to the nucleic acid biomarker. The first step of the amplification process is referred to as the target generation step, where the copy of the target to be amplified is made.<sup>81</sup>

Since the inner primer has a restriction site which gets incorporated in the newly generated target, this target enters into a cyclic phase where nicking, primer binding and extension can occur isothermally resulting in exponential growth. Although this isothermal amplification technique offers several benefits with a relatively simple enzyme system, the main disadvantages are the inability to amplify long target sequences and the requirement of a low operating temperature, which results in high background signal.<sup>82</sup>

### **1.3.2.2 Rolling circle amplification (RCA)**

RCA is an isothermal DNA amplification method, which can rapidly create multiple complementary copies of a circular nucleic acid template such as a plasmid (Figure 1.5).<sup>83, 84</sup> In contrast to SDA, where one copy of the template is produced in one cycle, RCA gives tandem-repeat complementary copies of the template as long the polymerase remains on the same circular template.<sup>83, 84</sup> The phi29 DNA polymerase is preferred for RCA because of its high processivity, fidelity and strong strand displacement ability.<sup>85</sup> As strand displacement in RCA requires a circular single stranded template it is therefore unsuitable for detecting a linear target. To avoid this limitation, researchers have developed a padlock probe which becomes circularized in the presence of a linear nucleic acid target followed by RCA.<sup>86, 87</sup>

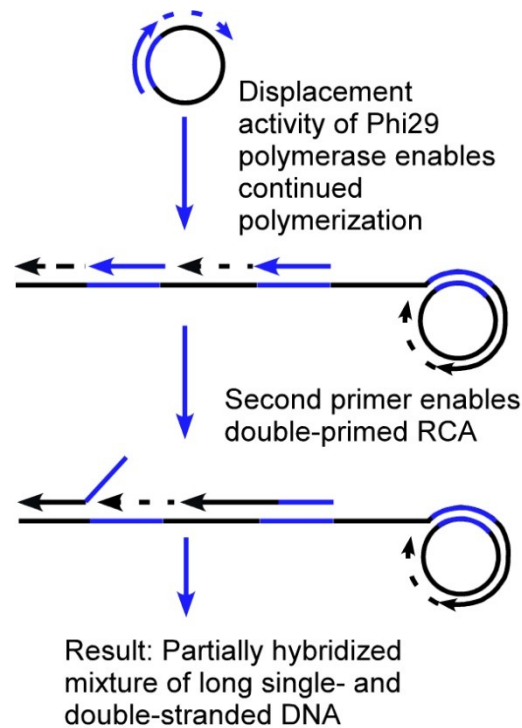


**Figure 1.5:** Schematic representation of rolling circle amplification (RCA). The primer can extend along the circular DNA template. After one complete cycle, the polymerase can displace the growing strand. This process can be repeated many times to give a tandem repeat of the same sequence in the amplified product. Image reproduced with permission from ref. 88. Copyright © 2013 The Royal Society of Chemistry.

### 1.3.2.3 Helicase-dependent isothermal amplification (HDA)

Instead of thermocycling as in regular PCR, the helicase-dependent amplification (HDA) procedure uses the unwinding ability of the enzyme helicase to denature the DNA duplex (Figure 1.6).<sup>89, 90</sup> This enzyme is utilized by the cell in DNA replication, prior to cell division in order to separate the genomic DNA strands, so that the primers can bind to the single stranded DNA allowing the DNA polymerase to start copying the genomic sequence. In HDA, after the helicase enzyme unwinds the target DNA duplex, the strands are kept separated

with the help of single strand binding proteins (SSB). The primers then hybridize and are extended by polymerase, followed by helicase unwinding of the resulting product duplex; the cycle continues yielding exponential amplification of the target sequence. Owing to its isothermal requirements, the HDA technology is being used for a simple and user-friendly nucleic acid test for the detection of *Clostridium difficile* bacteria, which causes an infectious diarrhea commonly associated with people with prior antibiotic therapy.<sup>91</sup>

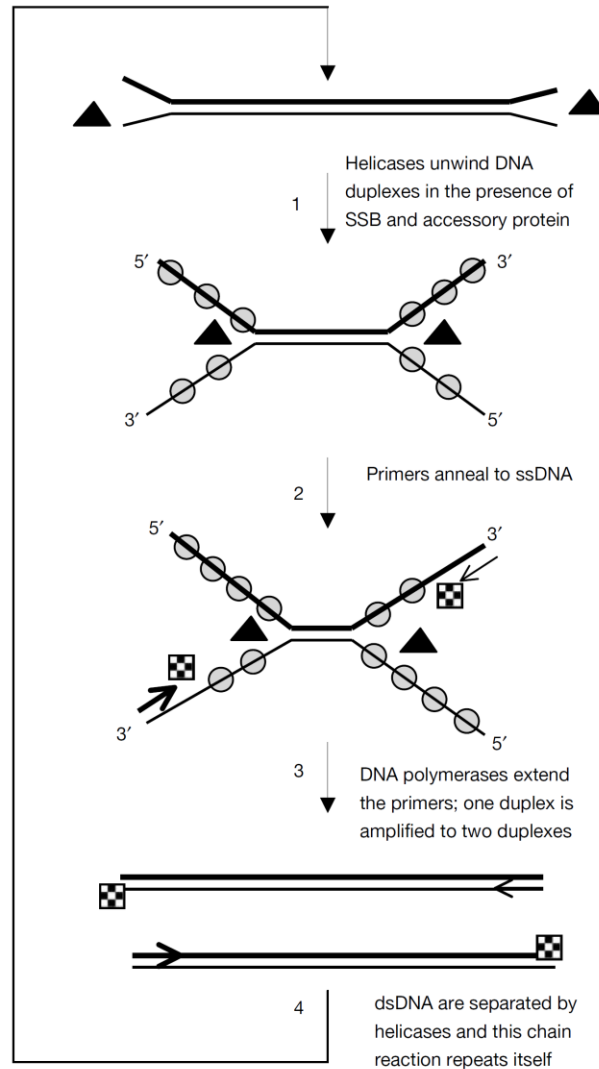


**Figure 1.6:** Schematic representation of helicase dependent amplification (HDA). Instead of thermocycling, the target DNA strands (thick line and thin lines) are separated by the helicase enzyme (black triangle) to allow the primers (lines with arrow head) to bind to the template. Single strand binding (SSB, grey circle) protein help stabilize the denatured DNA strands. The polymerase (mosaic square) now can extend the primers yielding isothermal amplification. Image reproduced with permission from ref. 90. Copyright © 2004 European Molecular Biology Organization.

#### **1.3.2.4 Nucleic acid sequence-based amplification (NASBA)**

Nucleic acid sequence-based amplification (NASBA) is an isothermal, transcription-mediated amplification system designed for the detection of RNA targets.<sup>92</sup> The unique characteristic of this method is the ability to detect single stranded RNA targets instead of duplex DNA (Figure 1.7). In addition, most DNA amplification methods produce double-stranded DNA (with the exception of RCA) whereas NASBA generates single-stranded products that are capable of hybridizing complementary strands for capture or downstream analysis. The enzymes used for this amplification process are reverse transcriptase, RNase H, and a DNA dependent RNA polymerase. A key feature of this process is the ability of RNase to hydrolyze the RNA strand in RNA:DNA heteroduplexes, which eliminates the need for denaturing the product complex by thermocycling. As described in Figure 1.7, the NASBA amplification process has two phases, a non-cyclic phase and cyclic phase. At first, in the non-cyclic phase, a DNA primer with a promoter sequence in the 5'-end (primer 1) hybridizes to the target RNA and is extended by an enzyme (reverse transcriptase (RT)) to form an RNA:DNA hybrid.<sup>92</sup> The RNA in the duplex is then cleaved by RNase, which leads to dissociation of the single-stranded DNA product (DNA(-)). This DNA binds with another primer (primer 2) to be extended by the RT enzyme giving a dsDNA product. Using this dsDNA, T7 RNA polymerase can form a single stranded RNA (RNA(-)) which now enters into the cyclic process of primer binding, RT extension, RNase cleavage, primer binding, RT extension and formation of single



(GAGTCNNNN<sup>^</sup>N) for N.BstNB restriction enzyme. In the first stage of amplification a short oligonucleotide trigger (X) is generated from genomic DNA target by the restriction enzyme. The template X'-X' contains the two copies of complementary sequence for the trigger (X') separated by the complementary sequence of cleavage site for the restriction enzyme. After trigger X binds to X'-X', a DNA polymerase will extend it to make a copy of the trigger X.<sup>94, 95</sup> After nicking the X-X product, the remaining part of the duplex will be extended by polymerase to replace the missing fragment, while the newly formed fragment (trigger X) activates hybridizing with other X'-X' templates for further amplification. In addition to the methods described above, isothermal amplification can also be achieved by an efficient primer designs with only one enzyme, DNA polymerase, as will be shown below.

#### **1.3.2.6 Loop-mediated isothermal amplification**

During the last decade, loop-mediated isothermal amplification, or LAMP, has been widely used for the rapid and simple detection of pathogenic microorganisms and several other diseases.<sup>96</sup> This method requires a DNA polymerase and four primers (F1C-F2, F3, B1-B2c, B3c) that recognize a total of six different regions on the target DNA (Figure 1.8).<sup>97</sup> At first, the inner primer (F1C-F2) recognizes part of both the sense and antisense sequence of the target DNA to initiate the LAMP process. The outer primer (F3) then displaces the single stranded inner primer extension product owing to the strand displacement ability of the DNA polymerase. After displacement of the extended F1C-F2 strand a loop forms owing to the F1c sequence originally on the F1c-F2 primer and the



F1 region that formed during primer extension. This new DNA strand acts as a template for DNA synthesis with another set of outer and inner primers (B1-B2c, B3c) that is hybridized to the other end of the template, leading to the formation of a dumb-bell shaped structure. The primers can bind to the single stranded part of the loop and continue amplification isothermally. The final amplification products adopt cauliflower like structures with multiple stem-loop DNA structures of inverted repeats of the target sequence. The smart amplification process version 2 (SMAP 2) is based on LAMP design to achieve a more rapid and sensitive SNP diagnosis.<sup>98</sup>

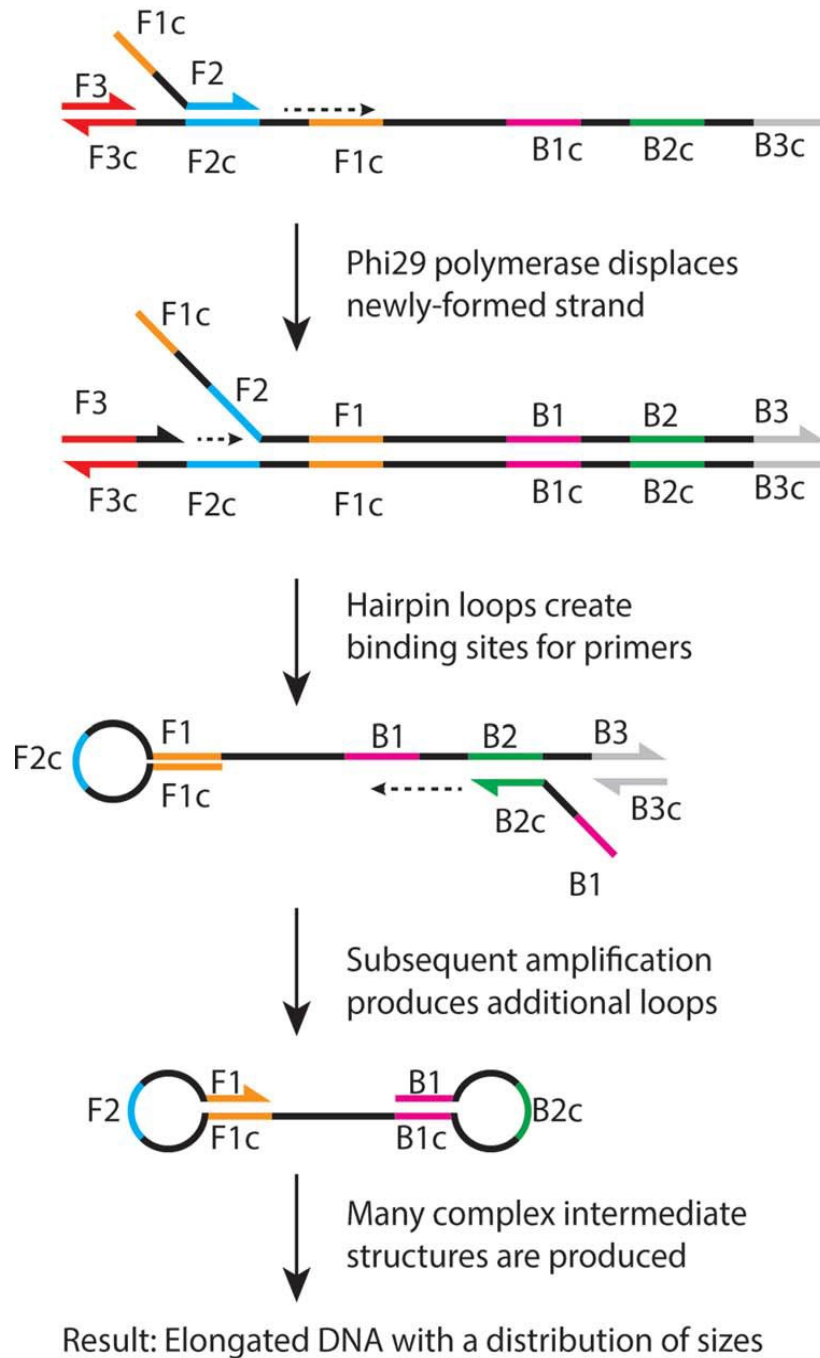


**Figure 1.8:** Schematic representation of the beginning steps of loop-mediated isothermal amplification (LAMP), see text for details. Image reproduced with permission from ref. 88. Copyright © 2013 The Royal Society of Chemistry.

### 1.3.2.7 Isothermal amplification using destabilization approach

Another approach to achieve isothermal amplification has focused on nonenzymatic systems based on peptides, DNA, and RNA.<sup>99-101</sup> Figure 1.9 shows a schematic diagram of an autocatalytic amplification system where the probes **A** and **B** reversibly bind to the template **T** to yield a ternary complex or nicked duplex **M**. The ternary complex **M** facilitates the formation of a bond (ligation) between the probes **A** and **B** by bringing their reactive ends in close proximity, which results in the formation of the **T** sequence. Consequently, the ternary complex **M** irreversibly converts to the duplex **D**. Reversible dissociation of the duplex **D** releases the newly formed template **T** which can act as a template for another cycle of amplification, by hybridization and ligation of another set of probes. The main obstacle of developing isothermal amplification methods with native DNA is that the product duplex **D** formed from the template directed ligation is much more stable than that of the nicked duplex **M**.

Usually thermocycling or mechanical intervention is used to release the template from the product duplex **D**. If the reaction runs isothermally, it will show parabolic growth rather than exponential growth due to product inhibition. Indeed parabolic growth was observed in the nonenzymatic self-replication of nucleic acids developed by von Kiedrowski based on an autocatalytic chemical ligation system.<sup>100</sup> In their ligation system, two protected complementary trideoxynucleotides, one of which contained a 3'-phosphate group, were ligated in the presence of 1-ethyl-3-(3-dimethylaminopropyl)carbodiimide (**EDC**) to yield a self-complementary hexadeoxynucleotide.<sup>100</sup> After dissociation, the product

duplex formed after ligation yielded two templates, which could initiate two new cycles of replication. However, the author found that the initial rate of reaction was proportional to the square root of the initial template concentration, which reflects the influence of product inhibition.<sup>102</sup> Zielinsky and Orgel reported a similar autocatalytic ligation system, where diribonucleotide analogues were ligated in the presence of carbodiimide (EDC) and a self-complementary tetraribonucleotide triphosphoramidate as a template.<sup>103</sup> This amplification system also followed the so-called square root law due to the product inhibition.<sup>103</sup>

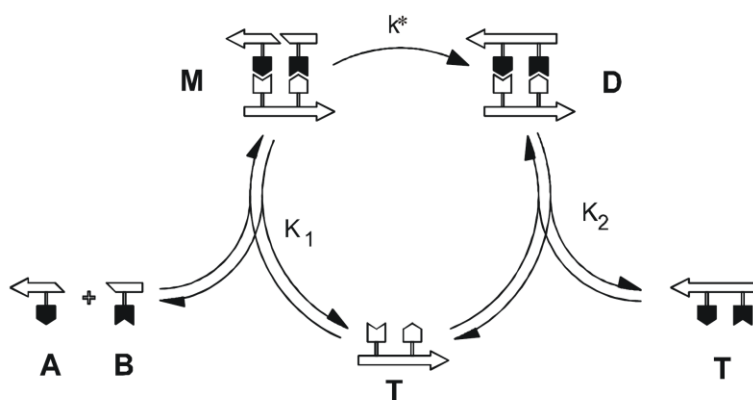


**Figure 1.9:** Schematic diagram of a nucleic acid self-replicating system. Template **T** reversibly binds to the probes **A** and **B** to facilitate the formation of new copy of **T**. Image reproduced with permission from ref. 104. Copyright © 1998 WILEY-VCH Verlag GmbH, Weinheim.

The autocatalytic replication systems are based on self-complementary oligonucleotides, however natural replication systems yield complementary strands instead. Therefore, to observe the replication of a complementary system, cross-catalytic amplification in a nonenzymatic ligation system was attempted, where the product of one cycle is the template for the other cycle.<sup>104</sup> Figure 1.10

shows the schematic diagram of cross-catalysis, where **AA** and **BB** represent the templates; **A**, **A'**, **B**, and **B'** represent the complementary probes.<sup>104</sup> This is identical to the ligase chain reaction described earlier in this chapter except that the probes are ligated by chemical means rather than a ligase enzyme.

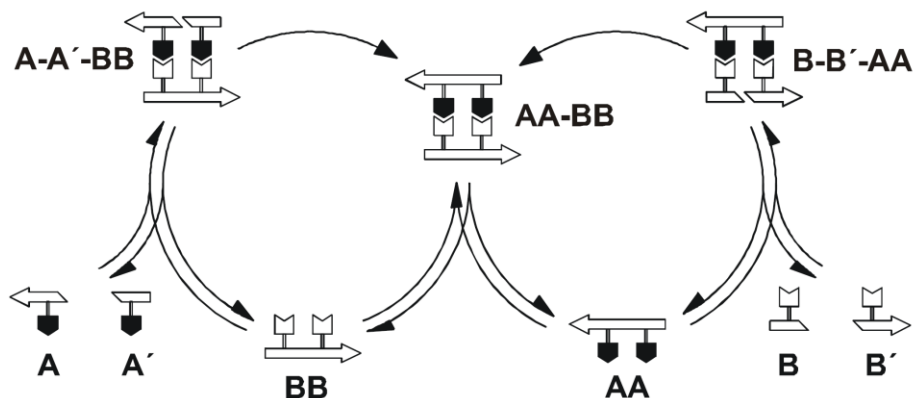


**Figure 1.10:** Schematic diagram of cross-catalytic amplification system. Using a cross-catalytic approach, it is possible to amplify non-self-complementary systems. Here the template **AA** catalyzed the formation of **BB** and vice versa. Image reproduced with permission from ref. 104. Copyright © 1998 WILEY-VCH Verlag GmbH, Weinheim.

In the cross-catalytic system, there are two pathways, both of which ultimately give the same template-product duplex. Since the product of one cycle acts as a catalyst for the other cycle, it is referred to as cross-catalysis. As reported by Kiedrowski and coworkers, the cross-catalytic self-replication of native oligonucleotide systems showed parabolic growth of the product due to product inhibition.<sup>104</sup> So, in order to observe exponential growth rather than parabolic growth the same group reported non-enzymatic exponential amplification of oligonucleotides on a solid support in a stepwise replication procedure called SPREAD (surface promoted replication and exponential amplification of DNA

analogues) (Figure 1.11).<sup>105</sup> The basic steps for SPREAD process are template immobilization on solid support, fragment hybridization, ligation (chemical), product release and re-immobilization to another part of the solid support. Each of the steps are very time-consuming (the ligation step itself was 40 hours long), therefore it is very tedious to study isothermal amplification using this method. Recently, another example of an isothermal non-enzymatic self-replicating system was reported by Lincoln and Joyce, where a catalytic 100-base RNAzyme system exhibited sigmoidal replication.<sup>106</sup> The authors found that a mismatched wobble pair between the RNAzyme and the RNA probes destabilized the product complex after RNA probe ligation, which allowed for sigmoidal amplification with a doubling rate of once per hour.<sup>106</sup> However, for this ligation chain reaction to operate a majority of the sequence had to be conserved to maintain the catalytic properties necessary for ligation. That means their amplification system is not very general. Therefore, this kind of amplification system may not be useful as a general method for detection of specific nucleic acid sequences.

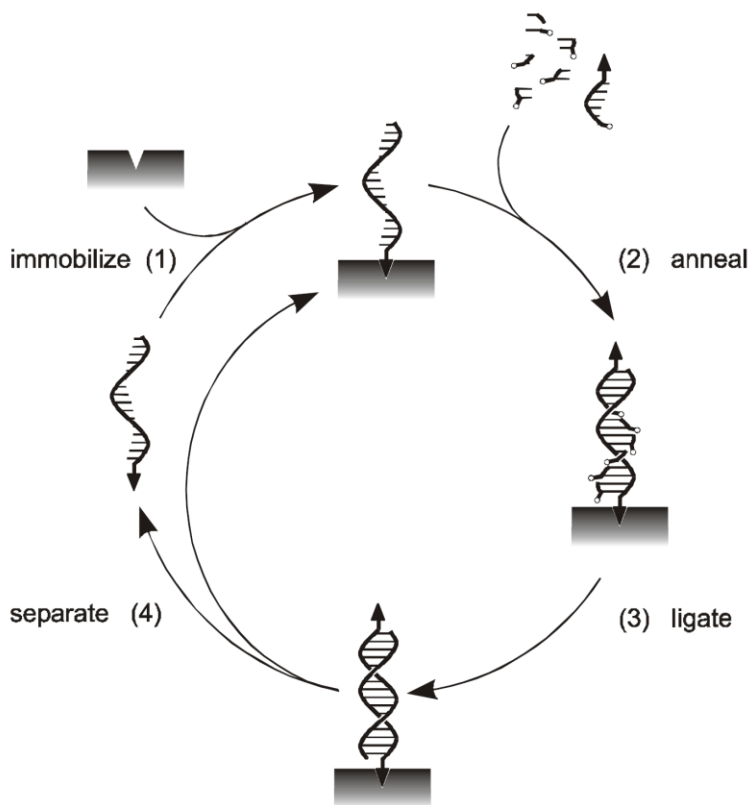


**Figure 1.11:** General steps of the SPREAD cycle: template immobilization, probe annealing, ligation, and dissociation of the product are repeated leading to an exponential rather than parabolic amplification of the DNA. Image reproduced with permission from ref. 105. Copyright © 1998 Nature Publishing Group

It is well known that the stability of the DNA duplex is dependent on the hydrogen bonding and base-stacking interactions within the duplex. Therefore, design strategies for isothermal amplification have focused on selective destabilization of the product duplex **D** without affecting the stability of the ternary complex **M**, so that one can find a temperature where complex **M** can form to allow ligation yet complex **D** can dissociate after ligation (Figure 1.9). One method of achieving isothermal amplification that has been explored in single-cycle ligation reactions involves the careful design of probe strands such

that a destabilizing modification is incorporated into the middle of the product duplex after ligation.<sup>107-109</sup> After ligation with such a destabilizing group, the stability of the product duplex **D** will be low enough to dissociate at the same temperature it formed.<sup>110, 111</sup> If the stabilities of the complexes before (**M**) and after (**D**) ligation are properly balanced, isothermal amplification should be achieved. Recently, several nonenzymatic isothermal amplification systems based on chemical ligation have been developed.<sup>108-111</sup> The Lynn group first demonstrated the idea of incorporating a modification in the terminal end of the ligating strands such that it formed a flexible linker in the middle of a duplex.<sup>108</sup> The Seitz group showed that isothermal amplification could be achieved in a single cycle using a DNA templated reaction followed by rearrangement by introducing PNA analogues of abasic groups into the ligation system to avoid product inhibition (Figure 1.12).<sup>110, 112</sup> In the Kool system, destabilization was achieved by introducing flexible linkers into the ligating strands (between the terminal nucleotide and the electrophilic end).<sup>113</sup> After ligation with a nucleophilic probe in the presence of target DNA, the resulting flexible linkers caused the product duplex to dissociate isothermally (Figure 1.13). All of these examples illustrated that introducing flexible linkers into the ligation system led to the selective destabilization of the product duplex and isothermal amplification of the complementary nucleic acid.



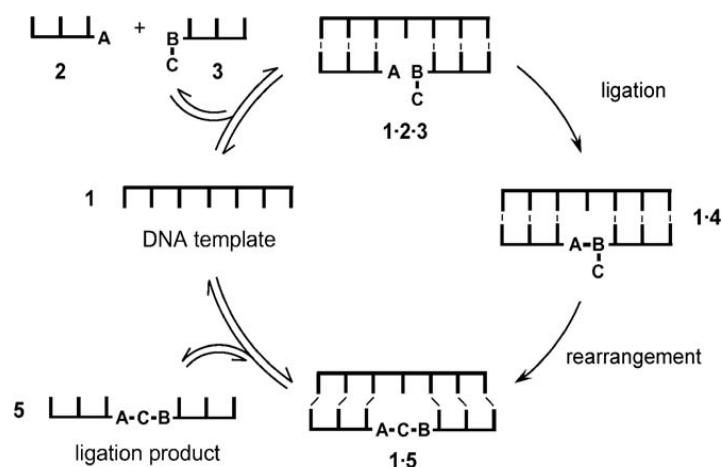


**Figure 1.12:** General scheme of destabilization of product duplex with ligation–rearrangement reactions. DNA template **1** catalyzed the ligation between **2** (terminus **A**, glycine thioester) and **3** (terminus **B-C**, isocysteine) to form **A-B-C** by bringing the probes closer. However, isothermal amplification was achieved due to the rearrangement of the **A-B-C** product (thioester linkage) to the **A-C-B** product (amide linkage) that destabilizes the duplex. Image reproduced with permission from ref. 110. Copyright © 2006 WILEY-VCH Verlag GmbH & Co. KGaA, Weinheim.

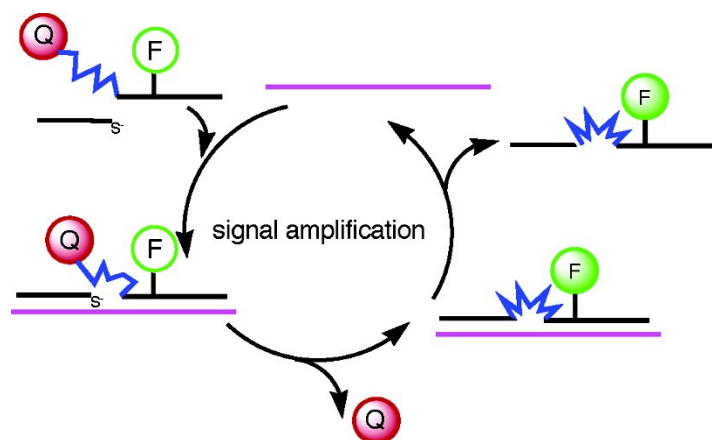


**Figure 1.13:** Schematic diagram of isothermal amplification by destabilization with a flexible linker. The template (purple strand) helps hybridizing the small probes (black strands) thus bringing the reactive ends closer to facilitate the ligation thereby releasing the quencher. The newly formed DNA strand can be released due to the presence of the flexible linker. Image reproduced with permission from ref. 113. Copyright © 2004 American Chemical Society.

## 1.4 Objectives

The goal of this thesis is to develop a simple, general and rapid isothermal DNA amplification method. As mentioned earlier the main obstacle of achieving isothermal amplification is that the product duplex formed after ligation or polymerization is much more stable than the DNA target:probe nicked duplex formed before ligation. For this reason, most popular DNA amplification techniques (PCR or LCR) use thermocycling to dissociate the product duplex for the next round of amplification. So if we can selectively modulate the stability of the product duplex without affecting the stability of the DNA nicked duplex before ligation, we will be able to achieve isothermal amplification. Current isothermal amplification techniques use a variety of tricks to destabilize the product duplex either by using a special primer design, a polymerase with strand displacement ability, a DNA unwinding enzyme, or nicking enzymes. As a result, most of the isothermal techniques require more than one enzyme and some of them require complex primer designs. To develop a point-of-care nucleic acid testing device, it is highly desirable to develop a simple isothermal nucleic acid amplification requiring less or no enzyme. The Lynn, Kool and Seitz groups addressed this problem by developing chemical ligation and destabilizing probe systems. To achieve isothermal DNA amplification, the authors designed the probes so that a destabilizing group got incorporated in the middle of the duplex. The flexible destabilizing groups explored in their work had a significant impact on the stability of the product duplex which helped them achieve isothermal amplification. One drawback of these chemical ligation systems that utilized

destabilization is that they did not result in exponential amplification of the DNA as they were not cross-catalytic. Additionally, their systems suffered from slow rates of ligation and high background reactions in the absence of target. As enzymatic ligation is faster and more specific than non-enzymatic ligation systems, we used enzymatic ligation to study isothermal amplification by destabilization.

The previous examples of amplification by destabilization incorporated the destabilizing groups into the small probe strands such that ligation positioned the destabilizing group in the middle of the product duplex. In contrast, our first aim in Chapter 2 was to incorporate destabilization into the DNA template for an enzymatic ligation system. Consequently, we replaced one of the bases from the template with different flexible and rigid linkers, so there would be no hydrogen bond in that place between the template and probe. We demonstrated that the ligated product duplex will be less stable than that of the native DNA duplex and will be released under isothermal conditions.

In the first part of Chapter 2, I will discuss how different destabilizing groups affect the stability of the duplex. Differences in stability are reflected in different melting temperatures,  $T_m$ , of the duplex. Next, we studied how the rate of ligation was affected by the presence of destabilizing groups in the template. To see whether we could achieve isothermal amplification, we utilized substoichiometric amounts of template and calculated the turnover number (TON, the average number of product formed per template). The variation of TON with the structural variation of the destabilizing linker will also be discussed. Finally,

the self-replication of a native target (whereby the destabilizing template is made in situ) and increased TON with a cross-catalytic approach will be discussed in the later part of the chapter.

While working on the single cycle amplification system in Chapter 2, we realized that abasic (**Ab**) and butyl (**Bu**) groups are the best among the different destabilizing groups that we studied. Due to the commercial availability and the chemical stability of the abasic group, we continued using the abasic group as a destabilizing group. While studying the amplification with single cycle, we also found that the concentration of enzyme had a huge impact on the rate of amplification. In Chapter 3, I will report our work on DNA amplification and replication with a higher concentration of enzyme, which led to rapid, sigmoidal amplification of target DNA. In addition, the rate of amplification with the abasic group will be compared with a mismatch as a destabilizing group. Finally, to address the sequence generality, we studied similar amplification behaviour with different DNA sequences suggesting DNA amplification using this destabilizing approach is general.

As the ligation reaction is very sensitive to the presence of mismatches in a specific position of the target DNA, this ligase-based isothermal amplification can also be used for detection of single nucleotide polymorphisms (SNPs), which result in single base pair mismatches with the probe DNA. In Chapter 4, I will show how our lesion-induced isothermal amplification (LIDA) method can be used to detect SNPs. In this chapter, we also showed our attempt to multiplex the SNP assay in order to detect specific mismatches in the target DNA. With

multiplexing, the background ligation was very high resulting in a poor discrimination ratio. Consequently, we separated the probe sets to match with a specific base, so that we could better discriminate between the matched target and mismatched targets. In the second part of the chapter, we will discuss the application of this isothermal amplification to the FRET based real-time detection of SNPs in the target DNA. We also explore combining our amplification method with target-induced disassembly of DNA-linked gold-nanoparticle (NP) aggregates, which has promise as a rapid, colorimetric platform.

For isothermal amplification systems described thus far, we used T4 DNA ligase that resulted in blunt-end ligation of our two sets of complementary probes, which ultimately triggered rapid amplification in the absence of the initial target. In order to reduce the background ligation so that we can lower the concentration of DNA target that we are able to detect, we studied in chapter 5 the isothermal amplification with different ligases: *E. coli*, T3 and T7 DNA ligase, as these three enzymes were reported to give less blunt-end ligation. Among these three enzymes T7 and *E. coli* DNA ligases improved the sensitivity by one and two orders of magnitude than that of T4 DNA ligase under the same experimental conditions. Since the amplification system we studied uses a pseudo-blunt end (one base overhang across from an abasic group), we hypothesized that if we used a true blunt end system the background problem might be solved. Our attempt to reduce background ligation using different true blunt end ligation systems is reported. In the final part of the chapter, we discuss the cross-catalytic amplification system with different bases across from the abasic site to find if

there is any specific base requirement for isothermal amplification using this destabilizing approach.

In Chapter 6, I provide general conclusions regarding the results of all the projects and proposed future work on developing an isothermal amplification system similar to LDR-PCR, so that we can achieve dual level of specificity to reduce background ligation. Another challenge for amplification using this destabilization approach is the ability to amplify longer DNA target or target with higher G:C content. One way of addressing the problem is to introduce multiple abasic sites in the amplification system. In my preliminary work it indicates that it is possible to amplify longer targets by introducing multiple abasic groups.

## 1.5 References

- 1) Whitman, W. B.; Coleman, D. C.; Wiebe, W. J.: Prokaryotes: the unseen majority. *Proc Natl Acad Sci* **1998**, *95*, 6578-83.
- 2) Horzinek, M. C.: The birth of virology. *Antonie Van Leeuwenhoek* **1997**, *71*, 15-20.
- 3) McKerrow, J. H.; Caffrey, C.; Kelly, B.; Loke, P.; Sajid, M.: Proteases in parasitic diseases. *Annu Rev Pathol* **2006**, *1*, 497-536.
- 4) Bowman, B. H.; White, T. J.; Taylor, J. W.: Human pathogenic fungi and their close nonpathogenic relatives. *Mol Phylogenet Evol* **1996**, *6*, 89-96.
- 5) Collinge, J.; Clarke, A. R.: A general model of prion strains and their pathogenicity. *Science* **2007**, *318*, 930-6.
- 6) Turner, J.; Begon, M.; Bowers, R. G.: Modelling pathogen transmission: the interrelationship between local and global approaches. *Proc Biol Sci* **2003**, *270*, 105-12.
- 7) Sakata, T.; Winzeler, E. A.: Genomics, systems biology and drug development for infectious diseases. *Mol Biosyst* **2007**, *3*, 841-8.
- 8) Mabey, D.; Peeling, R. W.; Ustianowski, A.; Perkins, M. D.: Diagnostics for the developing world. *Nat Rev Microbiol* **2004**, *2*, 231-40.
- 9) Peeling, R. W.; Smith, P. G.; Bossuyt, P. M. M.: A guide for diagnostic evaluations. *Nat Rev Micro* **2010**, S2-S6.
- 10) Chin, C. D.; Linder, V.; Sia, S. K.: Commercialization of microfluidic point-of-care diagnostic devices. *Lab Chip* **2012**, *12*, 2118-34.
- 11) Fu, E.; Yager, P.; Floriano, P. N.; Christodoulides, N.; McDevitt, J. T.: Perspective on diagnostics for global health. *IEEE Pulse* **2011**, *2*, 40-50.
- 12) Nichols, D.: Cultivation gives context to the microbial ecologist. *FEMS Microbiol Ecol* **2007**, *60*, 351-7.
- 13) Milks, M. L.; Sokolova, Y. Y.; Isakova, I. A.; Fuxa, J. R.; Mitchell, F.; Snowden, K. F.; Vinson, S. B.: Comparative effectiveness of light-microscopic techniques and PCR in detecting *Thelohania solenopsae*

- (Microsporidia) infections in red imported fire ants (*Solenopsis invicta*). *J Eukaryot Microbiol* **2004**, *51*, 187-91.
- 14) Fakruddin, M.; Mannan, K. S.; Andrews, S.: Viable but Nonculturable Bacteria: Food Safety and Public Health Perspective. *ISRN Microbiol* **2013**, *2013*, 703813.
  - 15) Iqbal, S. S.; Mayo, M. W.; Bruno, J. G.; Bronk, B. V.; Batt, C. A.; Chambers, J. P.: A review of molecular recognition technologies for detection of biological threat agents. *Biosens Bioelectron* **2000**, *15*, 549-78.
  - 16) Kumagai, I.; Tsumoto, K.: Antigen–Antibody Binding. In *eLS*; John Wiley & Sons, Ltd, **2001**.
  - 17) de Boer, E.; Beumer, R. R.: Methodology for detection and typing of foodborne microorganisms. *Int J Food Microbiol* **1999**, *50*, 119-130.
  - 18) Crowther, J. R.: ELISA. Theory and practice. *Methods Mol Biol* **1995**, *42*, 1-218.
  - 19) Huang, R.-P.; Lin, Y.; Chen, L.-P.; Yang, W.; Huang, R.: ELISA-based protein arrays: Multiplexed sandwich immunoassays. *Curr. Proteomics* **2004**, *1*, 199-210.
  - 20) Mistry, K. K.; Layek, K.; Mahapatra, A.; Roy Chaudhuri, C.; Saha, H.: A review on amperometric-type immunosensors based on screen-printed electrodes. *Analyst* **2014**, *139*, 2289-2311.
  - 21) Chen, C.-S.; Durst, R. A.: Simultaneous detection of *Escherichia coli* O157:H7, *Salmonella* spp. and *Listeria monocytogenes* with an array-based immunosorbent assay using universal protein G-liposomal nanovesicles. *Talanta* **2006**, *69*, 232-238.
  - 22) Banala, S.; Arts, R.; Aper, S. J. A.; Merckx, M.: No washing, less waiting: engineering biomolecular reporters for single-step antibody detection in solution. *Org Biomol Chem* **2013**, *11*, 7642-7649.
  - 23) Barken, K. B.; Haagenen, J. A.; Tolker-Nielsen, T.: Advances in nucleic acid-based diagnostics of bacterial infections. *Clin Chim Acta* **2007**, *384*, 1-11.



- 24) O'Connor, L.; Glynn, B.: Recent advances in the development of nucleic acid diagnostics. *Expert Review of Medical Devices* **2010**, *7*, 529-539.
- 25) Espy, M. J.; Uhl, J. R.; Sloan, L. M.; Buckwalter, S. P.; Jones, M. F.; Vetter, E. A.; Yao, J. D.; Wengenack, N. L.; Rosenblatt, J. E.; Cockerill, F. R., 3rd; Smith, T. F.: Real-time PCR in clinical microbiology: applications for routine laboratory testing. *Clin Microbiol Rev* **2006**, *19*, 165-256.
- 26) Battle, T. J.; Golden, M. R.; Suchland, K. L.; Counts, J. M.; Hughes, J. P.; Stamm, W. E.; Holmes, K. K.: Evaluation of laboratory testing methods for Chlamydia trachomatis infection in the era of nucleic acid amplification. *J Clin Microbiol* **2001**, *39*, 2924-7.
- 27) Vaneechoutte, M.; Van Eldere, J.: The possibilities and limitations of nucleic acid amplification technology in diagnostic microbiology. *J Med Microbiol* **1997**, *46*, 188-94.
- 28) Craw, P.; Balachandran, W.: Isothermal nucleic acid amplification technologies for point-of-care diagnostics: a critical review. *Lab Chip* **2012**, *12*, 2469-2486.
- 29) Fredriksson, S.; Gullberg, M.; Jarvius, J.; Olsson, C.; Pietras, K.; Gustafsdottir, S. M.; Ostman, A.; Landegren, U.: Protein detection using proximity-dependent DNA ligation assays. *Nat Biotechnol* **2002**, *20*, 473-7.
- 30) Gustafsdottir, S. M.; Nordengrahn, A.; Fredriksson, S.; Wallgren, P.; Rivera, E.; Schallmeiner, E.; Merza, M.; Landegren, U.: Detection of individual microbial pathogens by proximity ligation. *Clin Chem* **2006**, *52*, 1152-60.
- 31) Nindl, I.; Lorincz, A.; Mielzynska, I.; Petry, U.; Baur, S.; Kirchmayr, R.; Michels, W.; Schneider, A.: Human papilloma virus detection in cervical intraepithelial neoplasia by the second-generation hybrid capture microplate test, comparing two different cervical specimen collection methods. *Clin Diagn Virol* **1998**, *10*, 49-56.

- 32) Stoeva, S. I.; Lee, J.-S.; Thaxton, C. S.; Mirkin, C. A.: Multiplexed DNA Detection with Biobarcode Nanoparticle Probes. *Angew Chem Int Ed* **2006**, *45*, 3303-3306.
- 33) Das, J.; Cederquist, K. B.; Zaragoza, A. A.; Lee, P. E.; Sargent, E. H.; Kelley, S. O.: An ultrasensitive universal detector based on neutralizer displacement. *Nat Chem* **2012**, *4*, 642-648.
- 34) Klamp, T.; Camps, M.; Nieto, B.; Guasch, F.; Ranasinghe, R. T.; Wiedemann, J.; Petrášek, Z.; Schwille, P.; Klenerman, D.; Sauer, M.: Highly Rapid Amplification-Free and Quantitative DNA Imaging Assay. *Sci Rep* **2013**, *3*.
- 35) Bartlett, J. S.; Stirling, D.: A Short History of the Polymerase Chain Reaction. In *PCR Protocols*; Bartlett, J. S., Stirling, D., Eds.; Humana Press, **2003**; Vol. 226; pp 3-6.
- 36) Yang, S.; Rothman, R. E.; Hardick, J.; Kuroki, M.; Hardick, A.; Doshi, V.; Ramachandran, P.; Gaydos, C. A.: Rapid polymerase chain reaction-based screening assay for bacterial biothreat agents. *Acad Emerg Med* **2008**, *15*, 388-92.
- 37) Miller, M. B.; Tang, Y. W.: Basic concepts of microarrays and potential applications in clinical microbiology. *Clin Microbiol Rev* **2009**, *22*, 611-33.
- 38) Lo, Y. M.; Chan, K. C.: Introduction to the polymerase chain reaction. *Methods Mol Biol* **2006**, *336*, 1-10.
- 39) Kleppe, K.; Ohtsuka, E.; Kleppe, R.; Molineux, I.; Khorana, H. G.: Studies on polynucleotides. XCVI. Repair replications of short synthetic DNA's as catalyzed by DNA polymerases. *J Mol Biol* **1971**, *56*, 341-61.
- 40) Chien, A.; Edgar, D. B.; Trela, J. M.: Deoxyribonucleic acid polymerase from the extreme thermophile *Thermus aquaticus*. *J Bacteriol* **1976**, *127*, 1550-7.
- 41) Lawyer, F. C.; Stoffel, S.; Saiki, R. K.; Myambo, K.; Drummond, R.; Gelfand, D. H.: Isolation, characterization, and expression in *Escherichia*

- coli of the DNA polymerase gene from *Thermus aquaticus*. *J Biol Chem* **1989**, *264*, 6427-37.
- 42) Saiki, R. K.; Gelfand, D. H.; Stoffel, S.; Scharf, S. J.; Higuchi, R.; Horn, G. T.; Mullis, K. B.; Erlich, H. A.: Primer-directed enzymatic amplification of DNA with a thermostable DNA polymerase. *Science* **1988**, *239*, 487-91.
- 43) Pavlov, A. R.; Pavlova, N. V.; Kozyavkin, S. A.; Slesarev, A. I.: Recent developments in the optimization of thermostable DNA polymerases for efficient applications. *Trends Biotechnol* **2004**, *22*, 253-60.
- 44) Chou, Q.; Russell, M.; Birch, D. E.; Raymond, J.; Bloch, W.: Prevention of pre-PCR mis-priming and primer dimerization improves low-copy-number amplifications. *Nucleic Acids Res* **1992**, *20*, 1717-23.
- 45) D'Aquila, R. T.; Bechtel, L. J.; Videler, J. A.; Eron, J. J.; Gorczyca, P.; Kaplan, J. C.: Maximizing sensitivity and specificity of PCR by pre-amplification heating. *Nucleic Acids Res* **1991**, *19*, 3749.
- 46) Kaboev, O. K.; Luchkina, L. A.; Tret'iakov, A. N.; Bahrmand, A. R.: PCR hot start using primers with the structure of molecular beacons (hairpin-like structure). *Nucleic Acids Res* **2000**, *28*, E94.
- 47) Kebelmann-Betzing, C.; Seeger, K.; Dragon, S.; Schmitt, G.; Moricke, A.; Schild, T. A.; Henze, G.; Beyermann, B.: Advantages of a new Taq DNA polymerase in multiplex PCR and time-release PCR. *Biotechniques* **1998**, *24*, 154-8.
- 48) Kong, D.; Shen, H.; Huang, Y.; Mi, H.: PCR hot-start using duplex primers. *Biotechnol Lett* **2004**, *26*, 277-80.
- 49) Haqqi, T. M.; Sarkar, G.; David, C. S.; Sommer, S. S.: Specific amplification with PCR of a refractory segment of genomic DNA. *Nucleic Acids Res* **1988**, *16*, 11844.
- 50) Don, R. H.; Cox, P. T.; Wainwright, B. J.; Baker, K.; Mattick, J. S.: 'Touchdown' PCR to circumvent spurious priming during gene amplification. *Nucleic Acids Res* **1991**, *19*, 4008.

- 51) Saiki, R. K.; Bugawan, T. L.; Horn, G. T.; Mullis, K. B.; Erlich, H. A.: Analysis of enzymatically amplified beta-globin and HLA-DQ alpha DNA with allele-specific oligonucleotide probes. *Nature* **1986**, *324*, 163-6.
- 52) Innis, M. A.; Myambo, K. B.; Gelfand, D. H.; Brow, M. A.: DNA sequencing with *Thermus aquaticus* DNA polymerase and direct sequencing of polymerase chain reaction-amplified DNA. *Proc Natl Acad Sci* **1988**, *85*, 9436-40.
- 53) Mazars, G.-R.; Theillet, C.: Direct Sequencing by Thermal Asymmetric PCR #. In *T PCR Sequencing Protocols*, 1996; Vol. 65; pp 35-40.
- 54) Kubista, M.; Andrade, J. M.; Bengtsson, M.; Forootan, A.; Jonak, J.; Lind, K.; Sindelka, R.; Sjoback, R.; Sjogreen, B.; Strombom, L.; Stahlberg, A.; Zoric, N.: The real-time polymerase chain reaction. *Mol Aspects Med* **2006**, *27*, 95-125.
- 55) Morrison, T. B.; Weis, J. J.; Wittwer, C. T.: Quantification of low-copy transcripts by continuous SYBR Green I monitoring during amplification. *Biotechniques* **1998**, *24*, 954-8, 960, 962.
- 56) Wilhelm, J.; Pingoud, A.: Real-time polymerase chain reaction. *Chembiochem* **2003**, *4*, 1120-8.
- 57) Vogelstein, B.; Kinzler, K. W.: Digital PCR. *Proc Natl Acad Sci* **1999**, *96*, 9236-41.
- 58) Pohl, G.; Shih Ie, M.: Principle and applications of digital PCR. *Expert Rev Mol Diagn* **2004**, *4*, 41-7.
- 59) Diehl, F.; Li, M.; He, Y.; Kinzler, K. W.; Vogelstein, B.; Dressman, D.: BEAMing: single-molecule PCR on microparticles in water-in-oil emulsions. *Nat Methods* **2006**, *3*, 551-9.
- 60) Dressman, D.; Yan, H.; Traverso, G.; Kinzler, K. W.; Vogelstein, B.: Transforming single DNA molecules into fluorescent magnetic particles for detection and enumeration of genetic variations. *Proc Natl Acad Sci* **2003**, *100*, 8817-22.

- 61) Nakano, M.; Komatsu, J.; Matsuura, S.; Takashima, K.; Katsura, S.; Mizuno, A.: Single-molecule PCR using water-in-oil emulsion. *J Biotechnol* **2003**, *102*, 117-24.
- 62) Diehl, F.; Li, M.; Dressman, D.; He, Y.; Shen, D.; Szabo, S.; Diaz, L. A.; Goodman, S. N.; David, K. A.; Juhl, H.; Kinzler, K. W.; Vogelstein, B.: Detection and quantification of mutations in the plasma of patients with colorectal tumors. *Proc Natl Acad Sci* **2005**, *102*, 16368-16373.
- 63) Reyes, A. A.; Carrera, P.; Cardillo, E.; Ugozzoli, L.; Lowery, J. D.; Lin, C.-I. P.; Go, M.; Ferrari, M.; Wallace, R. B.: Ligase chain reaction assay for human mutations: the Sickle Cell by LCR assay. *Clin Chem* **1997**, *43*, 40-44.
- 64) Chernesky, M. A.; Marshall, R. L.; Petrich, A. K.: Infectious Disease Testing by LCR. In *Encyclopedia of Molecular Cell Biology and Molecular Medicine*; Wiley-VCH Verlag GmbH & Co. KGaA, **2006**.
- 65) Barany, F.: Genetic disease detection and DNA amplification using cloned thermostable ligase. *Proc Natl Acad Sci* **1991**, *88*, 189-93.
- 66) Landegren, U.; Kaiser, R.; Caskey, C. T.; Hood, L.: DNA diagnostics--molecular techniques and automation. *Science* **1988**, *242*, 229-37.
- 67) Landegren, U.; Kaiser, R.; Sanders, J.; Hood, L.: A ligase-mediated gene detection technique. *Science* **1988**, *241*, 1077-80.
- 68) Jarvius, J.; Nilsson, M.; Landegren, U.: Oligonucleotide ligation assay. *Methods Mol Biol* **2003**, *212*, 215-28.
- 69) Landegren, U.: Ligation-based DNA diagnostics. *Bioessays* **1993**, *15*, 761-5.
- 70) Besmer, P.; Miller, R. C., Jr.; Caruthers, M. H.; Kumar, A.; Minamoto, K.; Van de Sande, J. H.; Sidarova, N.; Khorana, H. G.: Studies on polynucleotides. CXVII. Hybridization of polydeoxynucleotides with tyrosine transfer RNA sequences to the r-strand of phi80psu + 3 DNA. *J Mol Biol* **1972**, *72*, 503-22.

- 71) Alves, A. M.; Carr, F. J.: Dot blot detection of point mutations with adjacently hybridising synthetic oligonucleotide probes. *Nucleic Acids Res* **1988**, *16*, 8723.
- 72) Wu, D. Y.; Wallace, R. B.: The ligation amplification reaction (LAR)--amplification of specific DNA sequences using sequential rounds of template-dependent ligation. *Genomics* **1989**, *4*, 560-9.
- 73) Luo, J.; Bergstrom, D. E.; Barany, F.: Improving the fidelity of *Thermus thermophilus* DNA ligase. *Nucleic Acids Res* **1996**, *24*, 3071-8.
- 74) Prchal, J. T.; Guan, Y. L.: A novel clonality assay based on transcriptional analysis of the active X chromosome. *Stem Cells* **1993**, *11 Suppl 1*, 62-5.
- 75) Pingle, M.; Rundell, M.; Das, S.; Golightly, L.; Barany, F.: PCR/LDR/Universal Array Platforms for the Diagnosis of Infectious Disease. In *Microarray Methods for Drug Discovery*; Chittur, S., Ed.; Humana Press, **2010**; Vol. 632; pp 141-157.
- 76) McNamara, D. T.; Thomson, J. M.; Kasehagen, L. J.; Zimmerman, P. A.: Development of a Multiplex PCR-Ligase Detection Reaction Assay for Diagnosis of Infection by the Four Parasite Species Causing Malaria in Humans. *J Clin Microbiol* **2004**, *42*, 2403-2410.
- 77) Marshall, R. L.; Laffler, T. G.; Cerney, M. B.; Sustachek, J. C.; Kratochvil, J. D.; Morgan, R. L.: Detection of HCV RNA by the asymmetric gap ligase chain reaction. *PCR Methods Appl* **1994**, *4*, 80-4.
- 78) Lee, H. H.; Chernesky, M. A.; Schachter, J.; Burczak, J. D.; Andrews, W. W.; Muldoon, S.; Leckie, G.; Stamm, W. E.: Diagnosis of *Chlamydia trachomatis* genitourinary infection in women by ligase chain reaction assay of urine. *Lancet* **1995**, *345*, 213-6.
- 79) Walker, G. T.; Fraiser, M. S.; Schram, J. L.; Little, M. C.; Nadeau, J. G.; Malinowski, D. P.: Strand displacement amplification--an isothermal, in vitro DNA amplification technique. *Nucleic Acids Res* **1992**, *20*, 1691-6.
- 80) Walker, G. T.; Little, M. C.; Nadeau, J. G.; Shank, D. D.: Isothermal in vitro amplification of DNA by a restriction enzyme/DNA polymerase system. *Proc Natl Acad Sci* **1992**, *89*, 392-6.

- 81) Walker, G. T.; Linn, C. P.; Nadeau, J. G.: DNA Detection by Strand Displacement Amplification and Fluorescence Polarization With Signal Enhancement Using a DNA Binding Protein. *Nucleic Acids Res* **1996**, *24*, 348-353.
- 82) Walker, G. T.: Empirical aspects of strand displacement amplification. *PCR Methods Appl* **1993**, *3*, 1-6.
- 83) Fire, A.; Xu, S. Q.: Rolling replication of short DNA circles. *Proc Natl Acad Sci* **1995**, *92*, 4641-5.
- 84) Liu, D.; Daubendiek, S. L.; Zillman, M. A.; Ryan, K.; Kool, E. T.: Rolling Circle DNA Synthesis: Small Circular Oligonucleotides as Efficient Templates for DNA Polymerases. *J Am Chem Soc* **1996**, *118*, 1587-1594.
- 85) Blanco, L.; Salas, M.: Characterization and purification of a phage phi 29-encoded DNA polymerase required for the initiation of replication. *Proc Natl Acad Sci* **1984**, *81*, 5325-9.
- 86) Nilsson, M.; Malmgren, H.; Samiotaki, M.; Kwiatkowski, M.; Chowdhary, B. P.; Landegren, U.: Padlock probes: circularizing oligonucleotides for localized DNA detection. *Science* **1994**, *265*, 2085-8.
- 87) Jonstrup, S. P.; Koch, J.; Kjems, J.: A microRNA detection system based on padlock probes and rolling circle amplification. *Rna* **2006**, *12*, 1747-52.
- 88) Hartman, M. R.; Ruiz, R. C. H.; Hamada, S.; Xu, C.; Yancey, K. G.; Yu, Y.; Han, W.; Luo, D.: Point-of-care nucleic acid detection using nanotechnology. *Nanoscale* **2013**, *5*, 10141-10154.
- 89) An, L.; Tang, W.; Ranalli, T. A.; Kim, H. J.; Wytiaz, J.; Kong, H.: Characterization of a thermostable UvrD helicase and its participation in helicase-dependent amplification. *J Biol Chem* **2005**, *280*, 28952-8.
- 90) Vincent, M.; Xu, Y.; Kong, H.: Helicase-dependent isothermal DNA amplification. *EMBO Rep* **2004**, *5*, 795-800.
- 91) Chow, W. H.; McCloskey, C.; Tong, Y.; Hu, L.; You, Q.; Kelly, C. P.; Kong, H.; Tang, Y. W.; Tang, W.: Application of isothermal helicase-dependent amplification with a disposable detection device in a simple

- sensitive stool test for toxigenic *Clostridium difficile*. *J Mol Diagn* **2008**, *10*, 452-8.
- 92) Compton, J.: Nucleic acid sequence-based amplification. *Nature* **1991**, *350*, 91-2.
- 93) Morabito, K.; Wiske, C.; Tripathi, A.: Engineering Insights for Multiplexed Real-Time Nucleic Acid Sequence-Based Amplification (NASBA): Implications for Design of Point-of-Care Diagnostics. *Mol Diagn Ther* **2013**, *17*, 185-192.
- 94) Van Ness, J.; Van Ness, L. K.; Galas, D. J.: Isothermal reactions for the amplification of oligonucleotides. *Proc Natl Acad Sci* **2003**, *100*, 4504-9.
- 95) Tan, E.; Erwin, B.; Dames, S.; Voelkerding, K.; Niemz, A.: Isothermal DNA amplification with gold nanosphere-based visual colorimetric readout for herpes simplex virus detection. *Clin Chem* **2007**, *53*, 2017-20.
- 96) Fu, S.; Qu, G.; Guo, S.; Ma, L.; Zhang, N.; Zhang, S.; Gao, S.; Shen, Z.: Applications of loop-mediated isothermal DNA amplification. *Appl Biochem Biotechnol* **2011**, *163*, 845-50.
- 97) Notomi, T.; Okayama, H.; Masubuchi, H.; Yonekawa, T.; Watanabe, K.; Amino, N.; Hase, T.: Loop-mediated isothermal amplification of DNA. *Nucleic Acids Res* **2000**, *28*, E63.
- 98) Mitani, Y.; Lezhava, A.; Kawai, Y.; Kikuchi, T.; Oguchi-Katayama, A.; Kogo, Y.; Itoh, M.; Miyagi, T.; Takakura, H.; Hoshi, K.; Kato, C.; Arakawa, T.; Shibata, K.; Fukui, K.; Masui, R.; Kuramitsu, S.; Kiyotani, K.; Chalk, A.; Tsunekawa, K.; Murakami, M.; Kamataki, T.; Oka, T.; Shimada, H.; Cizdziel, P. E.; Hayashizaki, Y.: Rapid SNP diagnostics using asymmetric isothermal amplification and a new mismatch-suppression technology. *Nat Methods* **2007**, *4*, 257-62.
- 99) Lee, D. H.; Granja, J. R.; Martinez, J. A.; Severin, K.; Ghadiri, M. R.: A self-replicating peptide. *Nature* **1996**, *382*, 525-528.
- 100) von Kiedrowski, G.: A Self-Replicating Hexadeoxynucleotide. *Angew Chem Int Ed* **1986**, *25*, 932-935.



- 101) Joyce, G. F. RNA evolution and the origins of life. *Nature* **1989**, 338, 217-224.
- 102) Patzke, V. v. K., G. Self replicating systems. *Arkivoc* **2007**, 293-310.
- 103) Zielinski, W. S.; Orgel, L. E. Autocatalytic synthesis of a tetranucleotide analogue. *Nature* **1987**, 327, 346-347.
- 104) Sievers, D.; von Kiedrowski, G. Self-Replication of Hexadeoxynucleotide Analogues: Autocatalysis versus Cross-Catalysis. *Chem Eur J* **1998**, 4, 629-641.
- 105) Luther, A.; Brandsch, R.; von Kiedrowski, G. Surface-promoted replication and exponential amplification of DNA analogues. *Nature* **1998**, 396, 245-248.
- 106) Lincoln, T. A.; Joyce, G. F. Self-Sustained Replication of an RNA Enzyme. *Science* **2009**, 323, 1229-1232.
- 107) Ye, J.; Gat, Y.; Lynn, D. G. Catalyst for DNA Ligation: Towards a Two-Stage Replication Cycle. *Angew Chem Int Ed* **2000**, 39, 3641-3643.
- 108) Zhan, Z.-Y. J.; Lynn, D. G. Chemical Amplification through Template-Directed Synthesis. *J Am Chem Soc* **1997**, 119, 12420-12421.
- 109) Silverman, A. P.; Kool, E. T. Detecting RNA and DNA with Templated Chemical Reactions. *Chem Rev* **2006**, 106, 3775-3789.
- 110) Dose, C.; Ficht, S.; Seitz, O. Reducing Product Inhibition in DNA-Template-Controlled Ligation Reactions. *Angew Chem Int Ed* **2006**, 45, 5369-5373.
- 111) Grossmann, T. N.; Strohbach, A.; Seitz, O. Achieving Turnover in DNA-Templated Reactions. *Chembiochem* **2008**, 9, 2185-2192.
- 112) Ficht, S.; Dose, C.; Seitz, O. As Fast and Selective as Enzymatic Ligations: Unpaired Nucleobases Increase the Selectivity of DNA-Controlled Native Chemical PNA Ligation. *Chembiochem* **2005**, 6, 2098-2103.
- 113) Abe, H.; Kool, E. T. Destabilizing Universal Linkers for Signal Amplification in Self-Ligating Probes for RNA. *J Am Chem Soc* **2004**, 126, 13980-13986.

## Chapter 2

### **Tuning DNA Stability to Achieve Turnover in Template for an Enzymatic Ligation Reaction**

Portions of this chapter are reproduced in part with permission from the

© Wiley VCH Verlag GmbH & Co from:

Kausar, A.\*, McKay, R. D.\*, Lam, J.\*, Bhogal, R. S., Tang, A. Y. and Gibbs-Davis, J. M. (2011), Tuning DNA Stability To Achieve Turnover in Template for an Enzymatic Ligation Reaction. *Angew Chem Int Ed*, 50: 8922–8926.doi: 10.1002/anie.201102579 \*Equal contribution

The synthesis of most of the destabilizing templates was performed by R. S. Bhogal and A. Y. Tang. Proof-of-concept experiments not contained herein and solid-phase synthesis of some of the other strands used was performed by R. D. McKay and J. Lam. Some of the melting experiments included herein were performed by A. Y. Tang, R. S. Bhogal and J. Lam.

## 2.1 Introduction

In the last decade, DNA-based systems have been developed that are capable of performing sophisticated functions initiated by molecular recognition. Key examples are the DNA walkers where directional motion or load pick-up, transfer, and release are achieved with molecular and spatial selectivity.<sup>1, 2</sup> Attempts to develop autonomous DNA self-replicating systems, however, without specific sequence requirements,<sup>3</sup> have in recent years lagged behind.<sup>4-6</sup> As one of the hallmarks of organisms is their ability to amplify information and materials through biocatalysis and self-replication,<sup>6, 7</sup> the development of truly biomimetic systems capable of integrated functions requires incorporating amplification into self-assembly and nanotechnology.<sup>8</sup> Not only do replicating DNA systems provide tools for DNA-based nanotechnology<sup>8</sup> and insights into the origins of life,<sup>6, 7, 9</sup> but they also can be used to isothermally amplify signal in DNA detection, which can simplify the requirements for point-of-care diagnostics.<sup>10</sup>

One method for introducing amplification into DNA-based systems involves generating turnover in DNA-templated processes.<sup>11</sup> To achieve turnover, the DNA template that facilitates the reaction of two complementary probe strands (Figure 2.1, steps A and B) must dissociate from the product after it has formed (Figure 2.1, step C). For ligation reactions, however, turnover is minimal under isothermal conditions owing to the enhanced affinity of the template for the ligated product.<sup>11</sup> Consequently, many detection strategies have focused on template-triggered scission and transfer reactions rather than ligations to avoid this product inhibition.<sup>11</sup> One method for introducing turnover into ligation

reactions exploits the sensitivity of DNA to destabilizing modifications present in the middle of a duplex.<sup>5, 12, 13</sup> By ligating strands at such a destabilizing site, one can modulate the stability of the hybridized complex without changing the temperature or any other reaction condition.<sup>14</sup> If the stabilities of the complexes before and after ligation are properly balanced, isothermal turnover should be achieved.

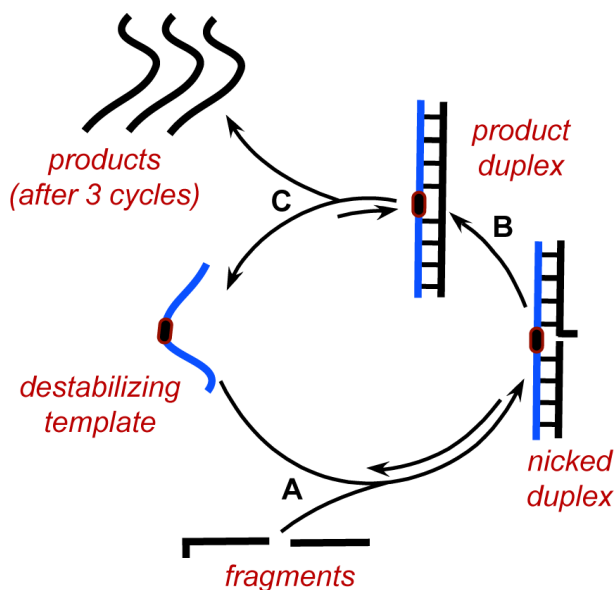


**Figure 2.1:** Isothermal turnover in DNA-templated ligation reactions using destabilizing templates.

In this chapter, I will discuss a general strategy for achieving turnover in template for ligations using T4 DNA ligase. Utilizing modified DNA template strands, the product duplex is destabilized after ligation. As a result, the template strand is released, freeing it to template more ligation reactions. Introducing turnover into simple, enzymatic ligation reactions provides an avenue for amplifying DNA-based assemblies constructed by enzymatic ligation.<sup>15-17</sup>

Isothermal ligation strategies also have potential applications in cross-catalytic replication of DNA, which represents a general method for amplifying any DNA sequence.<sup>6,7</sup>

## 2.2 Introduction of a destabilizing group for isothermal amplification

Two of the most successful examples of isothermal turnover in non-enzymatic, chemical ligation systems were reported by Kool and Seitz, which proved useful in DNA and mRNA detection.<sup>11, 13</sup> In the Kool system, destabilization was introduced in a ligating probe strand by adding an alkyl group between the terminal nucleotide and the electrophilic end.<sup>18</sup> After ligation with a nucleophilic probe using target DNA as a template, the resulting alkyl bridge caused the product duplex to dissociate. With this example in mind we

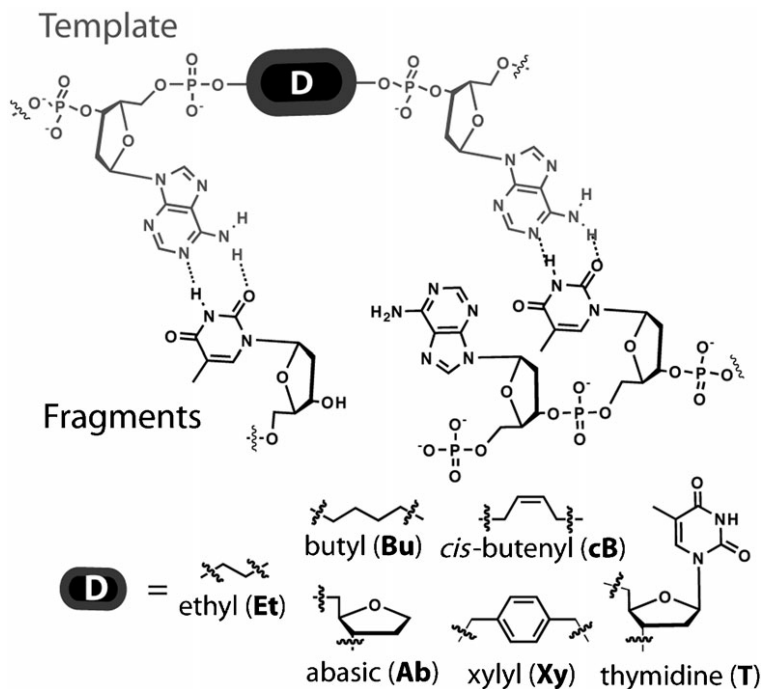


**Figure 2.2:** The nicked site prior to ligation. The destabilizing templates contain a modification (**D**) in place of a thymidine. The perfect template contains the complementary thymidine (**T**).

synthesized DNA templates containing short alkyl chains in place of a complementary nucleotide (Figure 2.2). We also investigated a model abasic DNA lesion known to destabilize DNA duplexes (Figure 2.2, **Ab**).<sup>19</sup> Previously, PNA analogues of abasic groups have been demonstrated by Seitz to avoid product inhibition<sup>20</sup> and improve selectivity<sup>21</sup> in chemical ligation systems using PNA. Here, the abasic group results in a template that is missing a base but still contains the canonical phosphate-sugar backbone.

## **2.3 Results and Discussions**

### **2.3.1 Tuning DNA stability with destabilizing groups**

Achieving the greatest turnover requires that the product duplex be less stable than the nicked duplex (Figure 2.1). However, because of multivalency<sup>22</sup> the product duplex is invariably more stable, even with the destabilizing modification. As a result, a more reasonable goal is to introduce a modification that renders the product and nicked duplexes closer in stability, so that a temperature can be found where both can form but remain labile. To determine whether the duplex stabilities of our destabilizing templates were optimal, we monitored their thermal dissociation behavior. The temperature at which half the duplex has dissociated is the melting temperature ( $T_m$ ), providing a way to compare duplex stabilities.

The thermal dissociation curves are shown for the nicked duplexes (template+two probes) and the product duplexes (template+product) in Figure 2.3 A and B, respectively. The 18-base sequence used in these experiments and the

position of the nicked site and destabilizing group are given in Figure 2.3C.

To illustrate the extent of destabilization, we compared these results with the behavior of a perfectly complementary system (Figure 2.3 A and B, black solid traces, where **D**=thymidine). For all of the destabilizing templates, the decrease in  $T_m$  between the nicked and corresponding product duplexes was 18–22 °C. In contrast, the  $T_m$  difference was 27 °C for the natural DNA system (Figure 2.3 D). The smaller  $\Delta T_m$  for the destabilized templates suggested that a temperature might be found where hybridization of the nicked duplex (Figure 2.1, step A) and dissociation of the product duplex (Figure 2.1, step C) were both possible. It still remain to be seen, however, whether the T4 DNA ligase, known to ligate mismatched DNA,<sup>23</sup> would tolerate nonnatural modifications on the DNA template strand.

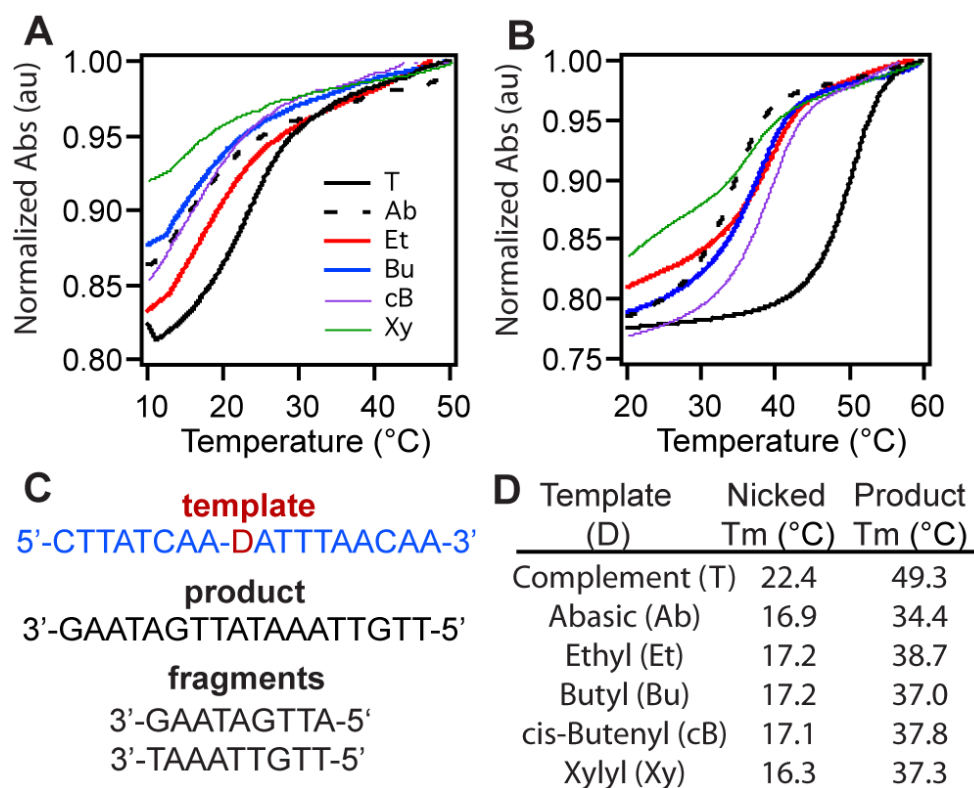


**Figure 2.3:** The thermal dissociation profiles of A) nicked duplexes (template:probes) and B) product duplexes (template:product). [DNA]=1.3  $\mu$ M per strand (pH 7.0, 20 mM PBS, 10 mM MgCl<sub>2</sub>). C) Sequence of strands where **D** is thymidine or a destabilizing group. D) Table of dissociation (melting) temperatures ( $T_m$ ).

### 2.3.2 Monitoring ligation with various destabilizing templates

In our ligation experiments, the template was mixed with the complementary reactive strands (containing a 3'-OH and 5'-phosphate at the ligation site) and 1 unit of T4 DNA ligase for each 15- $\mu$ L reaction.<sup>24</sup> We labeled the 5' end of one of the probes with fluorescein to follow ligation by fluorescent imaging after separation by denaturing polyacrylamide gel electrophoresis (PAGE). The gel image in Figure 2.4 A illustrates the ligation mixtures with one equivalent of template after 20 h of reaction time, where a product band was



evident for all of the destabilizing templates. This result is significant since it proves that T4 DNA ligase tolerates non-natural modifications to the DNA template near the site of ligation. It is important to note that ligation with all the destabilizing templates was hampered when the ligation site was opposite the 5' end rather than the 3' end of the destabilizing group (see Figure 2.5).

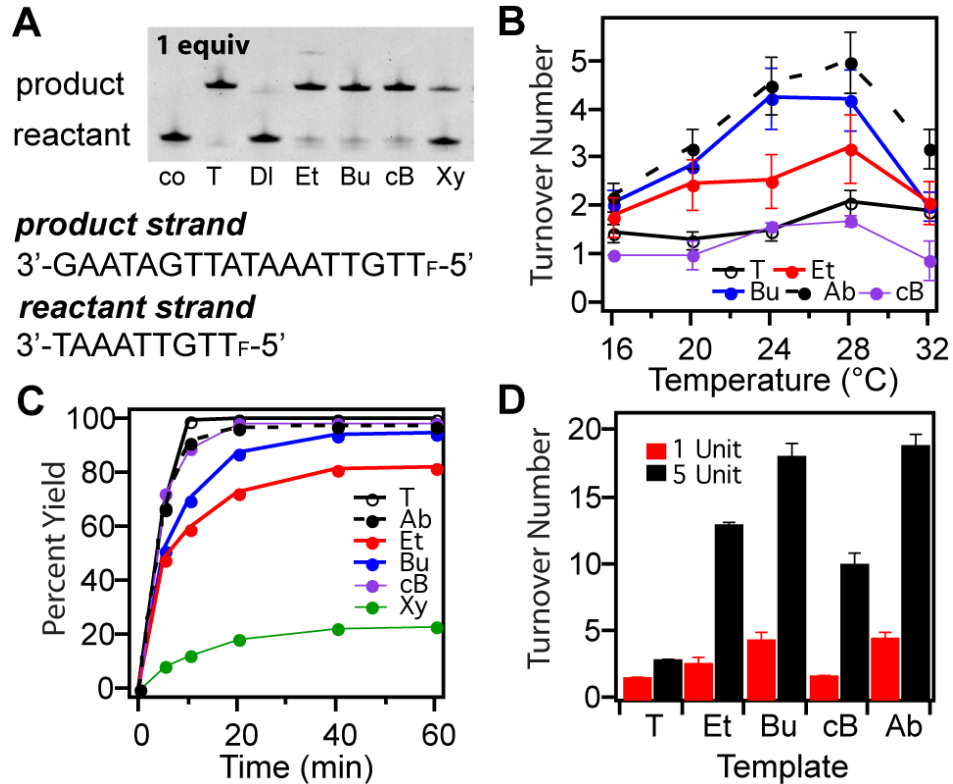


**Figure 2.4:** Template labels: **co** - no template; **T** thymidine; **del** deletion; **Et** ethyl; **Bu** butyl; **cB** *cis*-butenyl; **Xy** xylyl; **Ab** abasic. A) Fluorescent images of denaturing polyacrylamide gels for ligation mixtures using fluorescein-labeled thymine (**T<sub>F</sub>**) with 1 equiv template. B) Turnover number (TON) versus temperature for ligations with 0.01 equiv template. C) Percent yield versus time with 1 equiv template. D) TON versus enzyme concentration (1 unit vs. 5 unit) with 0.01 equiv template at 24 °C. Conditions unless otherwise noted: 1 equiv (1.4 μM) **T<sub>F</sub>**-labeled reactant, 1 unit T4 DNA ligase, 20 h, 16 °C.

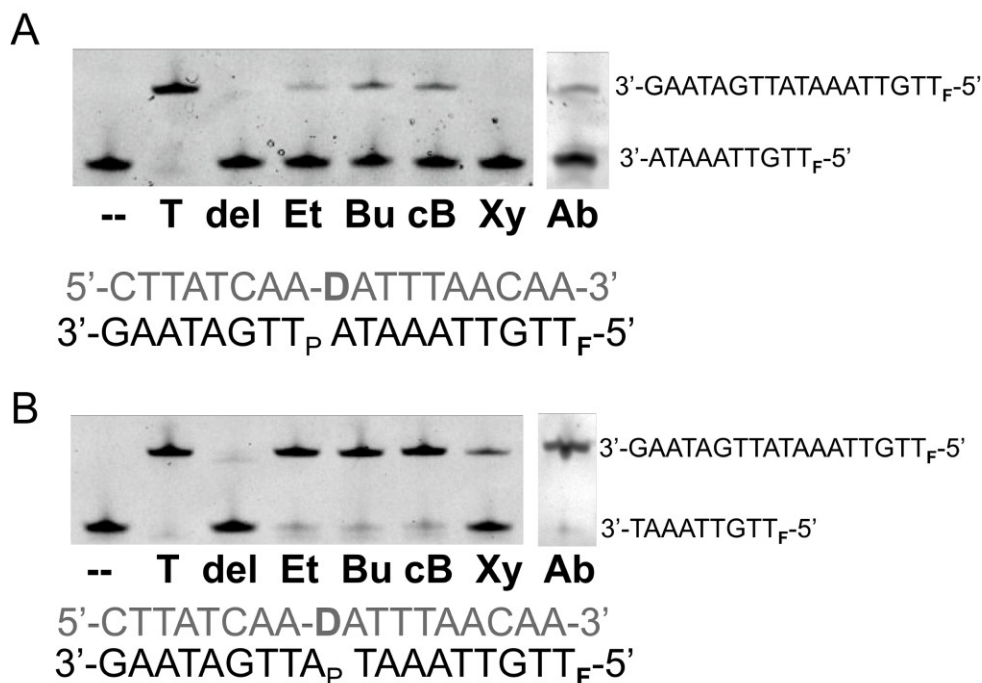


**Figure 2.5:** Template Labels: --, no template; (**T**) D = thymidine; (**del**) D = deletion; (**Et**) D = ethyl; (**Bu**) D = butyl; (**cB**) D = cis-butenyl; (**Xy**) D = xylyl; (**Ab**) D = abasic. Denaturing PAGE analysis of ligation reactions using one equivalent of different templates and two probe strands that position the nicked site on opposite ends of the destabilizing group. A) Ligation of 8-base and 10-base probes places the ligation site across from the 5' end of the destabilizing modification, which severely decreased the yield. B) In contrast, the reaction of two 9-base probes with the ligation site across from the 3' end of the destabilizing group proceeded smoothly.

### 2.3.3 Monitoring turnover with destabilizing templates

To determine whether these destabilizing templates could turn-over in the reaction, we next monitored the ligation reaction with substoichiometric amounts of template. At 20 °C, when 0.01 equivalents of complementary template (**T**) were used only 1.3 % of the fluorescent probe strand was ligated, indicating that the dissociation of the perfect product duplex was unfavorable. In contrast, using the same amount of an abasic template (**Ab**) led to 3.2 % of the ligated product. From

the ratio of [product]/[template] the turnover number (TON) was calculated. As shown in Figure 2.4 B, the degree of turnover for the perfect template (**T**) was between 1 and 2 for all reaction temperatures using 0.01 equivalents of template. In contrast, the turnover was greater than 2 for several of the destabilizing templates. The only inactive templates that yielded little or no ligated product under these substoichiometric conditions were the xylyl template (**Xy**) and a template containing a deletion of the thymidine (**del**, data not shown). With the *cis*-butenyl template, turnovers were between 0.9 and 1.7, which indicated that this rigid linkage did not promote catalytic behavior.

For all of the active destabilizing templates, the highest TON was observed at 28 °C, well above the melting temperature of their corresponding nicked duplexes (Figure 2.4 B). Specifically, the highest TON observed at this enzyme concentration was 5.0 for the abasic template (Figure 2.4 B, **Ab**). To explain the temperature trends, we propose that the decrease in nicked duplex stability at 28 °C is compensated by the higher rate of ligation or dissociation of the product duplex. At temperatures higher than 28 °C, however, the decrease in TON suggests that the formation of the nicked duplex becomes unfavorable. Importantly, at all temperatures, no background ligation was observed in the absence of template (Figure 2.4 A, **co**). The enzyme requires that the DNA to be double-stranded eliminated any background reaction illustrating a major advantage to this approach. Moreover, these results also suggest that employing a catalyst which favors double-stranded DNA might be a way to avoid non-templated background in chemical ligations.<sup>5</sup>

To see how the destabilizing template influenced the rate of ligation, we measured the yield versus time using one equivalent of template. As shown in Figure 2.4 C, within 10 min ligation was completed when natural DNA template (**T**) was used.<sup>25</sup> Most of the destabilizing templates are only a little slower with the **Ab** and **cB** template requiring 20 min, and the other templates requiring less than 40 min.<sup>26</sup> Comparing our results with those of chemical ligation methods that demonstrate lower rates of ligation<sup>18, 27</sup> indicates that faster ligation methods lead to greater turnover, which is consistent with previous reports on isothermal chemical ligation methods.<sup>20, 21</sup> The corresponding PAGE images of the kinetic experiments are given in Figure 2.6.

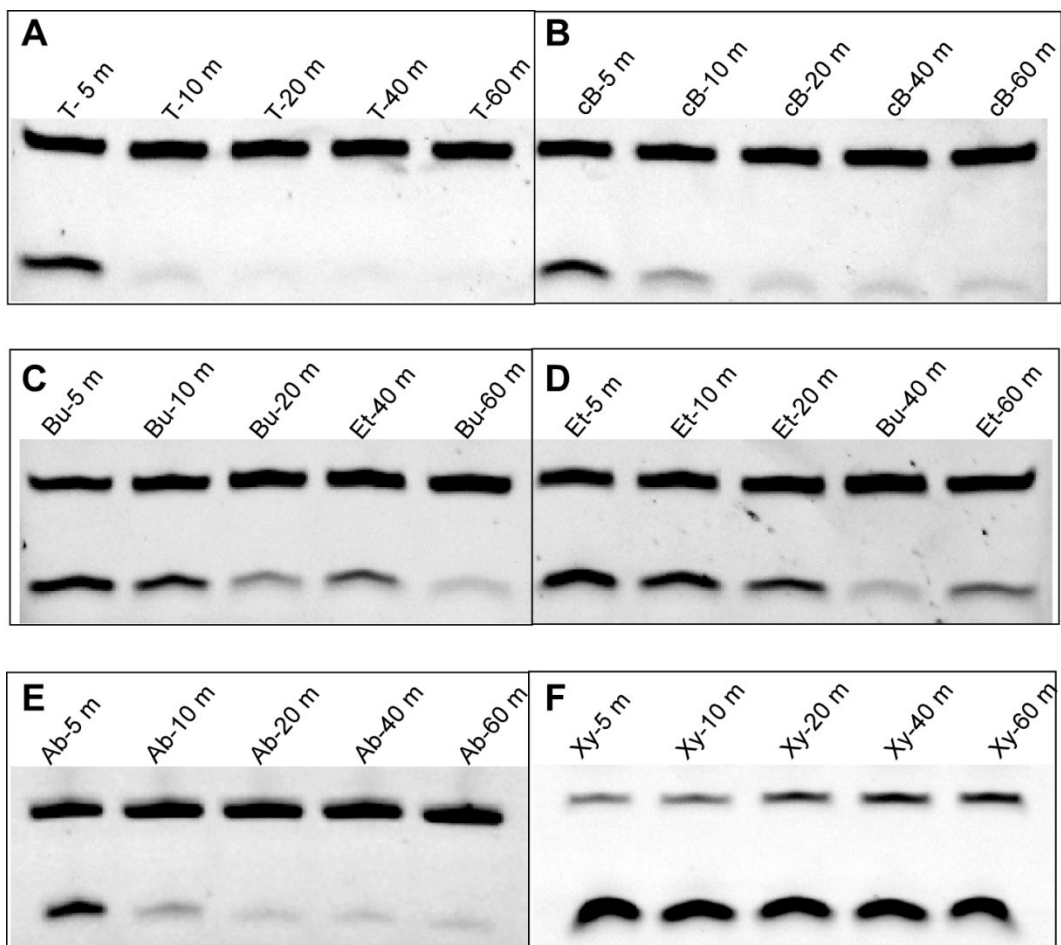


**Figure 2.6:** Representative PAGE images of the kinetics of ligation with different destabilizing templates A) regular template (**D=T**), B) cis-butenyl template (**D=cB**), C) butyl template (**D=Bu**), D) ethyl template (**D=Et**), E) abasic template (**D=Ab**) and F) xylyl template (**D=Xy**).

### 2.3.4 Effect of concentration of enzyme on turnover number (TON)

In the experiments described above we used the typical ligase concentration for ligating nicked duplexes of 1 Weiss unit enzyme per equivalent of fluorescent probe strand (1.4  $\mu\text{M}$ , 15  $\mu\text{L}$ ). To see whether increasing enzyme concentration would increase the amount of turnover, ligation reactions using concentrated enzyme (5 Weiss units per reaction) were performed with the same amount of template (0.01 equivalents). At higher enzyme concentration, the perfect DNA template (**T**) still exhibited a TON close to one. In contrast, the **Bu** and **Ab** templates generated 18 product strands per template (Figure 2.4 D), which is 5-fold higher than the maximum turnover number of 3.5 previously reported by the Seitz group using similar probe (1.2  $\mu\text{M}$ ) and template (12 nM) concentrations.<sup>20</sup> Although both Kool<sup>18</sup> and Seitz<sup>20</sup> report higher TONs (91.6 and 226, respectively) these were only achieved by increasing the probe:template ratio to 10 000, which facilitates dissociation of the product duplex. This required the use of HPLC or radio-imaging with PAGE, which allowed them to reliably distinguish 0.0916 % or 0.226 % of product formed from reactions with non-negligible background. In contrast, our approach has the advantage of no background reaction when template is absent. Moreover, T4 DNA ligase, standard DNA ligating groups, and the commercially available abasic destabilizing modifications should prove more accessible to non-synthetic labs than these chemical methods.

### 2.3.5 DNA self-replication with a cross-catalytic approach

This methodology for using catalytic amounts of template to amplify a DNA-ligated material made by T4 DNA ligase can be applied in smart, DNA-based systems. For example, an environmental stimulus can be used to release destabilizing template causing the amplification of a DNA material, like DNA-ligated gold nanoparticle aggregates.<sup>16</sup> If, however, one wanted to use this principle of destabilization for native DNA detection, another complementary

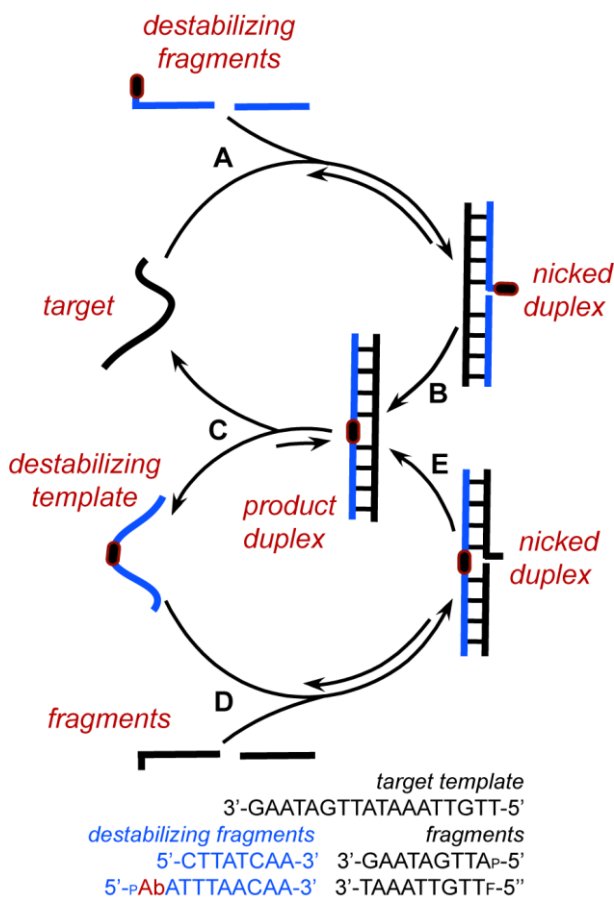


**Figure 2.7:** Cross-catalytic cycles with destabilizing probes.

ligation cycle must be included. Figure 2.7 illustrates a cross-catalytic replication strategy that can be initiated by a native DNA strand representing a target sequence. In this set of experiments, the destabilizing template is formed in situ by a ligation reaction templated by the natural DNA target (Figure 2.7, steps A and B). As a result of ligation, the same product duplex is formed as in the previous cycle. Consequently, the product:template duplex should be destabilized leading to the release of the original target and the newly formed destabilizing template (Figure 2.7, step C). This destabilizing template can now generate a copy of the original target template (Figure 2.7, steps D and E), which goes on to catalyze the formation of more destabilizing templates. As the product of each cycle is a template for the other, significant amplification of the original target should ensue.

To verify that we could observe cross-catalysis, we combined the probe strands listed in Figure 2.7, including a fluorescent modified probe corresponding to the bottom cycle ( $T_F$ , fluorescein-modified thymine). We then introduced a target DNA sequence which, although active in the top cycle, should have no effect on the fluorescein-labeled probe. Therefore, the formation of any fluorescent ligated product would signify cross-catalysis. Previous reports suggested that T4 DNA ligase would ligate a destabilizing probe terminated with a 5'-phosphate abasic group.<sup>28</sup> Indeed, as shown in Figure 2.8 target-initiated cross catalysis occurred for the **Ab**-substituted system. Not only did we observe self-replication in this two-cycle system, but we found this system also exhibited cross-catalytic TON (defined as [product]/[initial template]) greater than that for



the single catalytic cycle (TON 14 vs. 4.5; Figure 2.8, CC vs. SC, respectively). Decreasing the number of equivalents of template further increased the number of cross-catalytic turnovers (CC\*), indicating that dissociation is favored as the probe:template ratio becomes larger.<sup>18, 20</sup> The highest cross-catalytic turnover of 32 corresponds to the target undergoing on average 32 cycles of self-replication (Figure 2.8, CC\*). As a point of reference, our system exhibits the same number of self-replication cycles as shown by Albagli et al. in one of the few reported cross-catalytic chemical ligation systems applicable to DNA amplification and detection.<sup>29</sup> In their system, however, temperature cycling was used to achieve turnover, whereas our system requires no mechanical or thermal intervention.

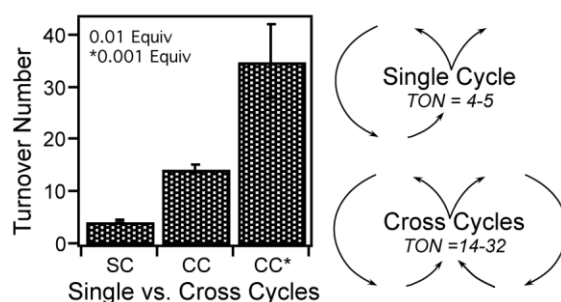


**Figure 2.8:** SC: Single-catalyst cycle using an abasic destabilizing template and probes. CC: Cross-catalytic cycle using target as template and probes, one of which contained an abasic group. Conditions: 0.01 equiv template (14 nM); \*0.001 equiv (1.4 nM); 1 unit T4 DNA ligase; 24 °C; 20 h.

For the cross-catalytic reactions using 1 Weiss unit of ligase and the 5'-phosphate abasic probe, we observed a small level of background (0.5 % and 3.7 % product at 20 and 24 °C, respectively, with no template present).<sup>30</sup> In contrast, the 5'-phosphate thymidine probe exhibited a large amount of

background (25 % ligation product at 20 °C) (Figure 2.9). The reason for the high background in the natural system is based on our probe design, which leads to a one-base overhang of thymidine on one probe and deoxyadenosine on the other. Ligation between “sticky-ends” can occur in the case of the native DNA due to complementary interactions, even when no template is present (Figure 2.9 B). Although this overhang exists in our **Ab**-modified system, replacing the thymidine with the abasic group prevents hydrogen bonding with the adenine, thus minimizing nonspecific joining of the probes. Consequently, very little background ligation is observed. In both cases, one equivalent of template prevents cross catalysis (see PAGE image in Figure 2.9). At this high concentration of template, dissociation from the ligated product is not favored. Consequently, the newly generated template for the second cycle is not released, preventing cross catalysis.

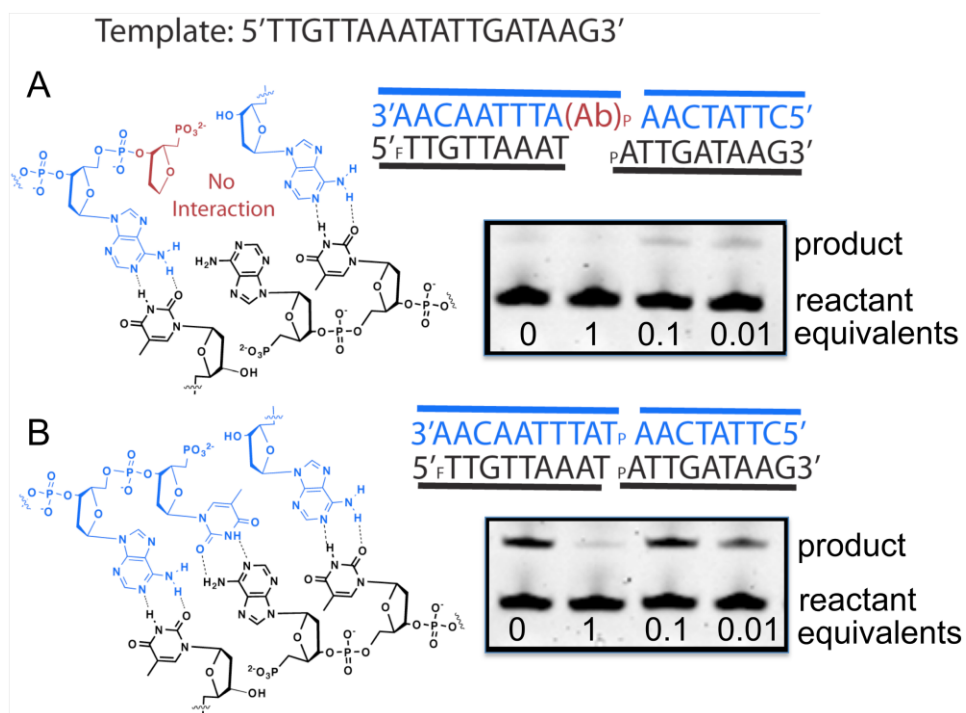


**Figure 2.9:** Cross-catalysis using varying equivalents of template (Sequence A). In these reactions there are four probe strands present, which can hybridize to form duplexes each with a one base overhang. The molecular structure, sequences, and PAGE analysis of: A) reactions between probes containing a 5'-abasic overhang and a 5'-deoxyadenosine overhang. B) reactions between probes containing a 5'-thymidine and 5'-deoxyadenosine overhang. Conditions: 20 h; 20 °C; 1 Unit T4 DNA ligase; 1 equivalent (1.4  $\mu$ M) fluorescein-labeled probe ( $T_F$ ); 2 equivalents of each other probe.

## 2.4 Conclusion

In conclusion, we have demonstrated that DNA templates for enzymatic ligation reactions can turn-over in the ligation cycle by introducing a destabilizing modification into the template strand. This work complements previous studies illustrating how destabilizing probes can be used to facilitate turnover.<sup>11, 13</sup>

Additionally, the turnover numbers observed in our system are higher than the best isothermal chemical ligation strategies at similar strand lengths, concentrations, and ratios.<sup>11, 13</sup> We have also taken this idea a step further by adding in another cycle that leads to a self-replicating DNA system using destabilization to overcome product inhibition. The success of the **Ab** templates in both cycles is especially promising as this phosphoramidite is commercially available allowing simple access to templates capable of turnover. Not only will this strategy enable advances in nanotechnology in the replication of DNA materials, but it should also be useful in isothermal target amplification for the broad field of DNA diagnostics. Finally, with simple destabilizing groups and rapid ligation methods, turnover and target-initiated self-replication are now possible, which should reinvigorate interest in autonomous DNA replication.<sup>4-6</sup>

## **2.5 Experimental**

### **2.5.1 General**

All of the destabilizing phosphoramidites, with the exception of the commercially available dSpacer group, were synthesized by Rohan Bhogal or Alexandra Tang. The corresponding destabilizing templates were also prepared as detailed below by Rohan Bhogal and Alexandra Tang. For completeness, these syntheses are included in this chapter. Several of the melting experiments were performed by Jade Lam, Rohan Bhogal and Alexandra Tang. Initial proof-of-concept ligation experiments were performed by Jade Lam and Rosalie McKay, but that data are not included in this chapter. Some DNA sequences were also

prepared by J. Lam and R. McKay and used herein. Chemicals were purchased from Fisher, VWR or Aldrich and used as received. Significantly, 2-cyanoethyl-N,N-diisopropylchloro phosphoramidite was purchased from Aldrich (cat # 302309-1G) and *cis*-2-butene-1,4-diol was purchased from Alfa Aesar (cat # A19182). Melting analyses of DNA-containing materials were performed using an HP 8453 diode-array spectrophotometer equipped with a HP 89090A Peltier temperature controller. The temperatures for DNA experiments were maintained using a Torrey Pines Scientific Echotherm Chilling/Heating Plate Model IC22. PAGE was performed using the Bio-Rad Mini-PROTEAN Tetra Cell System (cat. #165-8000). The gels were imaged using ImageQuant RT ECL Imager from GE Healthcare Life Science using UV transillumination. The DNA was synthesized on an Applied Biosystems Model 392 DNA/RNA Synthesizer. High-resolution mass spectrometry was performed on an Agilent Technologies 6220 Accurate-Mass TOF.  $^1\text{H}$ ,  $^{13}\text{C}$  and  $^{31}\text{P}$  NMR spectra were recorded on a Varian INOVA 400 FT-NMR spectrometer (399.795 MHz for  $^1\text{H}$  NMR, 100.538 MHz for  $^{13}\text{C}$  NMR, and 161.839 MHz for  $^{31}\text{P}$  NMR).  $^1\text{H}$  NMR data are reported as follows: chemical shift [multiplicity (b = broad, s = singlet, d = doublet, t = triplet, q = quartet, qn = quintet, and m = multiplet), integration, and peak assignments].  $^1\text{H}$  and  $^{13}\text{C}$  chemical shifts are reported in ppm downfield from tetramethylsilane (TMS).  $^{31}\text{P}$  chemical shifts are reported in ppm downfield from an external phosphoric acid standard.

## 2.5.2 Preparation of DNA strands

DNA was synthesized on an ABI 392 solid-phase synthesizer using Glen Research reagents. DNA strands were purified by Glen-Pak DNA Purification cartridges (cat. 60-5200-01) according to the DMT-On protocol. Standard nucleotide phosphoramidite and the following were used: Chemical Phosphorylation Reagent II (cat. 10-1901-90), Fluorescein-dT Phosphoramidite (cat. 10-1056-95), and dSpacer CE Phosphoramidite (cat 10-1914-90) for the abasic (**Ab**) template and probes. All other destabilizing templates were prepared from the corresponding protected diols with solid-phase synthesis. OligoCalc (<http://www.basic.northwestern.edu/biotools/oligocalc.html>) was used to determine the extinction coefficients where the destabilizing templates' absorptivity was assumed to be **DNA-II<sub>D</sub>**, with **D**=a deletion.

**Table 2.1.** DNA sequences used in this study

<b>DNA-I System</b>	
<b>DNA-I</b>	5'-TTGTTAAATATTGATAAG-3'
<b>DNA-II<sub>D</sub></b>	5'-CTTATCAADATTTAACAA-3'
<b>rDNA-Ia</b>	5'- <sub>F</sub> TTGTTAAAT-3'
<b>rDNA-IIa</b>	5'- <sub>p</sub> <b>D</b> ATTTAACAA-3'
<b>rDNA-Ib</b>	5'- <sub>p</sub> ATTGATAAG-3'
<b>rDNA-IIb*</b>	5'- <sub>F</sub> CTTATCAA-3'

**rDNA** = replicator DNA sequences; F = fluorescein, **D** = thymidine (**T**), abasic (**Ab**), deletion (**del**), ethyl (**Et**), butyl (**Bu**), cis-butenyl (**cB**), xylyl (**Xy**), ; P = phosphate \*In standard cross-catalysis experiments, **rDNA-IIb** contained no fluorescein label.

## 2.5.3 Synthesis of the destabilizing templates (strand DNA-II<sub>D</sub>, where D ≠ thymidine)

### 2.5.3.1 Preparation of dimethoxytrityl (DMT)-protected diols

The abasic template and 5'-phosphate abasic probe were prepared using the dSpacer CE Phosphoramidite according to the instructions from Glen Research and purified using the DMT-on procedure with their Glen-Pak solid-phase purification cartridges (Glen Research). All other destabilizing templates were prepared from the corresponding diols using the typical reactive groups and solid-phase synthesis. Specifically, the dimethoxytrityl (DMT)-protected phosphoramidites from ethyl,<sup>31</sup> xylyl, cis-butenyl,<sup>32</sup> and butyl<sup>33</sup> diol were prepared according to the following procedures. The resulting strands were purified using the DMT-on procedure with Glen-Pak solid phase purification cartridges (Glen Research). The characterization data for the xylyl derivative are listed below.

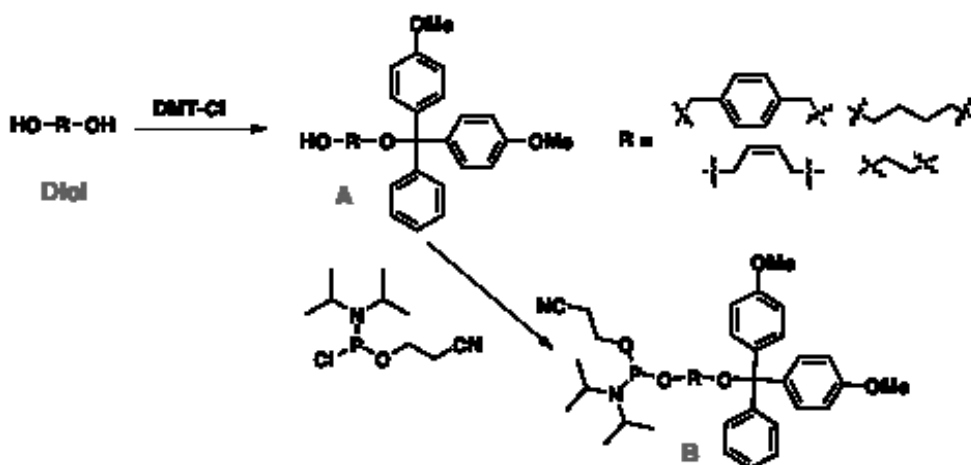


**Figure 2.10:** Scheme of synthesis of phosphoramidites with destabilizing modification.

### 2.5.3.2 Typical preparation of the mono-DMT protected diols (Figure 2.10, Compound A)

These syntheses were performed by A. Y. Tang and R. S. Bhogal. Excess diol (37 mmol) was weighed in a 50-mL round bottom flask equipped with a stir bar, dissolved in THF (15 mL) and cooled in an ice bath. Triethylamine (0.42 mL, 3.0 mmol) was added to the solution followed by the addition of dimethoxytrityl chloride (1.0 g, 3.0mmol) in THF (10 mL) over a period of ten minutes. The mixture was capped with a septum, allowed to reach room temperature, and stirred overnight. When the reaction was complete based on monitoring by TLC, the reaction mixture was rotovaped to dryness. The crude product was dissolved in dichloromethane (50 mL), and the organic layer was washed with aqueous sodium bicarbonate (2 x 50 mL). The aqueous washes were then combined and extracted with dichloromethane (50 mL). The organic phases were combined, dried over sodium sulfate, and concentrated using a rotary evaporator.

The crude products were purified using silica gel chromatography with an eluent mixture of 2:3 ethyl acetate to hexane. Yields: 2-[(4,4'-Dimethoxytrityl)oxy]ethanol 67.9%; 4-[(4,4'-Dimethoxytrityl)oxy]butanol 58.3%; 4-[(4,4'-Dimethoxytrityl)oxy]-2-cisbutenol 68.3%. The presence of the products was verified for all but the xylyl derivative by comparing their characterization data to the reported literature values.<sup>31-33</sup>



Characterization of xylyl derivative 4-[(4,4'-dimethoxytrityl)oxymethyl]benzyl alcohol

Yield: 76.5% <sup>1</sup>H NMR (CD<sub>2</sub>Cl<sub>2</sub>): δ 3.79 (s, 6H, Ar-OCH<sub>3</sub>), 4.14 (s, 2H, Ar-CH<sub>2</sub>O-), 4.67 (d, 2H, Ar-CH<sub>2</sub>OH), 6.85 (d, 4H, Ar-H), 7.23 (m, 1H, Ar-H), 7.23-7.40 (m, 10H, Ar-H), 7.50 (m, 2H, Ar-H) <sup>13</sup>C NMR (CD<sub>2</sub>Cl<sub>2</sub>): δ 55.60, 65.30, 65.77, 86.81, 113.49, 127.13, 127.27, 127.60, 128.22, 128.50, 130.42, 136.64, 138.96, 140.57, 145.65, 159.04. High-Resolution Mass Spectrometry: Found: 463.1875; Calc.: 463.1880; Diff (ppm) -1.13; Formula: C<sub>29</sub>H<sub>28</sub>NaO<sub>4</sub>; Ion (MNa)<sup>+</sup>.

**2.5.3.3 Preparation of the corresponding phosphoramidites (Figure 2.10, Compound B)**

These syntheses were performed by A. Y. Tang and R. S. Bhogal. The DMT-protected diol (0.26 mmol) was dissolved in DCM (5 mL) and added to a 50-mL round bottom flask equipped with a stir bar. *N,N*-Diisopropylethylamine (0.1 mL, 0.57 mmol) was then added to the round bottom flask, after which the solution was degassed with nitrogen gas for 10 minutes. The compound 2-cyanoethyl *N,N*-diisopropylchlorophosphoramidite (61.5 mg, 0.26 mmol) was weighed into a syringe and immediately added to the degassed solution. The round bottom flask was wrapped in foil, and the solution was stirred under nitrogen for 2 hours. The phosphoramidite is readily oxidized by air, so the reaction mixture was quickly concentrated to dryness and redissolved in 1 mL CDCl<sub>3</sub>. <sup>31</sup>P NMR confirmed the presence of the phosphoramidite by the distinctive signal at δ 149 ppm. The phosphoramidite solution in CDCl<sub>3</sub> was immediately coupled to the DNA on the solid-phase using syringe synthesis.

#### **2.5.3.4 Preparation of destabilized templates using the synthesized phosphoramidites**

These syntheses were performed by A. Y. Tang and R. S. Bhogal. The first half of the DNA strand was synthesized from the 3'-5' synthesis in the typical manner on the DNA synthesizer. Immediately after the nucleotide at the 10th position had been deprotected to generate a 5'-OH, the DNA was removed from the synthesizer. The CDCL<sub>3</sub> solution of phosphoramidite (0.5 mL) described above was placed in a syringe which was connected to the DNA solid-phase column. The tetrazole Activator solution (0.5 mL, Glen Research cat # 30-3100-52) was placed in another syringe, and this syringe was connected to the other end of the DNA column. The two solutions were mixed back and forth following typical syringe synthesis.<sup>34</sup> After reacting the phosphoramidite solution in this manner for 10 minutes with the DNA on the solid-phase, the solution was removed, and the solid-phase was washed with acetonitrile (2 x 1 mL). The column now containing the modified DNA on the solid-phase was then placed back on the synthesizer, and the synthesis was continued after the typical capping and oxidation steps were performed.

#### **2.5.4 Mass analysis of the DNA strands**

The modified DNA templates were characterized by MALDI-TOF using a matrix solution consisting of 2,4,6-trihydroxyacetophenone in 1:1 acetonitrile:water (20 mg/mL) combined in a 9:1 ratio with aqueous ammonium citrate solution (50 mg/mL). About 1 nmol of each DNA sample was dissolved in triethyl ammonium acetate (0.1 M TEAA, pH 7.0) and desalted using C18 Ziptip

pipette tips (ZipTip, Millipore) according to their procedure. After desalting, the DNA was finally eluted from the ZipTip using 5  $\mu$ L of matrix/ammonium citrate solution by repeating aspiration and dispersion three times and dispensing the sample into a microcentrifuge tube. The desalted DNA/matrix/ammonium citrate solution (0.6 to 1  $\mu$ L) was spotted on a MALDI target and allowed to dry. MALDI-MS was then performed on a Voyager Elite (Applied BioSystems, Foster City, CA, USA) time of flight-mass spectrometer in linear negative mode. Bovine insulin and Bovine insulin chain B were used to calibrate the instrument. The presence of the modifier was confirmed by comparing  $z \cdot m/z$  with the calculated values: Ethyl Template: Calc.: 5261, Found: 5260; Butyl Template: Calc.: 5289, Found: 5288; cis-Butenyl Template: Calc.: 5287, Found: 5283; Xylyl Template: Calc.: 5337, Found: 5336.

### **2.5.5 Thermal dissociation experiments**

These experiments were performed by myself, R. S. Bhogal, A. Y. Tang and J. Lam. 1.3 nmol of each DNA sequence (**DNA-II<sub>D</sub>** and **DNA-I** for the product duplex experiments and **DNA-II<sub>D</sub>**, **rDNA-Ia**, and **rDNA-Ib** for the nicked duplex experiments) were combined in PBS buffer (1.0 mL, 10 mM MgCl<sub>2</sub>, 20 mM PBS, pH 7.0) and hybridized for ca. 15 min. While stirring at 100 rpm, the absorbance readings at 260 nm were taken from 10 to 60 °C at 1 °C intervals, with 1 min hold time.

### **2.5.6 Melting profile analysis**

The maximum of the first derivative of the melting profile is often used to determine the melting temperature ( $T_m$ ). However, for the ternary complexes we

observed that the initial change in absorbance due to melting was often the steepest part of the transition, leading to a lower estimate of the melting temperature. Therefore, we selected another approach, which allows the  $T_m$  to be determined by fitting the following equation to the corrected melting profile.<sup>35,36</sup>

$$f(T) = \frac{1}{1 + \exp\left(\frac{\Delta H}{R} \left(\frac{1}{T} - \frac{1}{T_m}\right)\right)}$$

where  $f$  is the fraction of single-stranded DNA as a function of temperature.  $\Delta H$  was an additional fit parameter that was allowed to vary and influences the sharpness of the transition. The data were constrained to ensure that the fit was best at  $f(T) = 0.5$ , which led to the most accurate value for  $T_m$  (where  $f(T_m) = 0.5$ ).

### 2.5.7 Ligation experiments

Strand amounts: Single-cycle reactions: **rDNA-Ia** 1 equiv; **rDNA-Ib** 2 equiv; template (**DNA-II<sub>D</sub>**) 1 or 0.01 equiv. Cross-cycle reactions: **rDNA-Ia** 1 equiv; **rDNA-Ib** 2 equiv; **DNA-I** 0.01 or 0.001 equiv; **rDNA-IIb** 2 equiv; and 2 equiv of either strand **rDNA-IIa(D = T/Ab)**. In a typical ligation, where 1 equiv = 20.3 pmol, the appropriate amounts of DNA probes and template were first combined in water in a 400  $\mu\text{L}$  minicentrifuge tube to reach a final volume of 10  $\mu\text{L}$  and incubated at the desired reaction temperature. While several of these DNA solutions incubated, in a separate mini-centrifuge tube, T4 DNA ligase (8  $\mu\text{L}$ ) at lower concentration (1 unit  $\mu\text{L}^{-1}$ , Invitrogen cat. 15224-017) or higher concentration (5 unit  $\mu\text{L}^{-1}$ , Invitrogen cat. 46300-018) was mixed with ligation buffer (24  $\mu\text{L}$ , 5 $\times$  concentrated) and water (8  $\mu\text{L}$ ). A portion of this ligase mixture

(5  $\mu\text{L}$ ) was immediately added to each of the DNA solutions (final  $[\text{DNA}] = 1.4 \mu\text{M}$  for each equivalent). The reactions were then placed in a covered thermal incubator for 20 h unless otherwise noted. To stop ligation,  $\text{EDTA}_{(\text{aq})}$  (1  $\mu\text{L}$ , 0.5 M) was added for every unit of enzyme present. For the kinetic experiments, aliquots (3  $\mu\text{L}$ ) were removed from the bulk ligation mixture at various reaction times and placed in a separate microcentrifuge tube containing  $\text{EDTA}_{(\text{aq})}$  (1  $\mu\text{L}$ , 0.5 M). Samples were stored at 4  $^{\circ}\text{C}$  until analyzed by 15 % denaturing PAGE.

### **2.5.8 Denaturing Polyacrylamide Gel Electrophoresis**

The ligation mixtures were separated on a denaturing 15% polyacrylamide gel (0.75 mm thick, 10 wells). To prepare the gels, urea (4.8 g) was added to a 50-mL graduated cylinder equipped with a stir bar. In addition to the urea, concentrated Tris/Borate/EDTA (TBE) buffer (1 mL of 5 x TBE) and 40% *Acrylamide/Bis Solution* 19:1 (3.75 mL, Bio-Rad Cat.161-0144) were added to the cylinder, and the mixture was diluted to 10 mL with water. The mixture was then stirred and gently heated on a hot plate. After the urea had completely dissolved, aqueous ammonium persulfate (80  $\mu\text{L}$ , 10% w/v) and tetramethylethylenediamine (TEMED, 10.7  $\mu\text{L}$ ) were added to initiate polymerization. The gel was immediately poured into the gel casting system and was allowed to polymerize for one hour. Following this hour, the gels were used immediately or wrapped in paper towels soaked with running buffer and stored at room temperature overnight. Prior to introducing the ligation mixture, the gels were assembled in a Bio-Rad Mini-PROTEAN Tetra Cell that was then filled with running buffer (1 x TBE). In the meanwhile, the ligation samples were prepared for PAGE by adding

a concentrated solution of running dye (3  $\mu\text{L}$  of 0.25% w/v bromophenol blue in 80% w/v sucrose) to 15  $\mu\text{L}$  of each ligation mixture. Immediately before loading the samples, the wells were rinsed with a syringe containing running buffer to remove any accumulated urea. Finally, 4  $\mu\text{L}$  of the reaction/running dye mixture was loaded into each well, and the gel was run for 80 min at 175 V or until the running dye had travelled 75% down the gel. The gel was immediately imaged in a fluorescent imager with trans-UV illumination and a filter for the fluorescein fluorophore (Filter #4, *ImageQuant RT*). *ImageQuant TL* analysis software was used to analyze the data by quantifying the fluorescence emitted by each band. Baseline subtraction using the rolling ball method with a ball radius of 100 was selected for each image. Percent yield and TON were determined from the product and reactant band intensities and the number of equivalents of template using the following equations:

$$\% \text{ Yield} = \frac{I_{\text{Product Band}}}{I_{\text{Product Band}} + I_{\text{Reactant Band}}} \times 100\%$$

$$\text{TON} = \left( \frac{I_{\text{Product Band}}}{I_{\text{Product Band}} + I_{\text{Reactant Band}}} \right) \times \frac{1}{\text{Template Equivalent}}$$

For the cross-catalysis reactions where some product formed even in the absence of template, TON was determined by subtracting the product fraction formed in the control experiment according to:

$$\text{TON} = \left[ \left( \frac{I_{\text{Product Band}}}{I_{\text{Product Band}} + I_{\text{Reactant Band}}} \right)_{\text{Template}} - \left( \frac{I_{\text{Product Band}}}{I_{\text{Product Band}} + I_{\text{Reactant Band}}} \right)_{\text{No Template}} \right] \times \frac{1}{\text{Template Equivalents}}$$

### 2.5.8.1 PAGE analysis of strand purity

The destabilizing templates were analyzed by denaturing PAGE following the procedure described above and stained with Stain-All (Aldrich cat # E9379). One band corresponding to an 18-base strand was clearly visible for all of the destabilizing templates. The xylyl template showed evidence of decomposition, but the other templates appeared robust at room temperature in buffer for several weeks. The activity of the cis-butenyl template, however, increased with time suggesting some modification to the cis isomer had occurred. As a result both xylyl and cis-butenyl templates were used in ligation reactions within three days of dissolving the lyophilized samples in buffer or water (Figure 2.11).

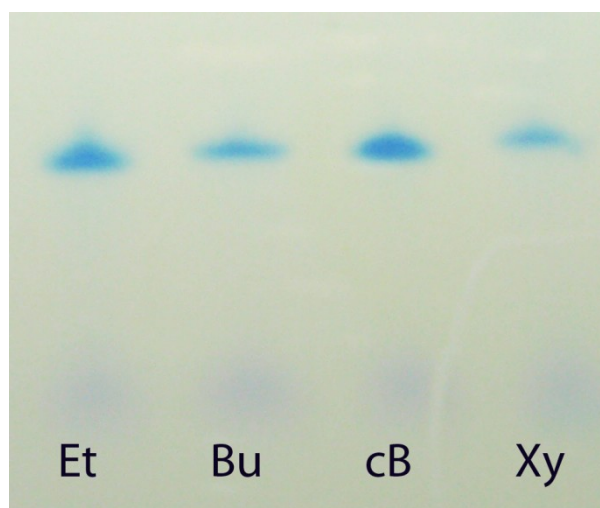


**Figure 2.11:** Stain-All stained denaturing PAGE gel of the destabilizing templates used in this study. The presence of one band corresponding to an 18-base strand indicates that the strands are nearly monodisperse after purification using the DMT-On procedure with Glen Pak cartridges. The faint spot at the bottom of the gel is the bromophenol blue running dye.

## 2.6 References

- 1) Gu, H.; Chao, J.; Xiao, S.-J.; Seeman, N. C.: A proximity-based programmable DNA nanoscale assembly line. *Nature* **2010**, *465*, 202-205.
- 2) Lund, K.; Manzo, A. J.; Dabby, N.; Michelotti, N.; Johnson-Buck, A.; Nangreave, J.; Taylor, S.; Pei, R.; Stojanovic, M. N.; Walter, N. G.; Winfree, E.; Yan, H.: Molecular robots guided by prescriptive landscapes. *Nature* **2010**, *465*, 206-210.
- 3) Lincoln, T. A.; Joyce, G. F.: Self-sustained replication of an RNA enzyme. *Science* **2009**, *323*, 1229-32.
- 4) Zielinski, W. S.; Orgel, L. E.: Autocatalytic synthesis of a tetranucleotide analogue. *Nature* **1987**, *327*, 346-347.
- 5) Ye, J.; Gat, Y.; Lynn, D. G.: Catalyst for DNA Ligation: Towards a Two-State Replication Cycle. *Angew Chem Int Ed* **2000**, *39*, 3641-3643.
- 6) Patzke, V.; von Kiedrowski, G.: Self replicating systems. *ARKIVOC* **2007**, 293-310.
- 7) Paul, N.; Joyce, G. F.: Minimal self-replicating systems. *Curr Opin Chem Biol* **2004**, *8*, 634-639.
- 8) Aldaye, F. A.; Palmer, A. L.; Sleiman, H. F.: Assembling Materials with DNA as the Guide. *Science* **2008**, *321*, 1795-1799.
- 9) Orgel, L. E.: Molecular Replication. *Nature* **1992**, *358*, 203-209.
- 10) Connolly, A. R.; Trau, M.: Isothermal Detection of DNA by Beacon-Assisted Detection Amplification. *Angew Chem Int Ed* **2010**, *49*, 2720-2723.
- 11) Grossmann, T. N.; Strohbach, A.; Seitz, O.: Achieving Turnover in DNA-Templated Reactions. *ChemBioChem* **2008**, *9*, 2185-2192.
- 12) Zhan, Z.-Y. J.; Lynn, D. G.: Chemical Amplification through Template-Directed Synthesis. *J Am Chem Soc* **1997**, *119*, 12420-12421.



- 13) Silverman, A. P.; Kool, E. T.: Detecting RNA and DNA with templated chemical reactions. *Chem Rev* **2006**, *106*, 3775-3789.
- 14) Li, X.; Chmielewski, J.: Peptide Self-Replication Enhanced by a Proline Kink. *J Am Chem Soc* **2003**, *125*, 11820-11821.
- 15) Mendel-Hartvig, M.; Kumar, A.; Landegren, U.: Ligase-mediated construction of branched DNA strands: a novel DNA joining activity catalyzed by T4 DNA ligase. *Nucleic Acids Res.* **2004**, *32*, e2.
- 16) Claridge, S. A.; Mastroianni, A. J.; Au, Y. B.; Liang, H. W.; Micheel, C. M.; Frechet, J. M. J.; Alivisatos, A. P.: Enzymatic Ligation Creates Discrete Multinanoparticle Building Blocks for Self-Assembly. *J. Am. Chem. Soc.* **2008**, *130*, 9598-9605.
- 17) Xue, X.; Zu, W.; Wang, F.; Liu, X.: Multiplex Single-Nucleotide Polymorphism Typing by Nanoparticle-Coupled DNA-Templated Reactions. *J. Am. Chem. Soc.* **2009**, *11668-11669*.
- 18) Abe, H.; Kool, E. T.: Destabilizing Universal Linkers for Signal Amplification in Self-Ligating Probes for RNA. *J. Am. Chem. Soc.* **2004**, *126*, 13980-13986.
- 19) Matray, T. J.; Kool, E. T.: Selective and Stable DNA Base Pairing without Hydrogen Bonds. *J. Am. Chem. Soc.* **1998**, *120*, 6191-6192.
- 20) Dose, C.; Ficht, S.; Seitz, O.: Reducing Product Inhibition in DNA-Template-Controlled Ligation Reactions. *Angew Chem Int Ed* **2006**, *45*, 5369-5373.
- 21) Ficht, S.; Dose, C.; Seitz, O.: As Fast and Selective as Enzymatic Ligations: Unpaired Nucleobases Increase the Selectivity of DNA-Controlled Native Chemical PNA Ligation. *ChemBioChem* **2005**, *6*, 2098-2103.
- 22) Mammen, M.; Choi, S.-K.; Whitesides, G. M.: Polyvalent Interactions in Biological Systems: Implications for Design and Use of Multivalent Ligands and Inhibitors. *Angew Chem Int Ed* **1998**, *37*, 2754-2794.
- 23) Alexander, R. C.; Johnson, A. K.; Thorpe, J. A.; Gevedon, T.; Testa, S. M.: Canonical nucleosides can be utilized by T4 DNA ligase as

universal template bases at ligation junctions. *Nucleic Acids Res.* **2003**, *31*, 3208-3216.

- 24) One unit is the amount of enzyme needed to catalyze the conversion of 1 nmol of <sup>32</sup>P-labeled pyrophosphate into ATP in 20 min at 37°C (Invitrogen). pp One unit is the amount of enzyme needed to catalyze the conversion of 1 nmol of <sup>32</sup>P-labeled pyrophosphate into ATP in 20 min at 37°C (Invitrogen).
- 25) The rate of ligation for perfect template should first be measured to verify the enzyme activity. If the enzyme is less active due to improper storage or handling, no turnover is observed.; pp The rate of ligation for perfect template should first be measured to verify the enzyme activity. If the enzyme is less active due to improper storage or handling, no turnover is observed.
- 26) We attribute the leveling off of the signal for the ethyl and butyl templates to subtle differences in the extinction coefficients used to calculate the DNA concentration. The leveling off of the xylyl suggests that most of the xylyl template is in a conformation that does not allow for hybridization or ligation.; pp We attribute the leveling off of the signal for the ethyl and butyl templates to subtle differences in the extinction coefficients used to calculate the DNA concentration. The leveling off of the xylyl suggests that most of the xylyl template is in a conformation that does not allow for hybridization or ligation.
- 27) Sando, S.; Abe, H.; Kool, E. T.: Quenched Auto-Ligating DNAs: Multicolor Identification of Nucleic Acids at Single Nucleotide Resolution. *J. Am. Chem. Soc.* **2004**, *126*, 1081-1087.
- 28) Goffin, C.; Verly, W. G.: T4 DNA ligase can seal a nick in double-stranded DNA limited by a 5'-phosphorylated base-free deoxyribose residue. *Nucleic Acids Res.* **1983**, *11*, 8103-8109.
- 29) Albagli, D.; Atta, R. V.; Cheng, P.; Huan, B.; Wood, M. L.: Chemical Amplification (CHAMP) by a Continuous Self-Replicating

Oligonucleotide-Based System. *J. Am. Chem. Soc.* **1999**, *121*, 6954-6955.

- 30) The more concentrated enzyme (5 units per reaction), capable of ligating blunt ends, displayed very high background under identical reaction conditions.; pp The more concentrated enzyme (5 units per reaction), capable of ligating blunt ends, displayed very high background under identical reaction conditions.
- 31) Fontanel, M. L.; Bazin, H.; Teoule, R.: Sterical recognition by T4 polynucleotide kinase of non-nucleosidic moieties 5'-attached to oligonucleotides. *Nucleic Acids Res* **1994**, *22*, 2022-7.
- 32) Ruhela, D.; Vishwakarma, R. A.: Iterative synthesis of Leishmania phosphoglycans by solution, solid-phase, and polycondensation approaches without involving any glycosylation. *J Org Chem* **2003**, *68*, 4446-56.
- 33) Lesiak, K.; Khamnei, S.; Torrence, P. F.: 2',5'-Oligoadenylate:antisense chimeras--synthesis and properties. *Bioconjug Chem* **1993**, *4*, 467-72.
- 34) Brown, T.; Brown, D. J. S.: *Oligonucleotides and Analogues*; Oxford University Press: New York, **1991**.
- 35) Borer, P. N.; Dengler, B.; Tinoco, I., Jr.; Uhlenbeck, O. C.: *J. Mol. Biol.* **1974**, *86*, 843-853.
- 36) Gibbs-Davis, J. M.; Schatz, G. C.; Nguyen, S. T.: Sharp Melting Transitions in DNA Hybrids without Aggregate Dissolution: Proof of Neighboring-Duplex Cooperativity. *J. Am. Chem. Soc.* **2007**, *129*, 15535-15540.

## Chapter 3

### **Rapid, Isothermal DNA Self-Replication Induced by a Destabilizing Lesion**

Portions of this chapter are reproduced in part with permission from the

© Wiley VCH Verlag GmbH & Co from:

Kausar, A., Mitran, C. J., Li, Y. and Gibbs-Davis, J. M. (2013), Rapid, Isothermal DNA Self-Replication Induced by a Destabilizing Lesion. *Angew Chem Int Ed*, 52: 10577–10581. doi: 10.1002/anie.201303225

Some proof-of-concept experiments not contained herein were performed by C. Mitran. Melting experiments were performed by myself, C. Mitran, and Y. Li. For the H-DNA system, the ligation experiments were performed by myself and Y. Li. Some of the single cycle kinetics serial ligation experiments were performed by C. Mitran. The *E.coli* plasmid was prepared by C. Mitran with help from the Campbell group and the other plasmid (CaYin0.6) was a gift from that group.

### 3.1 Introduction

One process that chemists have aimed to incorporate into artificial systems is self-replication.<sup>1-7</sup> Synthetic self-replicating systems use self-assembly or molecular recognition to initiate and propagate replication, which also gives insights into the origins of life.<sup>1-7</sup> For these synthetic processes to be functional as biomimetic models, they should demonstrate sigmoidal amplification at a constant temperature.<sup>3, 5</sup> However, synthetic replication processes based on biomolecules (like DNA) are plagued by product inhibition and competing background reactions which preventing these systems from exhibiting the sigmoidal growth characteristic of self-replication.<sup>5, 8-11</sup> One way that product inhibition has been avoided and exponential amplification achieved involved using stepwise procedures, whereby the composition of the system was physically modulated to facilitate replication.<sup>12</sup> This mechanical intervention, once every catalytic cycle, is similar to the need for thermal cycling in DNA replication strategies like the polymerase chain reaction, where heating is required to destabilize the product complex and turn over the reaction.<sup>13</sup>

For a system to be autonomous, the replication process must proceed with only one external intervention, the initial introduction of the target. Recently, Lincoln and Joyce reported the development of an autonomous, non-enzymatic self-replicating RNA system using a catalytic 100-base RNAzyme that exhibited sigmoidal replication.<sup>14</sup> The catalytic activities of the RNAzyme allowed it to ligate two probes that contained regions complementary to the RNAzyme as well as probes of the catalytically active domain. After ligation, this new catalytically

active RNA strand ligated another set of probe RNA to generate a copy of the original RNAzyme. Lincoln and Joyce found that the most active system contained a wobble G-U pair between the RNAzyme and the probes, which destabilized the product complex allowing for sigmoidal amplification with a doubling rate of once per hour. However, for this ligation chain reaction to operate a majority of the sequence had to be conserved to maintain the catalytic properties necessary for ligation.<sup>14</sup>

Our aim has been to develop a general isothermal DNA-amplification system based on a ligase chain reaction (LCR),<sup>15</sup> similar to strategies for DNA<sup>8, 10, 11</sup> and RNA<sup>9, 14</sup> amplification in non-enzymatic systems, as shown in the previous example, which would be useful in understanding the requirements for prebiotic oligonucleotide replication and have potential in DNA-based diagnostics of infectious diseases.<sup>16, 17</sup> Herein, we report a rapid sigmoidal amplification of DNA while circumventing the need for destabilizing enzymes or mechanical or thermal intervention using a destabilizing abasic lesion. The simplicity and generality of our method suggests that this strategy will be accessible to many laboratories. Moreover, although an enzyme is used to ligate the two strands in our strategy, turnover is a consequence of the destabilized DNA duplex. Hence, this work can aid the development of non-enzymatic nucleic acid self-replication systems using chemical-ligation methods.<sup>9-11, 18-20</sup>

### 3.2 Cross-catalytic amplification by destabilization

Similar to the RNAzyme system, cross-catalytic replication of DNA strands involves two coupled catalytic cycles where the product strand of one cycle is the template for the other cycle (Figure 3.1).<sup>3, 10</sup> In the first step of our isothermal LCR, a sequence (**DNA-I**) initiates the formation of its complement by hybridizing with two complementary probes, one of which contains a destabilizing abasic group in place of the complementary nucleotide at the 5'-phosphate terminus, to form a nicked duplex (Figure 3.1 A). After ligation of the two probes by T4 DNA ligase a new strand results, **DNA-II**, that is complementary to **DNA-I** with the exception of the central abasic nucleotide (Figure 3.1 B). Owing to the destabilizing effects of the abasic group on the product duplex, the product **DNA-II** will dissociate from **DNA-I** at the same temperature in which it was formed (Figure 3.1 C). The presence of a large excess of probes prevents the reannealing of **DNA-I** and **DNA-II**. **DNA-I** is then free to serve as a template for the formation of more **DNA-II** destabilizing strands. This approach for using destabilizing groups to achieve turnover in DNA-templated ligations was first shown by Lynn and co-workers<sup>21, 22</sup> and has now been demonstrated in several non-enzymatic single-cycle systems.<sup>19, 23</sup>

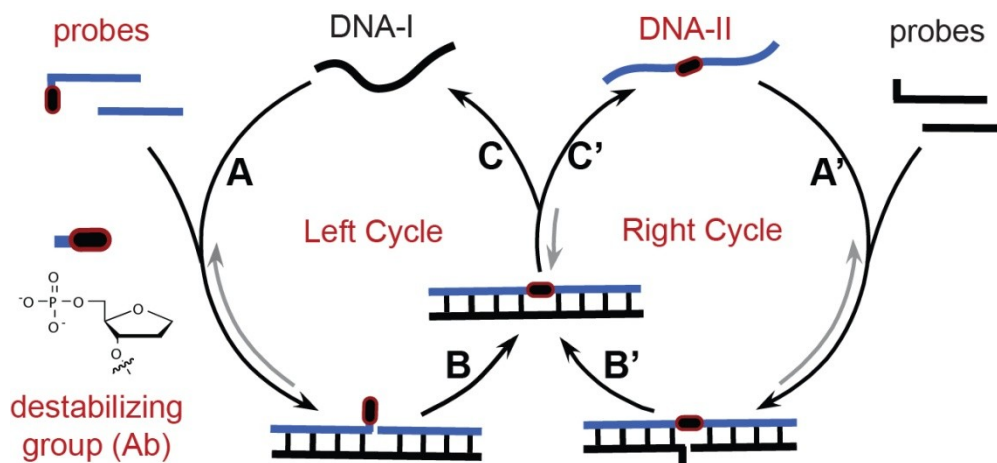


**Figure 3.1:** Cross-catalytic amplification of **DNA-I** using an abasic destabilizing group in an LCR. Left cycle: A **DNA-I** strand templates the formation of **DNA-II** (see text for details). Right cycle: The **DNA-II** formed in situ catalyzes the formation of a new **DNA-I** strand, which feeds back into the left cycle.

To achieve amplification of **DNA-I**, however, another catalytic cycle must be coupled to this first ligation process (Figure 3.1, right cycle). In this cycle, the **DNA-II** that was generated is complementary to two other probes that are present leading to hybridization and formation of another nicked duplex (Figure 3.1 B'). This nicked duplex is ligated, and then dissociates once again owing to the destabilizing abasic site (Figure 3.1 B', C'). The ligated product of the right cycle contains a sequence identical to **DNA-I** but with the addition of a fluorescent label (**F-DNA-I**). Our previous work indicated that 1',2'-dideoxyribose-5'-phosphate, a model abasic lesion (**Ab**), was an ideal destabilizing group that promoted isothermal replication and was compatible with ligation by T4 DNA ligase.<sup>24</sup> Unfortunately, our first efforts at cross-catalytic DNA self-replication by



destabilization were extremely slow, requiring 20 hours to achieve 31 replication cycles when one Weiss unit of enzyme<sup>25</sup> was used per 15  $\mu$ L reaction.<sup>24</sup>

### 3.2.1 Influence of enzyme concentration

Our previous work indicated that the concentration of the enzyme had a large impact on the turnover frequency for single-cycle experiments involving various destabilizing groups.<sup>24</sup> Therefore, to increase the replication rate we examined higher concentrations of T4 DNA ligase based on 2000 cohesive end units (or approximately seven Weiss units) per 15  $\mu$ L experiment.<sup>26</sup> With this commercially available high concentration of enzyme, we monitored the kinetics of the replication process for a reaction mixture containing all four probes (1.4  $\mu$ M and 2.8  $\mu$ M, fluorescently labeled and unlabeled, respectively) and either 14 nM or 0 nM **DNA-I** at time zero (Figure 3.2 A; and Figure 3.21 for PAGE images). Remarkably, self-replication occurred rapidly and consumed all of the probes for the reaction initiated with 14 nM **DNA-I**, as determined by gel electrophoresis (Figure 3.2 A, solid circles). The amount of **F-DNA-I** generated represented a 100-fold increase within 40 minutes, significantly faster than the reaction with low ligase concentration (31 copies in 20 hours). In contrast, decoupling the right cycle from the left cycle led to much slower **DNA-II** strand production and linear growth consistent with cross-catalysis being responsible for the rapid amplification (Figure 3.2 B and Figure 3.22 for PAGE images).

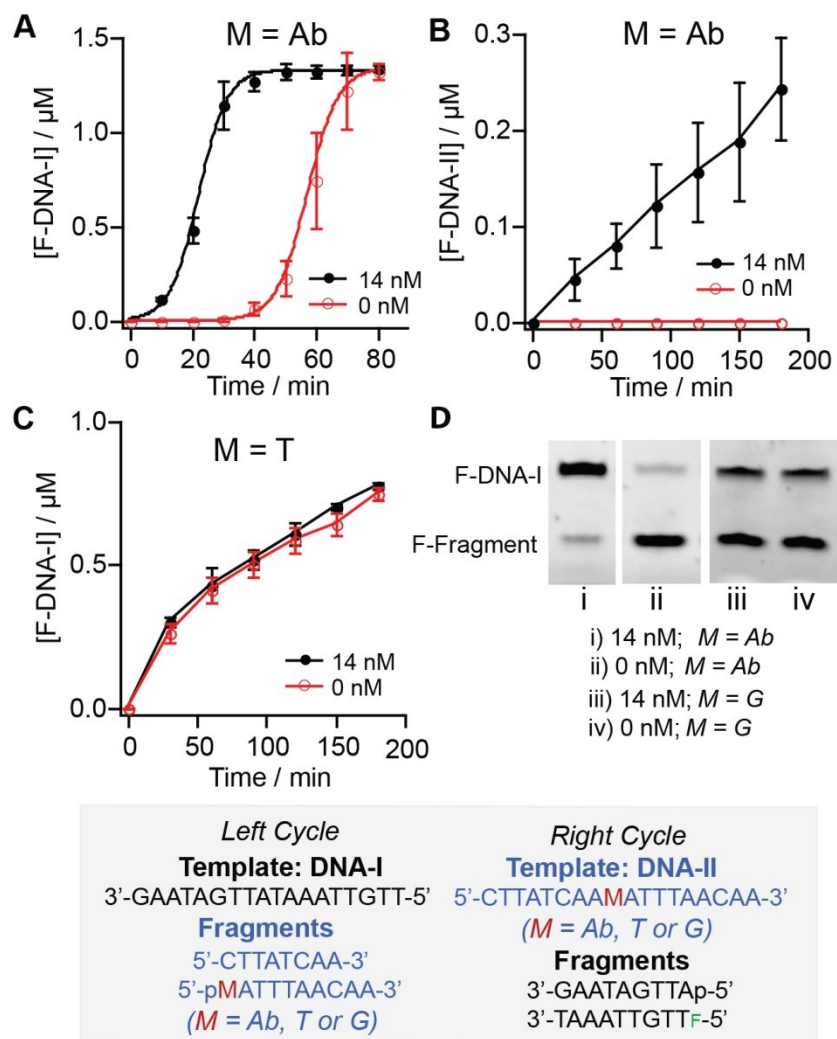


**Figure 3.2:** A) Cross-catalytic replication of **F-DNA-I** at 30 °C initiated by 14 nM or 0 nM **DNA-I** using destabilizing probes. B) Single (left) cycle amplification at 30 °C initiated by 14 nM and 0 nM **DNA-I** using destabilizing probes, one with a fluorescein, leading to the formation of the fluorescently labeled complement (**F-DNA-II**). C) Production of **F-DNA-I** at 30 °C initiated by 14 nM or 0 nM **DNA-I** using native DNA probes. D) Fluorescent images of polyacrylamide gels after electrophoretic separation. **F-DNA-I** formed at 30 °C: after 40 min (i, ii) or 180 min (iii, iv). Gray box: P=phosphate and T<sub>F</sub>=fluorescein-modified thymine.

In our cross-catalytic system, we also observed that the reaction without any initial **DNA-I** exhibited sigmoidal growth after an induction period of about 40 minutes (Figure 3.2 A, open circles), in contrast to the single-cycle experiment, where no reaction occurred without some initial **DNA-I** (Figure 3.2 B, open circles). We reasoned that small quantities of **DNA-I** or **DNA-II** were synthesized in the cross-catalytic system through pseudo-blunt-end ligation of the probes, as the probes present in each cycle were complementary to those in the opposite cycle. Such blunt-end ligation is known to occur in the presence of high concentrations of T4 DNA ligase.<sup>27</sup> (This reaction would be pseudo-blunt ended as there is a non-complementary one-base overhang, where the adenine is across from the abasic group.) The small quantities of **F-DNA-I** or **DNA-II** generated in this slow background process could then trigger cross-catalytic replication. Fitting the sigmoidal logistic growth function  $f(t)=a/(1+be^{-ct})$  to the data plotted in Figure 3.2 A allowed us to quantify the rate of replication, where  $a$  is the maximum concentration of **F-DNA-I** formed,  $b$  is the extent of sigmoidicity, and  $c$  is the exponential rate.<sup>14</sup> We observed that the rates were the same within error for the target-initiated and background-triggered reactions ( $0.22\pm 0.05 \text{ min}^{-1}$  versus  $0.20\pm 0.01 \text{ min}^{-1}$ , respectively), which indicated that the exponential growth came from the cross-catalysis not from the blunt-end reaction.

### **3.2.2 Cross-catalysis in the absence of a destabilizing group**

To determine the importance of the destabilizing group, we also examined replication in a native DNA system that contained the complementary thymidine rather than the abasic group (Figure 3.2 C and Figure 3.23 for PAGE images). The

**DNA-I**-initiated and background-triggered reactions exhibited the same kinetic profile, which did not have the sigmoidal shape characteristic of cross-catalytic replication (Figure 3.2 C). In this case, the background reaction was quite facile because it involved ligation of a one-base overhang between the native DNA probes (Figure 3.2, gray box, M=T). This native DNA ligation system failed to exhibit sigmoidal amplification at any temperature tested, indicating that the destabilizing group was essential to overcome product inhibition in the replication of an 18-base sequence (Figure 3.3).

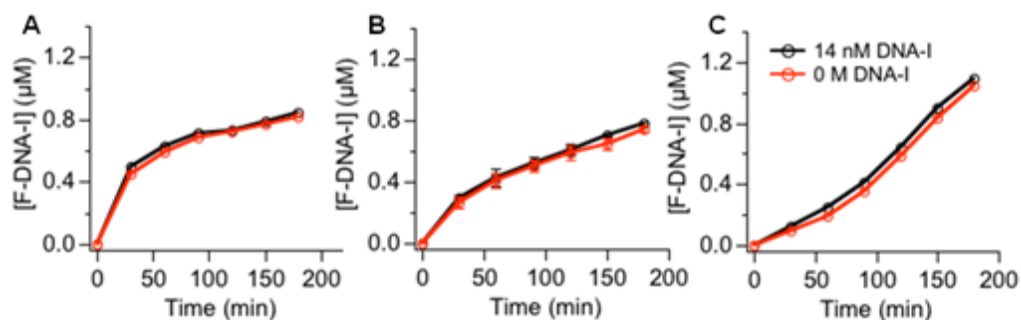


**Figure 3.3:** The concentration of **F-DNA-I** formed as a function of time using perfectly complementary replicators lacking an abasic group at A) 26 °C, B) 30 °C, and C) 34 °C. The black traces correspond to the experiment initiated with 14 nM **DNA-I** and the red traces correspond to the experiment initiated with no **DNA-I**. *Experimental conditions:* 14 nM **DNA-I**; 1.4 µM **rDNA-Ia**; 2.8 µM **rDNA-Ib**; 2.8 µM **rDNA-IIa** (*D = T*); 2.8 µM **rDNA-IIb**.

### 3.2.3 Cross-catalysis with a mismatch as the destabilizing group

Next, we attempted to use a mismatched base-pair (A:G) rather than the abasic group to destabilize the product duplex and facilitate turnover (Figure 3.2, gray box, M=G). However, this mismatched system also did not exhibit a significant difference between the template-initiated and background-triggered

reactions (Figure 3.2 D and 3.4). Thermal denaturation experiments indicated that the mismatch did not destabilize the product duplex as much as the presence of the abasic group, which explained the lack of cross-catalysis in the mismatched system (Figure 3.5). Specifically, the native **DNA-II:DNA-I** product duplex exhibited a dissociation, or melting, temperature ( $T_m$ ) of 49.2 °C, whereas the abasic-containing product duplex had a  $T_m$  of 34.0 °C. In contrast, the mismatch-containing product duplex had a  $T_m$  of 41.1 °C, consistent with less destabilization.

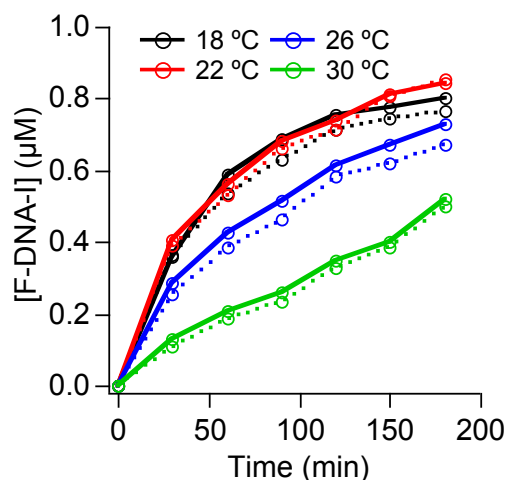


**Figure 3.4:** The concentration of **F-DNA-I** formed as a function of time at various temperatures using a replicator modified with a mismatch instead of an abasic group. The solid traces correspond to the experiment initiated with 14 nM **DNA-I** and the dotted traces correspond to the experiment initiated with no **DNA-I**. Sigmoidal amplification was not observed at any temperature indicating that the templated reaction was not favored and that the mismatch was not destabilizing enough to avoid product inhibition. *Experimental conditions:* 14 nM **DNA-I**; 1.4 μM **rDNA-Ia**; 2.8 μM **rDNA-Ib**; 2.8 μM **rDNA-IIa(D = G)**; 2.8 μM **rDNA-IIb**.

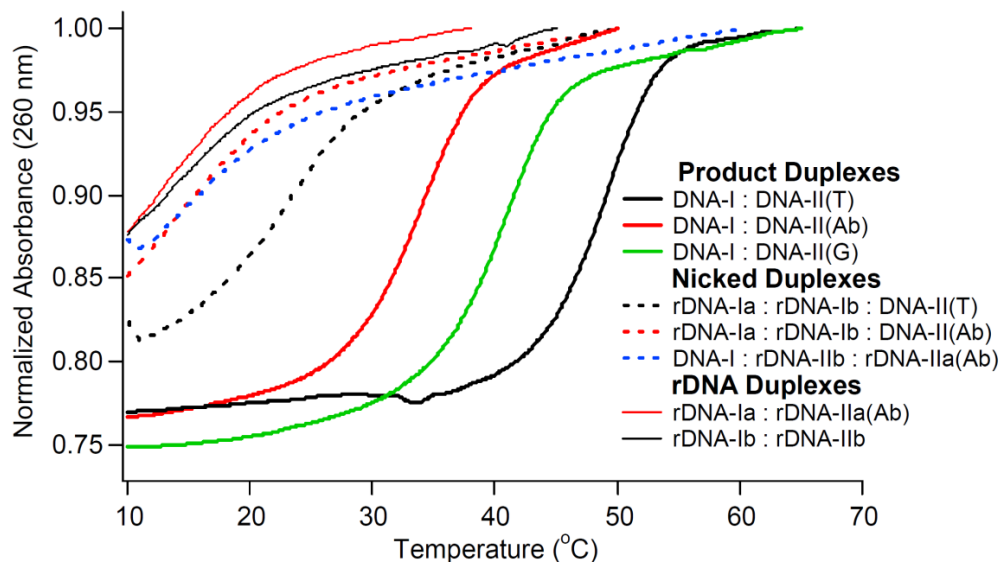


**Figure 3.5:** Melting profiles of the **DNA-I** system corresponding to the product duplex, nicked duplex and replicator (**rDNA**) duplexes. **DNA-II(T)** is the native DNA template, **DNA-II(Ab)** is the destabilizing template containing an abasic (**Ab**) group. **DNA-II(G)** is the destabilizing template containing an A:G mismatch instead of an abasic group.

### 3.2.4 Determining sequence generality

To test whether the presence of one abasic group for an 18 bp replicating system was a general method for self-replication, we prepared destabilizing probes complementary to a sequence associated with the hepatitis B virus (**H-DNA-I**),<sup>28</sup> which has a higher G:C content than our original **DNA-I:DNA-II** system. The corresponding DNA complexes had higher melting temperatures than that of the **DNA-I** system (Figure 3.6 and Table 3.1). Nevertheless significant destabilization was observed upon introducing the abasic group based on the depressed melting temperatures compared to the native DNA system.

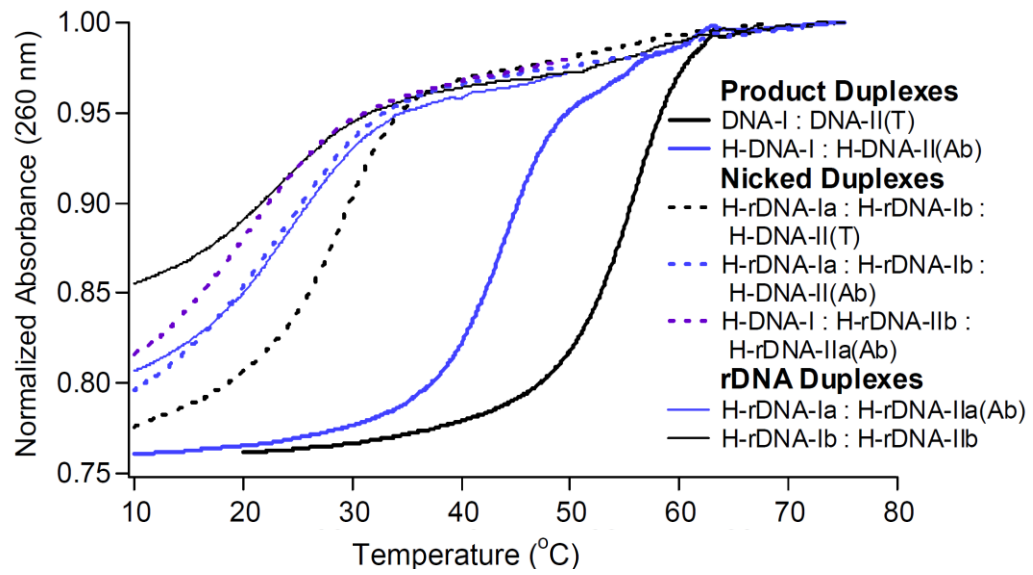


**Figure 3.6:** Melting profiles of the **H-DNA-I** system corresponding to the product duplex, nicked duplex and the replicator (**rDNA**) duplexes.

**Table 3.1.** Melting temperatures ( $T_m$ ) of duplexes formed during cross-catalytic replication.

<b>DNA-I System</b>		<b>H-DNA-I System</b>	
<b>Mixture</b>	<b><math>T_m</math> (°C)</b>	<b>Mixture</b>	<b><math>T_m</math> (°C)</b>
DNA-I:DNA-II ( $D = T$ )	49.2	H-DNA-I:H-DNA-II ( $D' = T$ )	55.4
DNA-I:DNA-II ( $D = Ab$ )	34.0	H-DNA-I:H-DNA-II ( $D' = Ab$ )	43.8
DNA-I:DNA-II ( $D = G$ )	41.1		
DNA-I:rDNA-IIa:rDNA-IIb( $D = T$ )	17.3	H-DNA-I:H-rDNA-IIa:H-rDNA-IIb ( $D' = A$ )	20.7
rDNA-Ia:rDNA-Ib:DNA-II( $D = T$ )	22.8	H-rDNA-Ia:H-rDNA-Ib:H-DNA-II ( $D' = A$ )	28.6
rDNA-Ia:rDNA-Ib:DNA-II( $D = Ab$ )	13.4	H-rDNA-Ia:H-rDNA-Ib:H-DNA-II ( $D' = Ab$ )	22.6
DNA-I:rDNA-IIa:rDNA-IIb( $D = Ab$ )	16.4	H-DNA-I:H-rDNA-IIa:H-rDNA-IIb ( $D' = Ab$ )	20.2
rDNA-Ia:rDNA-IIa ( $D = Ab$ )	12.8	H-rDNA-Ia:H-rDNA-IIa( $D' = Ab$ )	23.9
rDNA-Ib:rDNA-IIb	13.3	H-rDNA-Ib:H-rDNA-IIb	22.8

Despite the increase in the stability of the corresponding **H-DNA-I:H-DNA-II** product duplex, we still observed facile self-replication by simply increasing the replication temperature from 30 °C to 34 °C (Figure 3.7 and Figure 3.24 for PAGE images). The exponential rate determined for this system was slightly slower than that of the **DNA-I** sequence ( $0.10 \pm 0.02 \text{ min}^{-1}$ ), corresponding to a doubling rate of seven minutes.



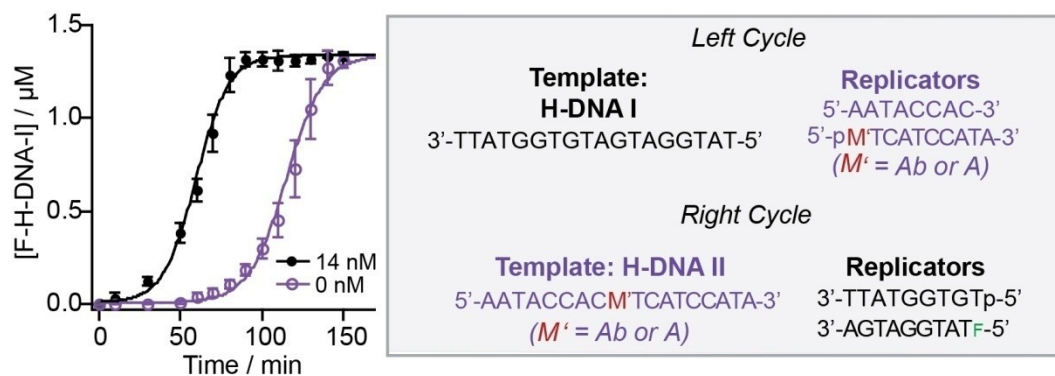


**Figure 3.7:** Cross-catalytic replication of **F-H-DNA-I** at 34 °C initiated by 14 nM or 0 nM **H-DNA-I** using destabilizing probes.

Varying the temperature of the cross-catalytic replication revealed that the process was highly temperature sensitive. As can be seen in the Figure 3.8, for amplification of the **H-DNA-I** system, the rate of amplification was very slow at 30 °C and very fast at 37 °C, however at 34 °C we observed an intermediate rate of amplification that resulted in a good separation between amplification with 14 nM initial target and no initial target. The **DNA-I** system followed the same trend, however, the optimum temperature for this system was 30 °C (Figure 3.9). This lower temperature was expected since the **DNA-I** system has a lower G:C content, reflecting a lower melting temperature of the product and nicked duplexes.

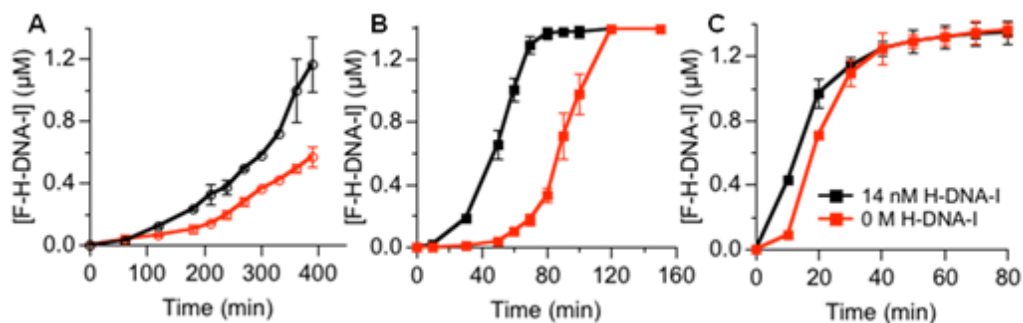


**Figure 3.8:** The concentration of **F-H-DNA-I** formed as a function of time using an abasic modified replicator at A) 30 °C, B) 34 °C, and C) 37 °C. The black traces correspond to the experiment initiated with 14 nM **H-DNA-I** and the red traces correspond to the experiment initiated with no **H-DNA-I**. Due to the higher G:C content for this system, the best separation between the template-initiated and background-initiated reactions was observed at 34 °C. *Experimental conditions:* 14 nM **H-DNA-I**; 1.4 µM **H-rDNA-Ia**; 2.8 µM **H-rDNA-Ib**; 2.8 µM **H-rDNA-IIa** ( $D' = Ab$ ); 2.8 µM **H-rDNA-IIb**.

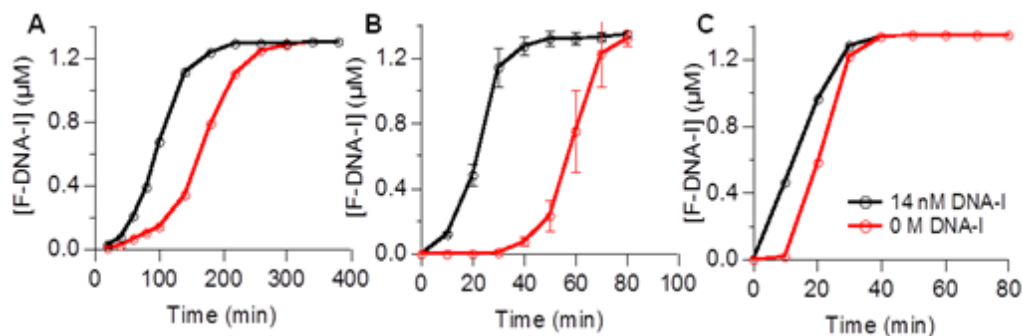


**Figure 3.9:** The concentration of **F-DNA-I** formed as a function of time using an abasic-modified replicator at A) 26 °C, B) 30 °C, and C) 34 °C. The black traces correspond to the experiment initiated with 14 nM **DNA-I** and the red traces correspond to the experiment initiated with no **DNA-I**. The reaction at 30°C led to rapid replication and good separation between the target-initiated and background-initiated reaction. *Experimental conditions:* 14 nM **DNA-I**; 1.4 µM **rDNA-Ia**; 2.8 µM **rDNA-Ib**; 2.8 µM **rDNA-IIa** ( $D = Ab$ ); 2.8 µM **rDNA-IIb**.

Temperature variation studies indicated that the ideal replication temperature was 10 °C below the  $T_m$  of the product duplex and 8 °C above the  $T_m$  of the probe:template nicked duplexes for the **H-DNA-I** system ( $T_m$  values correspond to 1.3  $\mu$ M per sequence; Figure 3.6, 3.8 and 3.10). For the **DNA-I** system the same relative temperature dependence was observed with the optimal replication temperature lying 4 °C below the  $T_m$  of the product duplex and approximately 15 °C above the melting temperature of the corresponding probe:template nicked duplexes (Figure 3.9 and 3.10). We conclude that the ideal temperature was great enough to facilitate product duplex dissociation yet still resulted in the formation of some nicked duplexes. Importantly, the more concentrated T4 DNA ligase compensated for the small amount of nicked duplexes present at this temperature.

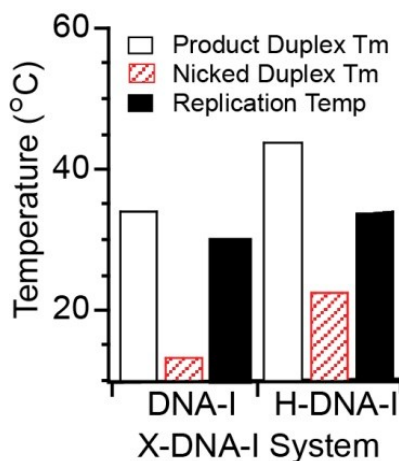


**Figure 3.10:** Melting temperatures ( $T_m$ ) of the product (white) and nicked (striped) duplexes for the **DNA-I** and **H-DNA-I** systems compared with the optimized replication temperature (black).

To verify that the template was primarily free during replication, not bound in the product duplex, the reaction order was determined from the rate law:  $\text{initial rate} \propto k[\text{template}]_0^p$ , where  $k$  is the rate constant for the templated reaction,  $[\text{template}]_0$  is the initial template concentration, and  $p$  is the reaction order of the template.<sup>5, 29</sup> We observed a linear dependence of the initial rate on the initial **DNA-I** concentration, indicating that  $p$  was close to one, which is a hallmark of exponential replicating systems (Figure 3.11).<sup>29</sup> A reaction order of one rather than 0.5 also suggested that the template strand present was primarily single-stranded or in the nicked rather than product duplex, which supported that product inhibition has been minimized in our system.<sup>5</sup>

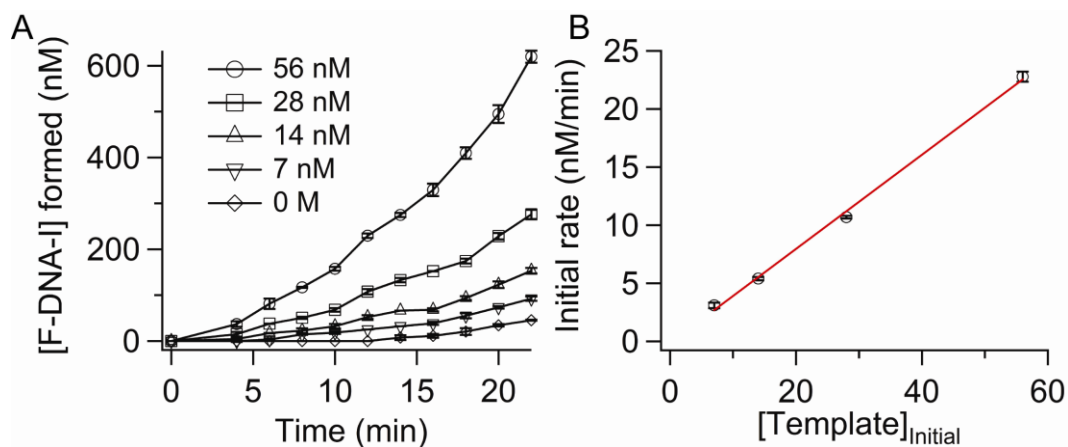


**Figure 3.11:** A) Formation of **F-DNA-I** as a function of initial **DNA-I** template concentration. B) Initial rate as a function of initial template concentration. The red line is a linear fit to the data ( $r^2 = 0.9978$ ).

### 3.2.5 Optimizing template-initiated replication by reducing the replicator concentration

To quantify the amount of self-replication, we measured the difference in fluorescent template formed between the target-initiated and background-triggered reactions ( $\Delta\mathbf{F-H-DNA-I}$ , Figure 3.12A); the maximum difference was then divided by the initial template concentration to yield the net number of target-initiated self-replication cycles. For example, the 14 nM **H-DNA-I** template-initiated reaction exhibited a maximum  $\Delta\mathbf{F-H-DNA-I}$  value of  $1.18 \pm 0.04 \mu\text{M}$ , which corresponded to  $85 \pm 3$  replication cycles (Figure 3.12 B). Reactions initiated with 1.4 nM template led to net replication cycles of  $780 \pm 40$  and  $310 \pm 50$  for the **DNA-I** and **H-DNA-I** systems, respectively (Figure 3.12 B).

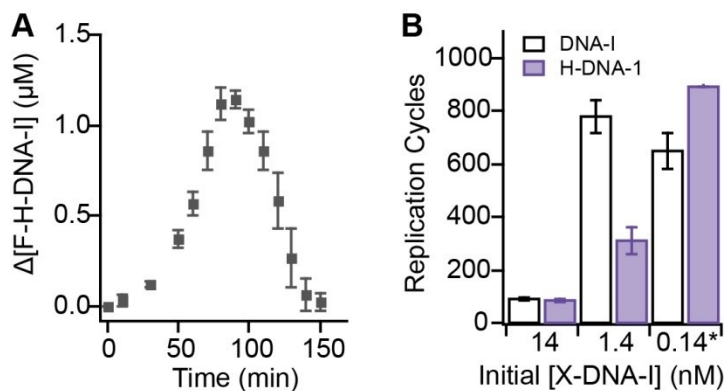


**Figure 3.12:** A) Difference in the concentration of **F-H-DNA-I** formed between the reaction initiated with 14 nM and 0 nM **H-DNA-I**. B) Number of template-initiated replication cycles as a function of initial template concentration (**DNA-I** = white; **H-DNA-I** = gray). \*=The probe concentrations were used at a fourfold dilution compared with the typical replication conditions.

To further increase the number of self-replication cycles required, we initiated the reaction with a lower template concentration; however, when the template concentrations were less than 1.4 nM the replication profile was the same as the background-triggered reaction. Therefore, we sought to delay the background reaction. We found that decreasing the probe concentration fourfold decreased the rate of the background blunt-end reaction, more so than its effect on the template-initiated reaction (Figure 3.13, 3.25, 3.26; Table 3.3 and 3.4). Consequently the time window increased which allowed us to initiate the reaction with 0.14 nM template and observe  $650 \pm 70$  and  $920 \pm 50$  self-replication cycles for the **DNA-I** and **H-DNA-I** systems, respectively (Figure 3.12 B, 0.14 nM). For the **H-DNA-I** system, we were also able to achieve an even lower detection limit and observed  $6000 \pm 600$  replication cycles with 14 pM initial **H-DNA-I** template.

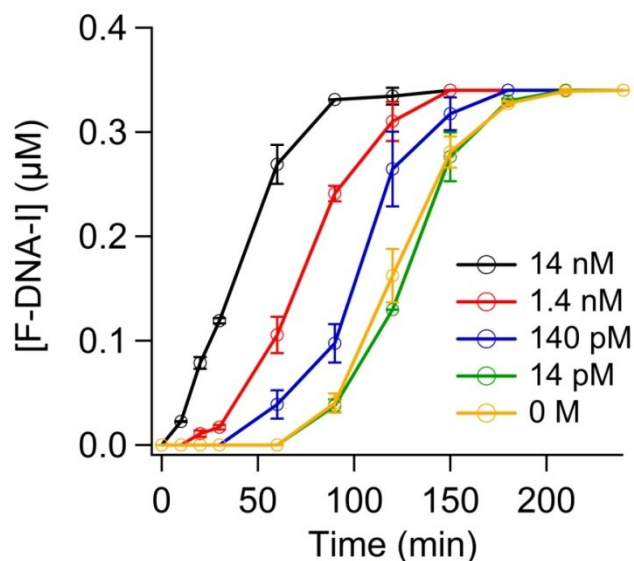


**Figure 3.13:** The concentration of **F-DNA-I** formed as a function of time with different concentrations of initial **DNA-I** template and lower replicator concentrations than standard conditions. *Experimental conditions:* 14 nM, 1.4 nM, 140 pM, 14 pM or 0 nM **DNA-I**; 0.35  $\mu\text{M}$  **rDNA-Ia**; 0.70  $\mu\text{M}$  **rDNA-Ib**; 0.70  $\mu\text{M}$  **rDNA-IIa**( $D = Ab$ ); 0.70  $\mu\text{M}$  **rDNA-IIb**; 30  $^{\circ}\text{C}$ .

It seemed likely that further reduction of the probe concentration would increase the observed replication cycles for our system. However, at probe concentrations below 0.35  $\mu\text{M}$  the replication process was difficult to monitor by fluorescent imaging after PAGE separation. Consequently, we attempted a step-wise serial ligation strategy, whereby **DNA-I** (140 fM) was combined with a low concentration of probes (0.14  $\mu\text{M}$  or tenfold more dilute than typical conditions). We also performed a control reaction lacking any initial **DNA-I**. After three hours, aliquots from the **DNA-I**-initiated and control experiment were added to two separate vessels containing the typical concentration of probes and more T4 DNA ligase (Figure 3.14). After approximately 40 minutes, we observed a difference in **F-DNA-I** concentration ( $\Delta\text{F-DNA-I}$ ) of  $0.10 \pm 0.03 \mu\text{M}$  between the

**DNA-I**-initiated and the control (background) reaction, which corresponded to  $2.7 \pm 0.9$  million replication cycles for the former in less than four hours (Figure 3.15; Table 3.3). Although the sensitivity achieved is quite promising, other parameters like the sequence length and composition as well as the reaction conditions need to be optimized for use in biodiagnostics.

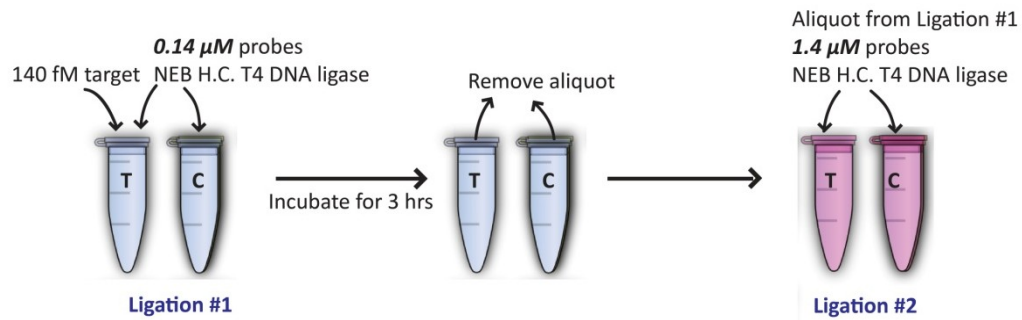


**Figure 3.14:** Schematic diagram of the serial ligation process.



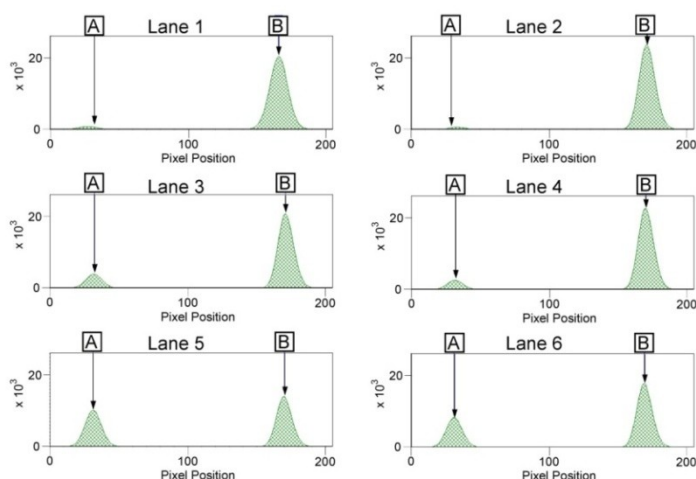
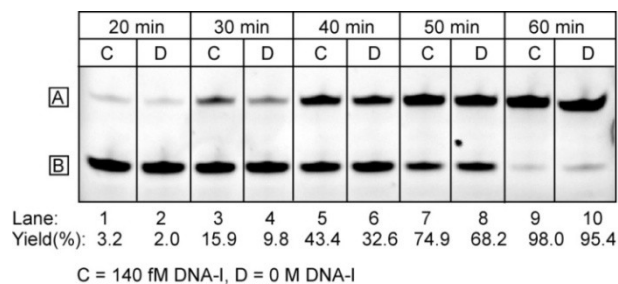


**Figure 3.15:** Top Panel: Representative gel image of serial ligation initiated 140 fM DNA-I at 30 °C. *Top band: F-DNA-I; bottom band: rDNA-Ia.* *Experimental conditions:* First Ligation: 140 fM or 0 M DNA-I; 0.14 μM rDNA-Ia; 0.28 μM rDNA-Ib; 0.28 μM rDNA-IIa (D = Ab); 0.28 μM rDNA-IIb. Second Ligation: 1.12 μM rDNA-Ia; 2.24 μM rDNA-Ib; 2.24 μM rDNA-IIa (D = Ab); 2.24 μM rDNA-IIb. Bottom Panels: Fluorescent intensity profiles of first six lanes shown in the top panel gel. The peak area of the band is proportional to the amount of F-DNA-I product formed (band A) or unreacted rDNA-Ia remaining (band B). Yield (%) = 100% x Area<sub>A</sub>/(Area<sub>A</sub>+ Area<sub>B</sub>).

### 3.2.6 Cross catalysis in the presence of non-complementary DNA

To operate as a diagnostic tool our method must be not only sensitive but capable of amplifying the target sequence in the presence of duplex DNA that is non-complementary to the replicators. As previously mentioned, a high enzyme concentration was essential to realize rapid, sigmoidal replication. Consequently, we were concerned that the presence of large quantities of non-complementary DNA would occupy many of the enzymes, significantly decreasing the rate of amplification. We found, however, that adding up to 100-fold excess of single-stranded non-complementary DNA similar in length to **DNA-I** or **H-DNA-I** had no effect on the rate of cross catalysis (Figure 3.16).

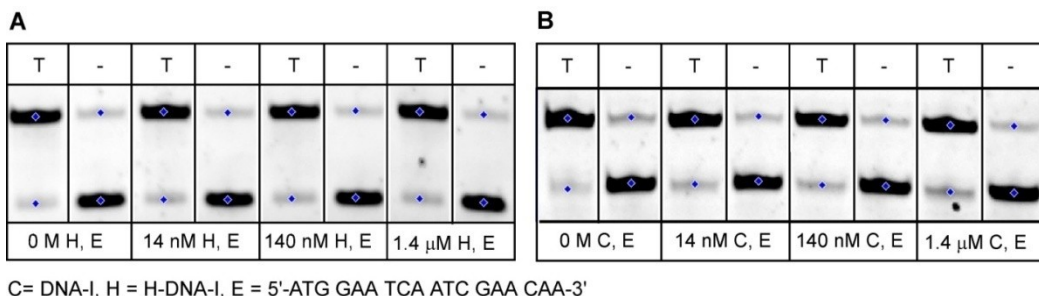


**Figure 3.16:** A) Representative gel images following cross-catalytic replication of **F-DNA-I** initiated by 14 nM (T) or 0 nM (-) **DNA-I** using destabilizing replicators (D = Ab) in the presence of other non-complementary DNA strands (**H-DNA-I** (H) and E) of different concentrations. *Top band: F-DNA-I; bottom band: rDNA-Ia. Experimental conditions:* 14 nM or 0 nM **DNA-I**; 1.4 μM **rDNA-Ia**; 2.8 μM **rDNA-Ib**; 2.8 μM **rDNA-IIa** (D = Ab); 2.8 μM **rDNA-IIb**; 30 °C, 40 min. B) Representative gel image of cross-catalytic replication of **F-H-DNA-I** at 34 °C initiated by 14 nM (T) or 0 nM (-) **H-DNA-I** using destabilizing replicators (D' = Ab) in the presence of other non-complementary DNA strands (**DNA-I** (C) and E) of different concentrations. *Top band: F-H-DNA-I; bottom band: H-rDNA-Ia.* The blue markers identify the location of the band determined by the imaging software. *Experimental conditions:* 14 nM or 0 nM **H-DNA-I**; 1.4 μM **H-rDNA-Ia**; 2.8 μM **H-rDNA-Ib**; 2.8 μM **H-rDNA-IIa** (D' = Ab); 2.8 μM **H-rDNA-IIb**; 34 °C, 40 min.

To ensure that discriminating the target-initiated reaction from the background was also possible in the presence of double-stranded non-complementary DNA, we introduced various amounts of salmon sperm genomic DNA into our cross-catalytic replication system. Figure 3.17 A illustrates that self-replication with 14 nM initial **DNA-I** is still readily observed after 40 minutes in the presence of up to 1.0 μg/μL salmon sperm DNA. Yet at concentrations exceeding this amount the rates of the target-initiated and background triggered reactions were significantly reduced. These experiments suggested that non-

complementary duplex DNA did slow down replication however rapid amplification was still possible as long as this DNA concentration was kept at or below 1.0  $\mu\text{g}/\mu\text{L}$ . Therefore, we performed a cross-catalytic amplification initiated by 140 pM **DNA-I** identical to that described previously but with the addition of 0.093  $\mu\text{g}/\mu\text{L}$  salmon sperm DNA. This mass concentration of genomic DNA would be equivalent to  $\sim 140$  pM if the genome of the target organism to be detected was 1,000,000 bp. The salmon genome is much larger ( $\sim 3$  billion bp), but many bacteria and viruses have genome sizes near 1 million base pairs. In the presence of 0.093  $\mu\text{g}/\mu\text{L}$  salmon sperm DNA, the difference between the target-initiated and background triggered reaction was easily discerned resulting in a turnover number of  $700 \pm 200$  similar to that observed in the reaction without salmon sperm ( $650 \pm 70$ ) (Figure. 3.17 B and 3.18 for PAGE images). These results highlight that our isothermal LCR process is not prevented by the presence of non-complementary genomic DNA, indicating that it may find use in biodiagnositics of infectious diseases. Greater sensitivity would be needed, however, to amplify DNA associated with organisms with larger genomes like salmon or humans.

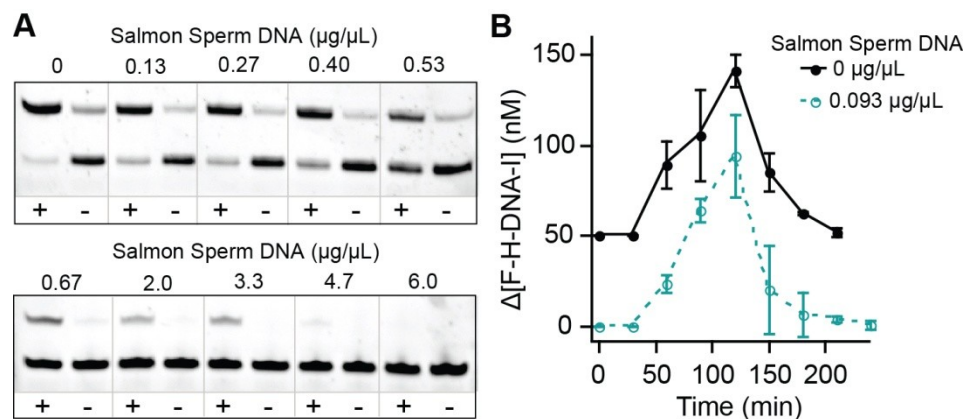


**Figure 3.17:** A) Fluorescent images after PAGE separation of cross-catalysis reactions initiated by 14 nM (+) or 0 M (-) **DNA-I** in the presence of varying amounts of salmon sperm DNA after 40 minutes reaction time. The top band is the self-replication product (**F-DNA-I**) and the bottom band is the unreacted replicator (**rDNA-Ia**). B) The difference in **F-DNA-I** formed between the reaction initiated with 140 pM and 0 nM **DNA-I** in the absence (black line) and presence (aqua dashed line) of salmon sperm DNA. The replicator concentrations were used at a four-fold dilution compared with the typical replication conditions. The time profile without salmon sperm has been offset by 50 nM to allow for comparison.

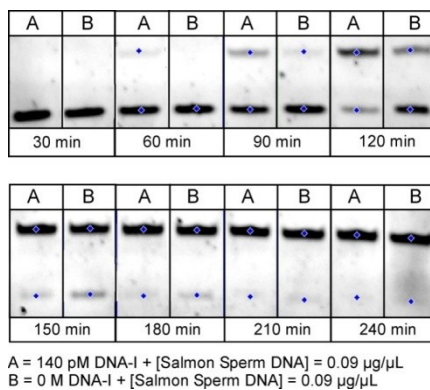


**Figure 3.18:** Representative gel image of cross-catalytic replication of **F-DNA-I** at 30 °C initiated by 140 pM, or 0 nM **DNA-I** in the presence of 0.09 µg/µL salmon sperm DNA. *Top band: F-DNA-I; bottom band: rDNA-Ia.* *Experimental conditions:* 140 pM or 0 M **DNA-I**; 0.35 µM **rDNA-Ia**; 0.7 µM **rDNA-Ib**; 0.7 µM **rDNA-IIa** ( $D = Ab$ ); 0.7 µM **rDNA-IIb**; 0.09 µg/µL salmon sperm DNA; 30 °C.

### 3.2.7 Cross catalysis initiated by double-stranded plasmid DNA

To determine whether our method was capable of amplifying a small sequence within a much larger double-stranded target - which is also relevant to its potential in biodiagnostics -we prepared probes complementary to a 6,100 bp plasmid containing the *E. coli* ligase gene (2016 bp, ECs3283). This plasmid was synthesized by inserting the *E. coli* ligase gene into the pBAD/His B vector (4100 bp). Another plasmid with a different gene that encoded for a fluorescent protein (CaYin0.6)<sup>28</sup> was prepared in a similar manner using the same vector and was implemented as a control. Four replicators were then prepared that would amplify an 18-base sequence unique to the *E. coli* ligase gene (**E-DNA-I**) (Figure 3.19 A). Similar to the **DNA-I** and **H-DNA-I** systems, the complementary replicators to **E-DNA-I** contained a model abasic group that would yield the destabilizing template upon ligation, while the other set of replicators yielded a fluorescently

labeled copy of **E-DNA-I** upon ligation (**F-E-DNA-I**, Table 3.1). Utilizing the control plasmid in a separate reaction with the four replicators accounted for the potential decrease in rate of both the target-initiated and background-triggered reactions in the presence of double-stranded non-complementary DNA (*vide supra*). To monitor cross-catalysis of the **E-DNA-I** sequence, the DNA replicators were first mixed with the complementary or control plasmid and heated to 95 °C for 10 minutes to denature the double-stranded plasmid. The mixture was then cooled to 37 °C allowing the replicators to hybridize with the complementary segment in the *E. coli* ligase gene for 20 minutes, at which point the T4 DNA ligase master mix was added. (This temperature was found to be the optimal replication temperature for the **E-DNA-I** sequence.) Within one hour, we were able to selectively amplify the **E-DNA-I** sequence within the *E. coli* ligase gene as illustrated by the difference in **F-E-DNA-I** product formed in the presence of complementary and non-complementary plasmid DNA (Figure 3.19 B and Figure 3.20 (gel images)). Significantly, this result demonstrates our ability to detect a particular DNA probe within a longer double-stranded DNA sequence, which is crucial for DNA-based detection of infectious disease. With further optimization, our amplification by destabilization method might prove useful in the isothermal amplification and detection of bacterial targets within real-world samples.

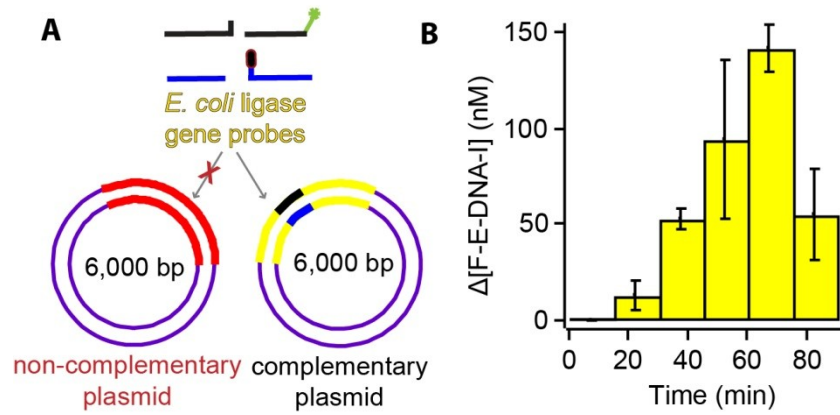
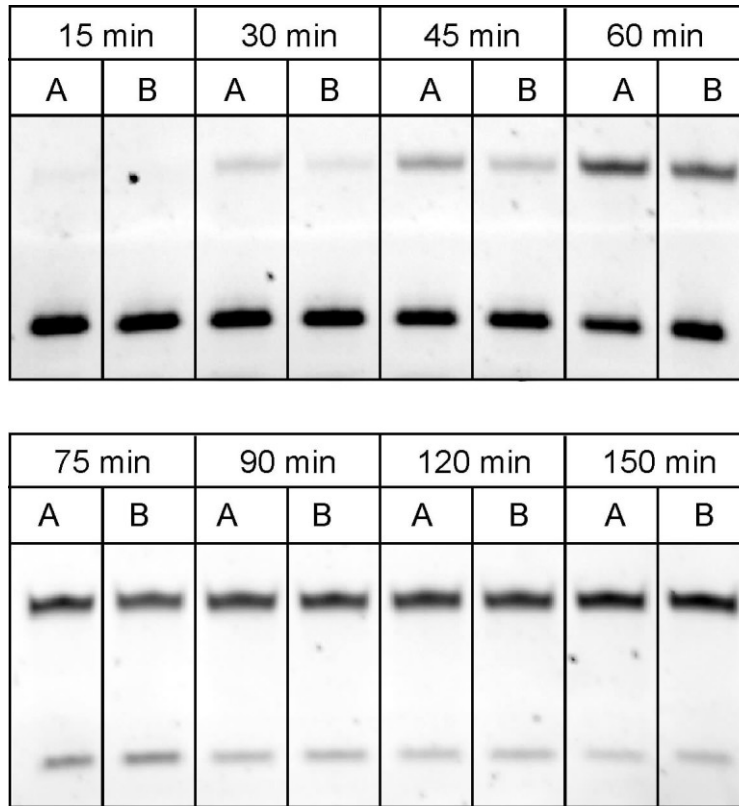


**Figure 3.19:** A) Schematic diagram illustrating the four probes capable of amplifying an 18 base sequence (**E-DNA-I**, *black segment*) within the plasmid containing the 2016 bp *E. coli* ligase gene (*yellow*). A non-complementary gene (*red*) of similar size to the *E. coli* ligase gene was inserted into the same vector to yield a similarly sized plasmid. B) The difference in **F-E-DNA-I** formed between the reaction initiated with 1.4 nM complementary plasmid and 1.4 nM non-complementary plasmid DNA.





A = 1.4 nM plasmid with *E. coli* gene, B = 1.4 nM CaYin0.6 plasmid

**Figure 3.20:** Representative gel image of cross-catalytic replication of **E-DNA-I** at 37 °C initiated by 1.4 nM *E. coli* plasmid or 1.4 nM CaYin0.6 plasmid DNA. *Top band: F-E-DNA-I; bottom band: E-rDNA-Ia.* Experimental conditions: 1.4 nM *E. coli* plasmid or 1.4 nM CaYin0.6 plasmid; 1.4 μM **E-rDNA-Ia**; 2.8 μM **E-rDNA-Ib**; 2.8 μM **E-rDNA-IIa** (D' = Ab); 2.8 μM **E-rDNA-IIb**; 37 °C.

### 3.3 Conclusions

In conclusion, we have shown that replacing one nucleotide with an abasic group in an 18-base sequence can alter the recognition properties of DNA allowing it to self-replicate in a ligase chain reaction. This general and simple strategy hints at the possibility that early replicating systems combined molecular recognition with destabilizing interactions to achieve turnover without temperature variation. This idea of structural destabilization being important in early replicating systems has also been proposed and demonstrated for the polymerization, rather than ligation, of non-enzymatically synthesized oligonucleotides, although these methods have yet to be extended to cross-catalytic replication.<sup>6, 30, 31</sup> Regarding the abasic modification, it is the most common lesion formed in DNA, because it can spontaneously occur through hydrolysis at the anomeric position of deoxyribose.<sup>32</sup> In RNA, abasic sites are less common owing to their slower formation.<sup>33, 34</sup> Nevertheless, it is reasonable to expect this lesion must have coexisted with the first replicating nucleotides. Finally, the strong dependence of the replication rates on the concentration of the enzyme reveals that the ligation step must be very rapid to achieve appreciable replication. Future work will examine fidelity and selection in this lesion-induced replication process.

## 3.4 Experimental Section

### 3.4.1 General

Thermal denaturation studies were performed by myself, Catherine Mitran and Yimeng Li using an HP 8453 diode-array spectrophotometer equipped with a HP 89090A Peltier temperature controller, and the melting curves were analyzed with ChemStation software. The temperatures for DNA ligation experiments were maintained using a Torrey Pines Scientific Echotherm Chilling/Heating Plate Model IC22. PAGE gels were imaged using ImageQuant RT ECL Imager from GE Healthcare Life Science using UV transillumination. The DNA was synthesized on an Applied Biosystems Model 392 DNA/RNA Synthesizer. MALDI-MS was performed on a Voyager Elite (Applied BioSystems, Foster City, CA) time of flight-mass spectrometer in linear negative mode. *Igor Pro v6.05A* (Wavemetrics, Oswego, OR) was used to fit the sigmoidal growth function to the data to determine the rate of replication.

### 3.4.2 DNA Preparation and Characterization

The DNA sequences for the **H-DNA-I** system were prepared and characterized by Yimeng Li. The DNA sequences for the **DNA-I** system were prepared and characterized by myself and Catherine Mitran. PCR primers were purchased from Integrated DNA Technologies (Coralville, IA). All other DNA strands were synthesized using standard phosphoramidite reagents and CPGs from Glen Research (Sterling, VA). Abasic groups were introduced with the dSpacer CE phosphoramidite and fluorescein was introduced with the Fluorescein-dT

phosphoramidite. The 5'-end of the appropriate replicator strands were phosphorylated using Chemical Phosphorylation Reagent II. All strands were deprotected and purified using the DMT-on method with Glen-Pak cartridges following the manufacturer's instructions. Strands were run on a polyacrylamide denaturing gel and imaged with Stain All (Aldrich cat # E9379) to confirm that the DNA strands were pure after purification on the Glen Pak cartridges. Strands were also characterized by MALDI-TOF as described in our previous work (Chapter 2).<sup>24</sup> Ultrapure genomic salmon sperm DNA was purchased from Invitrogen (catalog #15632011). T4 DNA ligase (2,000,000 cohesive end units/mL, catalog #M020T) and the corresponding ligase buffer were acquired from New England Biolabs.

**Table 3.2.** DNA Sequences.

<b>DNA-I System</b>	
DNA-I	5'-TTGTAAATATTGATAAG-3'
DNA-II <sub>D</sub>	5'-CTTATCAADATTTAACAA-3'
rDNA-Ia	5'- <sub>F</sub> TTGTAAAT-3'
rDNA-IIa	5'- <sub>p</sub> DATTTAACAA-3'
rDNA-Ib	5'- <sub>p</sub> ATTGATAAG-3'
rDNA-IIb*	5'- <sub>F</sub> CTTATCAA-3'
<b>H-DNA-I System</b>	
H-DNA-I	5'-TATGGATGATGTGGTATT-3'
H-DNA-II <sub>M</sub>	5'-AATACCACD''TCATCCATA-3'
H-rDNA-Ia	5'- <sub>F</sub> TATGGATGA -3'
H-rDNA-IIa	5'- <sub>p</sub> D''TCATCCATA-3'
H-rDNA-Ib	5'- <sub>p</sub> TGTGGTATT -3'
H-rDNA-IIb	5'-AATACCAC -3'
<b>E-DNA-I System</b>	
E-DNA-I	5'-ATGGAATCAATCGAACAA-3'
E-DNA-II <sub>M</sub>	5'- TTGTTTCGAD*TGATTCCAT-3'
E-rDNA-Ia	5'- <sub>F</sub> ATG GAA TCA -3'
E-rDNA-IIa	5'- <sub>p</sub> D''TGATTCCAT-3'
E-rDNA-Ib	5'- <sub>p</sub> ATCGAACAA-3'
E-rDNA-IIb	5'-TTGTTTCGA -3'

**rDNA** = replicator DNA sequences; F = fluorescein, D = Abasic, T or G; D' = Abasic or A; D'' = Abasic; P = phosphate \*In standard cross-catalysis experiments, rDNA-IIb contained no fluorescein label. The fluorescein-labeled strands were used only for the experiments depicted in Figure. 3.2 B.

### 3.4.3 MALDI characterization

**DNA-I:** calculated mass, 5552; measured, 5552. **rDNA-Ia (fluorescein-modified):** calculated mass, 3240; measured, 3240. **rDNA-Ib (5'-phosphate):** calculated mass, 2842; measured 2842. **DNA-II, D = T:** calculated mass, 5441; measured, 5440. **DNA-II, D = Ab:** calculated mass, 5317; measured, 5316. **DNA-II, D = G:** calculated mass, 5466; measured, 5465. **rDNA-IIa, D = T (5'-**

**phosphate**): calculated mass, 3090; measured, 3090. **rDNA-IIa, D = Ab (5'-phosphate)**: calculated mass, 2966; measured, 2969. **rDNA-IIa, D = G**: calculated mass, 3115; measured, 3115. **rDNA-IIb**: calculated mass, 2369; measured, 2369. **rDNA-IIb (fluorescein-modified)**: calculated mass, 2880; measured, 2881. **H-DNA-I**: calculated mass, 5600; measured, 5600. **H-rDNA-Ia (fluorescein-modified)**: calculated mass, 3290; measured, 3293. **H-rDNA-Ib (5'-phosphate)**: calculated mass, 2840; measured, 2841. **H-DNA-II, D' = A**: calculated mass, 5396; measured, 5395. **H-DNA-II, D' = Ab**: calculated mass, 5263; measured, 5263. **H-rDNA-IIa, D' = Ab (5'-phosphate)**: calculated mass, 2918; measured 2920. **H-rDNA-IIa, D' = A (5'-phosphate)**: calculated mass, 3051; measured, 3051. **H-rDNA-IIb**: calculated mass, 2363; measured, 2363.

#### 3.4.4 Thermal Denaturation (Melting) Studies

Due to hypochromicity, the absorbance at 260 nm by duplex DNA is less than that of single-stranded DNA. Consequently dissociation of the duplex can be observed by monitoring the absorbance at 260 nm as a function of temperature. The melting temperature ( $T_m$ ) corresponds to the temperature where 50% of the duplexes are dissociated and it is a common parameter for assessing DNA duplex stability. In a typical experiment, we combined 1.3 nmol of each DNA sequence without any fluorescein labels in 1 mL of PBS buffer (10 mM,  $MgCl_2$ , 20 mM PBS, pH 7.0). The mixture was allowed to equilibrate for at least 15 minutes while the instrument cooled to initial temperatures. Absorbance readings at 260 nm were taken from 10 to 65 °C at 1 °C intervals, with one minute hold time at each temperature. The samples were stirred at 100 rpm during the temperature-

variation experiment. The resulting profiles were baseline corrected by subtracting the absorbance at 350 nm.  $T_m$  values were determined from the software, which is based on the maximum of the first derivative of the melting transition.

### **3.4.5 Plasmid preparation**

The *E. coli* plasmid was prepared by Catherine Mitran and Hiofan Hoi as described in the following section. The non complementary plasmid was a gift from Yidan Ding in the Campbell lab at the University of Alberta and was also prepared in a similar manner. The **E-DNA-I** target sequence was contained within the *E. coli* ligase gene (ECs3283, gi 209764253, 2016 bp), which was inserted into the pBAD/His B vector (Invitrogen, 4100 bp). This was accomplished by PCR amplification of the *E. coli* ligase gene from electrocompetent *E. coli* strain DH10B (Invitrogen) using a 5' primer with a XhoI site and a 3' primer with an EcoRI site. The primer sequences used were: forward primer, 5'-GCA GGT GAG TAA CTC GAG CAT GGA ATC AAT CGA ACA AC-3' and reverse primer, 5'-GCC GAA TTC TCA GCT ACC CAG CAA A-3'. The cDNA was digested with XhoI and EcoRI restriction endonucleases (New England Biolabs) and ligated into similarly digested pBAD/His B (Invitrogen). The control plasmid (6170 bp) containing the CaYin0.6 gene<sup>35</sup> instead of the *E. coli* ligase gene was prepared in a similar way and was a gift from Ms. Yidan Ding in Dr. Robert Campbell's group. The PCR products and restriction digestion products were purified by gel electrophoresis and extracted using the QIAquick gel extraction kit (QIAGEN,

Valencia, CA). Plasmid DNA was purified using either the GeneJET Plasmid Miniprep Kit (Fermentas, ON). Dye terminator cycle sequencing using the BigDye (Applied Biosystems) was used to confirm the complete cDNA sequences for all fusion constructs. The sequence of the *E. coli* ligase gene containing the restriction sites was verified at the University of Alberta, Molecular Biology Service Unit (MBSU) prior to incorporation within the plasmid.

### 3.4.6 Ligation experiments

For ligation experiments, DNA replicators and template were first combined in water in a 600- $\mu$ L mini-centrifuge tube to reach a final volume of 10.00  $\mu$ L, at 1.5 times their final concentration. The DNA mixture was then incubated at the desired reaction temperature while the master mix containing the ligase was prepared. Typically, T4 DNA ligase (8.00  $\mu$ L) was mixed with ligation buffer (12.00  $\mu$ L, 10 x concentrated) and water (20.00  $\mu$ L). A portion of this ligase mixture (5.00  $\mu$ L) was immediately added to each DNA mixture resulting in 2,000 cohesive end units per 15- $\mu$ L reaction. The reactions were then placed in a covered thermal incubator. To stop ligation, aliquots (3.00  $\mu$ L) were removed at different times and immediately combined with EDTA<sub>(aq)</sub> (1  $\mu$ L, 0.5 M) to halt the ligation reaction. For the serial ligation reactions, DNA replicators and template were first combined in water in a 600- $\mu$ L mini-centrifuge tube to reach a final volume of 5.00  $\mu$ L, at 1.5 times their final concentration (final concentrations: [rDNA-Ia] = 0.140  $\mu$ M; all other replicators = 0.280  $\mu$ M; [DNA-I] = 140 fM or 0 M). Typical T4 DNA ligase master mix was then added (2.50  $\mu$ L) and the reaction was allowed to react for three hours. At this point, 5.00- $\mu$ L aliquots were taken



from the reactions, and each aliquot was added to a new 600- $\mu$ L mini-centrifuge tube containing higher replicator concentrations (8.75  $\mu$ L, [rDNA-Ia] = 2.32  $\mu$ M; all other replicators = 4.64  $\mu$ M). Master mix (5.00  $\mu$ L) was then added to this second ligation and the amount of **F-DNA-I** was monitored with time. All ligation experiments were analyzed by 15% denaturing PAGE. The percent yield was

determined from the gels according to:  $\%Yield = \frac{Band_{Product}}{Band_{Product} + Band_{Reactant}} \times 100\%$

as described in Chapter 2.<sup>24</sup> The concentration of product was determined by multiplying the percentage yield by the concentration of the fluorescent labeled replicator (the limiting replicator). Each ligation experiment was performed at least three times, and the serial ligation experiment was performed several times with different batches of enzyme. The list of experimental values for the **DNA-I**, **H-DNA-I**, and **E-DNA-I** systems are given in the Table 3.3 and 3.4. The reported values represent the average value  $\pm$  the standard deviation.

### 3.4.7 Plasmid detection

Plasmid detection was performed in a similar manner with some modifications. First, DNA replicators at the typical concentration (final [E-rDNA-Ia] = 1.4  $\mu$ M, all other final [replicator] = 2.8  $\mu$ M) and the plasmid DNA (final [plasmid] = 1.4 nM) were combined in Millipore water in a 600- $\mu$ L mini-centrifuge tube to reach a final volume of 10.00  $\mu$ L, at 1.5 times their final concentration. This mixture was then heated to 95  $^{\circ}$ C for 10 minutes, followed by incubation at 37  $^{\circ}$ C for 20 minutes before adding master mix (5.00  $\mu$ L) containing the T4 DNA ligase. The composition of the master mix was T4 DNA ligase (1.00

$\mu\text{L}$ , Invitrogen 5U/ $\mu\text{L}$  catalogue # 15224-041), ligation buffer (3.00  $\mu\text{L}$ , 5 x concentrated) and water (1.00  $\mu\text{L}$ ), and this master mix was incubated at 37 °C for 5 minutes before adding it to the ligation mixture. We note this buffer contains PEG unlike that of New England Biolabs, which unlike the other systems made this ligation faster without hurting discrimination between the gene-initiated and control experiments. These reactions were analyzed in the same manner as the ligation experiments described above.

### 3.4.8 Serial ligation experiments

For the serial ligation reactions, DNA replicators and template were first combined in water in a 600- $\mu\text{L}$  mini-centrifuge tube to reach a final volume of 5.00  $\mu\text{L}$ , at 1.5 times their final concentration (final concentrations: [**rDNA-Ia**] = 0.140  $\mu\text{M}$ ; all other replicators = 0.280  $\mu\text{M}$ ; [**DNA-I**] = 140 fM or 0 M). Typical T4 DNA ligase master mix was then added (2.50  $\mu\text{L}$ ) and the reaction was allowed to react for three hours. At this point, 5.00- $\mu\text{L}$  aliquots were taken from the reactions, and each aliquot was added to a new 600- $\mu\text{L}$  mini-centrifuge tube containing more replicators (8.75  $\mu\text{L}$ , [**rDNA-Ia**] = 2.32  $\mu\text{M}$ ; all other replicators = 4.64  $\mu\text{M}$ ). Master mix (5.00  $\mu\text{L}$ ) was then added to this second ligation and the amount of **F-DNA-I** was monitored with time.

### 3.4.9 Quantification of replication cycles

The percent yield was determined from the gels according to:

$$\%Yield = \frac{Band_{\text{product}}}{Band_{\text{product}} + Band_{\text{reactant}}} \times 100\% \text{ as described in our in Chapter 2. The}$$

concentration of product was determined by multiplying this percentage by the

concentration of the fluorescent labeled replicator (the limiting replicator). Each ligation experiment was performed at least three times, and the serial ligation experiment was performed several times with different batches of enzyme. The list of experimental values of replication cycles for the **DNA-I** system and **H-DNA-I** system are given (Table 3.3 and 3.4). The reported values represent the average value  $\pm$  the standard deviation. For the typical ligation reactions, the number of net replication cycles was determined from:

$$\text{Replication Cycles} = \frac{(\%Yield_{\text{initial template}} - \%Yield_{\text{no initial template}}) [\text{limiting replicator}]}{[\text{initial template}]}$$

For the serial ligation system, the number of net replication cycles was determined based on the concentration of initial template and limiting replicator concentration of the second-step ligation according to:

$$\text{Replication Cycles} = \frac{(\%Yield_{\text{initial template}} - \%Yield_{\text{no initial template}}) \cdot 1.12 \times 10^{-6} M}{140 \times 10^{-12} M \times \frac{5.0 \mu L}{18.75 \mu L}}$$

### 3.4.10 PAGE images

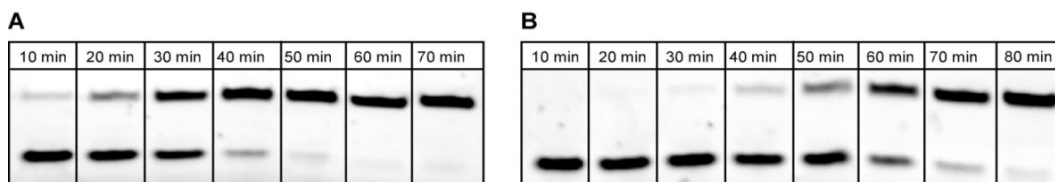


**Figure 3.21:** Representative gel images corresponding to the experiment shown in Figure 3.2 A following cross-catalytic replication of **F-DNA-I** initiated by A) 14 nM or B) 0 nM **DNA-I** using destabilizing replicators ( $D = Ab$ ). *Top band: F-DNA-I; bottom band: rDNA-Ia.* *Experimental conditions:* 14 or 0 nM **DNA-I**; 1.4  $\mu\text{M}$  **rDNA-Ia**; 2.8  $\mu\text{M}$  **rDNA-Ib**; 2.8  $\mu\text{M}$  **rDNA-IIa**( $D = Ab$ ); 2.8  $\mu\text{M}$  **rDNA-IIb**; 30 °C.

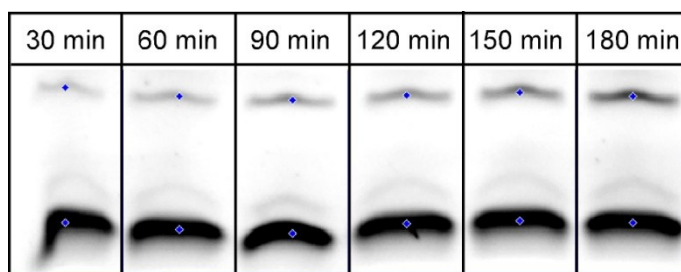
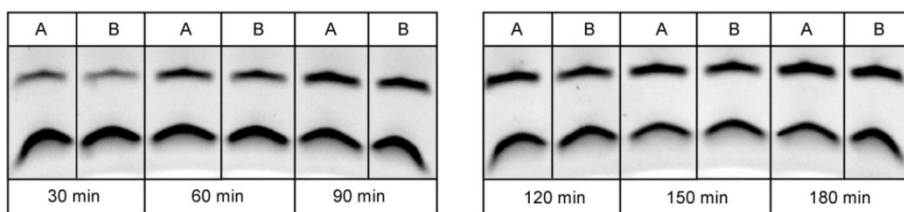


**Figure 3.22:** Representative gel images corresponding to the experiment shown in Figure 3.2 B following single cycle amplification of **F-DNA-II** (left cycle) initiated by 14 nM **DNA-I** using destabilizing replicators ( $D = Ab$ ), one of which contained a fluorescent label. *Top band: F-DNA-II; bottom band: rDNA-IIb\*.* The blue markers identify the location of the band determined by the imaging software. *Experimental conditions:* 14 nM **DNA-I**; 2.8  $\mu\text{M}$  **rDNA-IIa**( $D = Ab$ ); 1.4  $\mu\text{M}$  **rDNA-IIb\***; 30 °C.



A = 14 nM DNA-I, B = 0 M DNA-I

**Figure 3.23:** Representative gel images corresponding to the experiment shown in Figure. 3.2 C following cross-catalytic replication of **F-DNA-I** initiated by 14 nM or 0 nM **DNA-I** using native DNA replicators ( $D = T$ ). *Top band: F-DNA-I; bottom band: rDNA-Ia.* *Experimental conditions:* 14 or 0 nM **DNA-I**; 1.4  $\mu\text{M}$  **rDNA-Ia**; 2.8  $\mu\text{M}$  **rDNA-Ib**; 2.8  $\mu\text{M}$  **rDNA-IIa**( $D = T$ ); 2.8  $\mu\text{M}$  **rDNA-IIb**; 30  $^{\circ}\text{C}$ .

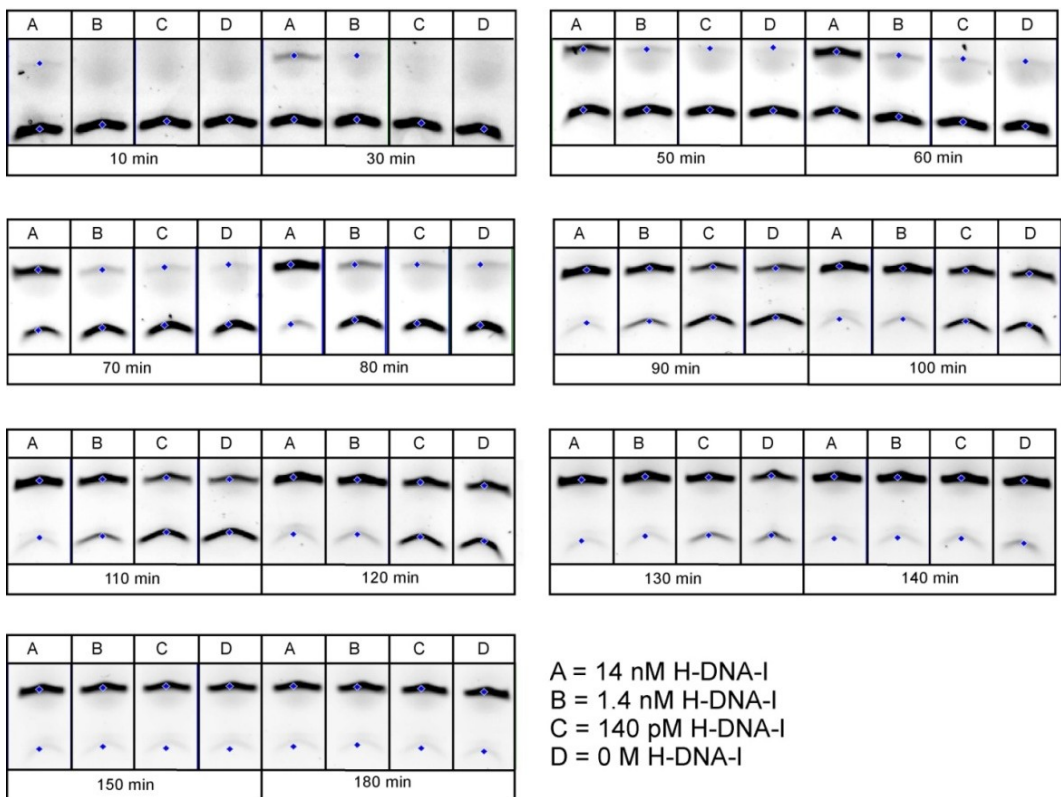


**Figure 3.24:** Representative gel image corresponding to the experiment shown in Figure 3.7 of cross-catalytic replication of **F-H-DNA-I** at 34 °C initiated by 14 nM, 1.4 nM, 140 pM, or 0 nM **H-DNA-I** using destabilizing replicators ( $D' = Ab$ ). *Top band: F-H-DNA-I; bottom band: H-rDNA-Ia.* The blue markers identify the location of the band determined by the imaging software. *Experimental conditions:* 14 nM, 1.4 nM, 140 pM, or 0 nM **H-DNA-I**; 1.4  $\mu$ M **H-rDNA-Ia**; 2.8  $\mu$ M **H-rDNA-Ib**; 2.8  $\mu$ M **H-rDNA-IIa** ( $D' = Ab$ ); 2.8  $\mu$ M **H-rDNA-IIb**; 34 °C.

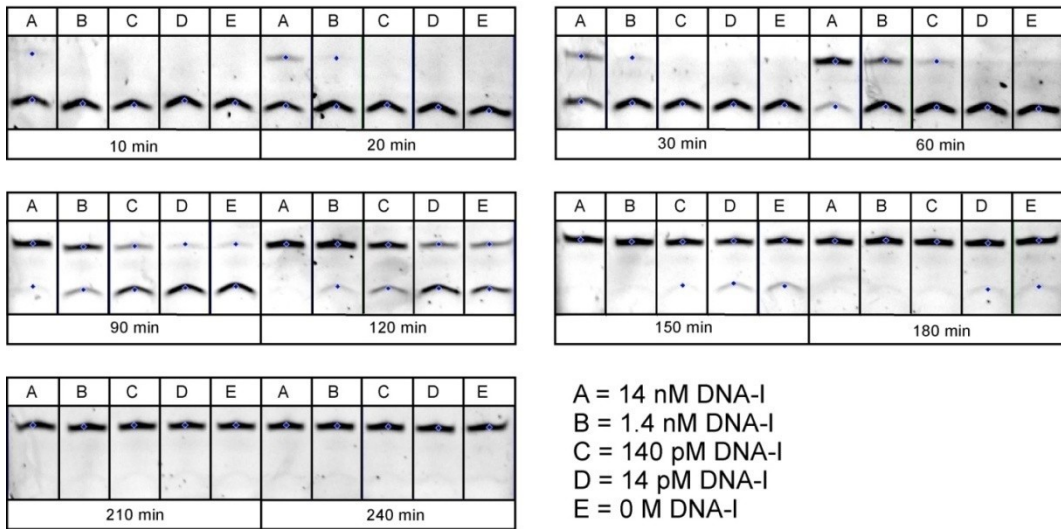
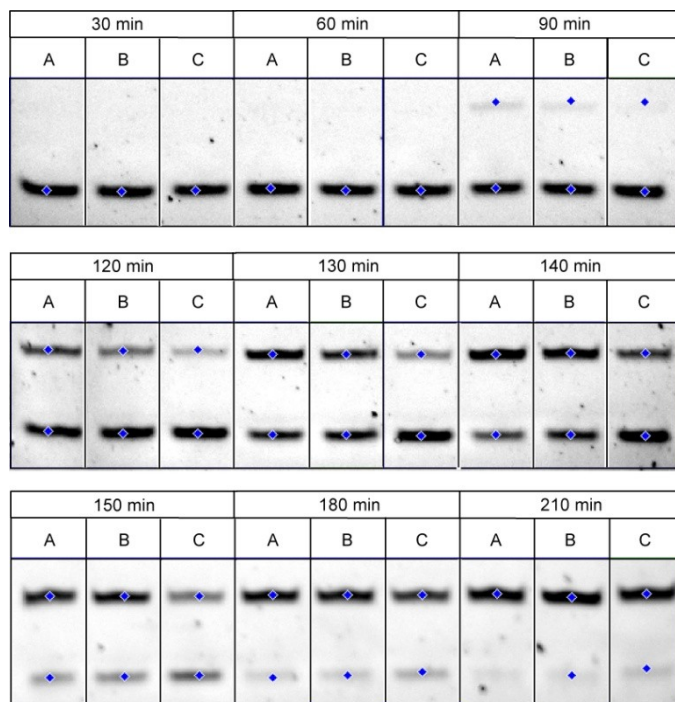


**Figure 3.25:** Representative gel image of cross-catalytic replication of **F-DNA-I** at 30 °C initiated by 14 nM, 1.4 nM, 140 pM, 14 pM or 0 nM **DNA-I** using a lower concentration of replicators. *Top band: F-DNA-I; bottom band: rDNA-Ia.* The blue markers identify the location of the band determined by the imaging software. *Experimental conditions:* 14 nM, 1.4 nM, 140 pM, 14 pM or 0 nM **DNA-I**; 0.35  $\mu$ M **rDNA-Ia**; 0.7  $\mu$ M **rDNA-Ib**; 0.7  $\mu$ M **rDNA-IIa** ( $D = Ab$ ); 0.7  $\mu$ M **rDNA-IIb**; 30 °C.



A = 140 pM, B = 14 pM, C = 0 M H-DNA-I

**Figure 3.26:** Representative gel image of cross-catalytic replication of **F-H-DNA-I** at 34 °C initiated by 140 pM, 14 pM or 0 M **H-DNA-I** using a lower concentration of destabilizing replicators. *Top band: F-H-DNA-I; bottom band: H-rDNA-Ia.* The blue markers identify the location of the band determined by the imaging software. *Experimental conditions:* 140 pM, 14 pM, or 0 M **H-DNA-I**; 0.35  $\mu$ M **H-rDNA-Ia**; 0.7  $\mu$ M **H-rDNA-Ib**; 0.7  $\mu$ M **H-rDNA-IIa** ( $D' = Ab$ ); 0.7  $\mu$ M **H-rDNA-IIb**; 34 °C.



### 3.4.11 Supporting tables

**Table 3.3.** Ligation results vs. initial template concentration for the **DNA-I** system.

Expt.	[DNA-I] (nM)	[F-DNA-I] Formed (nM)		$\Delta$ [F-DNA-I] Formed (nM)	Net Cycles	Replication	Time (min)
		With Template	Without Template			Average	
I	14	1,250	76.0	1,170	83.5		40
II	14	1,310	57.3	1,250	89.4	89±4	40
III	14	1,350	119	1,230	87.9		40
IV	14	1,360	51.1	1,310	93.7		40
I	1.4	1,390	354	1,040	743		50
II	1.4	1,310	165	1,150	821	780±40	50
III	1.4	1,240	146	1,090	780		50
I Dil.	0.14	272	175	97	690		120
II Dil.	0.14	281	201	80	570	650±70	120
III Dil.	0.14	241	143	98	700		120
I SL	0.00014	422	343	79	2,100,000		40
II SL	0.00014	524	365	159	4,270,000		40
III SL	0.00014	448	378	70	1,900,000	2,700,000 ±900,000	40
IV SL	0.00014	140	64.9	75	2,000,000		30
V SL	0.00014	495	371	124	3,300,000		40
VI SL	0.00014	470	359	111	2,980,000		40

Dil. = Experiments done with four-fold diluted replicators. SL = Serial ligation experiments.

**Table 3.4.** Ligation results vs. initial template concentration for the **H-DNA-I** system.

Expt.	[H-DNA-I] (nM)	[F-H-DNA-I] Formed (nM)		$\Delta$ [F-H-DNA-I] Formed (nM)	Net Replication Cycles		Time (min)
		With Template	Without Template			Average	
I	14	1,370	152	1,220	87.2		90
II	14	1,390	216	1,170	84.1		90
III	14	1,310	213	1,100	78.5		90
IV	14	1,400	186	1,210	86.6	85±3	90
V	14	1,400	191	1,210	86.2		90
VI	14	1,380	169	1,210	86.8		90
VII	14	1,340	177	1,160	82.9		90
I	1.4	733	290	443	317		100
II	1.4	711	382	330	236		100
III	1.4	691	294	397	284	310±50	100
IV	1.4	767	296	471	336		100
V	1.4	778	266	512	366		100
I Dil.	0.14	201	76.3	124	888		130
II Dil.	0.14	171	46.6	125	891	920±50	130
III Dil.	0.14	173	37.3	135	970		140
I Dil.	0.014	209	118	91	6500		140
II Dil.	0.014	189	114	74	5300	6000±600	140
III Dil.	0.014	147	62	85	6100		150

Dil. = Experiments done with four-fold diluted replicators.

### 3.5 References

- 1) Orgel, L. E.: Molecular replication. *Nature* **1992**, 358, 203-209.
- 2) Paul, N.; Joyce, G. F.: Minimal self-replicating systems. *Current Opinion in Chemical Biology* **2004**, 8, 634-639.
- 3) Volker Patzke, G. v. K.: Self replicating systems. *ARKIVOC* **2007**, 293-310.
- 4) Benner, S. A.; Chen, F.; Yang, Z.: Synthetic Biology, Tinkering Biology, and Artificial Biology: A Perspective from Chemistry. In *Chemical Synthetic Biology*; John Wiley & Sons, Ltd, **2011**; pp 69-106.
- 5) Taran, O.; von Kiedrowski, G.: Replicators: Components for Systems Chemistry. In *Chemical Synthetic Biology*; John Wiley & Sons, Ltd, **2011**; pp 287-319.
- 6) Szostak, J.: The eightfold path to non-enzymatic RNA replication. *J Syst Chem* **2012**, 3, 2.
- 7) Joyce, G. F.: Bit by Bit: The Darwinian Basis of Life. *PLoS Biol* **2012**, 10, e1001323.
- 8) von Kiedrowski, G.: A Self-Replicating Hexadeoxynucleotide. *Angew Chem Int Ed* **1986**, 25, 932-935.
- 9) Zielinski, W. S.; Orgel, L. E.: Autocatalytic synthesis of a tetranucleotide analogue. *Nature* **1987**, 327, 346-347.
- 10) Sievers, D.; von Kiedrowski, G.: Self-replication of complementary nucleotide-based oligomers. *Nature* **1994**, 369, 221-224.
- 11) von Kiedrowski, G.; Wlotzka, B.; Helbing, J.; Matzen, M.; Jordan, S.: Parabolic Growth of a Self-Replicating Hexadeoxynucleotide Bearing a 3'-5'-Phosphoamidate Linkage. *Angew Chem Int Ed* **1991**, 30, 423-426.
- 12) Luther, A.; Brandsch, R.; von Kiedrowski, G.: Surface-promoted replication and exponential amplification of DNA analogues. *Nature* **1998**, 396, 245-248.

- 13) Saiki, R.; Gelfand, D.; Stoffel, S.; Scharf, S.; Higuchi, R.; Horn, G.; Mullis, K.; Erlich, H.: Primer-directed enzymatic amplification of DNA with a thermostable DNA polymerase. *Science* **1988**, *239*, 487-491.
- 14) Lincoln, T. A.; Joyce, G. F.: Self-Sustained Replication of an RNA Enzyme. *Science* **2009**, *323*, 1229-1232.
- 15) Andras, S. C.; Power, J. B.; Cocking, E.; Davey, M.: Strategies for signal amplification in nucleic acid detection. *Mol Biotechnol* **2001**, *19*, 29-44.
- 16) Gill, P.; Ghaemi, A.: Nucleic Acid Isothermal Amplification Technologies—A Review. *Nucleosides, Nucleotides and Nucleic Acids* **2008**, *27*, 224-243.
- 17) Parida, M.; Sannarangaiah, S.; Dash, P. K.; Rao, P. V. L.; Morita, K.: Loop mediated isothermal amplification (LAMP): a new generation of innovative gene amplification technique; perspectives in clinical diagnosis of infectious diseases. *Rev Med Virol* **2008**, *18*, 407-421.
- 18) Ye, J.; Gat, Y.; Lynn, D. G.: Catalyst for DNA Ligation: Towards a Two-Stage Replication Cycle. *Angew Chem Int Ed* **2000**, *39*, 3641-3643.
- 19) Grossmann, T. N.; Strohbach, A.; Seitz, O.: Achieving Turnover in DNA-Templated Reactions. *ChemBioChem* **2008**, *9*, 2185-2192.
- 20) Schrum, J. P.; Ricardo, A.; Krishnamurthy, M.; Blain, J. C.; Szostak, J. W.: Efficient and Rapid Template-Directed Nucleic Acid Copying Using 2'-Amino-2',3'-dideoxyribonucleoside-5'-Phosphorimidazole Monomers. *J Am Chem Soc* **2009**, *131*, 14560-14570.
- 21) Zhan, Z.-Y. J.; Lynn, D. G.: Chemical Amplification through Template-Directed Synthesis. *J Am Chem Soc* **1997**, *119*, 12420-12421.
- 22) Luo, P.; Leitzel, J. C.; Zhan, Z.-Y. J.; Lynn, D. G.: Analysis of the Structure and Stability of a Backbone-Modified Oligonucleotide:

Implications for Avoiding Product Inhibition in Catalytic Template-Directed Synthesis. *J Am Chem Soc* **1998**, *120*, 3019-3031.

- 23) Silverman, A. P.; Kool, E. T.: Detecting RNA and DNA with Templated Chemical Reactions. *Chem Rev* **2006**, *106*, 3775-3789.
- 24) Kausar, A.; McKay, R. D.; Lam, J.; Bhogal, R. S.; Tang, A. Y.; Gibbs-Davis, J. M.: Tuning DNA Stability To Achieve Turnover in Template for an Enzymatic Ligation Reaction. *Angew Chem Int Ed* **2011**, *50*, 8922-8926.
- 25) Weiss, B.; Jacquemin-Sablon, A.; Live, T. R.; Fareed, G. C.; Richardson, C. C.: Enzymatic breakage and joining of deoxyribonucleic acid. VI. Further purification and properties of polynucleotide ligase from *Escherichia coli* infected with bacteriophage T4. *J Biol Chem* **1968**, *243*, 4543-55.
- 26) A cohesive end unit is the amount of enzyme needed to catalyze the ligation of 50 % of 0.12 M lambda DNA in 20  $\mu$ L in 30 minutes at 16 °C. One Weiss unit is equal to approximately 300 cohesive end units.
- 27) Lohman, G. J.; Tabor, S.; Nichols, N. M.: DNA ligases. *Curr Protoc Mol Biol* **2011**, *Chapter 3*, Unit3 14.
- 28) Abe, A.; Inoue, K.; Tanaka, T.; Kato, J.; Kajiyama, N.; Kawaguchi, R.; Tanaka, S.; Yoshiba, M.; Kohara, M.: Quantitation of hepatitis B virus genomic DNA by real-time detection PCR. *J Clin Microbiol* **1999**, *37*, 2899-903.
- 29) Levy, M.; Ellington, A. D.: Exponential growth by cross-catalytic cleavage of deoxyribozymogens. *Proc Natl Acad Sci* **2003**, *100*, 6416-6421.
- 30) Li, X. Y.; Hernandez, A. F.; Grover, M. A.; Hud, N. V.; Lynn, D. G.: Step-Growth Control in Template-Directed Polymerization. *Heterocycles* **2011**, *82*, 1477.
- 31) Li, X.; Zhan, Z.-Y. J.; Knipe, R.; Lynn, D. G.: DNA-Catalyzed Polymerization†. *J Am Chem Soc* **2002**, *124*, 746-747.

- 32) Loeb, L. A.; Preston, B. D.: Mutagenesis by Apurinic/Apyrimidinic Sites. *Ann Rev Genet* **1986**, *20*, 201-230.
- 33) Kochetkov, N. K.; Budovskii, E. I.: Hydrolysis of N-glycosidic Bonds in Nucleosides, Nucleotides, and their Derivatives. In *Organic Chemistry of Nucleic Acids*; Kochetkov, N. K., Budovskii, E. I., Eds.; Springer US, **1972**; pp 425-448.
- 34) Küpfer, P. A.; Leumann, C. J.: The chemical stability of abasic RNA compared to abasic DNA. *Nucleic Acids Res* **2007**, *35*, 58-68.
- 35) Ding, Y.; Ai, H. W.; Hoi, H.; Campbell, R. E.: Forster resonance energy transfer-based biosensors for multiparameter ratiometric imaging of Ca<sup>2+</sup> dynamics and caspase-3 activity in single cells. *Anal Chem* **2011**, *83*, 9687-93.

## **Chapter 4**

**Detection of SNPs using Lesion-Induced DNA**

**Amplification and Simplified Detection Strategies**

## 4.1 Introduction

A genetic mutation is defined as the changes to the DNA sequence of a particular gene. Commonly, genetic mutations are caused by radiation, mutagenic chemicals or errors during cellular DNA replication. Some DNA mutations may appear in the non-coding region therefore they have no effect on the organism, but some of the mutations can change the gene product (protein), which might lead to different diseases.<sup>1, 2</sup> A single nucleotide polymorphism (SNP) is a specific form of genetic variation, where the frequency of variation occurs at more than 1% in a population.<sup>3</sup> The detection of single nucleotide polymorphisms is very important in the diagnosis of human hereditary diseases, cancer diagnosis, pharmacogenomics and detection of disease resistant strains.<sup>4-8</sup> Recent works on SNP detection has focused on improving sensitivity and better discrimination between mismatches.<sup>9, 10</sup> Many of these methods involve amplification of the target sequence, followed by detection analysis to determine which allele is present. The most commonly used target sequence amplification methods are polymerase chain reaction (PCR),<sup>11, 12</sup> strand displacement amplification (SDA),<sup>13,</sup><sup>14</sup> rolling circle amplification (RCA),<sup>15, 16</sup> and the ligase chain reaction (LCR).<sup>17-19</sup> There are several commercially available SNP genotyping arrays (Affymetrix, Illumina) that are geared to genotype SNPs across the genome simultaneously with high accuracy. Indeed, these arrays are capable of analyzing millions of SNPs in one chip.<sup>20</sup> But for some diseases (e.g. multidrug drug resistant-tuberculosis (MDR-TB) or sickle cell anemia), it may be necessary to know the presence of a single base mismatch. For this purpose, it is optimal to develop a



simple assay. A diagnostic test kit developed by Cepheid (Xpert® MTB/RIF (rifampin-resistance mutations)) based on allele specific extension is a commercially available PCR-based kit for TB diagnosis that utilizes a temperature cycler. However, in addition to the high initial cost of the instrument (negotiated price for low income countries \$17,000), the cost per test is about \$10.<sup>21</sup> Furthermore, PCR based SNP detection is not very effective since the discrimination power of allele specific extension is low.<sup>22</sup> For this reason, polymerase based isothermal amplification methods like LAMP are not very suitable for SNP detection because of low discriminating power and difficulty in designing the primer, despite their simple instrumentation requirements.<sup>23</sup> In this chapter, we describe our efforts to develop a simple assay based on LCR that uses the effective discriminating ability of ligases to distinguish mismatches at a particular position on the target. Our goal is to keep the cost of analysis at a dollar per test either a colorimetric detection approach suitable for a simple handheld device. For this reason, the discrimination ratio of the amplification process has to be high enough to allow the difference in color that corresponds to the presence of a mismatch to be discerned by naked eye.

Due to their high sensitivity and better discriminating ability, LCR based methods have evolved as very promising molecular diagnostic techniques.<sup>17-19, 24-31</sup> For example, this technique has been used to identify the presence of specific genetic disorders such as sickle cell disease, which is caused by the presence of a single point mutation.<sup>18, 32, 33</sup> As described in Chapter 1 (Section 1.3.1.2), the DNA ligase is very specific for the 3'-nucleotide, which also allows for higher

discriminatory power against mismatches at the 3'-end of the ligation site.<sup>18, 24, 31</sup> Thus, the LCR process is very useful for detection of mismatches at specific positions in the target DNA.

In the LCR process, ligation of the two oligonucleotide probes by DNA ligase results in a longer product hybridized to the target strand. The stability of this product complex is much higher than the stability of the nicked duplex that existed prior to ligation. For this reason, a thermostable enzyme is required so that one can use thermocycling to separate the product from the target and hybridize a new set of probe strands. The cycle of denaturation, annealing and ligation is repeated many times leading to the exponential growth of the ligated product. To simplify the detection and remove the need for thermal cycling, several isothermal DNA amplification methods have been developed recently. Most of these isothermal DNA amplification methods are based on primer extension methods.<sup>34,35</sup> Since ligation has a better discriminating ability than primer extension reactions, hybrid methods have been developed that involve primer-extension based isothermal amplification coupled with ligation to achieve better discrimination.<sup>26-28, 36-38</sup> Generally, LCR amplification products are analyzed by heterogeneous methods like gel electrophoresis.<sup>39</sup> However, the main disadvantages of heterogeneous methods are that they involve multiple tedious and time consuming steps. To avoid these limitations, homogeneous methods have gained increasing attention because of their simplicity, shorter assay time, and absence of separation or washing steps. However, commonly used approaches for real-time homogeneous detection such as the Taqman probe,<sup>40</sup> molecular

beacon,<sup>41</sup> and double-stranded DNA (dsDNA) specific fluorescent dyes<sup>42</sup> are only applicable for polymerase based amplification methods.<sup>39</sup> These homogenous methods are not useful for LCR based methods since this is not a primer extension method but the amplification of ligated probes. Therefore, we aimed to design a simple, sensitive, and specific method for SNP detection by combining homogenous detection with a simple amplification step based on our novel destabilization-induced isothermal LCR process.

One example of a homogeneous detection method suitable for ligation detection is fluorescence (or Förster) resonance energy transfer, FRET, which is a useful technique for measuring distance-dependent interactions on a molecular level.<sup>43</sup> FRET is a radiation-free transfer of energy from an excited donor dye to an acceptor dye. In addition to the distance, the FRET process also depends on the overlap between the emission spectrum of the donor dye and the excitation spectrum of the acceptor as well as the correct dipole alignment of the dyes. If the distance between two dyes increases, the FRET efficiency decreases significantly. Based on this distance dependence, several FRET based ligation assays have been developed by modifying two probes with two fluorescent dyes of different colors which can act as a FRET pair.<sup>44-46</sup> In the first part of this chapter, I will evaluate the ability of our isothermal ligase-based lesion induced isothermal amplification (**LIDA**) method to detect SNPs based on polyacrylamide gel electrophoresis analysis. In the second part, I will discuss the application of LIDA to develop a FRET based real-time method of SNP detection. In the final part of the chapter, I will describe our work on developing a colorimetric platform for DNA detection

by combining isothermal amplification with target induced strand displacement in DNA-modified gold nanoparticle aggregates.

**Table 4.1.** DNA sequences used in this study

Sequence name	DNA sequence
<b>DNA-I(X) (X=T/G/C/A)</b>	5'-TTGTTA AAT AXT GATAAG-3'
<b>DNA-II<sub>D</sub>(D=Ab/T)</b>	5'-CTT ATC AAD ATT TAA CAA-3'
<b>r-Ia</b>	
<b>r-Ia</b>	5'-TTGTTAAAT-3'
<b>r-Ia(FAM)</b>	5'- <sub>FAM</sub> TTGTTAAAT-3'
<b>r-Ia(Cy5)</b>	5'- <sub>Cy5</sub> TTGTTAAAT-3'
<b>r-Ib (X)</b>	
<b>r-Ib (T)</b>	5'- <sub>p</sub> ATTGATAAG-3'
<b>r-Ib (A)</b>	5'- <sub>p</sub> AATGATAAG-3'
<b>r-Ib (G)</b>	5'- <sub>p</sub> AGTGATAAG-3'
<b>r-Ib (FAM)</b>	5'- <sub>p</sub> ATT <sub>FAM</sub> GATAAG-3' (FAM = Fluorescein)
<b>r-IIa<sub>D</sub></b>	
<b>r-IIa<sub>D</sub>(D=Ab)</b>	5'- <sub>p</sub> DATTTAACAA-3'
<b>r-IIb</b>	
<b>r-IIb</b>	5'-CTTATCAA-3'
<b>r-IIb-9(FAM)</b>	5'- <sub>FAM</sub> TCTTATCAA-3'
<b>r-IIb-13(FAM)T</b>	5'- <sub>FAM</sub> TTTTTCTTATCAT-3'
<b>r-IIb-13(FAM)C</b>	5'- <sub>FAM</sub> TTTTTCTTATCAC-3'

#### 4.2 Discrimination of mismatches in a ligation single cycle

In 1988, Landegren et al. developed a ligation based assay to show its suitability for distinguishing the SNP that causes sickle cell anaemia from the normal human *β globulin* gene.<sup>31</sup> It has subsequently become well known that the enzyme T4 DNA ligase is very sensitive to the presence of a mismatch at the 3'-end of the ligation site.<sup>31, 47</sup> Consequently, we designed our probes such that the mismatch would form across from the 3'-OH end of the ligation site. Our earlier work showed that T4 DNA ligase can tolerate abasic modifications both in the probe and the template, and the rate of ligation for the templated reaction (the

single cycle) is similar to that of native DNA.<sup>48, 49</sup> Thus, we studied the single cycle of ligation with different mismatches in the target (template) DNA (**DNA-I(X)**, where **X = T/G/C/A**) to see how much the ligation was affected by the presence of the mismatch using probes that were complementary to **DNA-I(T)**. As expected, the rate of ligation was very fast with the matched target (**X=T**), as the reaction was complete after 10 minutes. In contrast, there was no product formation in the presence of the mismatched target (**X= G/C/A**) after 10 minutes. Indeed, we found that the A:G, A:C, A:A mismatches yielded only 9%, 23% and 0 % respectively even after 18 hours (Figure 4.1). The high selectivity of the T4 DNA ligase for mismatches at the 3' position, yet its tolerance for the abasic at the 5' position, indicated that our DNA amplification by destabilization method would be perfectly suitable for the development of isothermal SNP detection.

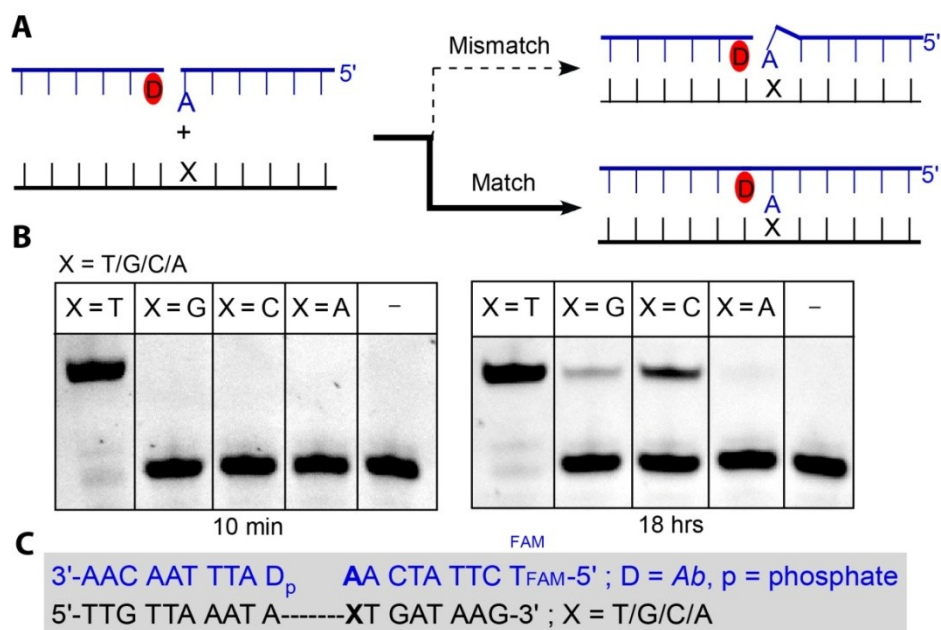


**Figure 4.1:** A) Schematic diagram of mismatch discrimination with T4 DNA ligase. B) PAGE images of ligation with match target, mismatch target and control ligation (-, no initial target) with T4 DNA ligase at 30 °C after 10 minutes and after 18 hours, and C) DNA sequences used. *Experimental conditions:* 1.4  $\mu\text{M}$  **r-IIb (FAM)**, 2.8  $\mu\text{M}$  **r-IIa<sub>Ab</sub>**, and 1.4  $\mu\text{M}$  of target **DNA-I(X)** (X=T/G/C/A) or no target at 30 °C, T4 DNA ligase 2000 cohesive end units (CEU) per 15  $\mu\text{L}$  ligation volume.

#### 4.3 Discrimination of mismatches with cross-catalysis

With one cycle of templated ligation, we achieved only linear amplification, which intrinsically requires a long time to amplify the target sequence initially present at low concentrations. In order to enhance the rate of amplification, we utilized a cross-catalytic approach for SNP detection based on our isothermal amplification method. The first step in our amplification process involves the hybridization of two small probe strands, one of which contains a destabilizing 5'-phosphate and abasic lesion, to the target sequence **DNA-I(X)**.

Following hybridization, the probes are ligated by T4 DNA ligase to form a destabilizing template (**DNA-II<sub>D</sub>**) in situ (Figure 4.2, Cycle 1). Here the probes only match with the target sequence that contains an internal thymidine (**DNA-I(T)**); all other bases at this position result in a mismatch with the terminus of one of the probes. As T4 DNA ligase is very sensitive to mismatches at the ligation site, the presence of the mismatched target should greatly decrease the rate of formation of the destabilizing template **DNA-II<sub>D</sub>**. If ligation occurs, the product **DNA-II<sub>D</sub>** should dissociate from **DNA-I(X)** owing to the presence of the destabilizing lesion in **DNA-II<sub>D</sub>**. Once dissociated, there is little chance for the DNA strands (**DNA-I(X)** and **DNA-II<sub>D</sub>**) to reanneal since there is a high concentration of complementary DNA probes present in the solution allowing **DNA-II<sub>D</sub>** to enter Cycle 2. Cycle 2 involves two probes complementary to the destabilizing **DNA-II<sub>D</sub>** template that are also present in the ligation mixture. The nicked duplex formed after hybridization with these probes can be ligated by T4 DNA ligase to give the **DNA-I(T)** strand (Figure 4.2, Cycle 2). **DNA-I(T)** is then released isothermally to template the formation of more **DNA-II<sub>D</sub>** in Cycle 3 (We note, Cycle 3 is the same as Cycle 1 for the matched target). Since the product of Cycle 2 acts as a template for Cycle 3, we expect exponential amplification of **DNA-I(T)** and its complement.<sup>49</sup> For the mismatched target, however, very little or no **DNA-II<sub>D</sub>** will be formed from Cycle 1, which will in turn hamper production of **DNA-I(T)** in Cycle 2. Therefore, any **DNA-I(T)** product formed from the mismatched target will be very close to that of the background reaction (vide supra).

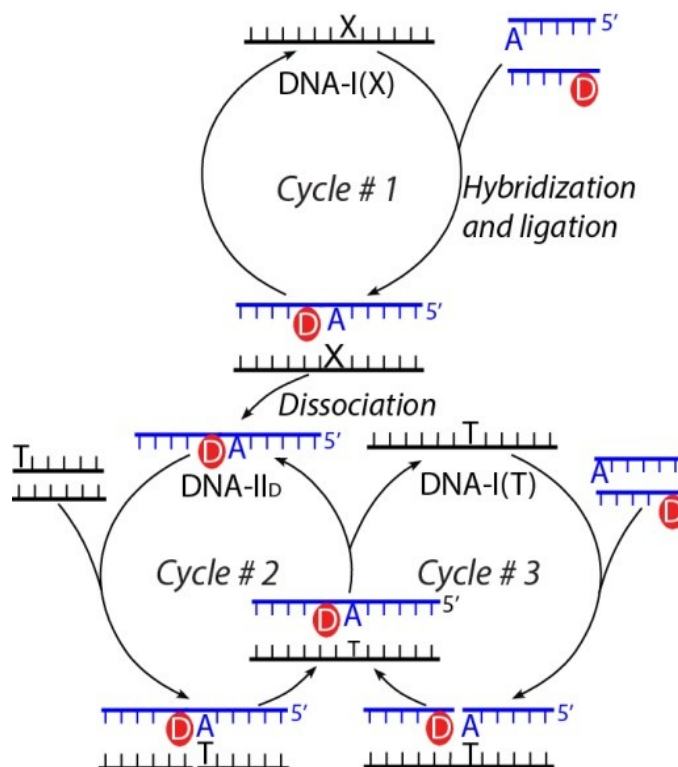


**Figure 4.2:** General scheme for isothermal cross-catalytic amplification of **DNA-I(X)** using an abasic destabilizing group in an LCR. Cycle 1: **DNA-I(X)** acts as a template for the formation of **DNA-II<sub>D</sub>** (see text for details). Cycle 2: The **DNA-II<sub>D</sub>** acts as template for formation of new **DNA-I(T)** strand, which is released isothermally to template more ligation in the Cycle 3 (same as Cycle 1 for the matched target).

To verify whether we could use this kind of isothermal amplification technique to detect the presence of mismatches in the target DNA, we studied the amplification with different matched and mismatched templates. As shown in Figure 4.3 A, the cross-catalytic formation of fluorescently labelled **DNA-I(T)** was complete after 50 min when 14 nM of the perfectly matched template **DNA-I(T)** was initially present. However with 14 nM of the mismatched templates, the cross-catalytic formation of fluorescently labelled **DNA-I(T)** was complete after



80 minutes. It is important to note that the amplification profiles with the mismatches are very similar to that of the background-triggered reaction (no initial **DNA-I(X)** present). These results suggest that our isothermal amplification method allows for the rapid detection of mismatches in a specific position on a DNA target sequence. To quantify how well this system was at differentiating the mismatches, we calculated the discrimination ratio, which is defined as the ratio of the **DNA-I(T)** formed from the cross-catalytic reactions initiated with the matched target to that of the mismatched target. The maximum discrimination ratios of the A:T match to the A:G, A:C and A:A mismatches were 35, 22 and 47, respectively. These values are greater than those in a recently reported method for ligase-based detection of SNPs in the literature, which indicated that our cross-catalytic approach enhances SNP selectivity.<sup>50</sup> Additionally, our approach has the advantage of requiring a simple probe design.

However, the presence of the background-triggered formation of **DNA-I(T)** limited the ability to detect nM levels; at lower initial target concentration, the formation of **DNA-I(T)** was indistinguishable for the target-initiated and background-triggered processes. Therefore, to slow the background-triggered process, we reduced the concentration of the probes as we had previously shown that allowed us to detect pM levels of target DNA. Using this lower probe concentration, we can discriminate 70 pM (1.02 fmol) of DNA from background with a widely dynamic range that spanned approximately 3 orders of magnitude. Moreover, the amount of **DNA-I(T)** formed after 80 minutes depended linearly on

the logarithm of the initial **DNA-I(T)** concentration, suggesting that our approach could be used to quantify the initial amount of target presents.

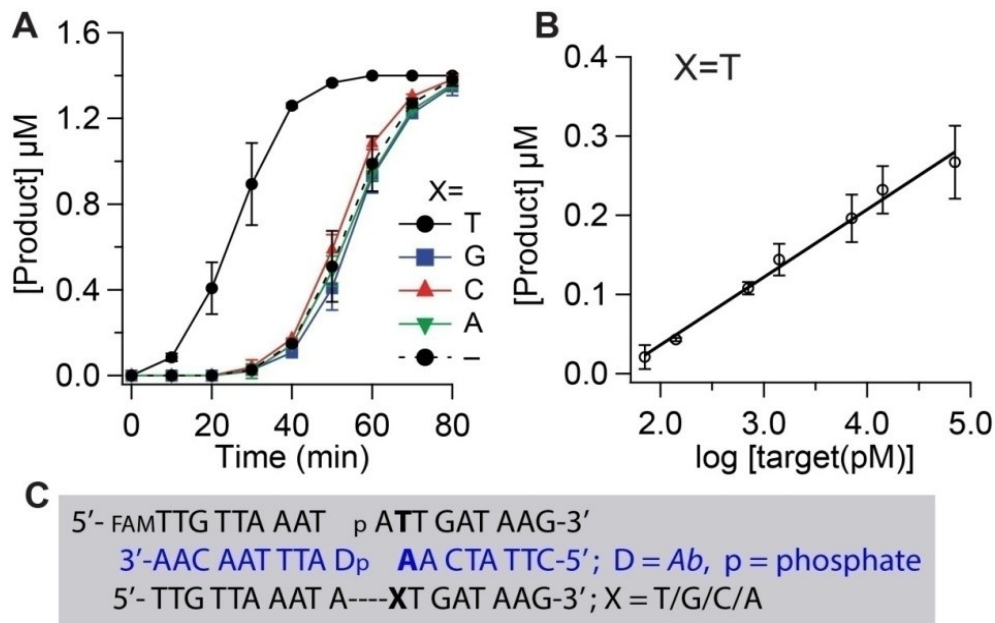


**Figure 4.3:** A) The kinetics of cross-catalytic amplification of **DNA-I(T)** initiated with different **DNA-I(X)** targets (matched or mismatched). The rate of amplification was faster with matched target (**X=T**), whereas the rate of amplification was slower in the presence of the mismatched targets (**X = G/C/A**). The background-triggered process is also shown (-, no initial template). *Experimental conditions:* 1.4  $\mu\text{M}$  **r-Ia(FAM)**, 2.8  $\mu\text{M}$  **r-Ib(T)**, 2.8  $\mu\text{M}$  **r-IIa<sub>Ab</sub>**, 2.8  $\mu\text{M}$  **r-IIb** and 14 nM **DNA-I(T)** at 30 °C, 2000 cohesive end unit (CEU) T4 DNA ligase per 15  $\mu\text{L}$  ligation volume. B) The amount of product formed depends linearly on the amount of matched target DNA (**DNA-I(T)**) initially present. C) DNA sequences used in this study. *Experimental conditions:* 340 nM **r-Ia(FAM)**, 680 nM **r-Ib(T)**, 680 nM **r-IIa<sub>Ab</sub>**, 680 nM **r-IIb** and different concentrations of target **DNA-I(T)** at 30 °C, 2000 CEU T4 DNA ligase per 15  $\mu\text{L}$  ligation volume.

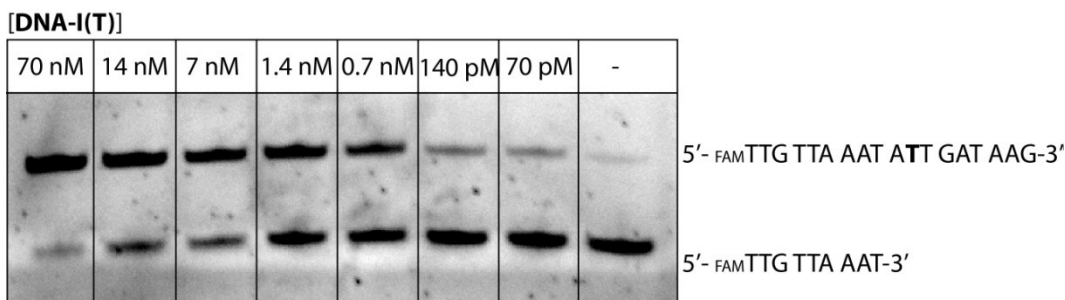


**Figure 4.4:** Representative PAGE image of the cross-catalytic amplification shown in Figure 4.3 B with different concentrations of initial target **DNA-I(T)**. *Experimental conditions:* 340 nM **r-Ia(FAM)**, 680 nM **r-Ib(T)**, 680 nM **r-IIa<sub>AB</sub>**, 680 nM **r-IIb** and different concentration of target **DNA-I(T)** at 30 °C, T4 DNA ligase 2000 CEU per 15  $\mu$ L ligation volume.

#### 4.3.1 Specific detection of mismatches

The above experiment for discrimination of mismatches can only reveal if a mismatch is present or not. In some cases, it may be necessary to know the type and the amount of the specific mismatch in the target DNA.<sup>51</sup> Since our isothermal amplification method is very good in discriminating mismatches in a particular position in the target, we attempted to multiplex the assay for detection of particular mismatches.

##### 4.3.1.1 Discrimination between T- and A-target

To develop an assay that could report on whether a T or A was present in the target sequence, we designed two probes of different lengths: a 9-nucleotide (nt) probe with a 3'-deoxyadenosine complementary to the T-target (**DNA-I(T)**) and a 13-nt probe with a 3'-thymidine complementary to the A-target (**DNA-I(A)**). To verify that the probes were selective, we combined T- or A- targets with both of the different length probes and another probe complementary to both



Next we attempted to multiplex the cross-catalytic amplification process. For this purpose, we added three more complementary probes to the ligation system. Upon ligation, these probes formed either A-target or T-target depending on whether the long or short destabilizing template was made in the first step, respectively. To delineate which product was forming, we utilized the probe sequences described in Figure 4.5, which allowed for the detection of the fluorescently labelled destabilizing template rather than the fluorescently labelled target (A- or T-target i.e., **DNA-I(X=A/T)**). Interestingly, unlike the single cycle experiments, we observed the formation of both products even though only one target was present. Moreover, the rate of formation of the mismatched product was faster than the background-triggered reaction. Specifically, when the T-target was present, we expected to see only the 19-nt product (T:A match), but as shown in Figure 4.6, we also observed the formation of the 23-nt product corresponding to the T:T mismatch after 30 minutes of reaction. Similarly, the A-target resulted in the preferential formation of the 23-nt product but a significant amount of the 19-nt product was also observed. For the A-target, the discrimination ratio for the T:A match over the A:A mismatch was 1.7, while the ratio for T:A match over T:T mismatch corresponding to the T-target system was 1.1. We reasoned the observed larger amount of product from the mismatched target in comparison to the reaction initiated with no template, is that the mismatched ligation became faster when there was a high concentration of probes present in the solution. Since all the probes (matched and mismatched) were present in a fairly high concentration and competing for the same spot in the template, the rate of

mismatched ligation was increased. The discrimination ratio was better for the T-target than the A-target, this is because for T-target we are comparing a T:A match over an A:A mismatch and for A-target we are comparing a T:A match over a T:T mismatch. This may be attributable to the higher stability of the T:T mismatch than that of the A:A mismatch, which leads to faster ligation with the former.<sup>52</sup> These observations of selectivity are similar to those reported with Taq DNA ligase where the authors observed more product formation that corresponded to a T:T mismatch compared with an A:A mismatch.<sup>18</sup>

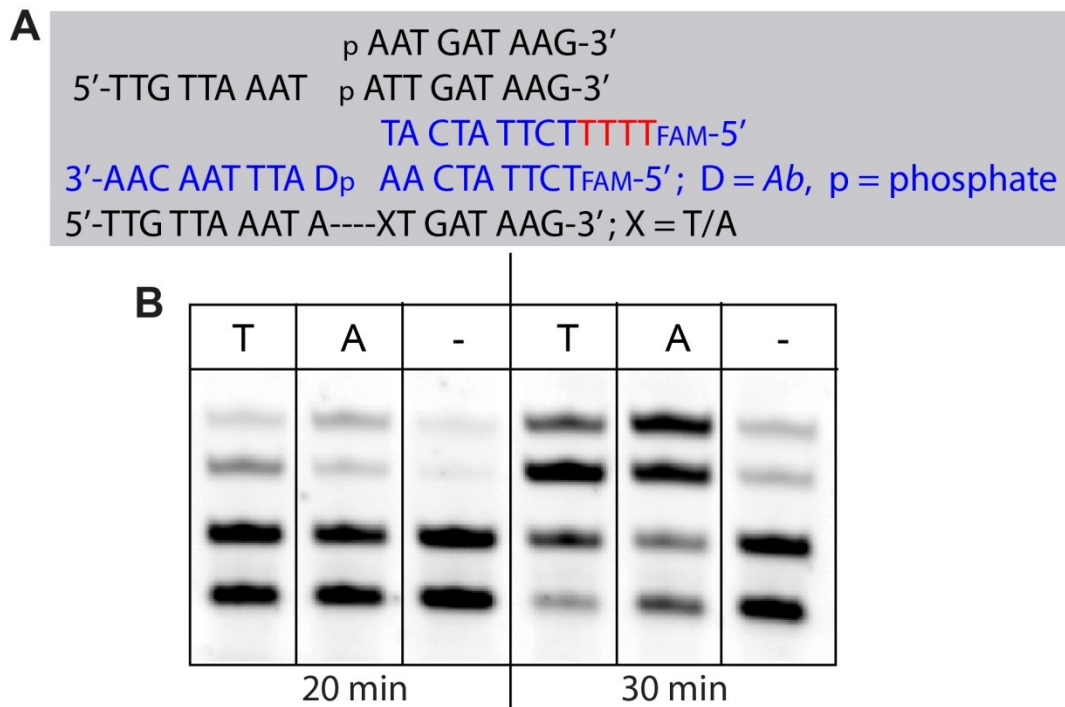


**Figure 4.6:** A) DNA sequences used for multiplexed assay. B) PAGE image of a multiplexed assay in the presence of all six probes after 20 min and 30 min of ligation. The reactions were initiated with 14 nM of the T-target (T), 14 nM of the A-target (A), or no target (-). *Experimental conditions:* 2.8  $\mu$ M **r-Ia**, 2.8  $\mu$ M **r-Ib(T)**, 2.8  $\mu$ M **r-Ib(A)**, 2.8  $\mu$ M **r-IIa<sub>Ab</sub>**, 1.4  $\mu$ M **r-IIb-9 (FAM)**, 1.4  $\mu$ M **r-IIb-13 (FAM)T**, and 14 nM of target **DNA-I(T/A)** or no target at 30 °C, T4 DNA ligase 2000 CEU per 15  $\mu$ L ligation volume.

In order to avoid the problem of high background with multiplexing, we studied separate cross-catalytic amplification with separate sets of four probes and either the matched target or mismatched target (Figure 4.7 A and B). For example, the set of probes containing the shorter fluorescent probe were complementary to the T-target, so A-target would be a mismatch (Figure 4.7 A). Consequently, we observed faster amplification of the short destabilizing template when 14 nM of the T-target was present compared with 14 nM of the A-target (Figure 4.7 C and E). Conversely, the second set of probes (Figure 4.7 B, longer fluorescent probe) which match with the A-target, yielded product faster when the A-target was initially present rather than the T-target (Figure 4.7 D and F). The discrimination ratio for the T:A match over the A:A mismatch was 11 and the ratio for the T:A match over the T:T mismatch was 3 based on the amount of product formed after 30 minutes. Clearly, the discrimination ratio is improved when we conducted the ligation with the separate sets of probes in separate containers. Furthermore, the mismatch-initiated reaction matched that of the background-triggered process under these conditions.

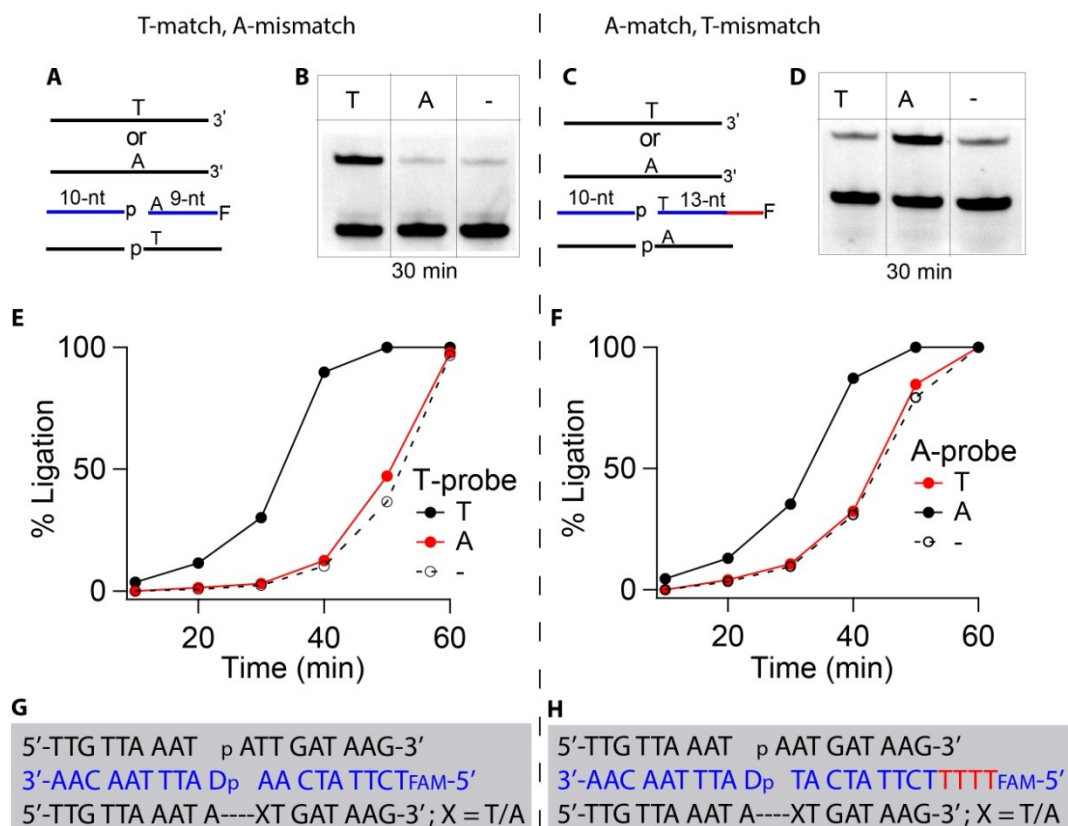


**Figure 4.7:** Cross-catalytic amplification with separate sets of probes. Schematic diagram of the DNA sequences used that: A) match with the T-target or C) match with the A-target. PAGE image of cross-catalytic amplification using: B) T-target specific probes including the short fluorescent probe and D) A-target specific probes including the long fluorescent probe. The reactions were initiated with 14 nM T-target (T), 14 nM A-target (A) or no target (-). Kinetics of cross-catalytic amplification using: E) the T-target specific (short) probes or F) the A-target specific (long) probes. DNA sequences of the corresponding set of G) T-target specific probes and H) A-target specific probes. *Experimental conditions:* 2.8  $\mu$ M **r-Ia**, 2.8  $\mu$ M **r-Ib(T)** or 2.8  $\mu$ M **r-Ib(A)**, 2.8  $\mu$ M **r-IIa<sub>Ab</sub>**, 1.4  $\mu$ M **r-IIb-9(FAM)** or 1.4  $\mu$ M **r-IIb-13(FAM)T**, and 14 nM of target **DNA-I(T/A)** or no target at 30 °C, T4 DNA ligase 2000 CEU per 15  $\mu$ L ligation volume.



#### 4.3.1.2 The discrimination between T- and G-target

In the above experiment, we showed the discrimination between A and T mismatches, but both of these assays were selective for the same match pair (T:A or A:T). Consequently, the stability of the product duplex was essentially the same, which allowed us to run both the A-target and T-target assays at the same temperature. If we want to compare different match pairs like T:A with G:C they might have different rates of amplification at the same temperature due to the higher stability of G:C compared to A:T. To determine if it was feasible to discriminate between a T-and G- target, we first tested the single cycle system made up of two separate sets of probes once again of different lengths that included a 9-nt probe with a 3'-A that matched with the T-target (**DNA-I(T)**) and a 13-nt probe with a 3'-C that matched with the G-target (**DNA-I(G)**). Consequently, we observed formation of the shorter complementary product (19-nt) in the presence of the T-target (T:A match) and longer complementary product (23-nt) in the presence of the G-target (G:C match), and no cross-product formed that corresponded with the T:C or G:A mismatches (Figure 4.8).

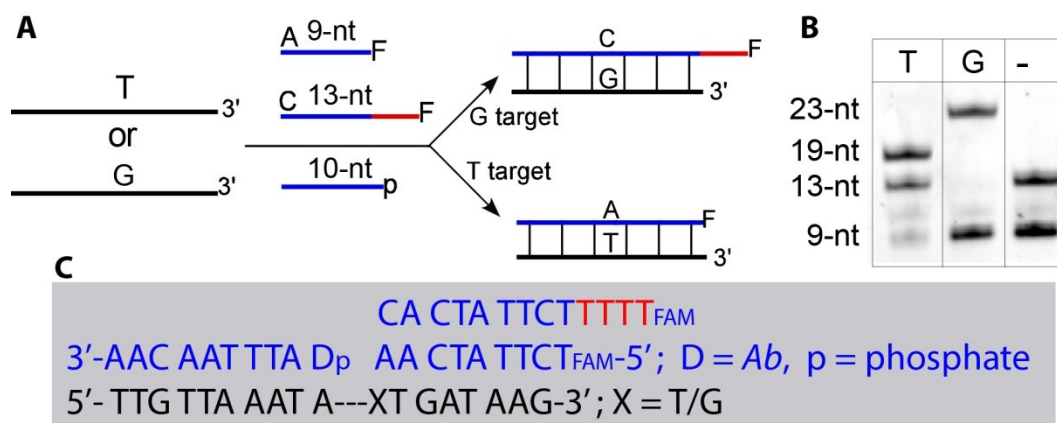


**Figure 4.8:** A) Schematic diagram of discrimination of T-target and G-target. Probes of different length give rise to different length product depending on the target presents in the solution. B) PAGE image of ligation reaction with T-target or G-target in the presence of **r-IIa<sub>Ab</sub>** (10-nt), **r-IIb(FAM)** and **r-IIb13(FAM)**C. C) DNA sequences used for this study. *Experimental conditions:* 1.4  $\mu$ M **r-IIb-9(FAM)**, 1.4  $\mu$ M **r-IIb-9(FAM)C**, 2.8  $\mu$ M **r-IIa<sub>Ab</sub>**, and 1.4  $\mu$ M of target **DNA-I(X)** (X=T/G) at 30 °C, T4 DNA ligase 400 CEU per 15  $\mu$ L ligation volume.

Similar to the A- and T-target, the T- and G-target also showed very good discrimination in the single-cycle experiment, so we attempted to multiplex the cross-catalytic amplification with T- and G-target as was tried for the T- and A-target system above. For this purpose, we added three more complementary probes to the ligation system resulting in a total of six probes. As a reminder, in this experiment either the short or long product that represents the in situ formed destabilizing template could form as both short and long probes were present. In contrast to the single cycle, we observed the formation of both products even if there was only one target present, as revealed by the PAGE image of a multiplexed assay in the presence of all six probes (Figure 4.9). Specifically, when the T-target was present, we expected to see only the 19-nt product (T:A

match), but as shown in Figure 4.9 we also observed the formation of the 23-nt product (T:C mismatch). The discrimination ratio for T-target over the G-mismatch was 5.5 and the ratio for G-target match over the T-target mismatch was 1.3 after 40 min indicating that there was selective amplification despite the high background for the mismatch-initiated reaction.

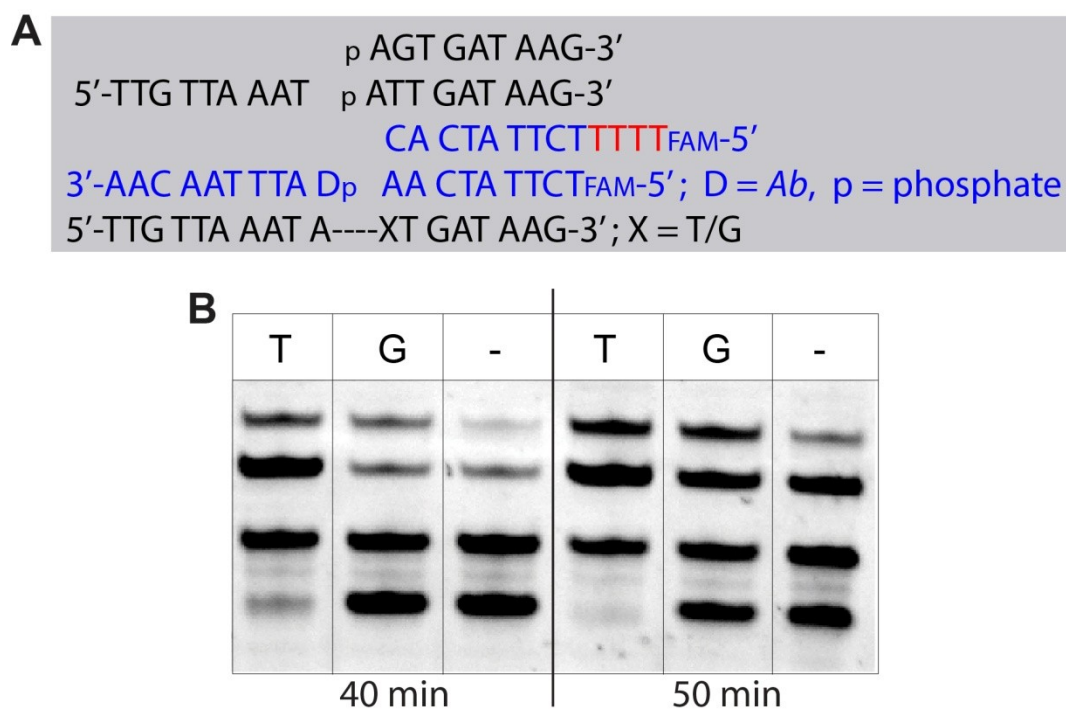


**Figure 4.9:** A) DNA sequences used for the multiplexed cross-catalysis for amplification of either a T- or G-target. B) A representative PAGE image of a multiplexed assay in the presence of all six probes after 40 min and 50 min of ligation initiated by T-target (T), G-target (G) or no target (-). *Experimental conditions:* 2.8  $\mu$ M **r-Ia**, 2.8  $\mu$ M **r-Ib(T)**, 2.8  $\mu$ M **r-Ib(G)**, 2.8  $\mu$ M **r-IIa<sub>Ab</sub>**, 1.4  $\mu$ M **r-IIb-9 (FAM)**, 1.4  $\mu$ M **r-IIb-13 (FAM)C**, and 14 nM of target **DNA-I(T/G)** or no target at 30 °C, T4 DNA ligase 2000 CEU per 15  $\mu$ L ligation volume.

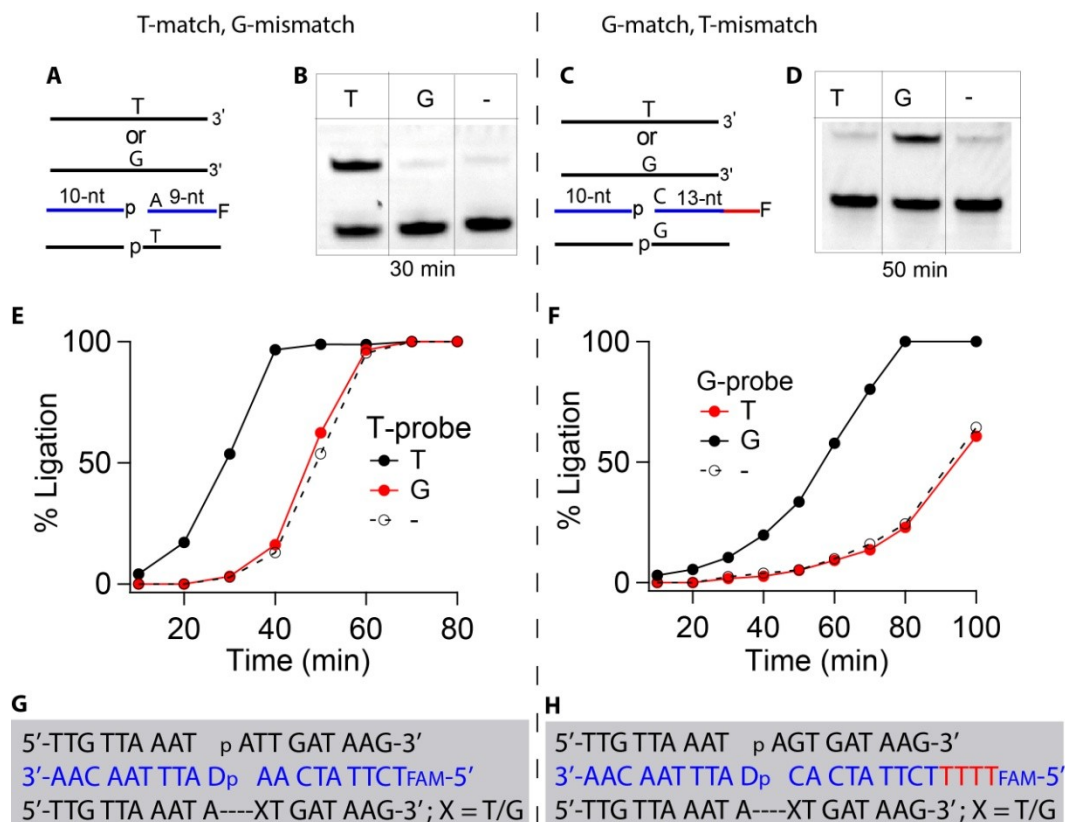


**Figure 4.10:** Cross-catalytic amplification with separate sets of four probes selective for either the T-target or the G-target. Schematic diagram of the DNA sequences: A) matched with T-target and C) matched with G-target. PAGE images of cross-catalytic amplification initiated by 14 nM T-target (T), G-target (G) or no target (-) using: B) T-target specific probes and D) G-target specific probes. Kinetics of cross-catalytic amplification for the reactions described above: E) with T-target specific probes and F) with G-target specific probes. DNA sequences of the target sequence and the G) T-target specific probes and H) the G-target specific probes. *Experimental conditions:* 2.8  $\mu$ M **r-Ia**, 2.8  $\mu$ M **r-Ib(T)** or 2.8  $\mu$ M **r-Ib(G)**, 2.8  $\mu$ M **r-IIa<sub>Ab</sub>**, 1.4  $\mu$ M **r-IIb-9 (FAM)** or 1.4  $\mu$ M **r-IIb-13 (FAM)C**, and 14 nM of target **DNA-I(T/G)** or no target at 30 °C, T4 DNA ligase 2000 CEU per 15  $\mu$ L ligation volume.

Due to the high background product formation with multiplexing, we once again decided to investigate the cross-catalytic amplification with separate sets of probes while comparing the matched target and mismatched target. The set of probes (with the shorter fluorescent probe) was complementary with T-target, so G-target will be a mismatch (Figure 4.10 A). In two separate reactions, we introduced the T-target and G-target to the four probe solution containing the shorter T-target specific fluorescent probe. As expected, we observed a faster rate of amplification for the T-target (T:A match) compared to the G-target (G:A mismatch) (Figure 4.10 B, E). Conversely, the second set of probes (with the longer fluorescent probe) which matched with G-target yielded faster product formation when G-target was present (G:C match) compared with the T-target (T:C mismatch) (Figure 4.10 C, D, F). The discrimination ratio for the T:A match over the G:A mismatch was 17 and the ratio for the G:C match over the T:C mismatch was 6. Once again, the discrimination ratio was improved when we studied the ligation with the separate set of probes in separate containers.

#### **4.3.2 FRET based detection**

Our gel based study is very efficient in the discrimination of single-base pair mismatches, but this procedure is very time-consuming and labor intensive. Therefore, we were interested in developing a system where we could monitor the ligation in real time using a simple device like a microplate reader. Real-time detection of ligation would be beneficial as this approach does not require tedious and time-consuming post-amplification processing, and can be amenable to automation. After developing a real-time detection method based on our

isothermal amplification process, we aimed to extend it to the detection of a SNP in the target DNA sequence.

As mentioned earlier, fluorescence (or Förster) resonance energy transfer, FRET, technique is used for measuring distance-dependent interactions on a molecular level.<sup>43</sup> If the distance between two dyes increases, the FRET efficiency decreases significantly. Using a FRET based approach we can develop a real-time assay since this approach does not require separation of the ligation product and the ligation can be monitored as the ligation proceeds. To develop real-time detection of a target DNA sequence based on FRET, we labelled two of the four probe strands with two different fluorescent labels (FAM and Cy5;  $R_0 = 44 \text{ \AA}$ ).<sup>53</sup> The two labels are well separated in their absorption wavelengths (FAM and Cy5 have maximum absorbance at 494 nm and 645 nm, respectively). As a result, this pair was expected to greatly lower background fluorescence as compared with more typical FRET pairs, such as FAM–TAMRA where a false signal appears from overlapping excitation of the donor and acceptor.<sup>44</sup> As can be seen from the excitation and emission spectra for the FAM and Cy5 fluorescent labels, there is an overlap between the FAM emission and Cy5 excitation spectra, while there is no overlap between the excitation spectrum of the donor FAM with the excitation spectrum of the acceptor Cy5 (Figure 4.11). These characteristics indicated that an effective FRET pair with minimal background fluorescence could be made from the Cy5 acceptor upon exciting the FAM donor. As mentioned earlier, FRET efficiency depends on the distance between the fluorophores. For the FAM-Cy5 pair, the Kool group reported the relationship between the distance and FRET

efficiency in a DNA-based system. The authors found that when the distance between the fluorophores was 3- to 7-nt apart, they observed the highest FRET efficiencies.<sup>44</sup> In our experiment however, we positioned the fluorophores 11-nt apart ( $\sim 37.4$  Å, 3.4 Å per base), as we were limited to the commercial availability of T<sub>FAM</sub> (as opposed to another nucleotide).<sup>54</sup> We were also concerned to have two bulky fluorophores close to the ligation site, which might affect the ligation by T4 DNA ligase.

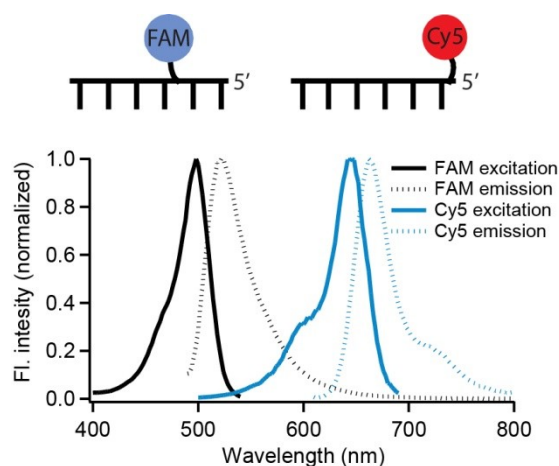


**Figure 4.11:** Normalized excitation and emission spectra of the fluorescein (FAM) and Cy5 labeled probes. For the FAM-probe, the  $\lambda_{em}$  was 521 nm and the  $\lambda_{ex}$  was 494 nm for the excitation and emission scans, respectively. For the Cy5-probe, the  $\lambda_{em}$  was 661 nm and the  $\lambda_{ex}$  was 645 nm for the excitation and emission scans, respectively.

#### 4.3.2.1 Detection of DNA-templated ligation with FRET for the single cycle system

To verify the efficiency of FRET at detecting the ligation process in real-time, at first we studied the single cycle kinetics of ligation with one equivalent of template and the two complementary fluorescent probes bearing the FAM and

Cy5 labels. Figure 4.12 A shows the schematic diagram of the DNA duplex formed after ligation, which brings the fluorophores in close proximity for the FRET process to occur. Upon exciting the ligation mixture at 485 nm, the emission intensity at 521 nm decreased and the emission intensity at 661 nm increased with time indicating that ligation was taking place (Figure 4.12 B and C). We found that using either the native template **DNA-II<sub>T</sub>** or the destabilizing template **DNA-II<sub>Ab</sub>**, led to efficient FRET. The FRET efficiency ( $(I_{661 \text{ nm}}/I_{521 \text{ nm}})$ ) levelled off after 15 minutes of ligation, which indicated that ligation was complete in 15 minutes, which was similar to the results from the gel based study where the ligation was completed after 10 min (Figure 4.13). Interestingly, the maximum FRET efficiency with **DNA-II<sub>T</sub>** was not very different from **DNA-II<sub>Ab</sub>**, which suggested that even the product duplex containing the destabilizing abasic group was stable enough at the ligation temperature (30 °C) for the FRET process to occur (Figure 4.12 and 4.13). Only a slight different in the FRET signal between the native and destabilizing templates indicated that the FRET process was slightly affected by the presence of the destabilizing group. It is interesting to note that the FRET process was not efficient in the absence of enzyme at 30 °C even if the target was present to hybridize the probes (Figure 4.12). So we conclude that the observation of FRET was the direct consequence of the ligation process.



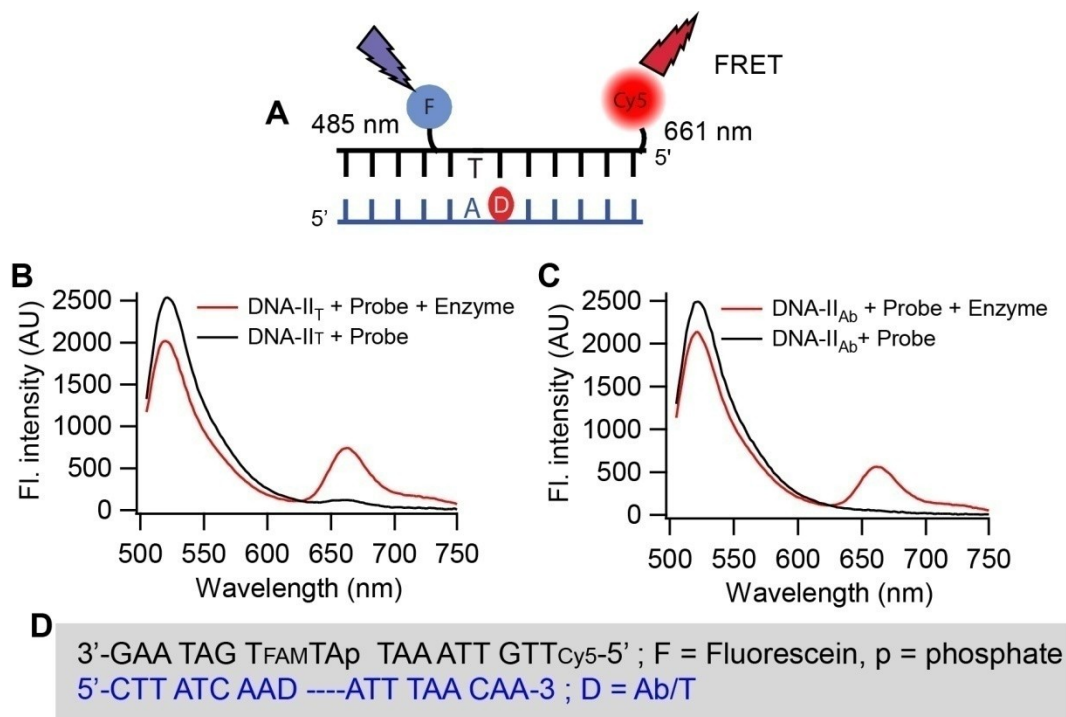


**Figure 4.12:** A) Schematic diagram of the FRET process. Upon excitation of the ligation mixture at 485 nm corresponding to FAM excitation, we observed the Cy5 emission at 661 nm. B) Fluorescent spectra of the DNA mixture containing the native template (D = T) and the FRET pair-labelled probes after 10 minutes in the absence and presence of ligation (no enzyme and with enzyme, respectively). C) Similar experiment to part B but with the destabilizing template DNA-II<sub>Ab</sub>. *Experimental conditions:* 1.4  $\mu$ M r-Ia(Cy5); 1.4  $\mu$ M r-Ib(FAM); 1.4  $\mu$ M DNA-II<sub>D</sub> (D=T or Ab); 30 °C, T4 DNA ligase 1000 CEU per 7.5  $\mu$ L ligation volume.



increase in FRET will be consistent with cross-catalysis (i.e. self-replication of **DNA-I(T)**). Figure 4.14 shows the intensity of the fluorescence emission of the donor and acceptor-modified strands at different times in the presence of the matched T-target **DNA-I(T)**. As expected, the fluorescence intensity of the donor decreased and the intensity of the acceptor increased with time, which was indicative of cross-catalytic amplification, as the fluorophores were attached to the probes in the second cycle.

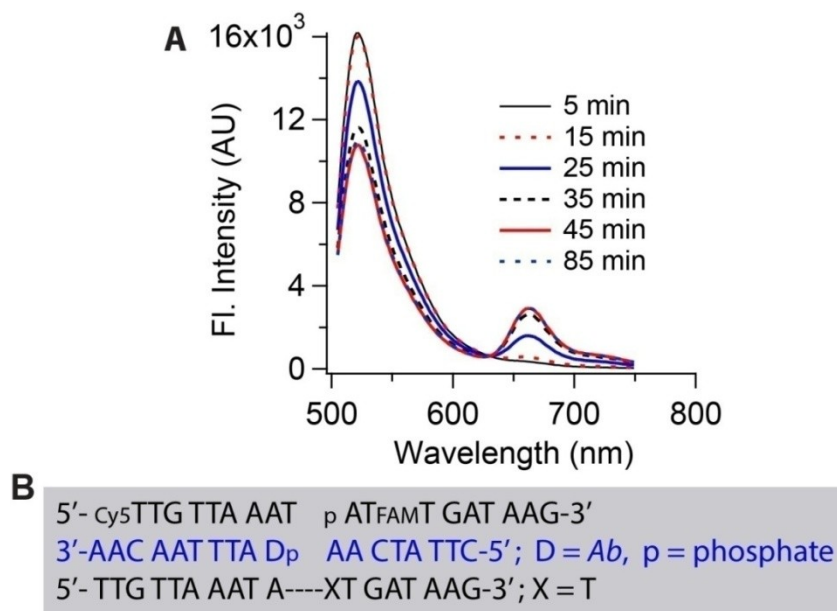


**Figure 4.14:** A) Real-time fluorescence spectra of the ligation mixture at different time point from the time of mixing with enzyme. The excitation wavelength is 485 nm. B) DNA sequences showing the position of the fluorophores used for cross-catalytic amplification. *Experimental conditions:* 1.4  $\mu\text{M}$  **r-Ia(Cy5)**, 1.4  $\mu\text{M}$  **r-Ib (FAM)**, 2.8  $\mu\text{M}$  **r-IIb**, 2.8  $\mu\text{M}$  **r-IIa<sub>Ab</sub>** and 14 nM of target **DNA-I(T)** at 30 °C, T4 DNA ligase 1000 CEU per 7.5  $\mu\text{L}$  ligation volume.

Since the rate of ligation was very slow for the single cycle experiments in the presence of mismatches (Section 4.2), the increase in FRET was expected to be much slower for the mismatched system compared with that of the matched target. Indeed, the fluorescence spectra after 35 min of amplification with different targets only exhibited significant FRET for the perfectly matched T-target **DNA-I(T)** (Figure 4.15). It is interesting to see that the FRET efficiency in the absence of target (background-triggered amplification) is almost overlapped with the mismatched target, which confirmed that the observed FRET from the mismatched targets is the result of the background ligation. These results indicate that if we could decrease the background-triggered amplification we would be able to achieve better discrimination between the matched target and mismatched target.

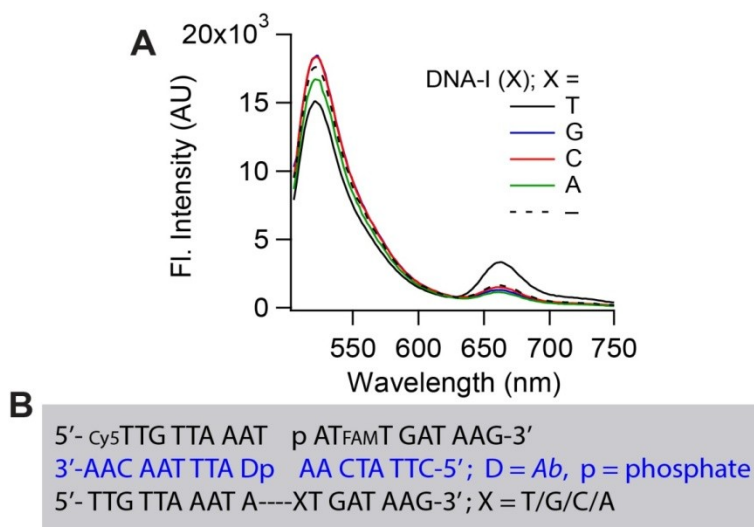


**Figure 4.15:** A) Difference in FRET signal with different mismatches at 30 °C after 35 minutes of mixing. B) DNA sequences used in this study. *Experimental conditions:* 1.4  $\mu$ M **r-Ia(Cy5)**, 1.4  $\mu$ M **r-Ib (FAM)**, 2.8  $\mu$ M **r-IIb**, 2.8  $\mu$ M **r-IIa<sub>Ab</sub>** and 14 nM of target **DNA-I(X)**, X= T/G/C/A or no target (-), T4 DNA ligase 1000 CEU per 7.5  $\mu$ L ligation volume.

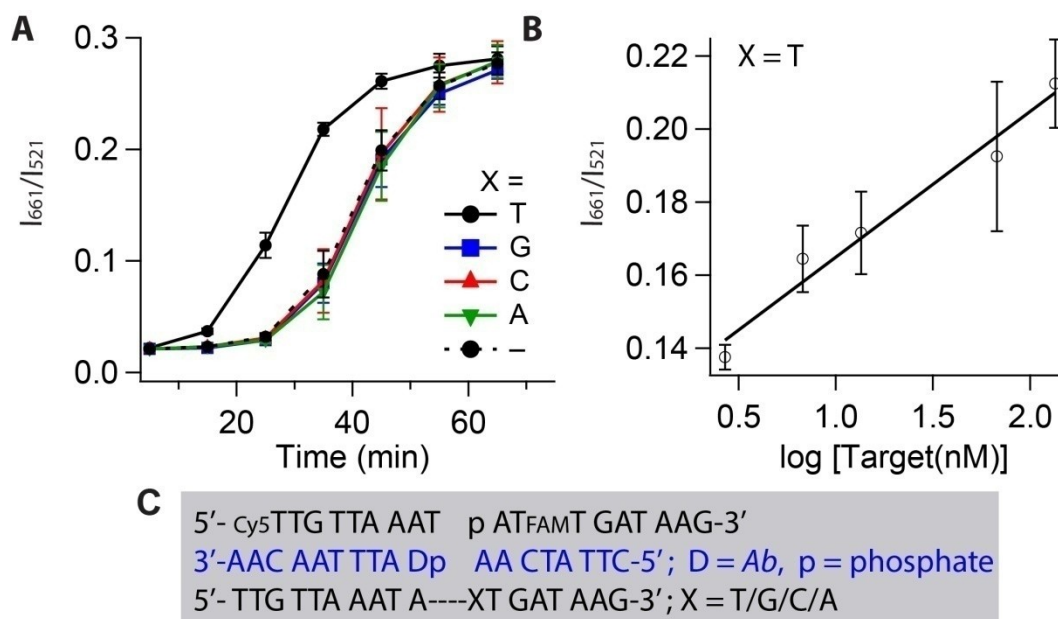


**Figure 4.16:** A) Plot of FRET efficiency with time for ligation with different targets (match or mismatch). 14 nM of the match target **DNA-I(T)** gives faster ligation, however mismatch targets shows slower ligation which is comparable to the background ligation. The background ligation was performed without any target DNA and detected in the same way as the targeted ligation. B) FRET efficiency linearly depends on the amount of match target DNA (**DNA-I(T)**) added. C) DNA sequences used in this study. *Experimental conditions:* For A, 1.4  $\mu\text{M}$  **r-Ia(Cy5)**, 1.4  $\mu\text{M}$  **r-Ib (FAM)**, 2.8  $\mu\text{M}$  **r-IIb**, 2.8  $\mu\text{M}$  **r-IIa<sub>Ab</sub>** and different concentrations of target **DNA-I(X)**, X= T/G/C/A or no target (-), T4 DNA ligase 1000 CEU per 7.5  $\mu\text{L}$  ligation volume. For B, the experiment run in a similar way with different concentration of target (**DNA-I(T)**).

In order to have a better understanding of the amplification behavior with different templates, we calculated the FRET efficiency as a function of time. We observed that the FRET efficiency in the presence of perfectly matched target increased much faster than that in the presence of mismatch (Figure 4.16 A). After

25 min, the FRET efficiency with matched DNA was four times higher than that for mismatched DNA (without background correction), which demonstrated the good selectivity of this method for detection of SNP (Figure 4.16). The discrimination ratios were improved after background correction (subtract the FRET efficiency at time  $t = 5$  minutes), the ratios of A:T match to the A:G, A:C and A:A mismatches were 11, 10 and 12 respectively. We note the discrimination ratio using FRET was much lower than that of the gel based study; part of the reason may be the maximum FRET efficiency was only 0.3, so we were monitoring the change in a small window. Finally, Figure 4.16 B reveals that the fluorescent efficiency depended linearly on the logarithm of the initial target DNA concentration ( $[DNA-I(T)]$ ) with a dynamic range of about 2 orders of magnitude. As shown earlier, using PAGE we can discriminate 70 pM (1.02 fmol) of target DNA, however, using the FRET based approach we can discriminate 2.7 nM (19.6 fmol) of target DNA which may be attributed to the low FRET efficiency.

### **4.3.3 Colorimetric detection of amplification with gold-nanoparticle**

We found that we could simplify our assay by combining our unique amplification process with real-time detection. To further simplify the DNA detection process such that it did not require a light source and detector (plate reader or fluorimeter), we attempted to develop a colorimetric approach, which does not require the use of expensive instrumentation. Since the discovery of the DNA-linked gold nanoparticle (NP) by Chad Mirkin and Paul Alivisatos in 1996, these materials have been extensively used by many researchers to develop colorimetric DNA detection.<sup>55-57</sup> One of the most important properties of the

DNA linked gold nanoparticle is that two types of nanoparticles each complementary to two halves of a target DNA sequence can reversibly bind together in the presence of the target DNA resulting in a large nanoparticle aggregate which leads to a color change from red to purple.<sup>55</sup> Since there are many DNA molecules attached to each NP, they can combine with other nanoparticles with the help of the linker DNA and form a three dimensional network of linked particle leading to a change in surface plasmon resonance (SPR), which is the main cause of color change. However, the hybridization (Figure 4.17) of DNA with gold nanoparticles to form an aggregate requires a long time, on the order of hours, in contrast to dissociation, which takes minutes. Consequently, it is desirable to develop assays based on dissociation rather than hybridization. Several years ago, Hazarika and co-workers demonstrated the reversible aggregation of DNA-modified gold NPs by using two complementary fueling oligonucleotides: one that linked the nanoparticles and the other that removed the linker leading to dissociation.<sup>58</sup> More recently, Trantakis et al. used the reversible assembly and disassembly of the nanoparticle aggregate to detect the presence of mismatches in the target DNA.<sup>59</sup> According to their report, it takes more than an hour to complete the disassembly process, which is not very practical if we want to develop a rapid test. Recently, one of our group members (Michael Lam) developed a similar target-induced disassembly of nanoparticle strategy (Figure 4.18). Mike found that the temperature had a significant role in the rate of the disassembly process (Unpublished work). By tuning the temperature close to the dissociation temperature ( $T_m$ ) (see Figure 4.19 for  $T_m$ ) of

the aggregate ( $T = T_m - 2\text{ }^\circ\text{C}$ ) it was possible to break the aggregate in less than 5 minutes. However, with his method it was possible to reliably detect down to 1.5 nM of target DNA using UV-vis absorbance spectroscopy, and the limit of detection based on a visual read out required even more target DNA. Therefore, to detect lower concentration of DNA, we decided to isothermally amplify the target DNA in a separate container and combine it with the NP-aggregate. If enough of the amplified target DNA was present, it should hybridize with the linker DNA and break the aggregate resulting in the color change from purple to red.

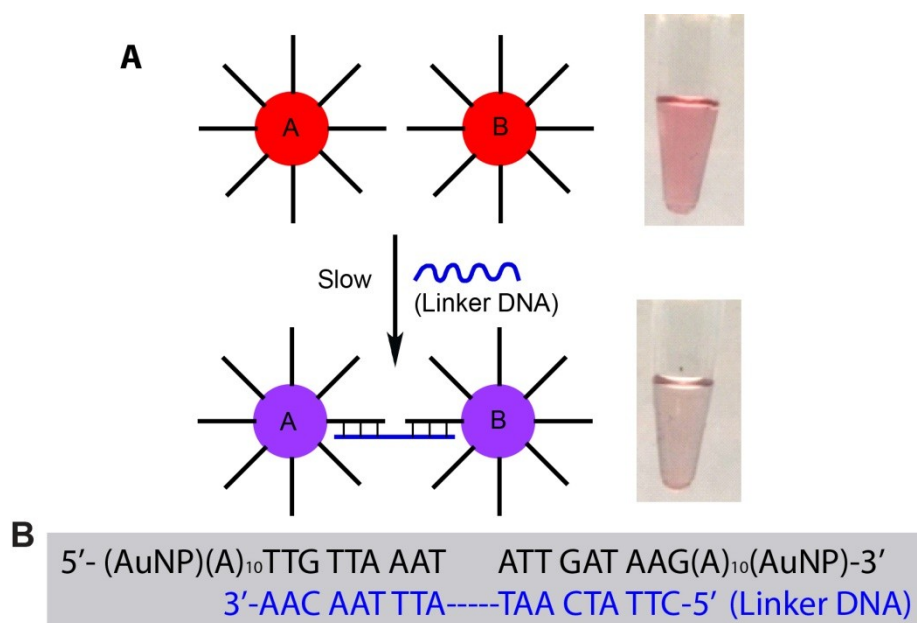


**Figure 4.17:** A) Schematic diagram of formation of NP-aggregate by hybridization of two NPs modified with non-complementary DNA sequences upon addition of the complementary linker DNA. Initially the color of the solution was red which became purple after hybridization (the color change is not very clear from this image but when we used a larger tube, we were able to see the color change more clearly). B) DNA sequences for nanoparticle functionalization and the linker DNA used for this study.



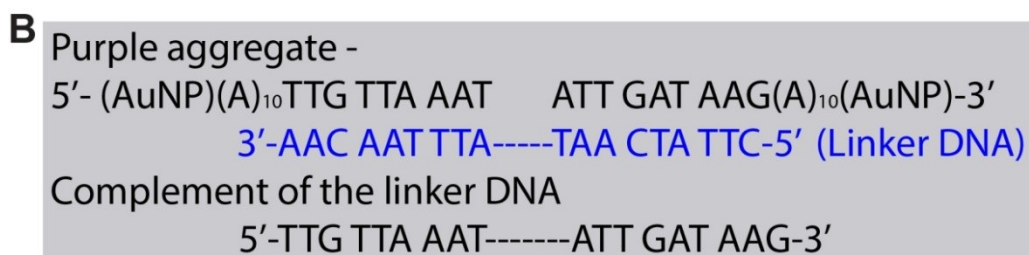
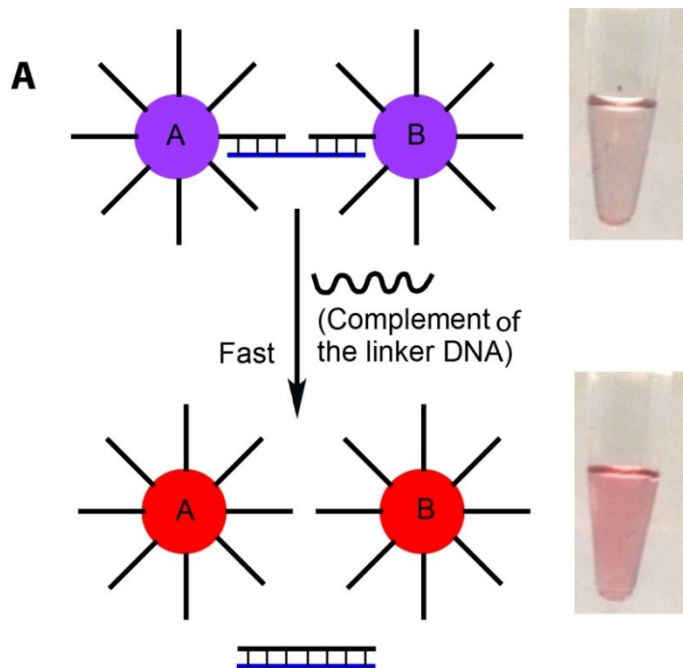


**Figure 4.18:** A) Schematic diagram of disassembly of aggregated DNA-linked gold NP by a complementary linker DNA (**DNA-II**) (blue strand). Initially the solution was purple because of the aggregate formation which changed to red color due to disassembly of the aggregate upon addition of the complementary DNA strand (**DNA-I**), it will hybridize to **DNA-II**. B) Schematic diagram showing the sequence used for the assembly and disassembly process.

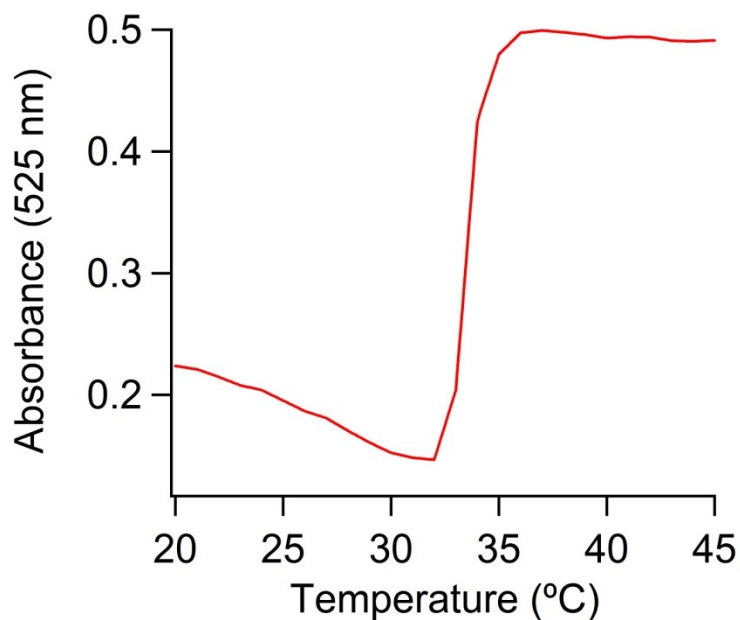


**Figure 4.19:** Thermal denaturation profile of the gold NP–DNA aggregate (Figure 4.17) formed by a linker DNA. Melting temperature of the duplex is 33.9 °C (Experiment performed by Michael Lam).

To prove our hypotheses, we amplified different initial concentrations of target DNA (**DNA-I(T)**) (140 nM, 14 nM, 1.4 nM, 140 pM, 14 pM, 0 M) using isothermal amplification method. After 40 minutes of amplification (the time where we see the maximum difference in product formation), we stopped the amplification by heating the ligation mixture at 95 °C for 10 minutes to denature the enzyme. We then cooled it down for another 10 minutes in the refrigerator (~ 4 °C). Next we added the ligation mixture to the NP aggregate immediately after taking the aggregate out of the refrigerator. After sitting at room temperature for 5 minutes, no color change was observed. However, after heating the sample to 32 °C (aggregate  $T_m$  is 33.9 °C, Figure 4.19) for 5 minutes, we observed color change from purple to red with 140 nM, 14 nM and 1.4 nM target. Figure 4.20 A shows a

picture of the tubes right after heating which was taken using a cell phone camera. A portion (10  $\mu$ L) of the same mixture was dropped onto a TLC plate, which was then scanned using a document scanner after drying in air (Figure 4.20 B). On the TLC plate, we observed better contrast than that observed for the solution. By incorporating our amplification method, we could easily observe 1.4 nM initial target DNA colorimetrically, which was not the case in the absence of amplification (data not shown-see the work of Michael Lam).

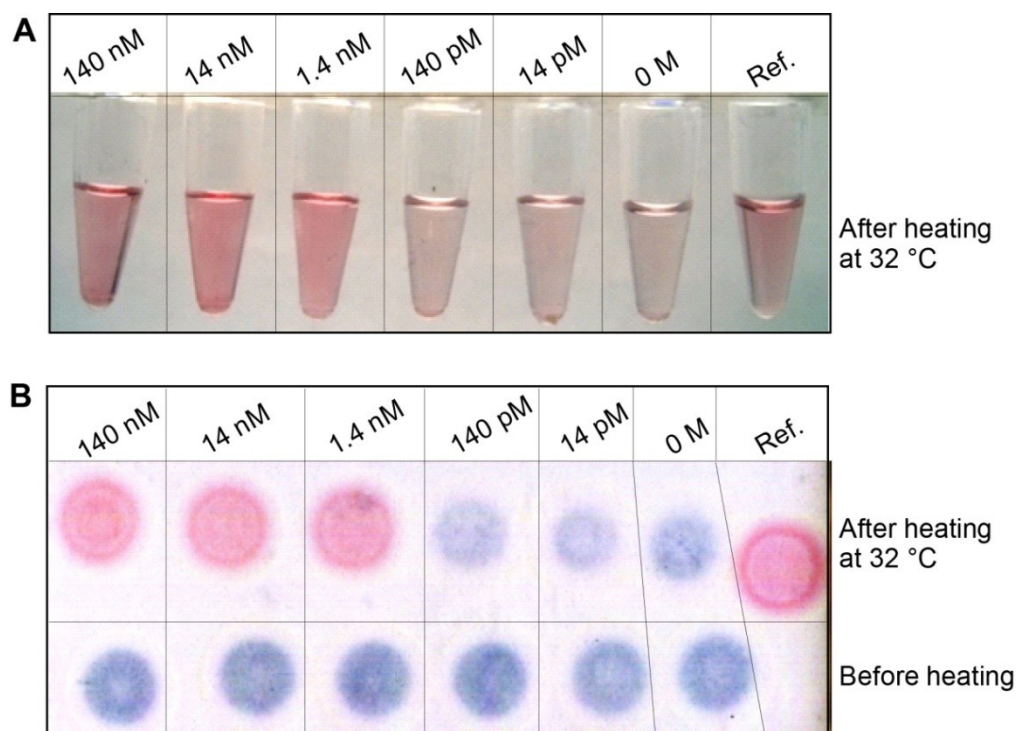


**Figure 4.20:** A) NP aggregates upon addition of the isothermally amplified target DNA mixture with different concentrations of initial target added for amplification. The picture was taken using a cell phone camera after heating the NP aggregate mixtures for five minutes. B) The ligation mixture was spotted on to TLC plate and image was taken using a document scanner which shows better contrast than in solution. In both cases, Ref. is the mixture of two NPs in the absence of the linker DNA (**DNA-II**).

In order to observe the color change spectroscopically, we studied target induced disassembly of nanoparticle aggregate using UV-visible absorbance spectroscopy. For this purpose, we placed 100  $\mu\text{L}$  of the NP aggregate in a cuvette and kept it at 32  $^{\circ}\text{C}$  for 5 minutes, while monitoring the change in absorbance. During the initial wait time, the absorbance of the solution decreased slightly, which we attribute to settling of the aggregate. After 5 minutes, we added the amplified target mixtures initiated with different amounts of target DNA, to the NP aggregate and we observed a rapid increase in the absorbance at 525 nm, which indicated that the amplified target DNA dissociated the aggregate by hybridizing with the linker strand (Figure 4.21 A). However, each experiment had a different starting absorbance, owing to the heterogeneity of the NP aggregate mixture, so it was difficult to compare the changes in the absorbance with different samples. To avoid this problem, we plotted the ratio of the absorbance at 525 nm and 520 nm ( $A(525 \text{ nm})/A(560 \text{ nm})$ ), with respect to time using similar ratiometric approach adopted by Shen et. al.<sup>60</sup> Initially, the NP-aggregate absorbed light with  $\lambda_{\text{max}}$  at 560 nm; as the amplified target-initiated disassembly process continued the absorbance gradually shifted to 525 nm ( $\lambda_{\text{max}}$ ). Using this ratio, all of the samples had almost the same starting point, which allowed us easier comparison of the absorbance changes for the reactions initiated with different target concentration (Figure 4.21 B). Using this method, we could reliably detect as little as 140 pM of target DNA.

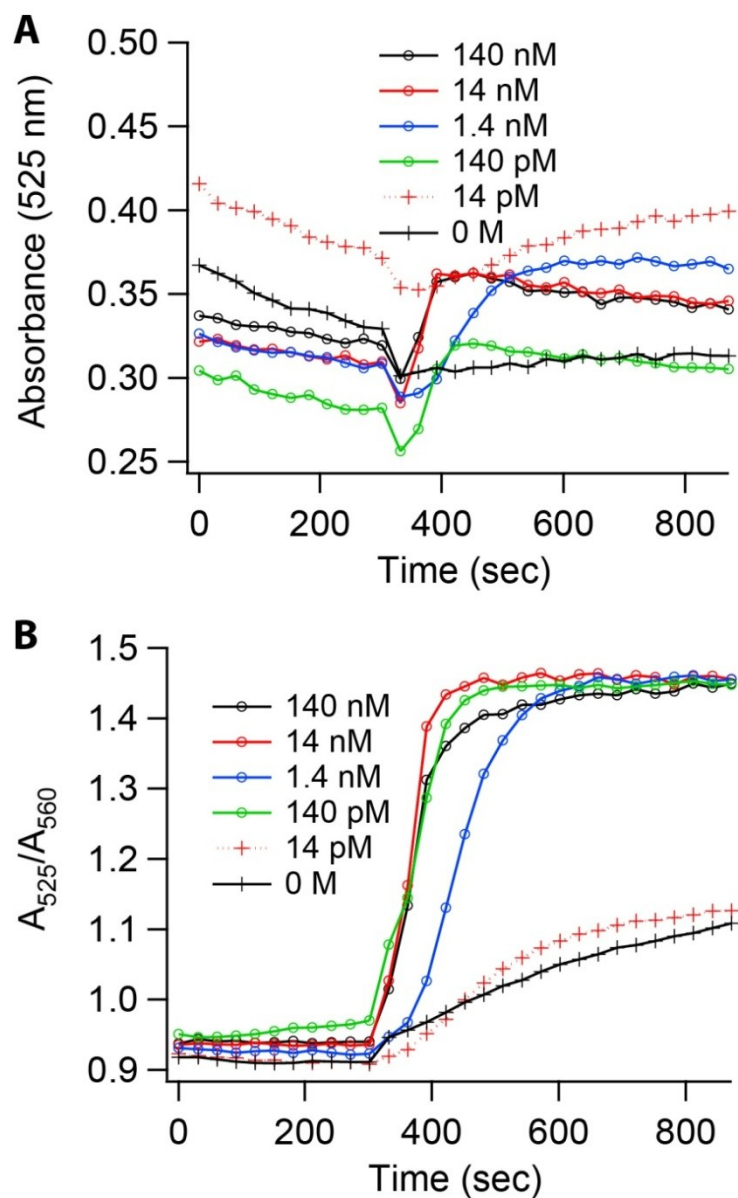


**Figure 4.21:** Monitoring the dissociation of the aggregate using UV-vis absorbance spectroscopy. The amplified DNA mixture was added after 300 seconds of keeping the solution at 32 °C, which was two degrees below the  $T_m$  of the aggregate. A) Absorbance changes with time and B) the ratio of absorbance at 525 nm to 560 nm with time.

#### 4.4 Conclusions

In this chapter, we have shown that our simple isothermal amplification method is very amenable to the detection of mismatches in a particular position in the target DNA sequence. The amplification product formation is linear with the logarithm of the initial concentration of the given target over 3 orders of magnitude. Our attempt to multiplex the assay did not lead to significant mismatch discrimination when both the matched and mismatched probes were present in the same reaction tube. However, separation of the probe sets for detecting a specific mismatch worked very well. As analysis of the ligation product by PAGE analysis was tedious and fairly time-consuming, we investigated the development of a simple method for SNP detection by combining isothermal amplification with real-time detection of SNPs using FRET and a microplate reader. The absence of FRET from direct excitation of the fluorophores Cy5 and fluorescein, makes it a good choice for real-time ligation detection based on FRET. In addition, the FRET efficiency can be improved by redesigning the probes such that the fluorophores stay closer to each other after ligation. Colorimetric assay is the simplest form of the assay since it does not require any instrument. Gold nanoparticle based colorimetric detection of target takes us one step closer to the development of a simple device for DNA detection. All of these approaches of combining isothermal amplification with simple detection are great, however, the presence of the background ligation in our amplification system limits the ability of this technique to detect low picomolar concentrations of DNA unless serial ligation is performed (Chapter 3). We can conclude that combining a

simple and sensitive amplification method with simple detection would facilitate a simple device for diseases diagnostics, which might potentially find application in a resource-limited area. Future work will focus on reducing background ligation, using a more efficient FRET probe design (possibly with different fluorophores or by changing the position of the fluorophore to get better FRET efficiency) and developing an instrument-free detection strategy suitable for a point-of-care kit.

## **4.5 Experimental**

### **4.5.1 Materials and instrumentation**

T4 DNA ligase was purchased from New England Biolabs. The temperatures for DNA ligation experiments were maintained using a Torrey Pines Scientific Echotherm Chilling/Heating Plate Model IC22. The polyacrylamide gel electrophoreses (PAGE) gels were imaged using ImageQuant RT ECL Imager from GE Healthcare Life Science using UV transillumination. The DNA was synthesized on an Applied Biosystems Model 392 DNA/RNA Synthesizer. Fluorescence spectra were measured in a Tecan Safire II plate reader using 384 well plates.

### **4.5.2 DNA synthesis and purification**

The sequences of the probes and targets are listed in Table 4.1 and 4.2. DNA was synthesized on an ABI 392 solid-phase synthesizer using Glen Research reagents. Strands were purified by Glen-Pak DNA Purification cartridges (cat. 60-5200-01) according to the DMT-On protocol. Standard nucleotide phosphoramidite and the following were used: 3'-thiol-modifier C3 S-S CPG (Glen Research Cat. # 20-

2933-41), 5'-thiol-modifier C6 (Glen Research Cat. # 10-1926-02), fluorescein-dT phosphoramidite (Glen Research Cat.# 10-1056-95), dSpacer CE phosphoramidite (Glen Research Cat.# 10-1914-90) (for abasic (**Ab**) group).

#### 4.5.3 PAGE-based ligation (single cycle and cross-catalysis)

Ligation was performed following the procedure described in Chapter 3. DNA composition of single cycle experiments (1 equiv = 10.2 pmol): 2 equiv. **r-IIa<sub>Ab</sub>**; 1 equiv. **r-IIb(FAM)**; 1 equiv. target **DNA-I(X)** (**X=T/G/C/A**) (final concentration of probes for one equiv = 1.4  $\mu$ M, final ligation volume 7.5  $\mu$ L). DNA composition of standard cross-catalysis reactions (1 equiv = 20.3 pmol): 1 equiv. **r-Ia(FAM)**; 2 equiv. **r-Ib**; 2 equiv. **r-IIb**; 2 equiv. **r-IIa<sub>D</sub>(D=Ab)** and 0.01 equiv of target **DNA-I(X)** (**X=T/G/C/A**) (final concentration of probes for one equiv = 1.4  $\mu$ M, final ligation volume 15  $\mu$ L). For cross-catalysis reactions performed at lower probe concentration as shown in Figure 4.3, the same probe ratio as above was used, but one equivalent was reduced to 2.54 pmol (final concentration of probes for one equiv = 340 nM, final ligation volume 7.5  $\mu$ L). Additionally, the appropriate amount of target DNA was used to reach the desired final concentration in 15  $\mu$ L.

#### 4.5.4 Denaturing Polyacrylamide Gel Electrophoresis

For the PAGE based study, the ligation mixtures were separated on a denaturing 15% polyacrylamide gel (0.75 mm thick, 10 wells). The details of the procedure are given in the Chapter 2 (Section 2.5.8).



#### **4.5.5 Real-time FRET experiments (single cycle and cross-catalysis)**

Real time FRET experiments utilized standard ligation mixtures very similar those described above for the PAGE based experiments except the total ligation volume was reduced to 7.5  $\mu\text{L}$ . Consequently, one equivalent was equal to 10.5 pmol in these experiments. At first, the DNA mixture and ligase mixture were also incubated at the desired ligation temperature for 10 minutes prior to mixing. During this time, the fluorescence spectrometer was turned on and set to the desired temperature. When the temperature of the instrument reached the desired ligation temperature, the ligase mixture (2.5  $\mu\text{L}$ , same composition as described above) was added to the DNA mixture (5.0  $\mu\text{L}$ ). The mixture was then vortexed thoroughly before being pipetted into one of the wells in the 384 well plate. The data was collected in the kinetic mode every 10 minutes for 85 minutes with the first data taken after 5 min of mixing the DNA solutions with the enzyme mixture. The following instrument settings were used: measurement mode fluorescence bottom; excitation  $\lambda = 485 \text{ nm}$ ; emission  $\lambda = 505\text{-}750 \text{ nm}$ ; excitation bandwidth = 10 nm; emission bandwidth = 10 nm; number of reads = 2; steps = 2 nm; gain = 60; integration = 500  $\mu\text{s}$ .

#### 4.5.6 Nanoparticle functionalization with DNA

The 3' or 5'terminal disulfide groups of the oligonucleotide strands were first cleaved by dissolving them in a 0.1 M dithiothreitol (DTT) phosphate buffer solution (0.1 M phosphate, pH 8.0) for 2 hours at room temperature and subsequently purified on a NAP column. For attachment to the gold nanoparticles, we used 3'- and 5'-thiolated DNA strands synthesized using 3'-Thiol-Modifier C3 S-S CPG and 5'-Thiol-Modifier C6 S-S phosphoramidite, respectively. Gold nanoparticles with an average diameter of 13 nm were prepared by Md. Delwar Sikder following the literature procedure.<sup>61</sup> To one mL of a gold colloid solution ( $5.6 \times 10^{12}$  particles/mL) 3 ml of water was added and then the purified cleaved thiolated oligonucleotide (20 nmol, ~1 mL) in buffer (0.05 M PBS, 0.05% SDS, pH 7.4). The same buffer was added to reach a final volume of 5 mL at which point the colloid was allowed to sit for two hours. The solution was then brought up to 0.6 M NaCl in 0.05 M NaCl increments by gradually adding a concentrated NaCl buffer (2 M NaCl, 10 mM PBS, 0.01% SDS pH 7.01). After the first increment of NaCl buffer was added to reach 0.05 M NaCl the solution was kept for 60 hours, thereafter the same buffer was added every hour to reach 0.6 M NaCl. After standing for 5 hours at 0.6 M NaCl, the nanoparticle solutions were centrifuged, decanted, and redispersed in 0.3 M NaCl, 10 mM PBS, 0.01 % SDS pH 7.01 (2 mL). These processes repeated at least 3 times to remove free DNA that did not bind to the nanoparticle. The final concentrations of the NP solutions were estimated from their measured absorption at 525 nm and published values for extinction coefficients of the unmodified particles ( $\epsilon_{525} = 2.4 \times 10^8 \text{ M}^{-1} \text{ cm}^{-1}$ ).<sup>62</sup>

#### 4.5.7 NP-based colorimetric detection

##### 4.5.7.1 Nanoparticle hybridization

First, the nanoparticles (NPs) were hybridized by combining NP A (0.15 pmol with respect to NPs), NP B (0.15 pmol with respect to NPs) and linker (6 pmol) in PBS buffer (100  $\mu$ L, 0.3 M NaCl, 10 mM PBS, pH 7.0). The mixture was allowed to sit overnight at 4 °C. Initially the solution was red but changed to purple after hybridization. The NP aggregates were stored at 4 °C until they were ready to be used.

**Table 4.2.** DNA sequences used for the nanoparticle study

Sequence name	DNA sequence
Linker DNA( <b>DNA-II<sub>T</sub></b> )	5'-CTT ATC AAD ATT TAA CAA-3'
Target DNA( <b>DNA-I(T)</b> )	5'-TTGTTA AAT AXT GATAAG-3'
NP A	5'-HS-(CH <sub>2</sub> ) <sub>6</sub> -A AAA AAAAAA TTGTTA AAT-3'
NP B	5'- ATT TAA CAA AAA AAAAAA A-(CH <sub>2</sub> ) <sub>3</sub> -SH-3'

##### 4.5.7.2 Cross-catalytic amplification followed by colorimetric detection

The DNA probes and target were combined in water in a 600- $\mu$ L minicentrifuge tube to reach a final volume of 6.67  $\mu$ L and incubated at the desired reaction temperature. In the meantime T4 DNA ligase 1.5  $\mu$ L (2000 CEU  $\mu$ L<sup>-1</sup>) was mixed with ligation buffer (2.25  $\mu$ L, 10X concentrated) and water (3.75  $\mu$ L). The ligase mixture (3.33  $\mu$ L) was immediately added to each of the DNA solutions (final [DNA] = 1.4  $\mu$ M for each equivalent). DNA components in the ligation mixture: 1 equiv **r-Ia**, 2 equiv **r-Ib**, 2 equiv **r-IIb**, 2 equiv **r-**

**IIa<sub>D</sub>(D=Ab)** and 0.01 or 0 equiv **DNA-I(T)**, 1 equiv = 13.5 pmol. The reactions were then placed in a covered thermal incubator. After 40 minutes, which is the time where we see maximum difference in product formation, we stopped the amplification by heating the ligation mixture at 95 °C for 10 min, then cooling it down for another 10 minutes in the refrigerator (~ 4 °C). Next we added the ligation mixture to the NP aggregate that had been stored in the refrigerator. The aggregate/amplification mixture was allowed to sit at room temperature for 5 minutes; there was no color change at this time. However, after heating the sample at 32 °C (Eppendorf Mastercycler® gradient) for 5 minutes, we observed a color change. For the UV-visible absorbance spectroscopy study, the samples were prepared in the same way as described for the colorimetric study.

## 4.6 References

- 1) Tom Strachan, A. P. R.: Chapter 9, Instability of the human genome: mutation and DNA repair. In *Hum Molec Genet. 2nd edition.*; Wiley-Liss: New York, **1999**.
- 2) Griffiths AJF, M. J., Suzuki DT, et al.: How DNA changes affect phenotype. In *An Introduction to Genetic Analysis. 7th edition.*; W. H. Freeman: New York, **2000**; Vol. How DNA changes affect phenotype.
- 3) Wang, D. G.; Fan, J. B.; Siao, C. J.; Berno, A.; Young, P.; Sapolsky, R.; Ghandour, G.; Perkins, N.; Winchester, E.; Spencer, J.; Kruglyak, L.; Stein, L.; Hsie, L.; Topaloglou, T.; Hubbell, E.; Robinson, E.; Mittmann, M.; Morris, M. S.; Shen, N.; Kilburn, D.; Rioux, J.; Nusbaum, C.; Rozen, S.; Hudson, T. J.; Lipshutz, R.; Chee, M.; Lander, E. S.: Large-scale identification, mapping, and genotyping of single-nucleotide polymorphisms in the human genome. *Science* **1998**, *280*, 1077-82.
- 4) Mhlanga, M. M.; Malmberg, L.: Using molecular beacons to detect single-nucleotide polymorphisms with real-time PCR. *Methods* **2001**, *25*, 463-71.
- 5) Yu, A.; Geng, H.; Zhou, X.: Quantify single nucleotide polymorphism (SNP) ratio in pooled DNA based on normalized fluorescence real-time PCR. *BMC Genomics* **2006**, *7*, 143.
- 6) Irizarry, K.; Kustanovich, V.; Li, C.; Brown, N.; Nelson, S.; Wong, W.; Lee, C. J.: Genome-wide analysis of single-nucleotide polymorphisms in human expressed sequences. *Nat Genet* **2000**, *26*, 233-6.
- 7) Kim, S.; Misra, A.: SNP genotyping: technologies and biomedical applications. *Annu Rev Biomed Eng* **2007**, *9*, 289-320.
- 8) Ramirez, M. V.; Cowart, K. C.; Campbell, P. J.; Morlock, G. P.; Sikes, D.; Winchell, J. M.; Posey, J. E.: Rapid Detection of Multidrug-Resistant Mycobacterium tuberculosis by Use of Real-Time PCR and High-Resolution Melt Analysis. *J Clin Microbiol* **2010**, *48*, 4003-4009.
- 9) Cottingham, K.: Product Review: Multiple choices for SNPs. *Anal Chem* **2004**, *76*, 179 A - 181 A.

- 10) Zhang, Y.; Guo, Y.; Quirke, P.; Zhou, D.: Ultrasensitive single-nucleotide polymorphism detection using target-recycled ligation, strand displacement and enzymatic amplification. *Nanoscale* **2013**, *5*, 5027-5035.
- 11) Mackay, I. M.; Arden, K. E.; Nitsche, A.: Real-time PCR in virology. *Nucleic Acids Res* **2002**, *30*, 1292-305.
- 12) Li, H.; Huang, J.; Lv, J.; An, H.; Zhang, X.; Zhang, Z.; Fan, C.; Hu, J.: Nanoparticle PCR: nanogold-assisted PCR with enhanced specificity. *Angew Chem Int Ed* **2005**, *44*, 5100-3.
- 13) Van Ness, J.; Van Ness, L. K.; Galas, D. J.: Isothermal reactions for the amplification of oligonucleotides. *Proc Natl Acad Sci* **2003**, *100*, 4504-9.
- 14) Wang, H. Q.; Liu, W. Y.; Wu, Z.; Tang, L. J.; Xu, X. M.; Yu, R. Q.; Jiang, J. H.: Homogeneous label-free genotyping of single nucleotide polymorphism using ligation-mediated strand displacement amplification with DNAzyme-based chemiluminescence detection. *Anal Chem* **2011**, *83*, 1883-9.
- 15) Li, J.; Deng, T.; Chu, X.; Yang, R.; Jiang, J.; Shen, G.; Yu, R.: Rolling circle amplification combined with gold nanoparticle aggregates for highly sensitive identification of single-nucleotide polymorphisms. *Anal Chem* **2010**, *82*, 2811-6.
- 16) Bi, S.; Li, L.; Zhang, S.: Triggered polycatenated DNA scaffolds for DNA sensors and aptasensors by a combination of rolling circle amplification and DNAzyme amplification. *Anal Chem* **2010**, *82*, 9447-54.
- 17) Wu, D. Y.; Wallace, R. B.: The ligation amplification reaction (LAR)--amplification of specific DNA sequences using sequential rounds of template-dependent ligation. *Genomics* **1989**, *4*, 560-9.
- 18) Barany, F.: Genetic disease detection and DNA amplification using cloned thermostable ligase. *Proc Natl Acad Sci* **1991**, *88*, 189-93.
- 19) Cao, W.: Recent developments in ligase-mediated amplification and detection. *Trends Biotechnol* **2004**, *22*, 38-44.

- 20) LaFramboise, T. Single nucleotide polymorphism arrays: a decade of biological, computational and technological advances. *Nucleic Acids Res* **2009**, *37*, 4181-4193.
- 21) [http://www.finddiagnostics.org/about/what\\_we\\_do/successes/find-negotiated-prices/xpert\\_mtb\\_rif.html](http://www.finddiagnostics.org/about/what_we_do/successes/find-negotiated-prices/xpert_mtb_rif.html)
- 22) Chen, X.; Sullivan, P. F. Single nucleotide polymorphism genotyping: biochemistry, protocol, cost and throughput. *Pharmacogenomics J* **2003**, *3*, 77-96.
- 23) Mori, Y.; Notomi, T. Loop-mediated isothermal amplification (LAMP): a rapid, accurate, and cost-effective diagnostic method for infectious diseases. *J Infect Chemother* **2009**, *15*, 62-69.
- 24) Luo, J.; Bergstrom, D. E.; Barany, F. Improving the fidelity of *Thermus thermophilus* DNA ligase. *Nucleic Acids Res* **1996**, *24*, 3071-3078.
- 25) Mano, J.; Oguchi, T.; Akiyama, H.; Teshima, R.; Hino, A.; Furui, S.; Kitta, K. Simultaneous detection of recombinant DNA segments introduced into genetically modified crops with multiplex ligase chain reaction coupled with multiplex polymerase chain reaction. *J Agric Food Chem* **2009**, *57*, 2640-2646.
- 26) Shi, C.; Eshleman, S. H.; Jones, D.; Fukushima, N.; Hua, L.; Parker, A. R.; Yeo, C. J.; Hruban, R. H.; Goggins, M. G.; Eshleman, J. R. LigAmp for sensitive detection of single-nucleotide differences. *Nat Meth* **2004**, *1*, 141-147.
- 27) Conze, T.; Shetye, A.; Tanaka, Y.; Gu, J.; Larsson, C.; Göransson, J.; Tavoosidana, G.; Söderberg, O.; Nilsson, M.; Landegren, U. Analysis of Genes, Transcripts, and Proteins via DNA Ligation. *Ann Rev Anal Chem* **2009**, *2*, 215-239.
- 28) Toubanaki, D. K.; Christopoulos, T. K.; Ioannou, P. C.; Flordellis, C. S. Identification of Single-Nucleotide Polymorphisms by the Oligonucleotide Ligation Reaction: A DNA Biosensor for Simultaneous Visual Detection of Both Alleles. *Anal Chem* **2008**, *81*, 218-224.

- 29) Psifidi, A.; Dovas, C.; Banos, G. Novel Quantitative Real-Time LCR for the Sensitive Detection of SNP Frequencies in Pooled DNA: Method Development, Evaluation and Application. *PLoS ONE* **2011**, *6*, e14560.
- 30) Wiedmann, M.; Wilson, W. J.; Czajka, J.; Luo, J.; Barany, F.; Batt, C. A. Ligase chain reaction (LCR)--overview and applications. *Genome Res* **1994**, *3*, S51-S64.
- 31) Landegren, U.; Kaiser, R.; Sanders, J.; Hood, L. A Ligase-Mediated Gene Detection Technique. *Science* **1988**, *241*, 1077-1080.
- 32) Reyes, A. A.; Carrera, P.; Cardillo, E.; Ugozzoli, L.; Lowery, J. D.; Lin, C.-I. P.; Go, M.; Ferrari, M.; Wallace, R. B. Ligase chain reaction assay for human mutations: the Sickle Cell by LCR assay. *Clin Chem* **1997**, *43*, 40-44.
- 33) Chernesky, M. A.; Marshall, R. L.; Petrich, A. K.: Infectious Disease Testing by LCR. In *Encyclopedia of Molecular Cell Biology and Molecular Medicine*; Wiley-VCH Verlag GmbH & Co. KGaA, 2006.
- 34) Yan, L.; Zhou, J.; Zheng, Y.; Gamson, A. S.; Roembke, B. T.; Nakayama, S.; Sintim, H. O. Isothermal amplified detection of DNA and RNA. *Molecular BioSystems* **2014**, *10*, 970-1003.
- 35) Craw, P.; Balachandran, W. Isothermal nucleic acid amplification technologies for point-of-care diagnostics: a critical review. *Lab Chip* **2012**, *12*, 2469-2486.
- 36) Qi, X.; Bakht, S.; Devos, K. M.; Gale, M. D.; Osbourn, A. L-RCA (ligation-rolling circle amplification): a general method for genotyping of single nucleotide polymorphisms (SNPs). *Nucleic Acids Res* **2001**, *29*, E116.
- 37) Pickering, J.; Bamford, A.; Godbole, V.; Briggs, J.; Scozzafava, G.; Roe, P.; Wheeler, C.; Ghouze, F.; Cuss, S. Integration of DNA ligation and rolling circle amplification for the homogeneous, end-point detection of single nucleotide polymorphisms. *Nucleic Acids Res* **2002**, *30*, e60.



- 38) Cheng, Y.; Zhao, J.; Jia, H.; Yuan, Z.; Li, Z. Ligase chain reaction coupled with rolling circle amplification for high sensitivity detection of single nucleotide polymorphisms. *Analyst* **2013**, *138*, 2958-2963.
- 39) Cheng, Y.; Du, Q.; Wang, L.; Jia, H.; Li, Z. Fluorescently Cationic Conjugated Polymer as an Indicator of Ligase Chain Reaction for Sensitive and Homogeneous Detection of Single Nucleotide Polymorphism. *Anal Chem* **2012**, *84*, 3739-3744.
- 40) Bardea, A.; Burshtein, N.; Rudich, Y.; Salame, T.; Ziv, C.; Yarden, O.; Naaman, R. Sensitive detection and identification of DNA and RNA using a patterned capillary tube. *Anal Chem* **2011**, *83*, 9418-9423.
- 41) Zheng, J.; Li, J.; Jiang, Y.; Jin, J.; Wang, K.; Yang, R.; Tan, W. Design of aptamer-based sensing platform using triple-helix molecular switch. *Anal Chem* **2011**, *83*, 6586-6592.
- 42) Cheng, Y.; Li, Z.; Zhang, X.; Du, B.; Fan, Y. Homogeneous and label-free fluorescence detection of single-nucleotide polymorphism using target-primed branched rolling circle amplification. *Anal Biochem* **2008**, *378*, 123-126.
- 43) Clegg, R. M.: Chapter 1 Förster resonance energy transfer—FRET what is it, why do it, and how it's done. In *Laboratory Techniques in Biochemistry and Molecular Biology*; Gadella, T. W. J., Ed.; Elsevier, **2009**; 1-57.
- 44) Abe, H.; Kool, E. T. Flow cytometric detection of specific RNAs in native human cells with quenched autoligating FRET probes. *Proc Natl Acad Sci* **2006**, *103*, 263-268.
- 45) Chen, X.; Livak, K. J.; Kwok, P.-Y. A Homogeneous, Ligase-Mediated DNA Diagnostic Test. *Genome Res* **1998**, *8*, 549-556.
- 46) Xu, Y.; Karalkar, N. B.; Kool, E. T. Nonenzymatic autoligation in direct three-color detection of RNA and DNA point mutations. *Nat Biotech* **2001**, *19*, 148-152.
- 47) Lohman, G. J. S.; Tabor, S.; Nichols, N. M.: DNA Ligases. In *Current Protocols in Molecular Biology*; John Wiley & Sons, Inc., **2001**.

- 48) Kausar, A.; McKay, R. D.; Lam, J.; Bhogal, R. S.; Tang, A. Y.; Gibbs-Davis, J. M. Tuning DNA Stability To Achieve Turnover in Template for an Enzymatic Ligation Reaction. *Angew Chem Int Ed* **2011**, *123*, 9084-9088.
- 49) Kausar, A.; Mitran, C. J.; Li, Y.; Gibbs-Davis, J. M. Rapid, Isothermal DNA Self-Replication Induced by a Destabilizing Lesion. *Angew Chem Int Ed* **2013**, *52*, 10577-10581.
- 50) Wang, H.; Li, J.; Wang, Y.; Jin, J.; Yang, R.; Wang, K.; Tan, W. Combination of DNA Ligase Reaction and Gold Nanoparticle-Quenched Fluorescent Oligonucleotides: A Simple and Efficient Approach for Fluorescent Assaying of Single-Nucleotide Polymorphisms. *Anal Chem* **2010**, *82*, 7684-7690.
- 51) Syvanen, A.-C. Accessing genetic variation: genotyping single nucleotide polymorphisms. *Nat Rev Genet* **2001**, *2*, 930-942.
- 52) Granzhan, A.; Kotera, N.; Teulade-Fichou, M.-P. Finding needles in a basestack: recognition of mismatched base pairs in DNA by small molecules. *Chem Soc Rev* **2014**, *43*, 3630-3665.
- 53) Sinden, R. R.: *DNA structure and function*; 1 ed., **1994**. pp. 398.
- 54) Kapanidis, A. N.; Weiss, S. Fluorescent probes and bioconjugation chemistries for single-molecule fluorescence analysis of biomolecules. *J Chem Phys* **2002**, *117*, 10953-10964.
- 55) Mirkin, C. A.; Letsinger, R. L.; Mucic, R. C.; Storhoff, J. J. A DNA-based method for rationally assembling nanoparticles into macroscopic materials. *Nature* **1996**, *382*, 607-609.
- 56) Rosi, N. L.; Mirkin, C. A. Nanostructures in Biodiagnostics. *Chem Rev* **2005**, *105*, 1547-1562.
- 57) Alivisatos, A. P.; Johnsson, K. P.; Peng, X.; Wilson, T. E.; Loweth, C. J.; Bruchez, M. P.; Schultz, P. G. Organization of 'nanocrystal molecules' using DNA. *Nature* **1996**, *382*, 609-611.
- 58) Hazarika, P.; Ceyhan, B.; Niemeyer, C. M. Reversible Switching of DNA-Gold Nanoparticle Aggregation. *Angew Chem Int Ed* **2004**, *43*, 6469-6471.

- 59) Trantakis, I. A.; Bolisetty, S.; Mezzenga, R.; Sturla, S. J. Reversible Aggregation of DNA-Decorated Gold Nanoparticles Controlled by Molecular Recognition. *Langmuir* **2013**, *29*, 10824-10830.
- 60) Shen, W.; Deng, H.; Gao, Z. Gold Nanoparticle-Enabled Real-Time Ligation Chain Reaction for Ultrasensitive Detection of DNA. *J Am Chem Soc* **2012**, *134*, 14678-14681.
- 61) Grabar, K. C.; Freeman, R. G.; Hommer, M. B.; Natan, M. J. Preparation and Characterization of Au Colloid Monolayers. *Anal Chem* **1995**, *67*, 735-743.
- 62) Stoeva, S. I.; Lee, J.-S.; Thaxton, C. S.; Mirkin, C. A. Multiplexed DNA Detection with Biobarcoded Nanoparticle Probes. *Angew Chem Int Ed* **2006**, *45*, 3303-3306.

## **Chapter 5**

### **The Influence of Ligase and Probe Architecture on Lesion-Induced DNA Amplification**

## 5.1 Introduction

In the previous chapters we have seen that the background ligation severely affected the ability to detect low concentrations of DNA. In chapter 3, we described our attempt to reduce the background ligation by reducing the probe concentration and by using a serial ligation strategy. In this chapter, I will discuss our attempts to reduce the background-triggered amplification process using different enzymes, which were reported to give no blunt end ligation, the source of our background reaction. Blunt end in a ligation system (as in LCR) is defined as a system where there are two small duplexes without having any extra base(s) in the ligating ends (Figure 5.1 A), whereas a sticky end is defined as a ligation system having one or more extra complementary overhanging bases (Figure 5.1 B). In the sticky end, if the terminal bases are complementary to each other DNA ligase can ligate them much faster than the blunt ends. In our amplification system, there is one base overhang in one terminal of one of the duplexes and one abasic (**Ab**) group in the terminal of the other duplex (Figure 5.1 C); as there is no interaction between the terminal base and **Ab** group we refer it as pseudo-blunt end system. Since the rate of blunt end ligation is always slower than that of sticky end ligation, we hypothesized that if we use true blunt end in the ligation system, the rate of background ligation would be decreased. To test this hypothesis, we designed several blunt end systems by introducing the abasic group in different positions in different probes. Cross-catalysis with different true blunt end systems is shown in the second part of the chapter. Finally, I will

describe the effect of different bases across from the abasic group in our regular cross-catalytic system.

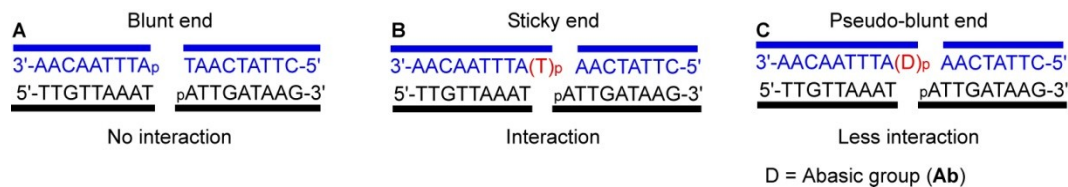


**Figure 5.1:** Schematic illustration of A) Blunt end B) Sticky end and C) Pseudo-blunt end systems.

## 5.2 Overview of DNA ligases

There are several different commercially available DNA ligases (T7, T3 and *E. coli* DNA ligase), which have been reported to give less blunt end ligation compared to T4 DNA ligase.<sup>1-3</sup> Among them, T7 and T3 DNA ligases are commercially available in a fairly high concentration (similar in activity with T4 DNA ligase). Before examining our lesion-induced DNA amplification process with different ligases, I will briefly describe each of the enzymes.

### 5.2.1 T7 DNA ligase

T7 DNA ligase is an ATP-dependent dsDNA ligase from bacteriophage T7, which catalyzes the formation of a phosphodiester bond between adjacent 5'-phosphate and 3'-hydroxyl groups of double stranded DNA.<sup>2, 4</sup> T7 DNA ligase is very efficient in cohesive end ligation and nick sealing, but the ligation of blunt ends is not very efficient. The activity of the T7 DNA ligase greatly depends on the concentration polyethylene glycol (PEG) present in the ligation buffer.<sup>2</sup> PEG increases macromolecular crowding, which mimics a higher DNA concentration

in solution.<sup>5</sup> Since ligation of blunt-end DNA does not happen appreciably in the presence of T7 DNA ligase, it can be particularly suitable for applications where both blunt ends and cohesive ends of DNA duplexes are present but only the cohesive ends needed to be joined.

### **5.2.2 T3 DNA ligase**

T3 DNA ligase is another example of an ATP-dependent dsDNA ligase from bacteriophage T3.<sup>3</sup> T3 DNA ligase exhibits a higher tolerance of monovalent cations (up to 1 M), which makes the enzyme a suitable choice for molecular biology protocols where a high salt concentration is required.<sup>3</sup> T3 DNA ligase is also very efficient for the ligation of cohesive DNA fragments, but less efficient for ligation of blunt-end DNA fragments. Similar to T7 DNA ligase, blunt end ligation is enhanced by the addition of PEG 6000 to the reaction.

### **5.2.3 *E. coli* DNA ligase**

*E. coli* DNA ligase is a NAD dependent dsDNA ligase from the lig gene in *E. coli*.<sup>6</sup> Like other ligases, *E. coli* DNA ligase catalyzes the formation of a phosphodiester bond between 5' phosphate and 3' hydroxyl groups in duplex DNA and joins restriction fragments having homologous cohesive ends.<sup>1,7</sup> Unlike T4 DNA ligase, *E. coli* DNA ligase does not join termini with blunt ends under normal reaction conditions, however, the addition of PEG has been reported to stimulate this activity.<sup>8</sup> *E. coli* DNA ligase requires NAD<sup>+</sup> as its AMP-donating cofactor. Due to its low blunt-end ligation efficiency, *E. coli* DNA ligase can be

used when a high specificity for cohesive end DNA joining or nick sealing is required.

### **5.3 Ligation with T7 DNA ligase**

#### **5.3.1 Lesion-induced DNA amplification with T7 DNA ligase**

At first, we examined the cross-catalytic amplification of our **DNA-I** system with commercially available T7 DNA ligase (3000 CEU/ $\mu$ L, New England Biolabs) with 7.5% PEG 6000 in the ligation buffer. Our prior work had shown that the optimum temperature for cross-catalytic amplification of the **DNA-I** system with T4 DNA ligase was 30 °C, so we studied the amplification using T7 DNA ligase at this temperature. Amplification with T7 DNA ligase at 30 °C was very slow yielding only ~ 8% **DNA-I** product after 2 hours (Figure 5.2 A). From the literature we found that the optimum temperature for ligation utilizing T7 DNA ligase was 25 °C. When cross-catalysis was conducted at 26 °C, we found that the rate of amplification was faster at this temperature (Figure 5.2 B). That is interesting as it brings the replication temperature further below the melting temperature of the product duplex. We were able to detect up to 140 pM of target DNA in the presence of 1.4  $\mu$ M of probes, whereas with T4 DNA ligase we could detect only 1.4 nM target DNA at similar probe concentrations. However, we note that the ligation with T7 DNA ligase was much slower compared with T4 DNA ligase requiring several hours to complete.



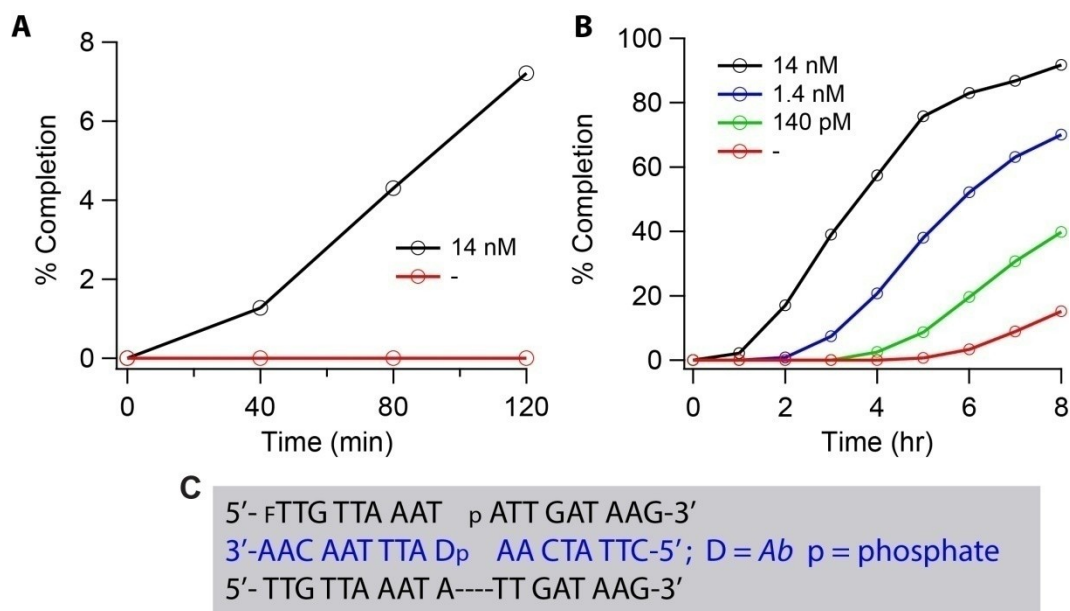


**Figure 5.2:** Kinetics of cross-catalytic amplification with T7 DNA ligase at: A) 30 °C and B) 26 °C. C) DNA sequences used for this study. *Experimental conditions:* 1.4  $\mu\text{M}$  **r-Ia(FAM)**, 2.8  $\mu\text{M}$  **r-Ib(A)**, 2.8  $\mu\text{M}$  **r-IIb**, 2.8  $\mu\text{M}$  **r-IIa<sub>Ab</sub>** and 0 nM (-), 140 pM, 1.4 nM or 14 nM target **DNA-I(A)**, Buffer 5, 3000 CEUs T7 DNA ligase per 15  $\mu\text{L}$  reaction. The naming of **DNA-I(A)** refers to the target sequence with an A in the 10th position from the 5' end, which is across from the abasic site upon hybridizing with the destabilizing probes. Note that this naming scheme is different than that used in Chapter 4, which focused on a different nucleotide position in the target sequence.

### 5.3.2 Single cycle ligation with T7 DNA ligase

To understand the different rates of amplification at different temperatures in the cross-catalytic system above, we studied the single cycle ligation with different templates and probes using one equivalent of template. This allows us to determine how the rate of ligation impacted turnover in the cross-catalytic system. As expected with the native DNA probes and template lacking any destabilizing

group the rate of ligation was very fast (~100% in 10 minutes) at all different temperatures explored from 22 °C to 30 °C (Figure 5.3 A and B). The rate was also fast when there was an abasic group only present in the DNA template (Figure 5.3 C). However, ligation with an abasic group in the probe was much slower and was incomplete after 10 minutes at all of the temperatures investigated (Figure 5.3 D). Ligation of the abasic probes did occur relatively quickly at 22 °C, but the rate of ligation was very slow at 30 °C (Figure 5.2 E). These results indicated that the cause of the slow cross-catalysis at 30 °C was the first cycle of ligation involving the target DNA templating the ligation of the destabilizing probes. The different temperature dependence of the T7 and T4 DNA ligase-catalyzed processes support the previous findings that both the rate of the ligation step as well as the rate of product duplex dissociation is very important to achieve rapid amplification.<sup>9</sup>

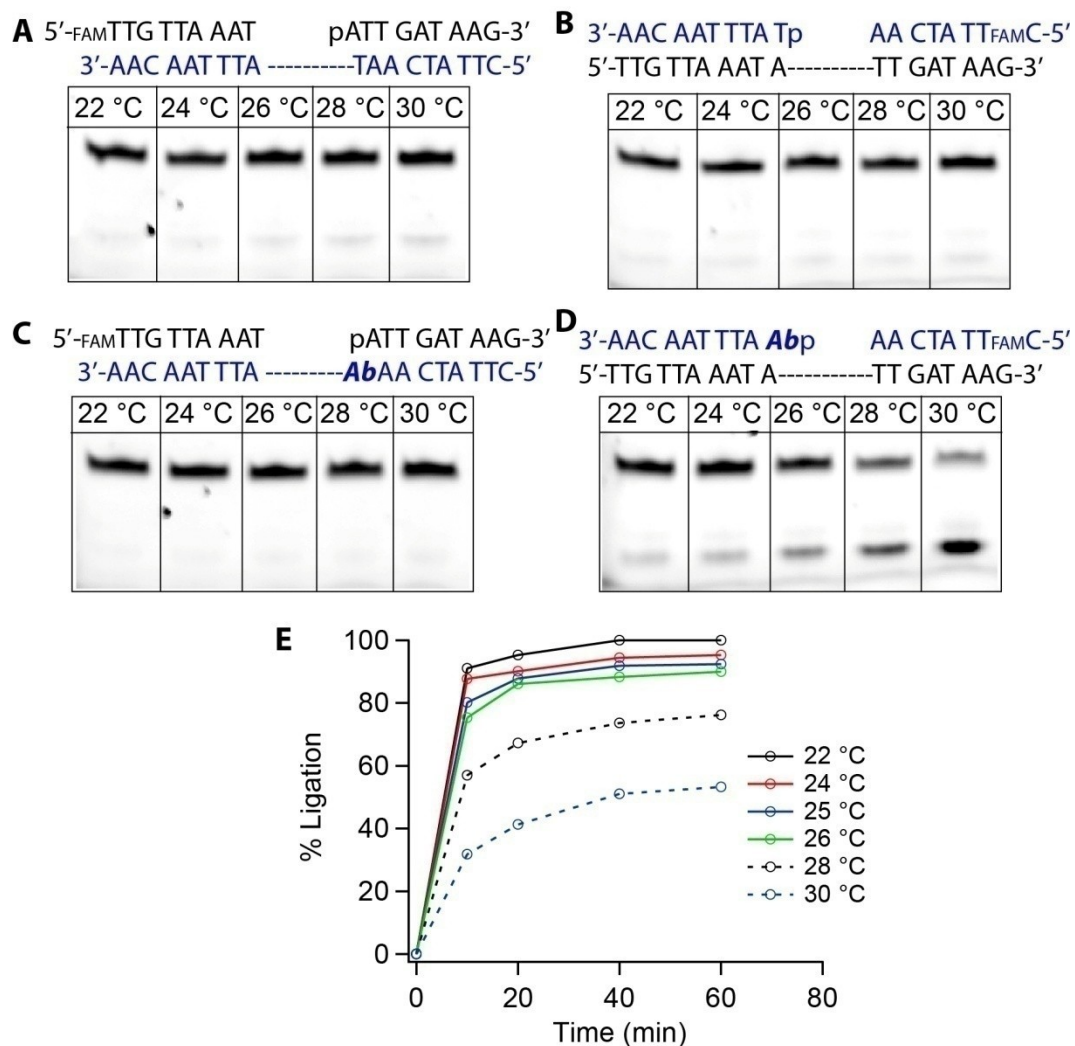


**Figure 5.3:** PAGE images of single cycle ligations after 10 minutes with: A-B) native DNA templates and probes C) a destabilizing template with native DNA probes and D) a native DNA template with a destabilizing probe (Ab = an abasic lesion). The top band is the ligation product while the bottom band is the fluorescently labeled probe. E) The kinetics of ligation of the destabilizing probes with a native DNA template (part D) at different temperatures. *Experimental conditions:* for all sets, [Template] = 1.4  $\mu$ M, [Fluorescent-DNA] = 1.4  $\mu$ M, [Non-fluorescent-DNA] = 2.8  $\mu$ M, [Enzyme] = T7 DNA ligase 3000 cohesive end units (CEUs) in Buffer 5 for 15  $\mu$ L ligation volume.

### 5.3.3 Cross-catalysis with different buffers with T7 DNA ligase

Although we found that T7 DNA ligase was useful in lowering the limit of detection, this enzyme still exhibited background-triggered amplification even in the absence of the initial target DNA. This background process once again decreased the sensitivity of our amplification method. For T7 DNA ligase, the rate of the blunt end ligation was known to depend strongly on the concentration of PEG in the ligation buffer.<sup>2</sup> Consequently, we varied the concentration of PEG in the ligation buffer to minimize the background reaction. As illustrated in Figure 5.4, in the absence of PEG no fluorescently labeled target (**F-DNA-I**) formed within 8 hours of observation, whereas if we increased the concentration of PEG to 3.8%, we observed the formation of target product. Under the latter conditions, amplification was still very slow with only ~ 30 % yield for amplification initiated by 14 nM **DNA-I** and ~0.5% yield for the background-triggered amplification after 8 hours (the percent yield is based on the percent of fluorescent probe that is converted to the ligated product **F-DNA-I**). With 7.5% PEG, the rate of amplification with initial target was much faster, but the background-triggered process was also faster than that observed with 3.8% PEG.

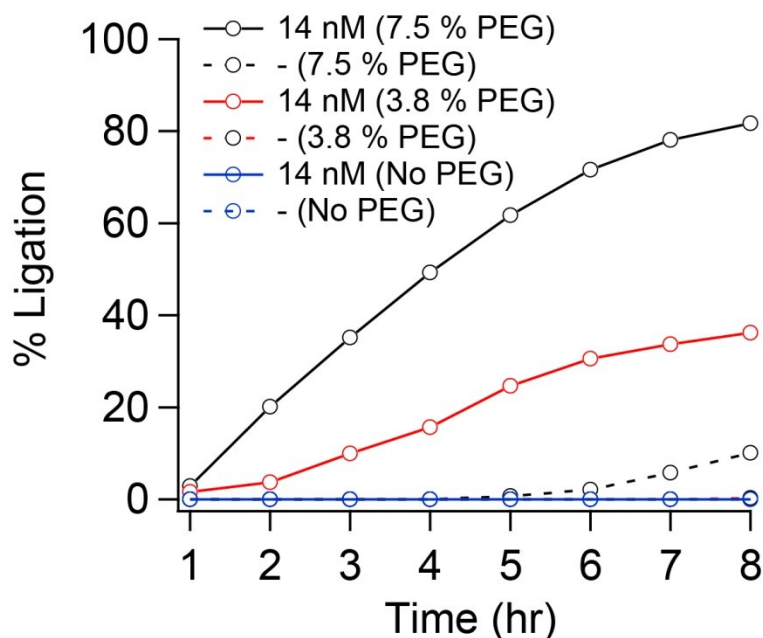


**Figure 5.4:** Cross-catalytic amplification utilizing T7 DNA ligase with different concentrations of PEG in the buffer (7.5 % (Buffer 5), 3.8 % (Buffer 6), 0 % (Buffer 1)). *Experimental conditions:* 1.4  $\mu\text{M}$  **r-Ia(FAM)**, 2.8  $\mu\text{M}$  **r-Ib(A)**, 2.8  $\mu\text{M}$  **r-IIb**, 2.8  $\mu\text{M}$  **r-IIa<sub>AB</sub>** and 0 nM (dotted lines) or 14 nM (solid lines) target **DNA-I(A)**, 3000 CEUs T7 DNA ligase per 15  $\mu\text{L}$  reaction, 26  $^{\circ}\text{C}$ . % Ligation is based on the percentage of fluorescent probe **r-Ia(FAM)** that is converted to the fluorescent labeled target sequence **F-DNA-I(A)**.

### 5.3.4 Cross-catalysis with high concentration T7 DNA ligase in PEG-free buffer

Since the presence of PEG greatly increased the rate of blunt end ligation, we hypothesized that if we used PEG-free buffer there would be no background reaction. But, as shown in Figure 5.4, the rate of the templated ligation was very slow in PEG-free buffer. One way to increase the rate of the templated reaction was to increase the concentration of enzyme. However, the highest commercially available concentration of the T7 DNA ligase enzyme is 3000 cohesive end units

(CEU)/ $\mu\text{L}$ , which was the concentration used in the PEG-variation experiment. Fortunately, we received some high concentration of T4, T3 and *E. coli* DNA ligase as a gift from an American company Enzymatics based in Massachusetts. The cross-catalytic amplification with this concentrated T7 DNA ligase (19650 CEU/ $\mu\text{L}$ ) in a PEG-free buffer proceeded well at different temperatures (Figure 5.5). Unfortunately, the rate of amplification with this high enzyme concentration was still very slow in PEG-free buffer.

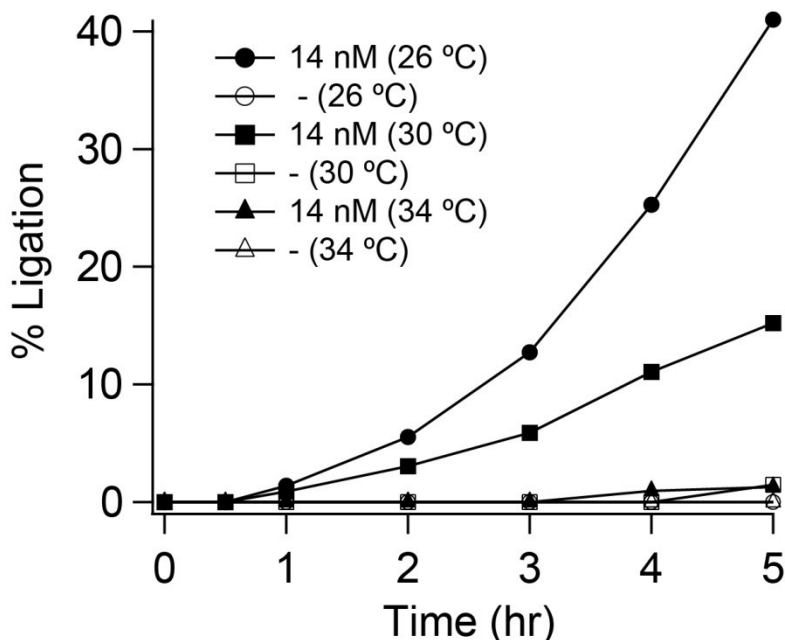


**Figure 5.5:** Cross-catalytic amplification with T7 DNA ligase at different temperatures in PEG-free buffer. *Experimental conditions:* **r-Ia(FAM) 1.4  $\mu\text{M}$ ; r-Ib(A) 2.8  $\mu\text{M}$ ; r-IIb 2.8  $\mu\text{M}$ ; r-IIa<sub>Ab</sub> 2.8  $\mu\text{M}$**  and 0 nM (open symbols) or 14 nM (solid symbols) target **DNA-I(A)**, 19650 CEUs T7 DNA ligase in Buffer 8 per 15  $\mu\text{L}$  reaction. *% Ligation* is based on the percentage of fluorescent probe **r-Ia(FAM)** that is converted to the fluorescent labeled target sequence **F-DNA-I(A)**.

#### 5.4 Cross-catalysis with *E. coli* ligase

*E. coli* DNA ligase is another example of a DNA ligase that is reported to give a slow rate of ligation of DNA duplexes with blunt ends. However this enzyme is also commercially available only in very low concentration (10 CEUs/ $\mu$ L). So we used the high concentration (260 CEU/ $\mu$ L) of *E. coli* DNA ligase received from Enzymatics in our lesion-induced cross-catalytic scheme. With this high concentration, it was possible to achieve a decent rate of amplification (> 80% ligation of the fluorescent probe in ~ 2 hours). Similar to T4 DNA ligase, this enzyme has the same optimum temperature (30 °C, Figure 5.6), but a slower rate of background (pseudo blunt-end) ligation, which enabled us to detect as little as 14 pM of target **DNA-I(A)** (Figure 5.7), which improved our sensitivity by two orders of magnitude compared with T4 DNA ligase.

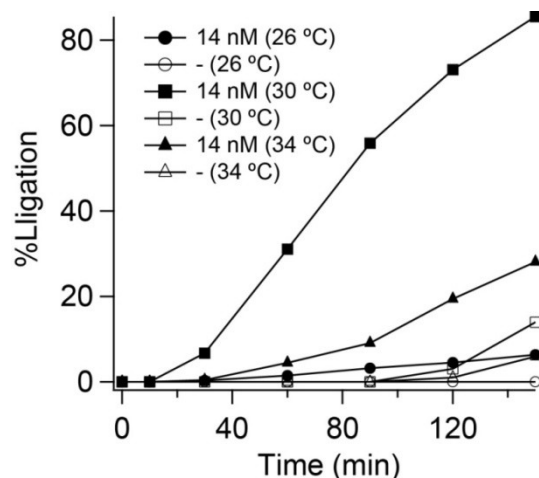


**Figure 5.6:** Kinetics of cross-catalysis with *E. coli* ligase at different temperatures. *Experimental conditions:* 1.4  $\mu\text{M}$  **r-Ia(FAM)**, 2.8  $\mu\text{M}$  **r-Ib(A)**, 2.8  $\mu\text{M}$  **r-IIb**, 2.8  $\mu\text{M}$  **r-IIa<sub>Ab</sub>** and 0 nM (open symbols) or 14 nM (solid symbols) target **DNA-I(A)**, 260 CEUs *E. coli* DNA ligase in Buffer 7 per 15  $\mu\text{L}$ . % *Ligation* is based on the percentage of fluorescent probe **r-Ia(FAM)** that is converted to the fluorescent labeled target sequence **F-DNA-I(A)**.

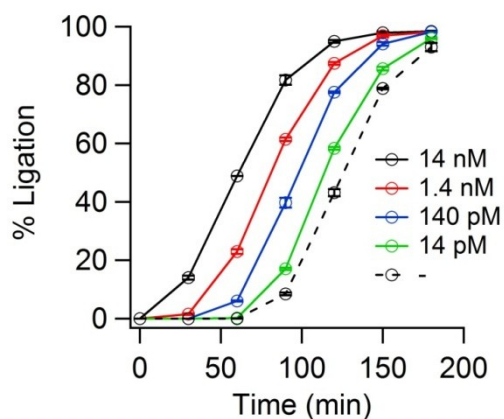


**Figure 5.7:** Kinetics of cross-catalysis with *E. coli* ligase with different concentrations of target DNA at 30 °C. *Experimental conditions:* 1.4  $\mu\text{M}$  **r-Ia(FAM)**; 2.8  $\mu\text{M}$  **r-Ib(A)**; 2.8  $\mu\text{M}$  **r-IIb**; 2.8  $\mu\text{M}$  **r-IIa<sub>Ab</sub>**; 0 nM (-), 1.4 nM, 140 pM or 14 nM target **DNA-I(A)**; 260 CEUs *E. coli* DNA ligase in Buffer 7 per 15  $\mu\text{L}$  reaction.



## 5.5 Cross-catalysis with T3 DNA ligase

We also examined T3 DNA ligase to measure its ability to catalyze our lesion-induced DNA amplification process. Figure 5.8 shows the cross-catalytic amplification with the **DNA-I(A)** system at different temperatures with T3 DNA ligase. The rate of amplification was faster at 30 °C than 26 °C and 34 °C, but none of the temperatures were free from the background-triggered process. Additionally, the rate of amplification was much slower than that with T4 DNA ligase, which we attribute to the lack of PEG in the ligation buffer. The addition of PEG in the buffer might improve the rate of amplification, but it is also likely to increase the rate of background ligation, so we did not pursue those experiments.

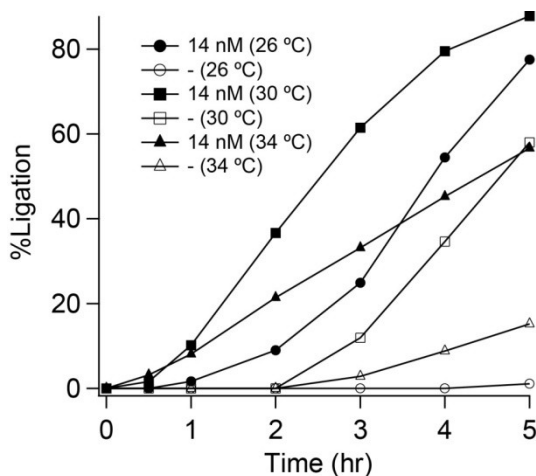


**Figure 5.8:** Kinetics of cross-catalysis with T3 DNA ligase at different temperatures. *Experimental conditions:* 1.4  $\mu\text{M}$  **r-Ia(FAM)**, 2.8  $\mu\text{M}$  **r-Ib(A)**, 2.8  $\mu\text{M}$  **r-IIb**, 2.8  $\mu\text{M}$  **r-IIa<sub>Ab</sub>** and 0 nM (open symbols) or 14 nM (solid symbols) target **DNA-I(A)**, 18870 CEUs T3 DNA ligase in Buffer 8 per 15  $\mu\text{L}$  reaction. % *Ligation* is based on the percentage of fluorescent probe **r-Ia(FAM)** that is converted to the fluorescent labeled target sequence **F-DNA-I(A)**.

## 5.6 Cross-catalysis with different blunt end system

In the above examples, we saw that varying the ligase to reduce the background ligation worked for some of the ligases explored, but the improvements were not significant enough to make our lesion-induced DNA amplification method viable for nucleic acid diagnostics. To make the amplification system more sensitive we aimed to further reduce the background ligation by varying the probe architecture. The amplification systems described so far utilized probe sequences that had one base overhang across from the abasic group (Figure 5.1-5.8). As this design is not perfectly blunt end, we refer to it as pseudo-blunt end as there should be no interactions between the abasic group and the one-base overhang. As all ligases joins overhangs much faster than blunt ends, we decided to redesign our probes by moving the abasic group one or two bases from the probe terminus to make a true blunt end. All the probes we designed for making the blunt end systems are 9-bases long (Figure 5.9). The first two sets had the abasic group one-base or two-bases inside from the 5'-end. In fact, we could make a probe having a 5'-terminal abasic group, but in that case the ligation site in the second cycle will be across from 5'-end of the **Ab** group. As shown earlier in Chapter 2 (Figure 2.5), the ligation was severely affected when the ligation site was across from the 5'-end of the **Ab** group. When we studied the cross-catalytic amplification we found that the rate of target-initiated amplification with these probes that formed a blunt end was very slow, as we observed formation of very small amount of product formation even after 20 hours of amplification (Figure 5.9).

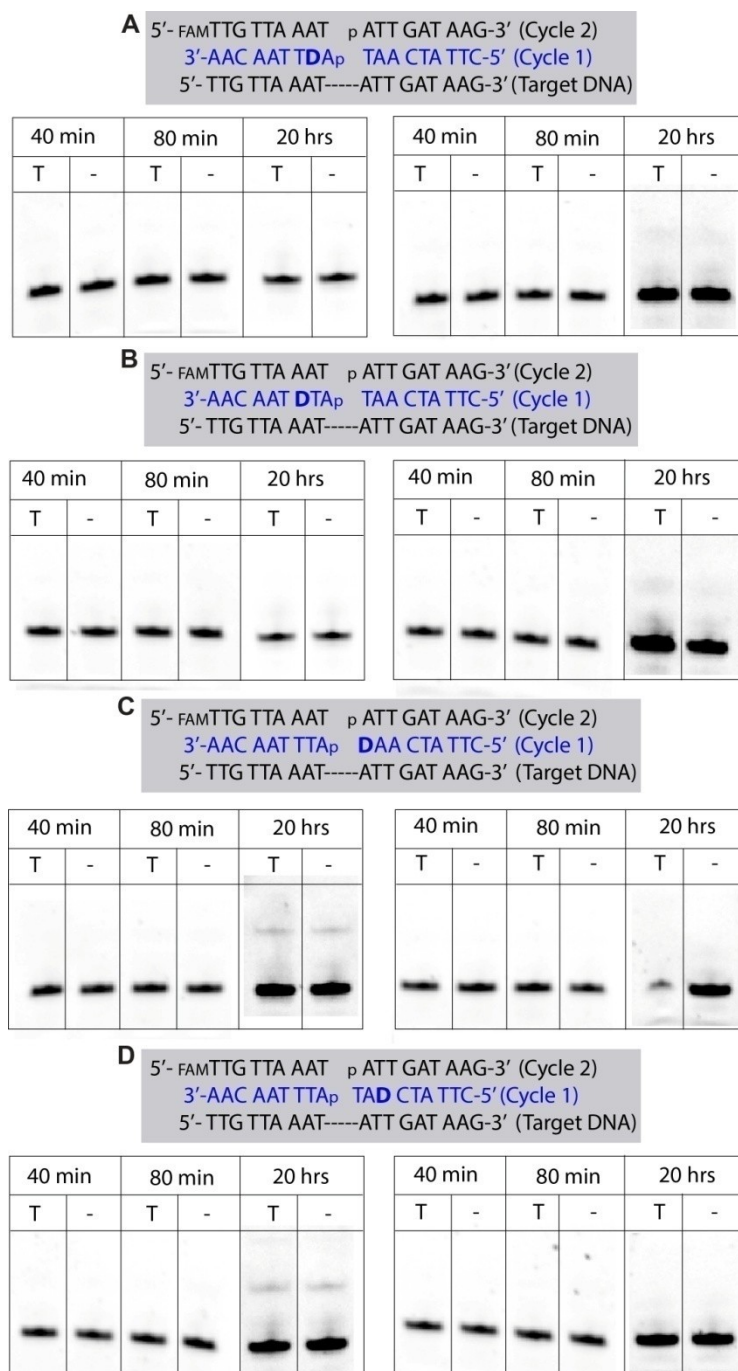


**Figure 5.9:** Cross-catalytic amplification with different blunt-end systems at 30 °C with T7 (left images) and *E. coli* DNA ligase (right images). For all [Target] = 14 nM, [Fluorescent-DNA] = 1.4 μM, [Non-fluorescent-DNA] = 2.8 μM, [Enzyme] = *E. coli* DNA ligase 260 CEU/μL in Buffer 7, T7 DNA ligase 19650 CEU/ μL in Buffer 8 for 15 μL ligation volume.

To diagnose why the cross-catalysis did not occur or was incredibly slow, we studied the single cycle ligation reaction using one equivalent of template with the probes having the **Ab** group at different positions. As expected, the ligation with the native DNA template and probes was very fast with all different ligases (Figure 5.10, lane 1 and 4). For T4 DNA ligase, we also observed ligation for all of the single cycle ligation reactions consisting of destabilizing probes with a native DNA template (Figure 5.10 B, lanes 1-3). The standard probes used in our pseudo-blunt end system containing a terminal 5' abasic phosphate exhibited fast ligation with T4 DNA ligase, slightly slower than that of the native DNA probes (Figure 5.10 B, lane 1 and 4, respectively). The probes that resulted in blunt end probe duplexes (lanes 2 and 3), however, were significantly slower in these single cycle reactions, but appreciable amounts of ligation had occurred for these probes after 60 minutes. In contrast, the ligation of the same probes with T3 DNA ligase was very slow yielding very little product after one hour (Figure 5.10 C, lanes 2 and 3). Finally, no ligation product formed from these probes with the internal destabilizing groups when either T7 or *E. coli* DNA ligase was used even after 60 minutes (lanes 2 and 3, Figure 5.10 D and E, respectively). We infer that the reason we failed to observe any cross-catalytic amplification with T7 and *E. coli* DNA ligases as described above stemmed from the slow rate of ligation for this destabilizing probe design. These results illustrated that different ligases have very different tolerances of lesions in the nicked complex. Unfortunately, none of the blunt-end systems were particularly promising as replacements for our pseudo-blunt end architecture using T7 or *E. coli* DNA ligase. Previous work in

the group done by Katie Mitran indicated that using “blunt end” probes with T4 DNA ligase did lower the limit of detection 100-fold compared with the pseudo-blunt end probes, however the amplification process became very slow, requiring hours to complete (data not shown). Finally, it might be worth exploring cross-catalysis using the blunt end probes with T3 DNA ligase, but it is likely to also result in very slow kinetics given the slower ligation rates observed for T3 DNA ligase compared with T4 DNA ligase (Figure 5.10 C vs. B, respectively).

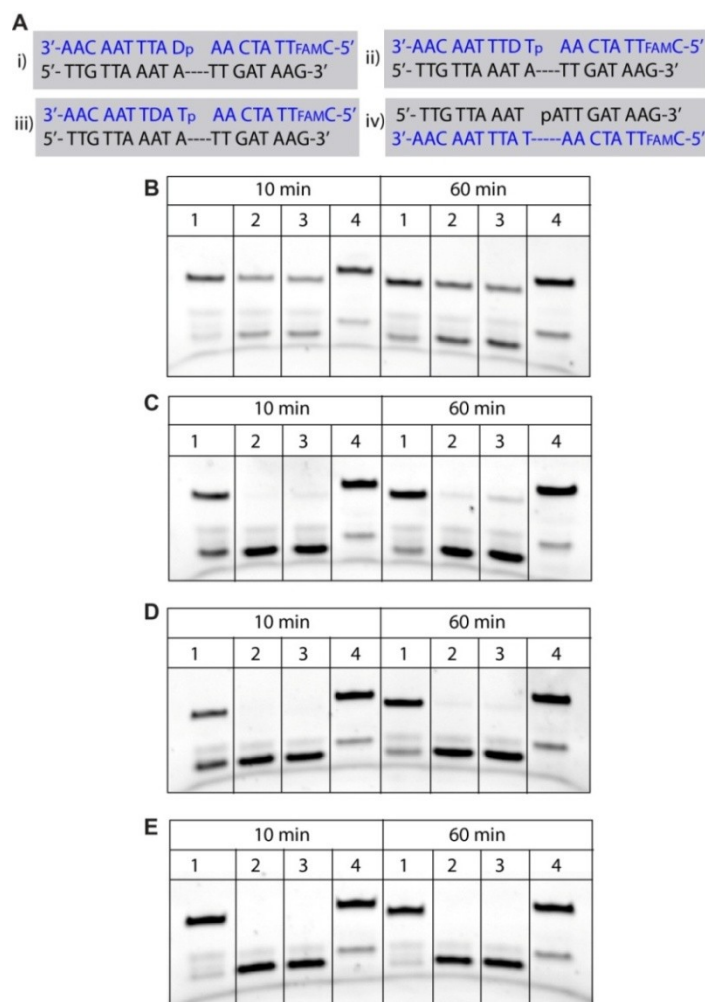
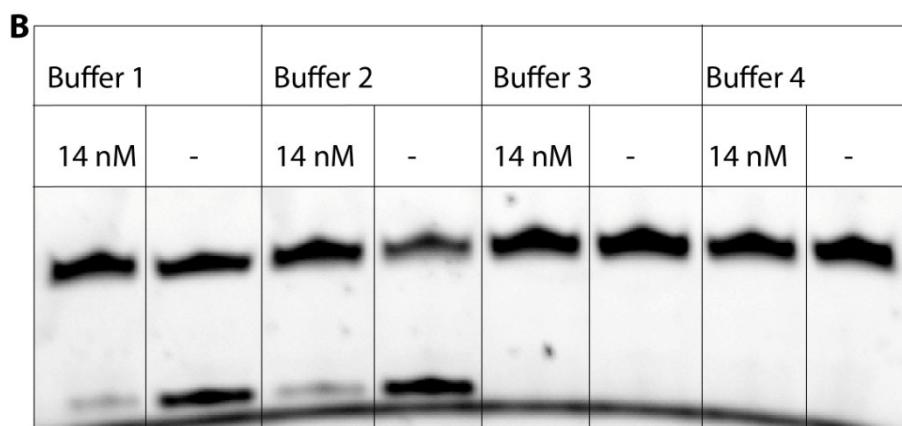
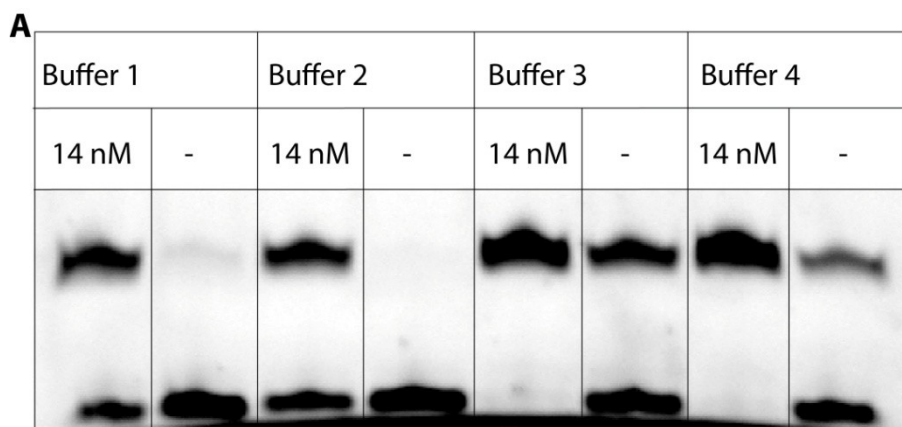


**Figure 5.10:** Single cycle ligation reactions with different destabilizing probes and different ligases at 25 °C. A) The different probe architectures explored contained: (i) a terminal destabilizing phosphate; (ii) and (iii) internal destabilizing groups; and (iv) no destabilizing groups. (D = a model abasic destabilizing group; FAM = fluorescein and P = phosphate.) PAGE images of the ligation mixtures, where the lane label refers to the specific probes and target listed in (A), using: B) T4 DNA ligase; C) T3 DNA ligase; D) T7 DNA ligase; and E) *E. coli* DNA ligase. *Experimental conditions:* 1.4 μM template; 1.4 μM fluorescent-probe; 2.8 μM each non-fluorescent probes; 400 CEUs T4 DNA ligase in Buffer 1, 19650 CEUs T7 DNA ligase in Buffer 8, 18870 CEUs T3 DNA ligase /μL in Buffer 8 or 260 CEUs *E. coli* DNA ligase in Buffer 7 for a 15 μL ligation volume.

## **5.7 Attempts to reduce background-triggered amplification with ATP and spermidine**

It was reported several decades ago that blunt end ligation could be selectively inhibited by changing the concentration of ATP or by the addition of spermidine in the buffer.<sup>10</sup> For this purpose, we have studied the cross-catalytic amplification with different concentrations of ATP and spermidine (Figure 5.11). Buffer 1 was the regular DNA ligase buffer with 1 mM ATP. To determine how ATP influenced the ligation process, we prepared Buffer 2 consisting of a higher ATP concentration (4.2 mM ATP). Using our standard destabilizing probe (i.e., with the 5' abasic phosphate), we observed a slower rate of amplification for both template-initiated and background-triggered amplification in buffer 2 compared with the standard buffer 1, but the effect was not significant. To determine the influence of spermidine, we compared ligation in buffer 1 with buffer 3 which had the regular ATP concentration (1 mM) with 18.1 mM spermidine. To our surprise, the background-triggered amplification was significantly faster than that observed in buffer 1. The same was true for the reaction initiated with 14 nM target. However, the fastest amplification rates were observed for both the template-initiated and background-triggered reactions with Buffer 4, which contained 3.8 mM ATP and 16.2 mM spermidine. Further optimization using different additives is required to maximize the difference in yield between the amplification mixtures with and without initial template.



Buffer 1 : 1 mM ATP  
 Buffer 2 : 4.2 mM ATP  
 Buffer 3 : 1 mM ATP + 18.1 mM spermidine  
 Buffer 4 : 3.8 mM ATP + 16.2 mM spermidine

**Figure 5.11:** PAGE images of cross-catalytic amplifications using standard destabilizing probes after A) 40 minutes and B) 80 minutes with different buffers containing different amount of ATP and spermidine. *Experimental conditions:* 1.4  $\mu$ M **r-Ia(FAM)**; 2.8  $\mu$ M **r-Ib(A)**; 2.8  $\mu$ M **r-IIb**; 2.8  $\mu$ M **r-IIa<sub>Ab</sub>**; 0 nM (-) or 14 nM target **DNA-I(A)**; 2000 CEUs T4 DNA ligase per 15  $\mu$ L reaction; 30 °C.



## 5.8 Varying the deoxynucleotide across from the abasic group

When designing destabilizing probes for our lesion-induced DNA amplification strategy, one of the questions that arose was whether there was any influence of the nucleobase (A/T/G/C) across from the abasic group. In both the **DNA-I** and **H-DNA-I** systems from Chapter 3, there was a deoxyadenosine (A) across from the abasic group. For the **E-DNA-I** system also therein, there was an A across from the abasic, which indicated that either a pyrimidine or purine was acceptable to T4 DNA ligase across from the abasic lesion. Indeed, one might suspect that since there is no hydrogen bonding and pi-stacking interaction there should be no effect of the base across from the abasic site. To determine the influence of the base across from this destabilizing group, we studied cross-catalytic amplification with different templates (Y in Figure 5.12). For this purpose, we purchased different target **DNA-I(Y)** strands and synthesized four probes (**r1b(Y)**) to match with the corresponding targets.

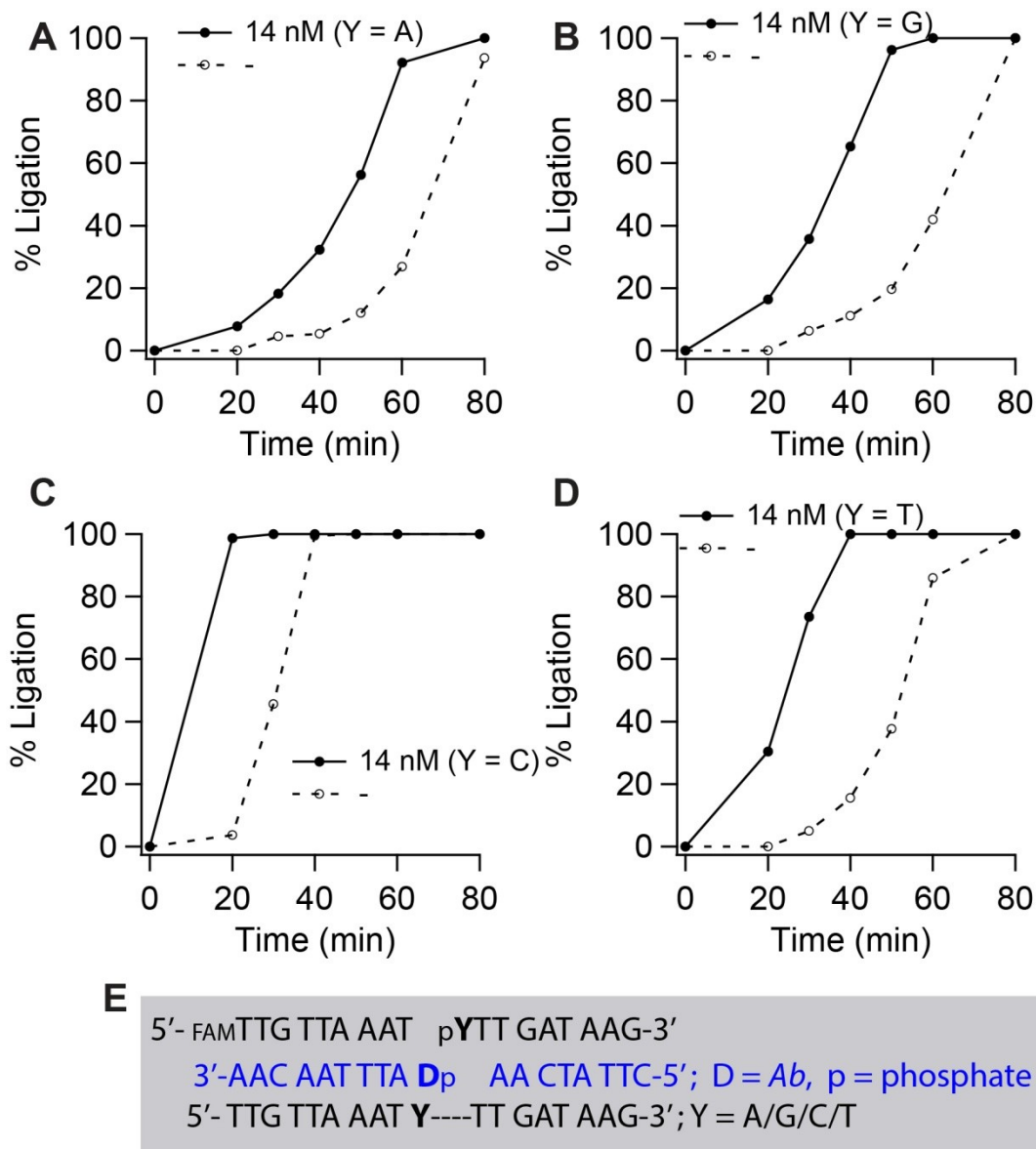


**Figure 5.12:** Cross-catalytic amplification of different amplification systems with T4 DNA ligase at 30 °C. *Experimental conditions:* 1.4 μM **r-Ia(FAM)**, 2.8 μM **r-Ib(A)**, 2.8 μM **r-IIb**, 2.8 μM **r-IIa<sub>Ab</sub>** and 14 nM of target **DNA-I(Y)**, Y = A/T/C/G, T4 DNA ligase 2000 CEU/μL in Buffer 1 for 15 μL ligation volume. % *Ligation* is based on the percentage of fluorescent probe **r-Ia(FAM)** that is converted to the fluorescent labeled target sequence **F-DNA-I(Y)**.

Cross-catalytic amplification of different templates with their matched set of probes showed that all of the different nucleobases were tolerated in the amplification process. The amplification profiles, however, varied significantly from each other (Figure 5.12). Specifically, the most significant difference in the amplification profile was observed with **DNA-I(C)** and the corresponding probe set. This target exhibited a rate of amplification that was much faster than Y = A,T, or G under the same experimental conditions.

We inferred from this observation that the rate of ligation was faster with **DNA-I(C)** and **r1b(C)**. In order to test this hypothesis, we studied separately the single cycle ligation reaction for both cycles in the cross-catalytic scheme with the native **DNA-I(Y)** template and destabilizing probes and the destabilizing template and native DNA probes, which showed that the rate of the single cycle ligation did follow the same trend as the rate of cross-catalytic amplification (Figure 5.13).

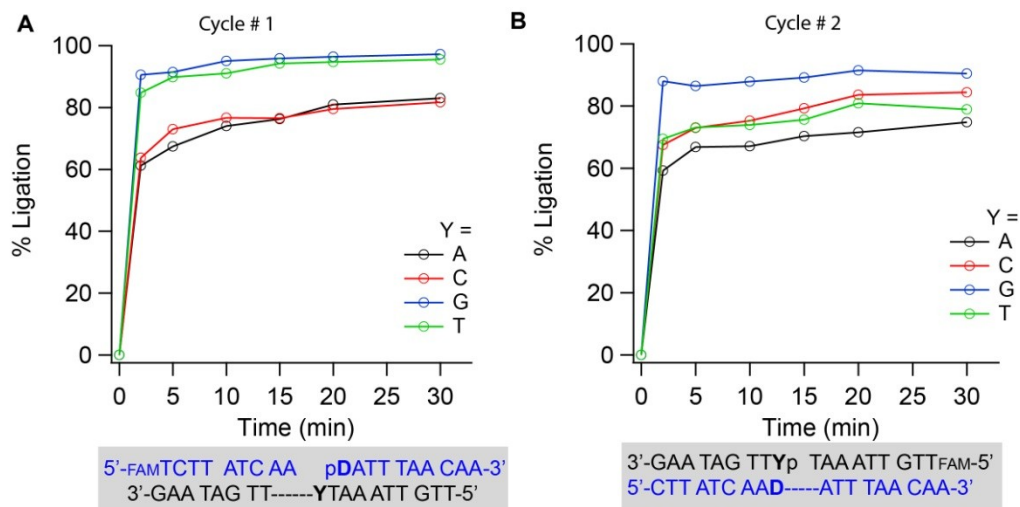


**Figure 5.13:** The kinetics of the single cycle ligation for the two cycles present in cross-catalysis at 30 °C consisting of: A) the cycle with the native target DNA template (**DNA-I(Y)**) and destabilizing probes and B) the cycle with the destabilizing template **DNA-II<sub>D</sub>** and native DNA probes (**r-Ia(FAM)** and **r-Ib(Y)**). *Experimental conditions:* 1.4 μM template; 1.4 μM fluorescent probe; 2.8 μM each non-fluorescent probe; 400 CEUs T4 DNA ligase in Buffer 1 per 15 μL reaction. % *Ligation* is based on the percentage of fluorescent probe that is converted to the fluorescent labeled ligation product.

Although the single-cycle experiments did not shed much light, when we studied the thermal stability of the DNA product duplexes (**DNA-II<sub>Ab</sub>:DNA-I(Y)**), the rapid amplification of the **DNA-I(C)** system was easier to understand. Specifically, we found that the dissociation or melting temperature ( $T_m$ ) was 32.2 °C for the **DNA-II<sub>Ab</sub>:DNA-I(C)** product duplex, which was much lower than that observed for the product duplexes containing **DNA-I(G)**, **DNA(A)** or **DNA-I(T)** ( $T_m = 34.6$  °C, 35.9 °C, and 34.7 °C respectively) (Figure 5.14). The lower  $T_m$  of the **DNA-II<sub>Ab</sub>:DNA-I(C)** duplex suggested that dissociation of the product duplex

was faster for this system allowing for the faster rate of amplification. Additionally, the variation in  $T_m$  for the different product duplexes indicated that the optimum temperature for amplification would be different for each system. To verify this, we next studied the cross-catalytic amplification at different temperatures with **DNA-I(C)** (Figure 5.15). For this system, the optimum temperature was 30 °C, as was found for the **DNA-I(A)** system. So we conclude that even though the  $T_m$  and the rate of amplification are different, there is no special base requirement for the isothermal amplification to work.

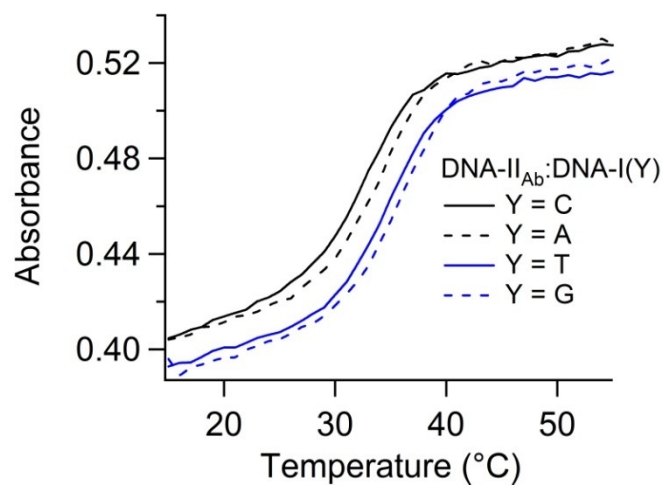


**Figure 5.14:** Thermal denaturation (melting) profiles of different DNA duplexes (**DNA-II<sub>Ab</sub>:DNA-I(Y)**).

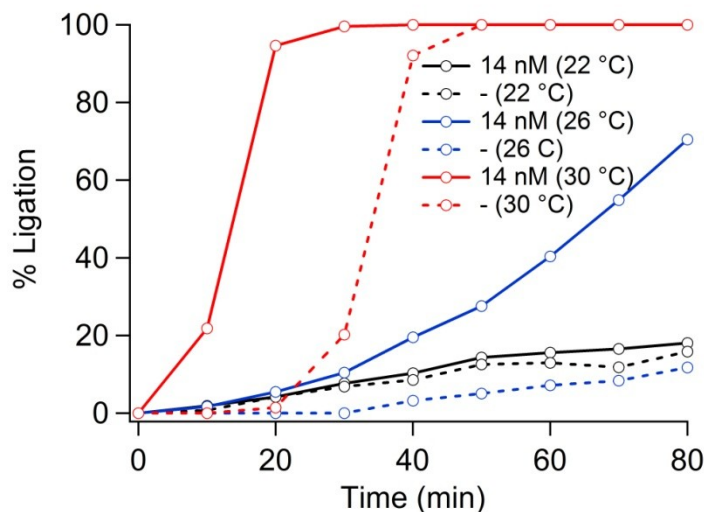


**Figure 5.15:** Cross-catalytic amplification of **DNA-I (C)** at different temperatures with T4 DNA ligase. *Experimental conditions:* 1.4  $\mu\text{M}$  **r-Ia(FAM)**; 2.8  $\mu\text{M}$  **r-Ib (C)**; 2.8  $\mu\text{M}$  **r-IIb**; 2.8  $\mu\text{M}$  **r-IIa<sub>AB</sub>**; 0 nM (-; dotted lines) or 14 nM (solid lines) target **DNA-I(C)**; 2000 CEUs T4 DNA ligase in Buffer 1 per 15  $\mu\text{L}$  reaction.

Finally, we were also interested to see how the cross-catalytic amplification was affected with different targets with the probes that match completely with only one of the targets. For this purpose, we studied cross-catalytic amplification with 14 nM of different target **DNA-I(Y)** with the probes matching with **DNA-I(A)** (Figure 5.16) The rate of amplification was similar with templates containing an A, T or G across from the abasic group; however the rate of amplification with the template containing a C across from abasic ( $Y = C$ ) was faster than the other templates even though there was only 1% (14 nM) of the target and the probes matched the  $Y = A$  target. But the rate of amplification with **DNA-I(C)** was much slower than that of the one shown in Figure 5.15 where

probes (**r-Ib (C)** and others) matched with target **DNA-I(C)**. The results indicated that the effect of different bases across from the abasic group would be minimized if we initiated amplification with lower concentrations of target. Therefore, we will be able to develop an amplification system without worrying about what is across from the abasic site. In that case, one of the limitations of our amplification system would be the inability to detect the presence of mismatch across from the abasic site.

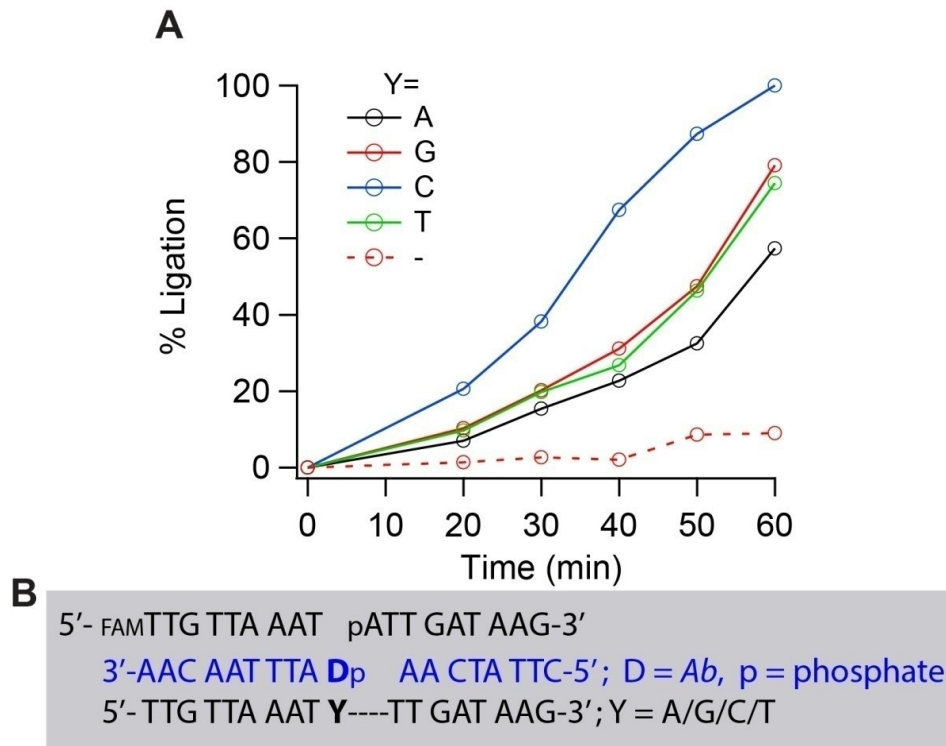


**Figure 5.16:** Cross-catalytic amplification with different templates with probe set matching with **DNA-I(Y = A)** at 30 °C with T4 DNA ligase. *Experimental conditions:* 1.4 μM **r-Ia(FAM)**, 2.8 μM **r-Ib(A)**, 2.8 μM **r-IIb**, 2.8 μM **r-IIa<sub>Ab</sub>** and 0 nM (-) or 14 nM of target **DNA-I(Y)** Y = A/T/C/G, T4 DNA ligase 2000 CEU/μL in Buffer 1 for 15 μL ligation volume. % Ligation is based on the percentage of fluorescent probe **r-Ia(FAM)** that is converted to the fluorescent labeled target sequence **F-DNA-I(A)**.

## 5.9 Conclusions

First of all, we found that all the DNA ligases explored (T3, T7 and *E. coli*) can tolerate an abasic site in the template and ligating probe strands for specific positions of the abasic group. In our attempt to reduce background with different DNA ligases, we found T7 DNA ligase and *E. coli* DNA ligase were suitable catalysts. For cross-catalytic amplification with *E. coli* DNA ligase we could achieve two orders of magnitude better sensitivity than that of T4 DNA ligase with similar probe concentrations. Amplification with T3 DNA ligase exhibited similar behavior to T4 DNA ligase. Since the T3 enzyme has a higher salt tolerance than T4 DNA ligase, this enzyme may be best where there is salt and other contaminants in the sample.<sup>3</sup> Even though it is reported that the rate of blunt end ligation is very slow with those enzymes, due to the exponential nature of our amplification system, the background-triggered amplification process showed appreciable yield, which kept our detection limits high.

For the blunt end systems, none of those designed gave us appreciable amplification with either T7 or *E. coli* DNA ligase. The main reason appeared to be the slower rate of ligation of the probes having the abasic group one or two bases inside from the ligation site. However, ligation of the same blunt-end system with T4 DNA ligase gave us two orders of magnitude better discrimination than that of the pseudo-blunt end systems (unpublished work done by Katie Mitran). Finally, our lesion-induced DNA amplification method operated well with different bases across from the abasic group, giving us the greatest



latitude when designing new ligation systems for new targets. Even though each base acted differently, we can conclude that there is no special base requirement for the probe design.

## 5.10 Experimental Section.

### 5.10.1 General Materials

Most of the DNA sequences used in this chapter were synthesized using the procedure described in Chapter 2. The **DNA-I (Y)** strands were purchased from IDT-DNA (without HPLC purification). High concentration DNA ligases (T3, T7 and *E.coli*) were received as a gift from Enzymatics (Beverly, MA). T4 DNA ligase was purchased from New England Biolabs.

### 5.10.2 DNA Sequences

Some of the DNA sequences used in this study are given in Table 5.1. Other DNA are mentioned in the appropriate section.

**Table 5.1:** DNA sequences used in this study

Sequence name	DNA sequence
<b>DNA-I(Y)</b> ( $Y = A/T/C/G$ )	5'-TTGTTA AAT YTT GATAAG-3'
<b>DNA-II<sub>D</sub></b> ( $D = Ab/T$ )	5'-CTT ATC AAD ATT TAA CAA-3'
<b>r-Ia</b>	
r-Ia(FAM)	5'- <sup>FAM</sup> TTGTTAAAT-3'
<b>r-Ib</b>	
r-Ib ( $Y = A/T/C/G$ )	5'- <sub>p</sub> YTTGATAAG-3'
<b>r-IIa<sub>D</sub></b>	
r-IIa <sub>D</sub> ( $D = Ab$ )	5'- <sub>p</sub> DATTTAACAA-3'
<b>r-IIb</b>	
r-IIb	5'-CTTATCAA-3'

### 5.10.3 Ligation buffers

The composition of different buffers (final concentration in the ligation mixtures) used are given below:

**Buffer 1:** 50 mM Tris-HCl, 10 mM MgCl<sub>2</sub>, 1 mM ATP, 10 mM DTT, pH 7.5 @ 25°C, from New England Biolabs.

**Buffer 2:** 50 mM Tris-HCl, 10 mM MgCl<sub>2</sub>, 1+3.2 mM ATP, 10 mM DTT, pH 7.5 @ 25°C, from New England Biolabs. Extra ATP added from 10 mM ATP solution from New England Biolabs.

**Buffer 3:** 50 mM Tris-HCl, 10 mM MgCl<sub>2</sub>, 1 mM ATP, 10 mM DTT, 18.1 mM spermidine pH 7.5 @ 25°C, from New England Biolabs. Spermidine added from 85.1 mM solution.

**Buffer 4:** 50 mM Tris-HCl, 10 mM MgCl<sub>2</sub>, 1+2.8 mM ATP, 10 mM DTT, 16.2 mM spermidine, pH 7.5 @ 25°C, from New England Biolabs. Spermidine added from 85.1 mM solution. Extra ATP added from 10 mM ATP solution from New England Biolabs.

**Buffer 5:** 66 mM Tris-HCl, 10 mM MgCl<sub>2</sub>, 1 mM ATP, 1 mM DTT, 7.5% Polyethylene glycol (PEG 6000) pH 7.6 @ 25°C, from New England Biolabs

**Buffer 6:** 58 mM Tris-HCl, 10 mM MgCl<sub>2</sub>, 1 mM ATP, 1 mM DTT, 3.8% Polyethylene glycol (PEG 6000) pH 7.6 @ 25°C. Prepared by mixing (1:1) buffer 1 and 5.

**Buffer 7:** 30 mM Tris-HCl, 4 mM MgCl<sub>2</sub>, 26 μM NAD, 1 mM DTT, 50 μg/ml BSA pH 8 @ 25°C from Enzymatics.

**Buffer 8:** 50 mM Tris-HCl, 10 mM MgCl<sub>2</sub>, 1 mM ATP, 10 mM DTT, pH 7.5 @ 25°C, from Enzymatics.

#### **5.10.4 Ligation experiments**

Unless otherwise described, both single cycle and cross-catalytic amplification were studied using the same protocol described in Chapter 3 (Section 3.4.6).

#### **5.10.5 Thermal denaturation experiments**

Melting experiments was done following the procedure described in Chapter 3 (Section 3.4.4).

#### **5.10.6 Unit definitions (Reproduced from respective company websites, [www.neb.com](http://www.neb.com) / [www.enzymatics.com/](http://www.enzymatics.com/))**

##### **NEB T4 DNA ligase:**

One unit is defined as the amount of enzyme required to give 50% ligation of HindIII fragments of  $\lambda$  DNA (5' DNA termini concentration of 0.12  $\mu$ M, 300- $\mu$ g/ml) in a total reaction volume of 20  $\mu$ l in 30 minutes at 16°C in 1X T4 DNA Ligase Reaction Buffer (Buffer 1).

##### **NEB T7 DNA ligase:**

One unit is defined as the amount of enzyme required to give 50% ligation of 100 ng HindIII fragments of  $\lambda$  DNA in a total reaction volume of 20  $\mu$ l in 30 minutes at 25°C in 1X T7 DNA Ligase Reaction Buffer (Buffer 5).

**Enzymatics T7 DNA ligase:**

1 unit is defined as the amount of *E.coli* DNA ligase required to ligate 50% of 100 ng DNA fragments with cohesive termini in 30 minutes at 25°C (in same buffer as Buffer 5).

**Enzymatics T3 DNA ligase:**

1 unit is defined as the amount of T3 DNA ligase required to ligate 50% of 100 ng DNA fragments with cohesive termini in 30 minutes at 23°C in 50 mM Tris-HCl, 300 mM NaCl, 0.5 mM ATP, 1 mM DTT, pH 8.0 @ 25°C.

**Enzymatics *E. coli* DNA ligase:**

1 unit is defined as the amount of T7 DNA ligase required to ligate 50% of 100 ng DNA fragments with cohesive termini in 30 minutes at 23°C in Buffer 7.

## 5.11 References

- 1) Lohman, G. J. S.; Tabor, S.; Nichols, N. M.: DNA Ligases. In *Curr Protoc Mol Biol*; John Wiley & Sons, Inc., **2011**.
- 2) Doherty, A. J.; Ashford, S. R.; Subramanya, H. S.; Wigley, D. B.: Bacteriophage T7 DNA Ligase: Overexpression, Purification, Crystallization, And Characterization. *J Biol Chem* **1996**, *271*, 11083-11089.
- 3) Cai, L.; Hu, C.; Shen, S.; Wang, W.; Huang, W.: Characterization of Bacteriophage T3 DNA Ligase. *J Biochem* **2004**, *135*, 397-403.
- 4) Subramanya, H. S.; Doherty, A. J.; Ashford, S. R.; Wigley, D. B.: Crystal Structure of an ATP-Dependent DNA Ligase from Bacteriophage T7. *Cell* **1996**, *85*, 607-615.
- 5) Lund, A. H.; Duch, M.; Skou Pedersen, F. Increased Cloning Efficiency by Temperature-Cycle Ligation. *Nucleic Acids Res* **1996**, *24*, 800-801.
- 6) Panasenko, S. M.; Alazard, R. J.; Lehman, I. R. A simple, three-step procedure for the large scale purification of DNA ligase from a hybrid lambda lysogen constructed in vitro. *J Biol Chem* **1978**, *253*, 4590-4592.
- 7) Okayama, H.; Berg, P. High-efficiency cloning of full-length cDNA. *Molec Cell Biol* **1982**, *2*, 161-170.
- 8) Hayashi, K. i.; Nakazawa, M.; Ishizaki, Y.; Hiraoka, N.; Obayashi, A. Stimulation of intermolecular ligation with E. coli DNA ligase by high concentration of monovalent cations in polyethylene glycol solutions. *Nucleic Acids Res* **1985**, *13*, 7979-7992.
- 9) Kausar, A.; Mitran, C. J.; Li, Y.; Gibbs-Davis, J. M. Rapid, Isothermal DNA Self-Replication Induced by a Destabilizing Lesion. *Angew Chem Int Ed* **2013**, *52*, 10577-10581.
- 10) Ferretti, L.; Sgaramella, V. Specific and reversible inhibition of the blunt end joining activity of the T4 DNA ligase. *Nucleic Acids Res* **1981**, *9*, 3695-3705.

## **Chapter 6**

### **General Conclusions and Future Plans**

## 6.1 General Conclusions

The goal of this thesis was to develop a simple, general and rapid isothermal DNA amplification and detection method. The main obstacle of achieving isothermal amplification is that the product duplex formed after ligation or polymerization is much more stable than the DNA duplex before ligation. For this reason, the most popular DNA amplification techniques (LCR/PCR) use thermocycling to dissociate the product duplex for the next round of amplification. In order to develop isothermal amplification such that we do not have to use thermocycling, we developed an amplification system such that the product duplex after ligation is selectively destabilized more than the stability of the DNA duplex before ligation.

At first, to achieve isothermal DNA amplification in a single ligation cycle, we designed different templates with destabilizing linkers in the middle of the DNA sequence. In Chapter 2, we demonstrated that the different destabilizing groups had a significant impact on the stability of the duplex, which helped us achieve isothermal amplification. The difference in stability was reflected in different melting temperatures,  $T_m$ . We showed that the  $T_m$  of the duplex decreased about 12-16 °C in the presence of different destabilizing linkers, while the  $T_m$  of the nicked duplexes decreased by about 5.2-6.1°C. As a result, the stability difference ( $T_m$  difference) between the product duplexes and nicked duplexes with destabilizing linkers became smaller compared with native DNA, which was a requirement for isothermal DNA amplification. The ligation of two complementary fragments in the presence of different templates (native or

destabilizing) showed that the ligation was almost unaffected by the presence of the destabilizing modifications (with few exceptions). The study of isothermal amplification with reduced template concentrations in a single cycle experiment revealed that isothermal amplification was possible with destabilizing templates. Among the different destabilizing groups, abasic (**Ab**) and a butyl (**Bu**) linker gave us the best turnover number (**TON**). In particular, the isothermal amplification with **Ab** template was very promising as this modification can be introduced using commercially available phosphoramidites with solid-phase DNA synthesis.

The kinetics of amplification with one cycle showed that the amplification was linear with time. In addition, the concentration of enzyme had a huge impact on the rate of amplification. Even with the high concentration of enzyme, however, with one cycle of amplification we always observed linear amplification. Therefore, in order to achieve exponential amplification we coupled one more cycle into our ligation system. We refer to these two coupled ligation cycles as cross-catalytic amplification. In Chapter 3, we have shown the rate of DNA amplification was greatly improved with cross-catalytic amplification and higher concentration of enzyme leading to the observation of rapid exponential amplification and self-replication of DNA in the presence of **Ab** as a destabilizing group. As a point of comparison, the cross-catalytic amplification with native DNA did not give any target selective amplification, and the rate of amplification was very slow. More importantly, the amplification system seemed to be general, since we were able to amplify different 18 base



pairs target DNA sequences without any specific sequence requirements. However, different DNA sequences had different optimum temperatures depending on the different G:C content in the target DNA. We have shown that tweaking the backbone of DNA with an abasic group can improve the self-replication and amplification of nucleic acid in a ligase chain reaction (LCR). In addition, the isothermal system worked well in the presence of genomic DNA (Salmon sperm) and was able to detect a specific DNA sequence in plasmid DNA, suggesting that our isothermal amplification method might be able to detect a specific target DNA sequence in genomic DNA.

Since the ligation reaction is very sensitive to the presence of mismatches in the target DNA, our LCR based isothermal amplification was applied in the detection of single nucleotide polymorphisms (SNPs). In Chapter 4, we have shown that our isothermal amplification method was amenable to the detection of mismatches in a particular position in the target DNA sequence. Using this method, we observed a high discrimination ratio between the match pair and different mismatch pairs. However, attempts to multiplex the assay did not lead to significant mismatch discrimination when both the matched and mismatched probes were present in the same reaction tube. However, separating the probe sets specific for particular nucleotides for detecting a specific mismatch worked very well. In order to develop a simple method of SNP detection, we then combined the isothermal amplification process with real-time detection using FRET and a microplate reader. The FRET based approach was very easy and time-efficient, as we could analyze multiple samples at a time without requiring separation of the

ligation product from the reaction mixture. The absence of background FRET from the direct excitation of the fluorescein when using fluorophore Cy5 as the acceptor made it a good choice for real-time ligation detection. In the future, the distance between the FRET pair needs to be optimized to balance between the rate of ligation and the FRET efficiency. To further simplify the detection, we developed a gold-nanoparticle based colorimetric approach by combining with isothermal amplification. In this approach, purple gold nanoparticle aggregate was disassembled by amplification product resulting in color change to red reflecting the amount of original target presented before amplification. Although the amplification and detection steps were separate, gold nanoparticle based colorimetric assay represented a very simple form of detection as it did not require any instrument other than a simple heater with temperature control.

The T4 DNA ligase enzyme used in our isothermal amplification system can perform nick sealing as well as ligate sticky ends and blunt ends, which resulted in the formation of a small amount of target sequence, which could then amplify to large amounts. This background-triggered amplification kept the detection limit higher than we would have liked for our system (140 fM or 14 pM with or without serial ligation). To reduce the background ligation, so that we could achieve a lower limit of detection, we studied our isothermal amplification process with *E. coli*, T3 and T7 DNA ligases. Among these three enzymes, T7 and *E. coli* DNA ligases yielded one and two orders of magnitude better sensitivity based on the lower limit of detection than that of T4 DNA ligase under the same experimental conditions (Chapter 5). It is important to note that all the

DNA ligases (T3, T7 and *E. coli*) we studied can tolerate **Ab** site in the template and probe at specific positions. However, our attempt to reduce the background with true blunt end system was not successful using these enzymes, partly because of the low tolerance of the **Ab** group when it was positioned one or two nucleotides away from the ligation site. All the ligation system we used to study isothermal amplification had the nucleotide deoxyadenine (**A**) across from abasic (**Ab**) group. Therefore, we studied the cross-catalytic amplification with same target having different nucleotides (**A/T/C/G**) across from the **Ab** (10th position from 5'). The amplification profiles were slightly different with different targets. Even though each base acts slightly differently, we concluded that there is no special base requirement for our amplification system and we are free to design the probes for an amplification system with different bases across from **Ab** site.

To summarize, we have develop a simple, rapid and general strategy for amplification of target specific DNA sequence by modifying it with a simple destabilizing group. This lesion-induced DNA amplification system appeared to be general and can work in the presence of genomic DNA. Since the technique is based on a ligase chain reaction, it is very sensitive to the presence of mismatch, which enabled us to detect the presence of SNPs in the target DNA. Finally, we were able to simplify the detection by combining this isothermal amplification method with simple read-outs like FRET-based and gold NP-based detection. Future work will focus on reducing background ligation, using a more efficient FRET probe design (possibly with different fluorophores or by changing the position of the fluorophore to get better FRET efficiency) and developing an

instrument-free detection strategy suitable for a point-of-care kit. We hope that finding or engineering a DNA ligase to eliminate the background ligation will take our amplification strategy one step closer to the development of a point-of-care device. It should be noted that, the lowest concentration of DNA that can be detected by LIDA using the serial ligation approach is 140 fM. However, the concentration of DNA in clinical samples is much lower. For example in case of hepatitis B (HBV) the clinically relevant concentration is 20,000 IU/ml (100,000 copies/ml) or 166 attomolar (aM,  $10^{-18}$  M) and for *Plasmodium falciparum* the lowest positive diagnosis corresponds to 2 parasites/ $\mu$ L (3.3 aM).<sup>1,2</sup> Therefore, to apply our amplification system for analyzing clinical samples we have to improve the limit of detection by at least  $\sim 3$  orders of magnitude.

## **6.2 Future Plans**

### **6.2.1 Reducing background ligation using dual LDR-PCR with destabilization**

Background ligation in the isothermal ligase chain reaction (LCR) based amplification system we have developed is one of the key limitations to achieve sensitive detection. It is well known that PCR and LCR are very sensitive methods for DNA amplification and detection. Since ligase is very sensitive to the presence of mismatches in the 3'-end of the ligating strand, ligase based amplification systems are better than polymerase based amplification for discrimination of mismatches. As described in Chapter 1, one of the drawbacks of the LCR process is that the probes that are complementary to the target sequences

are also complementary to each other. Therefore, DNA ligase can ligate them even if there is no target present in the solution resulting in a false positive signal. To overcome this problem, the ligase detection reaction (LDR) has been combined with PCR to generate a LDR-PCR approach.<sup>3</sup> In this approach, product of the target-induced ligation using LDR is amplified by PCR using outside primers which results in less background ligation due to the absence of double-stranded probes.<sup>4</sup>

To avoid the problem of background ligation in our isothermal amplification system I have designed an amplification system similar to LDR-PCR (Figure 6.1). In this process, where the first cycle of amplification will be catalyzed by a DNA ligase, one of two probes complementary to the target sequence contains a destabilizing group (**D**) between the terminal base and a phosphate group. Owing to the presence of the destabilizing group the product strand will be released isothermally producing a destabilizing template in situ. If we introduce another probe that is partially complementary to the destabilizing template, a DNA polymerase will be able to extend the primer. The probe to be extended by DNA polymerase is designed such that it is long enough to cross the destabilizing group in the template. From the data on single cycle amplification reported in this thesis we are confident that the ligase mediated first cycle of amplification will work. An experiment similar to the second cycle with DNA polymerase studied by Akemi Darlington in the Gibbs-Davis group showed that extension of a primer in the presence of an abasic group in the template is possible (unpublished work). The next challenge for this project will be combining two

cycles together as there may have different optimum temperatures for DNA ligase and DNA polymerase. The idea of using two enzymes will be great since we will get very specific amplification in both cycles and there will be no background ligation. Since the cyclic amplification is initiated by a DNA ligase we can expect to have good discrimination for mismatches in the target DNA.

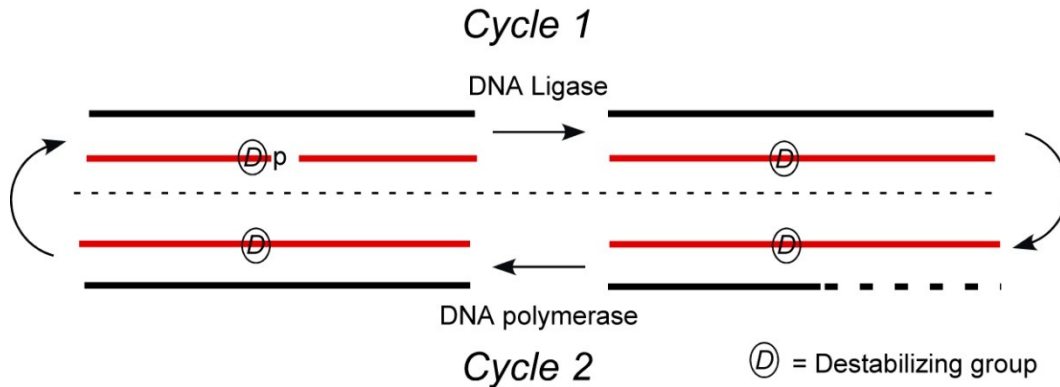


**Figure 6.1:** Schematic representation of isothermal LDR-PCR amplification.

### 6.2.2 Isothermal amplification of longer targets using LIDA

Another challenge with our amplification by destabilization approach is the difficulty in amplifying longer DNA targets or target sequences with higher G:C content. One way of addressing the problem is to introduce multiple abasic sites into the amplification system. My preliminary work indicates that it is possible to amplify longer target sequences by introducing multiple abasic groups. To amplify longer targets (27 nt instead of our typical 18 nt), we introduced three destabilizing groups in the two probes: one of the probes contained one destabilizing group in the middle of the sequence and another at the 5' phosphate terminus (Figure 6.2). The other probe contained only one destabilizing group

present in the middle of the duplex. Once ligated, the stability of the product duplex should be much lower despite its length, so that it can dissociate to allow amplification isothermally.

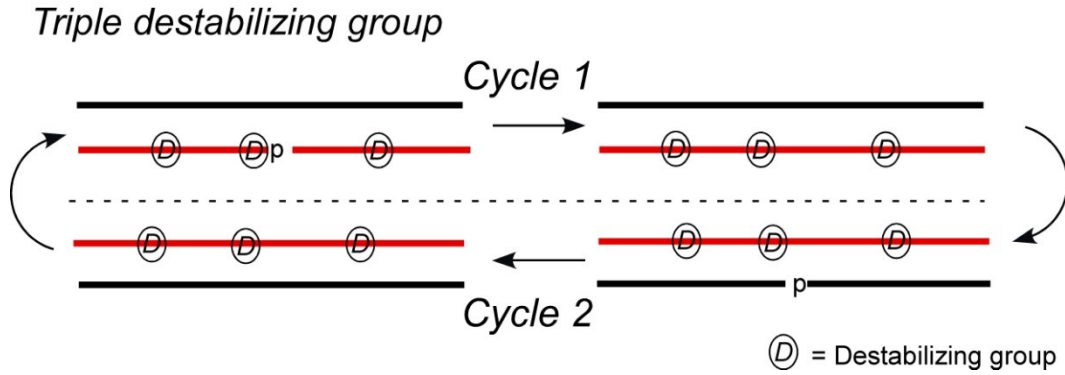


**Figure 6.2:** Schematic representation of isothermal lesion-induced amplification of a longer target.

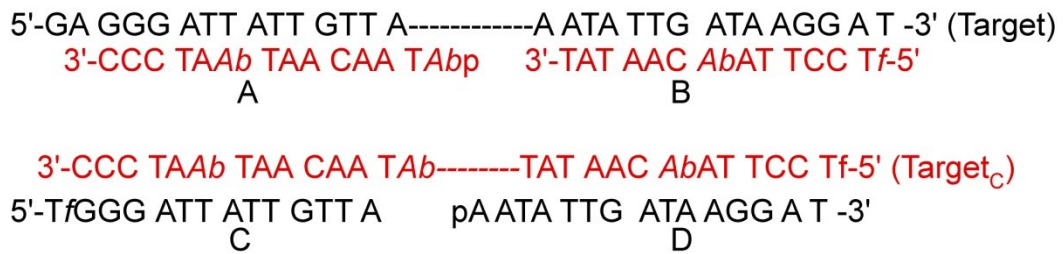


**Figure 6.3:** DNA sequences used in LIDA of a longer target.

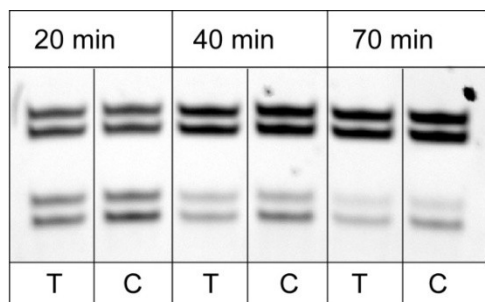


**Figure 6.4:** PAGE image of cross-catalytic amplification with 14 nM Target or 0 M, 2.8  $\mu$ M A, 1.4  $\mu$ M B, 1.4  $\mu$ M C and 2.8  $\mu$ M D DNA sequences used isothermal amplification of longer target, temperature 37  $^{\circ}$ C, T4 DNA ligase 2000unit/15 $\mu$ L. T = 14 nM Target, C= No target, two bands in the PAGE images are due to two labeled probes.

In a preliminary experiment with the DNA sequences shown in Figure 6.3, we have seen that with three destabilizing groups the melting temperature of the duplex decreased from 59.0  $^{\circ}$ C to 36.4  $^{\circ}$ C, which is a huge drop in the stability of the duplex. Initial cross-catalytic amplification of 14 nM of 27-nt target DNA with four probes at 37  $^{\circ}$ C showed that the rate of amplification was very rapid at that temperature (Figure 6.4). However, the rate of background ligation was also very high at this temperature. The temperature used for the isothermal amplification was above the melting temperature of the product duplex (experiment done before checking the melting temperature of the duplex), which is likely the reason for the high background ligation. According to the temperature variation experiments in Chapter 3 we found that the ideal temperature for amplification was always lower than the melting temperature of the product duplex. Therefore, there are different parameters that need to be studied to find an



optimum condition for amplification: the temperature and the position of the abasic group to find the right balance in stability for both probes. Furthermore, we can use the same idea of multiple abasic groups to amplify DNA sequences with higher G:C content.

### **6.3 Challenges:**

The goal strategy of the development of POCT is the simplification of the devices so that the end user can do the testing without the help of any expert. Blood glucose test and pregnancy tests are examples of the simplest form of a POCT device, where the patient can do their test by themselves. For example, in pregnancy tests, the patient just needs to add a certain volume of their urine sample in a specific part of the device and wait for the color to appear after a certain time to know if the test is positive or not. Therefore, it is a very easy one step process.

Due to high sensitivity and specificity, there have been a lot of focus to develop a simple nucleic acid based POCT device. These are some of the major challenges we need to overcome to develop a robust, reliable and widely applicable nucleic acid testing device.

#### **6.3.1 Sample Preparation.**

Generally, nucleic acid based testing consists of three components, sample preparation, nucleic acid amplification and detection. Depending on the disease, there can be different kinds of samples; it can be blood, urine, sputum, or saliva. It

would be ideal if a user can directly use these samples for analysis. However with the available technology it is important to have some form of sample preparation and it is considered a bottleneck in developing POCT devices. Sometimes, enzymes used for amplification might stop working in the presence of other impurities in the sample. Therefore, even if we have a very good amplification system sample preparation will be one of the major challenges for simplifying the POCT device.

Using our amplification system, most of the data shown used pure synthesized DNA, when we used the same samples contaminated with genomic DNA, we found that the rate of amplification slowed down. This may be due to the amount of available enzyme used for ligation was lower as the enzyme can sit on double stranded DNA, which reduces the overall concentration of unbound enzyme in solution. If we want to analyze crude samples without purifying or with minimal purification, we have to improve the sensitivity of the amplification as a slower target-initiated reaction makes it difficult to distinguish from the background reaction. Therefore, reduction or elimination of the background ligation is very important to improve the sensitivity of the assay.

### **6.3.2 Ease of Use**

In order for the POCT device to be widely accepted the operation of the device has to be easy enough to be operated by a non-expert. The device should be designed to have minimum steps to minimize the work. Therefore, procedural simplicity is another important parameter that needs to be considered in order to

develop a low cost, and reliable device. Our amplification method mostly relies on PAGE and FRET based assays, which are very tedious and need an expert to run and analyze. Therefore, developing a colorimetric assay or electrochemical assay will be the most effective way of simplifying the detection.

### **6.3.3 Stability of the Reagent**

One of the advantages of POCT devices is that they can be used anywhere where the patient needs to use it, therefore the device has to be robust and reliable enough to work in different weather conditions (humidity and temperature). Another important consideration for POCT devices is the stability of the reagents and the storage conditions. Since most of the DNA amplification systems require enzyme and other reagents, stability of the reagents in ambient condition is very important for development of a widely applicable POCT device. Our amplification method used T4 DNA ligase; this enzyme is not thermostable and is not stable at room temperature for long ( $< \sim 1$  day). Therefore, the assay developed using this enzyme would likely fail in the point-of-care setting. To avoid this limitation, finding or engineering an enzyme that is stable at room temperature for a significant amount of time is very important to develop a device applicable in remote areas.

## 6.4 References

- 1) Valsamakis, A. Molecular Testing in the Diagnosis and Management of Chronic Hepatitis B. *Clin Microbiol Rev* **2007**, *20*, 426-439.
- 2) Taylor, B.; Howell, A.; Martin, K.; Manage, D.; Gordy, W.; Campbell, S.; Lam, S.; Jin, A.; Polley, S.; Samuel, R.; Atrazhev, A.; Stickel, A.; Birungi, J.; Mbonye, A.; Pilarski, L.; Acker, J.; Yanow, S. A lab-on-chip for malaria diagnosis and surveillance. *Malaria J* **2014**, *13*, 179.
- 3) Pingle, M.; Rundell, M.; Das, S.; Golightly, L.; Barany, F.: PCR/LDR/Universal Array Platforms for the Diagnosis of Infectious Disease. In *Microarray Methods for Drug Discovery*; Chittur, S., Ed.; Methods in Molecular Biology; Humana Press, 2010; Vol. 632; pp 141-157.
- 4) McNamara, D. T.; Thomson, J. M.; Kasehagen, L. J.; Zimmerman, P. A. Development of a Multiplex PCR-Ligase Detection Reaction Assay for Diagnosis of Infection by the Four Parasite Species Causing Malaria in Humans. *J Clin Microbiol* **2004**, *42*, 2403-2410

## Bibliography

1. Abe, A.; Inoue, K.; Tanaka, T.; Kato, J.; Kajiyama, N.; Kawaguchi, R.; Tanaka, S.; Yoshida, M.; Kohara, M.: Quantitation of hepatitis B virus genomic DNA by real-time detection PCR. *J Clin Microbiol* **1999**, *37*, 2899-903.
2. Abe, H.; Kool, E. T. Destabilizing Universal Linkers for Signal Amplification in Self-Ligating Probes for RNA. *J Am Chem Soc* **2004**, *126*, 13980-13986.
3. Abe, H.; Kool, E. T. Flow cytometric detection of specific RNAs in native human cells with quenched autoligating FRET probes. *Proc Natl Acad Sci* **2006**, *103*, 263-268.
4. Albagli, D.; Atta, R. V.; Cheng, P.; Huan, B.; Wood, M. L.: Chemical Amplification (CHAMP) by a Continuous Self-Replicating Oligonucleotide-Based System. *J. Am. Chem. Soc.* **1999**, *121*, 6954-6955.
5. Aldaye, F. A.; Palmer, A. L.; Sleiman, H. F.: Assembling Materials with DNA as the Guide. *Science* **2008**, *321*, 1795-1799.
6. Alexander, R. C.; Johnson, A. K.; Thorpe, J. A.; Gevedon, T.; Testa, S. M.: Canonical nucleosides can be utilized by T4 DNA ligase as universal template bases at ligation junctions. *Nucleic Acids Res.* **2003**, *31*, 3208-3216.
7. Alivisatos, A. P.; Johnsson, K. P.; Peng, X.; Wilson, T. E.; Loweth, C. J.; Bruchez, M. P.; Schultz, P. G. Organization of 'nanocrystal molecules' using DNA. *Nature* **1996**, *382*, 609-611.
8. Alves, A. M.; Carr, F. J.: Dot blot detection of point mutations with adjacently hybridising synthetic oligonucleotide probes. *Nucleic Acids Res* **1988**, *16*, 8723.
9. An, L.; Tang, W.; Ranalli, T. A.; Kim, H. J.; Wytiaz, J.; Kong, H.: Characterization of a thermostable UvrD helicase and its participation in helicase-dependent amplification. *J Biol Chem* **2005**, *280*, 28952-8.

10. Andras, S. C.; Power, J. B.; Cocking, E.; Davey, M.: Strategies for signal amplification in nucleic acid detection. *Mol Biotechnol* **2001**, *19*, 29-44.
11. Banala, S.; Arts, R.; Aper, S. J. A.; Merkx, M.: No washing, less waiting: engineering biomolecular reporters for single-step antibody detection in solution. *Org Biomol Chem* **2013**, *11*, 7642-7649.
12. Barany, F.: Genetic disease detection and DNA amplification using cloned thermostable ligase. *Proc Natl Acad Sci* **1991**, *88*, 189-93.
13. Bardea, A.; Burshtein, N.; Rudich, Y.; Salame, T.; Ziv, C.; Yarden, O.; Naaman, R. Sensitive detection and identification of DNA and RNA using a patterned capillary tube. *Anal Chem* **2011**, *83*, 9418-9423.
14. Barken, K. B.; Haagensen, J. A.; Tolker-Nielsen, T.: Advances in nucleic acid-based diagnostics of bacterial infections. *Clin Chim Acta* **2007**, *384*, 1-11.
15. Bartlett, J. S.; Stirling, D.: A Short History of the Polymerase Chain Reaction. In *PCR Protocols*; Bartlett, J. S., Stirling, D., Eds.; Humana Press, **2003**; Vol. 226; pp 3-6.
16. Battle, T. J.; Golden, M. R.; Suchland, K. L.; Counts, J. M.; Hughes, J. P.; Stamm, W. E.; Holmes, K. K.: Evaluation of laboratory testing methods for Chlamydia trachomatis infection in the era of nucleic acid amplification. *J Clin Microbiol* **2001**, *39*, 2924-7.
17. Benner, S. A.; Chen, F.; Yang, Z.: Synthetic Biology, Tinkering Biology, and Artificial Biology: A Perspective from Chemistry. In *Chemical Synthetic Biology*; John Wiley & Sons, Ltd, **2011**; pp 69-106.
18. Besmer, P.; Miller, R. C., Jr.; Caruthers, M. H.; Kumar, A.; Minamoto, K.; Van de Sande, J. H.; Sidarova, N.; Khorana, H. G.: Studies on polynucleotides. CXVII. Hybridization of polydeoxynucleotides with tyrosine transfer RNA sequences to the r-strand of phi80psu + 3 DNA. *J Mol Biol* **1972**, *72*, 503-22.
19. Bi, S.; Li, L.; Zhang, S.: Triggered polycatenated DNA scaffolds for DNA sensors and aptasensors by a combination of rolling circle amplification and DNAzyme amplification. *Anal Chem* **2010**, *82*, 9447-54.

20. Blanco, L.; Salas, M.: Characterization and purification of a phage phi 29-encoded DNA polymerase required for the initiation of replication. *Proc Natl Acad Sci* **1984**, *81*, 5325-9.
21. Borer, P. N.; Dengler, B.; Tinoco, I., Jr.; Uhlenbeck, O. C.: *J. Mol. Biol.* **1974**, *86*, 843-853.
22. Bowman, B. H.; White, T. J.; Taylor, J. W.: Human pathogenic fungi and their close nonpathogenic relatives. *Mol Phylogenet Evol* **1996**, *6*, 89-96.
23. Brown, T.; Brown, D. J. S.: *Oligonucleotides and Analogues*; Oxford University Press: New York, **1991**.
24. Cai, L.; Hu, C.; Shen, S.; Wang, W.; Huang, W.: Characterization of Bacteriophage T3 DNA Ligase. *J Biochem* **2004**, *135*, 397-403.
25. Cao, W.: Recent developments in ligase-mediated amplification and detection. *Trends Biotechnol* **2004**, *22*, 38-44.
26. Chen, C.-S.; Durst, R. A.: Simultaneous detection of Escherichia coli O157:H7, Salmonella spp. and Listeria monocytogenes with an array-based immunosorbent assay using universal protein G-liposomal nanovesicles. *Talanta* **2006**, *69*, 232-238.
27. Chen, X.; Livak, K. J.; Kwok, P.-Y. A Homogeneous, Ligase-Mediated DNA Diagnostic Test. *Genome Res* **1998**, *8*, 549-556.
28. Chen, X.; Sullivan, P. F. Single nucleotide polymorphism genotyping: biochemistry, protocol, cost and throughput. *Pharmacogenomics J* **2003**, *3*, 77-96.
29. Cheng, Y.; Du, Q.; Wang, L.; Jia, H.; Li, Z. Fluorescently Cationic Conjugated Polymer as an Indicator of Ligase Chain Reaction for Sensitive and Homogeneous Detection of Single Nucleotide Polymorphism. *Anal Chem* **2012**, *84*, 3739-3744.
30. Cheng, Y.; Li, Z.; Zhang, X.; Du, B.; Fan, Y. Homogeneous and label-free fluorescence detection of single-nucleotide polymorphism using target-primed branched rolling circle amplification. *Anal Biochem* **2008**, *378*, 123-126.

31. Cheng, Y.; Zhao, J.; Jia, H.; Yuan, Z.; Li, Z. Ligase chain reaction coupled with rolling circle amplification for high sensitivity detection of single nucleotide polymorphisms. *Analyst* **2013**, *138*, 2958-2963.
32. Chernesky, M. A.; Marshall, R. L.; Petrich, A. K.: Infectious Disease Testing by LCR. In *Encyclopedia of Molecular Cell Biology and Molecular Medicine*; Wiley-VCH Verlag GmbH & Co. KGaA, **2006**.
33. Chien, A.; Edgar, D. B.; Trela, J. M.: Deoxyribonucleic acid polymerase from the extreme thermophile *Thermus aquaticus*. *J Bacteriol* **1976**, *127*, 1550-7.
34. Chin, C. D.; Linder, V.; Sia, S. K.: Commercialization of microfluidic point-of-care diagnostic devices. *Lab Chip* **2012**, *12*, 2118-34.
35. Chou, Q.; Russell, M.; Birch, D. E.; Raymond, J.; Bloch, W.: Prevention of pre-PCR mis-priming and primer dimerization improves low-copy-number amplifications. *Nucleic Acids Res* **1992**, *20*, 1717-23.
36. Chow, W. H.; McCloskey, C.; Tong, Y.; Hu, L.; You, Q.; Kelly, C. P.; Kong, H.; Tang, Y. W.; Tang, W.: Application of isothermal helicase-dependent amplification with a disposable detection device in a simple sensitive stool test for toxigenic *Clostridium difficile*. *J Mol Diagn* **2008**, *10*, 452-8.
37. Claridge, S. A.; Mastroianni, A. J.; Au, Y. B.; Liang, H. W.; Micheel, C. M.; Frechet, J. M. J.; Alivisatos, A. P.: Enzymatic Ligation Creates Discrete Multinanoparticle Building Blocks for Self-Assembly. *J. Am. Chem. Soc.* **2008**, *130*, 9598-9605.
38. Clegg, R. M.: Chapter 1 Förster resonance energy transfer—FRET what is it, why do it, and how it's done. In *Laboratory Techniques in Biochemistry and Molecular Biology*; Gadella, T. W. J., Ed.; Elsevier, **2009**; Vol. Volume 33; pp 1-57.
39. Collinge, J.; Clarke, A. R.: A general model of prion strains and their pathogenicity. *Science* **2007**, *318*, 930-6.
40. Compton, J.: Nucleic acid sequence-based amplification. *Nature* **1991**, *350*, 91-2.



41. Connolly, A. R.; Trau, M.: Isothermal Detection of DNA by Beacon-Assisted Detection Amplification. *Angew Chem Int Ed* **2010**, *49*, 2720-2723.
42. Conze, T.; Shetye, A.; Tanaka, Y.; Gu, J.; Larsson, C.; Göransson, J.; Tavoosidana, G.; Söderberg, O.; Nilsson, M.; Landegren, U. Analysis of Genes, Transcripts, and Proteins via DNA Ligation. *Ann Rev Anal Chem* **2009**, *2*, 215-239.
43. Cottingham, K.: Product Review: Multiple choices for SNPs. *Anal Chem* **2004**, *76*, 179 A - 181 A.
44. Craw, P.; Balachandran, W. Isothermal nucleic acid amplification technologies for point-of-care diagnostics: a critical review. *Lab Chip* **2012**, *12*, 2469-2486.
45. Crowther, J. R.: ELISA. Theory and practice. *Methods Mol Biol* **1995**, *42*, 1-218.
46. D'Aquila, R. T.; Bechtel, L. J.; Videler, J. A.; Eron, J. J.; Gorczyca, P.; Kaplan, J. C.: Maximizing sensitivity and specificity of PCR by pre-amplification heating. *Nucleic Acids Res* **1991**, *19*, 3749.
47. Das, J.; Cederquist, K. B.; Zaragoza, A. A.; Lee, P. E.; Sargent, E. H.; Kelley, S. O.: An ultrasensitive universal detector based on neutralizer displacement. *Nat Chem* **2012**, *4*, 642-648.
48. de Boer, E.; Beumer, R. R.: Methodology for detection and typing of foodborne microorganisms. *Int J Food Microbiol* **1999**, *50*, 119-130.
49. Diehl, F.; Li, M.; Dressman, D.; He, Y.; Shen, D.; Szabo, S.; Diaz, L. A.; Goodman, S. N.; David, K. A.; Juhl, H.; Kinzler, K. W.; Vogelstein, B.: Detection and quantification of mutations in the plasma of patients with colorectal tumors. *Proc Natl Acad Sci* **2005**, *102*, 16368-16373.
50. Diehl, F.; Li, M.; He, Y.; Kinzler, K. W.; Vogelstein, B.; Dressman, D.: BEAMing: single-molecule PCR on microparticles in water-in-oil emulsions. *Nat Methods* **2006**, *3*, 551-9.
51. Ding, Y.; Ai, H. W.; Hoi, H.; Campbell, R. E.: Forster resonance energy transfer-based biosensors for multiparameter ratiometric imaging of Ca<sup>2+</sup>

- dynamics and caspase-3 activity in single cells. *Anal Chem* **2011**, *83*, 9687-93.
52. Doherty, A. J.; Ashford, S. R.; Subramanya, H. S.; Wigley, D. B.: Bacteriophage T7 DNA Ligase: Overexpression, Purification, Crystallization, And Characterization. *J Biol Chem* **1996**, *271*, 11083-11089.
53. Don, R. H.; Cox, P. T.; Wainwright, B. J.; Baker, K.; Mattick, J. S.: 'Touchdown' PCR to circumvent spurious priming during gene amplification. *Nucleic Acids Res* **1991**, *19*, 4008.
54. Dose, C.; Ficht, S.; Seitz, O. Reducing Product Inhibition in DNA-Template-Controlled Ligation Reactions. *Angew Chem Int Ed* **2006**, *45*, 5369-5373.
55. Dressman, D.; Yan, H.; Traverso, G.; Kinzler, K. W.; Vogelstein, B.: Transforming single DNA molecules into fluorescent magnetic particles for detection and enumeration of genetic variations. *Proc Natl Acad Sci* **2003**, *100*, 8817-22.
56. Espy, M. J.; Uhl, J. R.; Sloan, L. M.; Buckwalter, S. P.; Jones, M. F.; Vetter, E. A.; Yao, J. D.; Wengenack, N. L.; Rosenblatt, J. E.; Cockerill, F. R., 3rd; Smith, T. F.: Real-time PCR in clinical microbiology: applications for routine laboratory testing. *Clin Microbiol Rev* **2006**, *19*, 165-256.
57. Fakruddin, M.; Mannan, K. S.; Andrews, S.: Viable but Nonculturable Bacteria: Food Safety and Public Health Perspective. *ISRN Microbiol* **2013**, *2013*, 703813.
58. Ferretti, L.; Sgaramella, V. Specific and reversible inhibition of the blunt end joining activity of the T4 DNA ligase. *Nucleic Acids Res* **1981**, *9*, 3695-3705.
59. Ficht, S.; Dose, C.; Seitz, O.: As Fast and Selective as Enzymatic Ligations: Unpaired Nucleobases Increase the Selectivity of DNA-Controlled Native Chemical PNA Ligation. *ChemBioChem* **2005**, *6*, 2098-2103.

60. Fire, A.; Xu, S. Q.: Rolling replication of short DNA circles. *Proc Natl Acad Sci* **1995**, *92*, 4641-5.
61. Fontanel, M. L.; Bazin, H.; Teoule, R.: Sterical recognition by T4 polynucleotide kinase of non-nucleosidic moieties 5'-attached to oligonucleotides. *Nucleic Acids Res* **1994**, *22*, 2022-7.
62. Fredriksson, S.; Gullberg, M.; Jarvius, J.; Olsson, C.; Pietras, K.; Gustafsdottir, S. M.; Ostman, A.; Landegren, U.: Protein detection using proximity-dependent DNA ligation assays. *Nat Biotechnol* **2002**, *20*, 473-7.
63. Fu, E.; Yager, P.; Floriano, P. N.; Christodoulides, N.; McDevitt, J. T.: Perspective on diagnostics for global health. *IEEE Pulse* **2011**, *2*, 40-50.
64. Fu, S.; Qu, G.; Guo, S.; Ma, L.; Zhang, N.; Zhang, S.; Gao, S.; Shen, Z.: Applications of loop-mediated isothermal DNA amplification. *Appl Biochem Biotechnol* **2011**, *163*, 845-50.
65. Gibbs-Davis, J. M.; Schatz, G. C.; Nguyen, S. T.: Sharp Melting Transitions in DNA Hybrids without Aggregate Dissolution: Proof of Neighboring-Duplex Cooperativity. *J. Am. Chem. Soc.* **2007**, *129*, 15535-15540.
66. Gill, P.; Ghaemi, A.: Nucleic Acid Isothermal Amplification Technologies—A Review. *Nucleosides, Nucleotides and Nucleic Acids* **2008**, *27*, 224-243.
67. Goffin, C.; Verly, W. G.: T4 DNA ligase can seal a nick in double-stranded DNA limited by a 5'-phosphorylated base-free deoxyribose residue. *Nucleic Acids Res.* **1983**, *11*, 8103-8109.
68. Grabar, K. C.; Freeman, R. G.; Hommer, M. B.; Natan, M. J. Preparation and Characterization of Au Colloid Monolayers. *Anal Chem* **1995**, *67*, 735-743.
69. Granzhan, A.; Kotera, N.; Teulade-Fichou, M.-P. Finding needles in a basestack: recognition of mismatched base pairs in DNA by small molecules. *Chem Soc Rev* **2014**, *43*, 3630-3665.

70. Griffiths AJF, M. J., Suzuki DT, et al.: How DNA changes affect phenotype. In *An Introduction to Genetic Analysis. 7th edition.*; W. H. Freeman: New York, **2000**; Vol. How DNA changes affect phenotype.
71. Grossmann, T. N.; Strohbach, A.; Seitz, O.: Achieving Turnover in DNA-Templated Reactions. *ChemBioChem* **2008**, *9*, 2185-2192.
72. Gu, H.; Chao, J.; Xiao, S.-J.; Seeman, N. C.: A proximity-based programmable DNA nanoscale assembly line. *Nature* **2010**, *465*, 202-205.
73. Gustafsdottir, S. M.; Nordengrahn, A.; Fredriksson, S.; Wallgren, P.; Rivera, E.; Schallmeiner, E.; Merza, M.; Landegren, U.: Detection of individual microbial pathogens by proximity ligation. *Clin Chem* **2006**, *52*, 1152-60.
74. Haqqi, T. M.; Sarkar, G.; David, C. S.; Sommer, S. S.: Specific amplification with PCR of a refractory segment of genomic DNA. *Nucleic Acids Res* **1988**, *16*, 11844.
75. Hartman, M. R.; Ruiz, R. C. H.; Hamada, S.; Xu, C.; Yancey, K. G.; Yu, Y.; Han, W.; Luo, D.: Point-of-care nucleic acid detection using nanotechnology. *Nanoscale* **2013**, *5*, 10141-10154.
76. Hayashi, K. i.; Nakazawa, M.; Ishizaki, Y.; Hiraoka, N.; Obayashi, A. Stimulation of intermolecular ligation with E. coli DNA ligase by high concentration of monovalent cations in polyethylene glycol solutions. *Nucleic Acids Res* **1985**, *13*, 7979-7992.
77. Hazarika, P.; Ceyhan, B.; Niemeyer, C. M. Reversible Switching of DNA–Gold Nanoparticle Aggregation. *Angew Chem Int Ed* **2004**, *43*, 6469-6471.
78. Horzinek, M. C.: The birth of virology. *Antonie Van Leeuwenhoek* **1997**, *71*, 15-20.
79. Huang, R.-P.; Lin, Y.; Chen, L.-P.; Yang, W.; Huang, R.: ELISA-based protein arrays: Multiplexed sandwich immunoassays. *Curr. Proteomics* **2004**, *1*, 199-210.
80. Innis, M. A.; Myambo, K. B.; Gelfand, D. H.; Brow, M. A.: DNA sequencing with *Thermus aquaticus* DNA polymerase and direct

- sequencing of polymerase chain reaction-amplified DNA. *Proc Natl Acad Sci* **1988**, *85*, 9436-40.
81. Iqbal, S. S.; Mayo, M. W.; Bruno, J. G.; Bronk, B. V.; Batt, C. A.; Chambers, J. P.: A review of molecular recognition technologies for detection of biological threat agents. *Biosens Bioelectron* **2000**, *15*, 549-78.
  82. Irizarry, K.; Kustanovich, V.; Li, C.; Brown, N.; Nelson, S.; Wong, W.; Lee, C. J.: Genome-wide analysis of single-nucleotide polymorphisms in human expressed sequences. *Nat Genet* **2000**, *26*, 233-6.
  83. Jarvius, J.; Nilsson, M.; Landegren, U.: Oligonucleotide ligation assay. *Methods Mol Biol* **2003**, *212*, 215-28.
  84. Jonstrup, S. P.; Koch, J.; Kjems, J.: A microRNA detection system based on padlock probes and rolling circle amplification. *Rna* **2006**, *12*, 1747-52.
  85. Joyce, G. F. RNA evolution and the origins of life. *Nature* **1989**, *338*, 217-224.
  86. Joyce, G. F.: Bit by Bit: The Darwinian Basis of Life. *PLoS Biol* **2012**, *10*, e1001323.
  87. Kaboev, O. K.; Luchkina, L. A.; Tret'iakov, A. N.; Bahrmand, A. R.: PCR hot start using primers with the structure of molecular beacons (hairpin-like structure). *Nucleic Acids Res* **2000**, *28*, E94.
  88. Kapanidis, A. N.; Weiss, S. Fluorescent probes and bioconjugation chemistries for single-molecule fluorescence analysis of biomolecules. *J Chem Phys* **2002**, *117*, 10953-10964.
  89. Kausar, A.; McKay, R. D.; Lam, J.; Bhogal, R. S.; Tang, A. Y.; Gibbs-Davis, J. M.: Tuning DNA Stability To Achieve Turnover in Template for an Enzymatic Ligation Reaction. *Angew Chem Int Ed* **2011**, *50*, 8922-8926.
  90. Kausar, A.; Mitran, C. J.; Li, Y.; Gibbs-Davis, J. M. Rapid, Isothermal DNA Self-Replication Induced by a Destabilizing Lesion. *Angew Chem Int Ed* **2013**, *52*, 10577-10581.

91. Kebelmann-Betzing, C.; Seeger, K.; Dragon, S.; Schmitt, G.; Moricke, A.; Schild, T. A.; Henze, G.; Beyermann, B.: Advantages of a new Taq DNA polymerase in multiplex PCR and time-release PCR. *Biotechniques* **1998**, *24*, 154-8.
92. Kim, S.; Misra, A.: SNP genotyping: technologies and biomedical applications. *Annu Rev Biomed Eng* **2007**, *9*, 289-320.
93. Klamp, T.; Camps, M.; Nieto, B.; Guasch, F.; Ranasinghe, R. T.; Wiedemann, J.; Petrášek, Z.; Schwille, P.; Klenerman, D.; Sauer, M.: Highly Rapid Amplification-Free and Quantitative DNA Imaging Assay. *Sci Rep* **2013**, *3*.
94. Kleppe, K.; Ohtsuka, E.; Kleppe, R.; Molineux, I.; Khorana, H. G.: Studies on polynucleotides. XCVI. Repair replications of short synthetic DNA's as catalyzed by DNA polymerases. *J Mol Biol* **1971**, *56*, 341-61.
95. Kochetkov, N. K.; Budovskii, E. I.: Hydrolysis of N-glycosidic Bonds in Nucleosides, Nucleotides, and their Derivatives. In *Organic Chemistry of Nucleic Acids*; Kochetkov, N. K., Budovskii, E. I., Eds.; Springer US, **1972**; pp 425-448.
96. Kong, D.; Shen, H.; Huang, Y.; Mi, H.: PCR hot-start using duplex primers. *Biotechnol Lett* **2004**, *26*, 277-80.
97. Kubista, M.; Andrade, J. M.; Bengtsson, M.; Forootan, A.; Jonak, J.; Lind, K.; Sindelka, R.; Sjoback, R.; Sjogreen, B.; Strombom, L.; Stahlberg, A.; Zoric, N.: The real-time polymerase chain reaction. *Mol Aspects Med* **2006**, *27*, 95-125.
98. Kumagai, I.; Tsumoto, K.: Antigen–Antibody Binding. In *eLS*; John Wiley & Sons, Ltd, **2001**.
99. Küpfer, P. A.; Leumann, C. J.: The chemical stability of abasic RNA compared to abasic DNA. *Nucleic Acids Res* **2007**, *35*, 58-68.
100. LaFramboise, T. Single nucleotide polymorphism arrays: a decade of biological, computational and technological advances. *Nucleic Acids Res* **2009**, *37*, 4181-4193.

101. Landegren, U.: Ligation-based DNA diagnostics. *Bioessays* **1993**, *15*, 761-5.
102. Landegren, U.; Kaiser, R.; Caskey, C. T.; Hood, L.: DNA diagnostics--molecular techniques and automation. *Science* **1988**, *242*, 229-37.
103. Landegren, U.; Kaiser, R.; Sanders, J.; Hood, L. A Ligase-Mediated Gene Detection Technique. *Science* **1988**, *241*, 1077-1080.
104. Lawyer, F. C.; Stoffel, S.; Saiki, R. K.; Myambo, K.; Drummond, R.; Gelfand, D. H.: Isolation, characterization, and expression in *Escherichia coli* of the DNA polymerase gene from *Thermus aquaticus*. *J Biol Chem* **1989**, *264*, 6427-37.
105. Lee, D. H.; Granja, J. R.; Martinez, J. A.; Severin, K.; Ghadiri, M. R.: A self-replicating peptide. *Nature* **1996**, *382*, 525-528.
106. Lee, H. H.; Chernesky, M. A.; Schachter, J.; Burczak, J. D.; Andrews, W. W.; Muldoon, S.; Leckie, G.; Stamm, W. E.: Diagnosis of *Chlamydia trachomatis* genitourinary infection in women by ligase chain reaction assay of urine. *Lancet* **1995**, *345*, 213-6.
107. Lesiak, K.; Khamnei, S.; Torrence, P. F.: 2',5'-Oligoadenylate:antisense chimeras--synthesis and properties. *Bioconjug Chem* **1993**, *4*, 467-72.
108. Levy, M.; Ellington, A. D.: Exponential growth by cross-catalytic cleavage of deoxyribozymogens. *Proc Natl Acad Sci* **2003**, *100*, 6416-6421.
109. Li, H.; Huang, J.; Lv, J.; An, H.; Zhang, X.; Zhang, Z.; Fan, C.; Hu, J.: Nanoparticle PCR: nanogold-assisted PCR with enhanced specificity. *Angew Chem Int Ed* **2005**, *44*, 5100-3.
110. Li, J.; Deng, T.; Chu, X.; Yang, R.; Jiang, J.; Shen, G.; Yu, R.: Rolling circle amplification combined with gold nanoparticle aggregates for highly sensitive identification of single-nucleotide polymorphisms. *Anal Chem* **2010**, *82*, 2811-6.
111. Li, X. Y.; Hernandez, A. F.; Grover, M. A.; Hud, N. V.; Lynn, D. G.: Step-Growth Control in Template-Directed Polymerization. *Heterocycles* **2011**, *82*, 1477.

112. Li, X.; Chmielewski, J.: Peptide Self-Replication Enhanced by a Proline Kink. *J Am Chem Soc* **2003**, *125*, 11820-11821.
113. Li, X.; Zhan, Z.-Y. J.; Knipe, R.; Lynn, D. G.: DNA-Catalyzed Polymerization†. *J Am Chem Soc* **2002**, *124*, 746-747.
114. Lincoln, T. A.; Joyce, G. F.: Self-Sustained Replication of an RNA Enzyme. *Science* **2009**, *323*, 1229-1232.
115. Liu, D.; Daubendiek, S. L.; Zillman, M. A.; Ryan, K.; Kool, E. T.: Rolling Circle DNA Synthesis: Small Circular Oligonucleotides as Efficient Templates for DNA Polymerases. *J Am Chem Soc* **1996**, *118*, 1587-1594.
116. Lo, Y. M.; Chan, K. C.: Introduction to the polymerase chain reaction. *Methods Mol Biol* **2006**, *336*, 1-10.
117. Loeb, L. A.; Preston, B. D.: Mutagenesis by Apurinic/Apyrimidinic Sites. *Ann Rev Genet* **1986**, *20*, 201-230.
118. Lohman, G. J.; Tabor, S.; Nichols, N. M.: DNA ligases. *Curr Protoc Mol Biol* **2011**, *Chapter 3*, Unit3 14.
119. Lund, A. H.; Duch, M.; Skou Pedersen, F. Increased Cloning Efficiency by Temperature-Cycle Ligation. *Nucleic Acids Res* **1996**, *24*, 800-801.
120. Lund, K.; Manzo, A. J.; Dabby, N.; Michelotti, N.; Johnson-Buck, A.; Nangreave, J.; Taylor, S.; Pei, R.; Stojanovic, M. N.; Walter, N. G.; Winfree, E.; Yan, H.: Molecular robots guided by prescriptive landscapes. *Nature* **2010**, *465*, 206-210.
121. Luo, J.; Bergstrom, D. E.; Barany, F. Improving the fidelity of *Thermus thermophilus* DNA ligase. *Nucleic Acids Res* **1996**, *24*, 3071-3078.
122. Luo, P.; Leitzel, J. C.; Zhan, Z.-Y. J.; Lynn, D. G.: Analysis of the Structure and Stability of a Backbone-Modified Oligonucleotide: Implications for Avoiding Product Inhibition in Catalytic Template-Directed Synthesis. *J Am Chem Soc* **1998**, *120*, 3019-3031.
123. Luther, A.; Brandsch, R.; von Kiedrowski, G. Surface-promoted replication and exponential amplification of DNA analogues. *Nature* **1998**, *396*, 245-248.



124. Mabey, D.; Peeling, R. W.; Ustianowski, A.; Perkins, M. D.: Diagnostics for the developing world. *Nat Rev Microbiol* **2004**, *2*, 231-40.
125. Mackay, I. M.; Arden, K. E.; Nitsche, A.: Real-time PCR in virology. *Nucleic Acids Res* **2002**, *30*, 1292-305.
126. Mammen, M.; Choi, S.-K.; Whitesides, G. M.: Polyvalent Interactions in Biological Systems: Implications for Design and Use of Multivalent Ligands and Inhibitors. *Angew Chem Int Ed* **1998**, *37*, 2754–2794.
127. Mano, J.; Oguchi, T.; Akiyama, H.; Teshima, R.; Hino, A.; Furui, S.; Kitta, K. Simultaneous detection of recombinant DNA segments introduced into genetically modified crops with multiplex ligase chain reaction coupled with multiplex polymerase chain reaction. *J Agric Food Chem* **2009**, *57*, 2640-2646.
128. Marshall, R. L.; Laffler, T. G.; Cerney, M. B.; Sustachek, J. C.; Kratochvil, J. D.; Morgan, R. L.: Detection of HCV RNA by the asymmetric gap ligase chain reaction. *PCR Methods Appl* **1994**, *4*, 80-4.
129. Matray, T. J.; Kool, E. T.: Selective and Stable DNA Base Pairing without Hydrogen Bonds. *J. Am. Chem. Soc.* **1998**, *120*, 6191-6192.
130. Mazars, G.-R.; Theillet, C.: Direct Sequencing by Thermal Asymmetric PCR#. In *T PCR Sequencing Protocols*, 1996; Vol. 65; pp 35-40.
131. McKerrow, J. H.; Caffrey, C.; Kelly, B.; Loke, P.; Sajid, M.: Proteases in parasitic diseases. *Annu Rev Pathol* **2006**, *1*, 497-536.
132. McNamara, D. T.; Thomson, J. M.; Kasehagen, L. J.; Zimmerman, P. A.: Development of a Multiplex PCR-Ligase Detection Reaction Assay for Diagnosis of Infection by the Four Parasite Species Causing Malaria in Humans. *J Clin Microbiol* **2004**, *42*, 2403-2410.
133. Mendel-Hartvig, M.; Kumar, A.; Landegren, U.: Ligase-mediated construction of branched DNA strands: a novel DNA joining activity catalyzed by T4 DNA ligase. *Nucleic Acids Res.* **2004**, *32*, e2.
134. Mhlanga, M. M.; Malmberg, L.: Using molecular beacons to detect single-nucleotide polymorphisms with real-time PCR. *Methods* **2001**, *25*, 463-71.

135. Milks, M. L.; Sokolova, Y. Y.; Isakova, I. A.; Fuxa, J. R.; Mitchell, F.; Snowden, K. F.; Vinson, S. B.: Comparative effectiveness of light-microscopic techniques and PCR in detecting *Thelohania solenopsae* (Microsporidia) infections in red imported fire ants (*Solenopsis invicta*). *J Eukaryot Microbiol* **2004**, *51*, 187-91.
136. Miller, M. B.; Tang, Y. W.: Basic concepts of microarrays and potential applications in clinical microbiology. *Clin Microbiol Rev* **2009**, *22*, 611-33.
137. Mirkin, C. A.; Letsinger, R. L.; Mucic, R. C.; Storhoff, J. J. A DNA-based method for rationally assembling nanoparticles into macroscopic materials. *Nature* **1996**, *382*, 607-609.
138. Mistry, K. K.; Layek, K.; Mahapatra, A.; Roy Chaudhuri, C.; Saha, H.: A review on amperometric-type immunosensors based on screen-printed electrodes. *Analyst* **2014**, *139*, 2289-2311.
139. Mitani, Y.; Lezhava, A.; Kawai, Y.; Kikuchi, T.; Oguchi-Katayama, A.; Kogo, Y.; Itoh, M.; Miyagi, T.; Takakura, H.; Hoshi, K.; Kato, C.; Arakawa, T.; Shibata, K.; Fukui, K.; Masui, R.; Kuramitsu, S.; Kiyotani, K.; Chalk, A.; Tsunekawa, K.; Murakami, M.; Kamataki, T.; Oka, T.; Shimada, H.; Cizdziel, P. E.; Hayashizaki, Y.: Rapid SNP diagnostics using asymmetric isothermal amplification and a new mismatch-suppression technology. *Nat Methods* **2007**, *4*, 257-62.
140. Morabito, K.; Wiske, C.; Tripathi, A.: Engineering Insights for Multiplexed Real-Time Nucleic Acid Sequence-Based Amplification (NASBA): Implications for Design of Point-of-Care Diagnostics. *Mol Diagn Ther* **2013**, *17*, 185-192.
141. Mori, Y.; Notomi, T. Loop-mediated isothermal amplification (LAMP): a rapid, accurate, and cost-effective diagnostic method for infectious diseases. *J Infect Chemother* **2009**, *15*, 62-69.
142. Morrison, T. B.; Weis, J. J.; Wittwer, C. T.: Quantification of low-copy transcripts by continuous SYBR Green I monitoring during amplification. *Biotechniques* **1998**, *24*, 954-8, 960, 962.

143. Nakano, M.; Komatsu, J.; Matsuura, S.; Takashima, K.; Katsura, S.; Mizuno, A.: Single-molecule PCR using water-in-oil emulsion. *J Biotechnol* **2003**, *102*, 117-24.
144. Nichols, D.: Cultivation gives context to the microbial ecologist. *FEMS Microbiol Ecol* **2007**, *60*, 351-7.
145. Nilsson, M.; Malmgren, H.; Samiotaki, M.; Kwiatkowski, M.; Chowdhary, B. P.; Landegren, U.: Padlock probes: circularizing oligonucleotides for localized DNA detection. *Science* **1994**, *265*, 2085-8.
146. Nindl, I.; Lorincz, A.; Mielzynska, I.; Petry, U.; Baur, S.; Kirchmayr, R.; Michels, W.; Schneider, A.: Human papilloma virus detection in cervical intraepithelial neoplasia by the second-generation hybrid capture microplate test, comparing two different cervical specimen collection methods. *Clin Diagn Virol* **1998**, *10*, 49-56.
147. Notomi, T.; Okayama, H.; Masubuchi, H.; Yonekawa, T.; Watanabe, K.; Amino, N.; Hase, T.: Loop-mediated isothermal amplification of DNA. *Nucleic Acids Res* **2000**, *28*, E63.
148. O'Connor, L.; Glynn, B.: Recent advances in the development of nucleic acid diagnostics. *Expert Review of Medical Devices* **2010**, *7*, 529-539.
149. Okayama, H.; Berg, P. High-efficiency cloning of full-length cDNA. *Molec Cell Biol* **1982**, *2*, 161-170.
150. Orgel, L. E.: Molecular replication. *Nature* **1992**, *358*, 203-209.
151. Panasenko, S. M.; Alazard, R. J.; Lehman, I. R. A simple, three-step procedure for the large scale purification of DNA ligase from a hybrid lambda lysogen constructed in vitro. *J Biol Chem* **1978**, *253*, 4590-4592.
152. Parida, M.; Sannarangaiah, S.; Dash, P. K.; Rao, P. V. L.; Morita, K.: Loop mediated isothermal amplification (LAMP): a new generation of innovative gene amplification technique; perspectives in clinical diagnosis of infectious diseases. *Rev Med Virol* **2008**, *18*, 407-421.
153. Patzke, V. v. K., G. Self replicating systems. *Arkivoc* **2007**, 293-310.
154. Paul, N.; Joyce, G. F.: Minimal self-replicating systems. *Curr Opin Chem Biol* **2004**, *8*, 634-639.

155. Pavlov, A. R.; Pavlova, N. V.; Kozyavkin, S. A.; Slesarev, A. I.: Recent developments in the optimization of thermostable DNA polymerases for efficient applications. *Trends Biotechnol* **2004**, *22*, 253-60.
156. Peeling, R. W.; Smith, P. G.; Bossuyt, P. M. M.: A guide for diagnostic evaluations. *Nat Rev Micro* **2010**, S2-S6.
157. Pickering, J.; Bamford, A.; Godbole, V.; Briggs, J.; Scozzafava, G.; Roe, P.; Wheeler, C.; Ghouze, F.; Cuss, S. Integration of DNA ligation and rolling circle amplification for the homogeneous, end-point detection of single nucleotide polymorphisms. *Nucleic Acids Res* **2002**, *30*, e60.
158. Pingle, M.; Rundell, M.; Das, S.; Golightly, L.; Barany, F.: PCR/LDR/Universal Array Platforms for the Diagnosis of Infectious Disease. In *Microarray Methods for Drug Discovery*; Chittur, S., Ed.; Humana Press, **2010**; Vol. 632; pp 141-157.
159. Pohl, G.; Shih Ie, M.: Principle and applications of digital PCR. *Expert Rev Mol Diagn* **2004**, *4*, 41-7.
160. Prchal, J. T.; Guan, Y. L.: A novel clonality assay based on transcriptional analysis of the active X chromosome. *Stem Cells* **1993**, *11 Suppl 1*, 62-5.
161. Psifidi, A.; Dovas, C.; Banos, G. Novel Quantitative Real-Time LCR for the Sensitive Detection of SNP Frequencies in Pooled DNA: Method Development, Evaluation and Application. *PLoS ONE* **2011**, *6*, e14560.
162. Qi, X.; Bakht, S.; Devos, K. M.; Gale, M. D.; Osbourn, A. L-RCA (ligation-rolling circle amplification): a general method for genotyping of single nucleotide polymorphisms (SNPs). *Nucleic Acids Res* **2001**, *29*, E116.
163. Ramirez, M. V.; Cowart, K. C.; Campbell, P. J.; Morlock, G. P.; Sikes, D.; Winchell, J. M.; Posey, J. E.: Rapid Detection of Multidrug-Resistant Mycobacterium tuberculosis by Use of Real-Time PCR and High-Resolution Melt Analysis. *J Clin Microbiol* **2010**, *48*, 4003-4009.
164. Reyes, A. A.; Carrera, P.; Cardillo, E.; Ugozzoli, L.; Lowery, J. D.; Lin, C.-I. P.; Go, M.; Ferrari, M.; Wallace, R. B.: Ligase chain reaction assay

- for human mutations: the Sickle Cell by LCR assay. *Clin Chem* **1997**, *43*, 40-44.
165. Rosi, N. L.; Mirkin, C. A. Nanostructures in Biodiagnostics. *Chem Rev* **2005**, *105*, 1547-1562.
166. Ruhela, D.; Vishwakarma, R. A.: Iterative synthesis of Leishmania phosphoglycans by solution, solid-phase, and polycondensation approaches without involving any glycosylation. *J Org Chem* **2003**, *68*, 4446-56.
167. Saiki, R. K.; Bugawan, T. L.; Horn, G. T.; Mullis, K. B.; Erlich, H. A.: Analysis of enzymatically amplified beta-globin and HLA-DQ alpha DNA with allele-specific oligonucleotide probes. *Nature* **1986**, *324*, 163-6.
168. Saiki, R. K.; Gelfand, D. H.; Stoffel, S.; Scharf, S. J.; Higuchi, R.; Horn, G. T.; Mullis, K. B.; Erlich, H. A.: Primer-directed enzymatic amplification of DNA with a thermostable DNA polymerase. *Science* **1988**, *239*, 487-91.
169. Sakata, T.; Winzeler, E. A.: Genomics, systems biology and drug development for infectious diseases. *Mol Biosyst* **2007**, *3*, 841-8.
170. Sando, S.; Abe, H.; Kool, E. T.: Quenched Auto-Ligating DNAs: Multicolor Identification of Nucleic Acids at Single Nucleotide Resolution. *J. Am. Chem. Soc.* **2004**, *126*, 1081-1087.
171. Schrum, J. P.; Ricardo, A.; Krishnamurthy, M.; Blain, J. C.; Szostak, J. W.: Efficient and Rapid Template-Directed Nucleic Acid Copying Using 2'-Amino-2',3'-dideoxyribonucleoside-5'-Phosphorimidazolide Monomers. *J Am Chem Soc* **2009**, *131*, 14560-14570.
172. Shen, W.; Deng, H.; Gao, Z. Gold Nanoparticle-Enabled Real-Time Ligation Chain Reaction for Ultrasensitive Detection of DNA. *J Am Chem Soc* **2012**, *134*, 14678-14681.
173. Shi, C.; Eshleman, S. H.; Jones, D.; Fukushima, N.; Hua, L.; Parker, A. R.; Yeo, C. J.; Hruban, R. H.; Goggins, M. G.; Eshleman, J. R. LigAmp for sensitive detection of single-nucleotide differences. *Nat Meth* **2004**, *1*, 141-147.

174. Sievers, D.; von Kiedrowski, G. Self-Replication of Hexadeoxynucleotide Analogues: Autocatalysis versus Cross-Catalysis. *Chem Eur J* **1998**, *4*, 629-641.
175. Sievers, D.; von Kiedrowski, G.: Self-replication of complementary nucleotide-based oligomers. *Nature* **1994**, *369*, 221-224.
176. Silverman, A. P.; Kool, E. T. Detecting RNA and DNA with Templated Chemical Reactions. *Chem Rev* **2006**, *106*, 3775-3789.
177. Sinden, R. R.: *DNA structure and function*; 1 ed., 1994. pp. 398.
178. Stoeva, S. I.; Lee, J.-S.; Thaxton, C. S.; Mirkin, C. A. Multiplexed DNA Detection with Biobarcode Nanoparticle Probes. *Angew Chem Int Ed* **2006**, *45*, 3303-3306.
179. Subramanya, H. S.; Doherty, A. J.; Ashford, S. R.; Wigley, D. B.: Crystal Structure of an ATP-Dependent DNA Ligase from Bacteriophage T7. *Cell* **1996**, *85*, 607-615.
180. Syvanen, A.-C. Accessing genetic variation: genotyping single nucleotide polymorphisms. *Nat Rev Genet* **2001**, *2*, 930-942.
181. Szostak, J.: The eightfold path to non-enzymatic RNA replication. *J Syst Chem* **2012**, *3*, 2.
182. Tan, E.; Erwin, B.; Dames, S.; Voelkerding, K.; Niemz, A.: Isothermal DNA amplification with gold nanosphere-based visual colorimetric readout for herpes simplex virus detection. *Clin Chem* **2007**, *53*, 2017-20.
183. Taran, O.; von Kiedrowski, G.: Replicators: Components for Systems Chemistry. In *Chemical Synthetic Biology*; John Wiley & Sons, Ltd, **2011**; pp 287-319.
184. Taylor, B.; Howell, A.; Martin, K.; Manage, D.; Gordy, W.; Campbell, S.; Lam, S.; Jin, A.; Polley, S.; Samuel, R.; Atrazhev, A.; Stickel, A.; Birungi, J.; Mbonye, A.; Pilarski, L.; Acker, J.; Yanow, S. A lab-on-chip for malaria diagnosis and surveillance. *Malaria J* **2014**, *13*, 179.
185. Tom Strachan, A. P. R.: Chapter 9, Instability of the human genome: mutation and DNA repair. In *Hum Molec Genet. 2nd edition.*; Wiley-Liss: New York, **1999**.

186. Toubanaki, D. K.; Christopoulos, T. K.; Ioannou, P. C.; Flordellis, C. S. Identification of Single-Nucleotide Polymorphisms by the Oligonucleotide Ligation Reaction: A DNA Biosensor for Simultaneous Visual Detection of Both Alleles. *Anal Chem* **2008**, *81*, 218-224.
187. Trantakis, I. A.; Bolisetty, S.; Mezzenga, R.; Sturla, S. J. Reversible Aggregation of DNA-Decorated Gold Nanoparticles Controlled by Molecular Recognition. *Langmuir* **2013**, *29*, 10824-10830.
188. Turner, J.; Begon, M.; Bowers, R. G.: Modelling pathogen transmission: the interrelationship between local and global approaches. *Proc Biol Sci* **2003**, *270*, 105-12.
189. Valsamakis, A. Molecular Testing in the Diagnosis and Management of Chronic Hepatitis B. *Clin Microbiol Rev* **2007**, *20*, 426-439.
190. Van Ness, J.; Van Ness, L. K.; Galas, D. J.: Isothermal reactions for the amplification of oligonucleotides. *Proc Natl Acad Sci* **2003**, *100*, 4504-9.
191. Vaneechoutte, M.; Van Eldere, J.: The possibilities and limitations of nucleic acid amplification technology in diagnostic microbiology. *J Med Microbiol* **1997**, *46*, 188-94.
192. Vincent, M.; Xu, Y.; Kong, H.: Helicase-dependent isothermal DNA amplification. *EMBO Rep* **2004**, *5*, 795-800.
193. Vogelstein, B.; Kinzler, K. W.: Digital PCR. *Proc Natl Acad Sci* **1999**, *96*, 9236-41.
194. Volker Patzke, G. v. K.: Self replicating systems. *ARKIVOC* **2007**, 293-310.
195. von Kiedrowski, G.: A Self-Replicating Hexadeoxynucleotide. *Angew Chem Int Ed* **1986**, *25*, 932-935.
196. von Kiedrowski, G.; Wlotzka, B.; Helbing, J.; Matzen, M.; Jordan, S.: Parabolic Growth of a Self-Replicating Hexadeoxynucleotide Bearing a 3'-5'-Phosphoamidate Linkage. *Angew Chem Int Ed* **1991**, *30*, 423-426.
197. Walker, G. T.: Empirical aspects of strand displacement amplification. *PCR Methods Appl* **1993**, *3*, 1-6.

198. Walker, G. T.; Fraiser, M. S.; Schram, J. L.; Little, M. C.; Nadeau, J. G.; Malinowski, D. P.: Strand displacement amplification--an isothermal, in vitro DNA amplification technique. *Nucleic Acids Res* **1992**, *20*, 1691-6.
199. Walker, G. T.; Linn, C. P.; Nadeau, J. G.: DNA Detection by Strand Displacement Amplification and Fluorescence Polarization With Signal Enhancement Using a DNA Binding Protein. *Nucleic Acids Res* **1996**, *24*, 348-353.
200. Walker, G. T.; Little, M. C.; Nadeau, J. G.; Shank, D. D.: Isothermal in vitro amplification of DNA by a restriction enzyme/DNA polymerase system. *Proc Natl Acad Sci* **1992**, *89*, 392-6.
201. Wang, D. G.; Fan, J. B.; Siao, C. J.; Berno, A.; Young, P.; Sapolsky, R.; Ghandour, G.; Perkins, N.; Winchester, E.; Spencer, J.; Kruglyak, L.; Stein, L.; Hsie, L.; Topaloglou, T.; Hubbell, E.; Robinson, E.; Mittmann, M.; Morris, M. S.; Shen, N.; Kilburn, D.; Rioux, J.; Nusbaum, C.; Rozen, S.; Hudson, T. J.; Lipshutz, R.; Chee, M.; Lander, E. S.: Large-scale identification, mapping, and genotyping of single-nucleotide polymorphisms in the human genome. *Science* **1998**, *280*, 1077-82.
202. Wang, H. Q.; Liu, W. Y.; Wu, Z.; Tang, L. J.; Xu, X. M.; Yu, R. Q.; Jiang, J. H.: Homogeneous label-free genotyping of single nucleotide polymorphism using ligation-mediated strand displacement amplification with DNAzyme-based chemiluminescence detection. *Anal Chem* **2011**, *83*, 1883-9.
203. Wang, H.; Li, J.; Wang, Y.; Jin, J.; Yang, R.; Wang, K.; Tan, W. Combination of DNA Ligase Reaction and Gold Nanoparticle-Quenched Fluorescent Oligonucleotides: A Simple and Efficient Approach for Fluorescent Assaying of Single-Nucleotide Polymorphisms. *Anal Chem* **2010**, *82*, 7684-7690.
204. Weiss, B.; Jacquemin-Sablon, A.; Live, T. R.; Fareed, G. C.; Richardson, C. C.: Enzymatic breakage and joining of deoxyribonucleic acid. VI. Further purification and properties of polynucleotide ligase from



- Escherichia coli infected with bacteriophage T4. *J Biol Chem* **1968**, *243*, 4543-55.
205. Whitman, W. B.; Coleman, D. C.; Wiebe, W. J.: Prokaryotes: the unseen majority. *Proc Natl Acad Sci* **1998**, *95*, 6578-83.
206. Wiedmann, M.; Wilson, W. J.; Czajka, J.; Luo, J.; Barany, F.; Batt, C. A. Ligase chain reaction (LCR)--overview and applications. *Genome Res* **1994**, *3*, S51-S64.
207. Wilhelm, J.; Pingoud, A.: Real-time polymerase chain reaction. *Chembiochem* **2003**, *4*, 1120-8.
208. Wu, D. Y.; Wallace, R. B.: The ligation amplification reaction (LAR)--amplification of specific DNA sequences using sequential rounds of template-dependent ligation. *Genomics* **1989**, *4*, 560-9.
209. Xu, Y.; Karalkar, N. B.; Kool, E. T. Nonenzymatic autoligation in direct three-color detection of RNA and DNA point mutations. *Nat Biotech* **2001**, *19*, 148-152.
210. Xue, X.; Zu, W.; Wang, F.; Liu, X.: Multiplex Single-Nucleotide Polymorphism Typing by Nanoparticle-Coupled DNA-Templated Reactions. *J. Am. Chem. Soc.* **2009**, *11668-11669*.
211. Yan, L.; Zhou, J.; Zheng, Y.; Gamson, A. S.; Roembke, B. T.; Nakayama, S.; Sintim, H. O. Isothermal amplified detection of DNA and RNA. *Molecular BioSystems* **2014**, *10*, 970-1003.
212. Yang, S.; Rothman, R. E.; Hardick, J.; Kuroki, M.; Hardick, A.; Doshi, V.; Ramachandran, P.; Gaydos, C. A.: Rapid polymerase chain reaction-based screening assay for bacterial biothreat agents. *Acad Emerg Med* **2008**, *15*, 388-92.
213. Ye, J.; Gat, Y.; Lynn, D. G. Catalyst for DNA Ligation: Towards a Two-Stage Replication Cycle. *Angew Chem Int Ed* **2000**, *39*, 3641-3643.
214. Yu, A.; Geng, H.; Zhou, X.: Quantify single nucleotide polymorphism (SNP) ratio in pooled DNA based on normalized fluorescence real-time PCR. *BMC Genomics* **2006**, *7*, 143.

215. Zhan, Z.-Y. J.; Lynn, D. G. Chemical Amplification through Template-Directed Synthesis. *J Am Chem Soc* **1997**, *119*, 12420-12421.
216. Zhang, Y.; Guo, Y.; Quirke, P.; Zhou, D.: Ultrasensitive single-nucleotide polymorphism detection using target-recycled ligation, strand displacement and enzymatic amplification. *Nanoscale* **2013**, *5*, 5027-5035.
217. Zheng, J.; Li, J.; Jiang, Y.; Jin, J.; Wang, K.; Yang, R.; Tan, W. Design of aptamer-based sensing platform using triple-helix molecular switch. *Anal Chem* **2011**, *83*, 6586-6592.
218. Zielinski, W. S.; Orgel, L. E. Autocatalytic synthesis of a tetranucleotide analogue. *Nature* **1987**, *327*, 346-347.